THE UNIVERSITY OF CHICAGO

AVIAN SLEEP ARCHITECTURE AND MOTOR REPLAY

A DISSERTATION SUBMITTED TO

THE FACULTY OF THE DIVISION OF THE BIOLOGICAL SCIENCES

AND THE PRITZKER SCHOOL OF MEDICINE

IN CANDIDACY FOR THE DEGREE OF

DOCTOR OF PHILOSOPHY

INTERDISCIPLINARY SCIENTIST TRAINING PROGRAM:

COMPUTATIONAL NEUROSCIENCE

BY

SOPHIA V. CANAVAN

CHICAGO, ILLINOIS

DECEMBER 2019

Table of Contents

LIST OF FIGURES ..... **VIII**

LIST OF TABLES ..... **X**

ACKNOWLEDGMENTS ..... **XI**

ABSTRACT ..... **XIV**

CHAPTER 1. INTRODUCTION **1**

THE QUESTION OF SLEEP 1

Sleep drive and sleep deprivation *2*

Sleep and memory *4*

Passive hypotheses of sleep *6*

Specialized sleep *7*

SLEEP ARCHITECTURE: A BRIEF INTRODUCTION 8

REM *9*

SWS *12*

Intermediate sleep: stage 2 and transition to REM *15*

Intermediate sleep: other forms *17*

Sleep architecture outside of mammals: initial comments *17*

SONGBIRDS AS A MODEL ORGANISM 18

The songbird brain *21*

Why study sleep in birds? *24*

FUNCTIONAL EFFECTS OF SLEEP ON MEMORY: SONGBIRDS 26

Memory encoding and initial learning *26*

Song maintenance *28*

Consolidation and reconsolidation *29*

Summary *30*

SLEEP AND MEMORY IN MAMMALS 31

Functional effects *32*

REM and sleep deprivation *33*

The Motor Sequence Task *34*

Language learning *35*

Does sleep affect learning independent of the hippocampus? *36*

Sleep correlates of procedural memory *37*

By what mechanism do specific stages of sleep affect memory? *40*

SLEEP REPLAY IN MAMMALS 40

Hippocampal sleep replay ... *40*
Other forms of replay ... *45*
Summary: mammalian sleep replay ... *47*
SLEEP REPLAY IN SONGBIRDS ... 47
Evoked replay ... *47*
Spontaneous replay ... *50*
What is the function of song replay? ... *53*
Is song replay related to sleep structure? ... *55*
Summary ... *56*
EVOLUTION OF SLEEP IN BIRDS ... 57
The traditional view: rudimentary REM ... *58*
The hypothesis of convergent evolution ... *59*
Early experimental limitations ... *60*
Recent studies in songbirds: unexpected similarities ... *61*
Basal birds ... *61*
The hypothesis of common ancestry ... *62*
THE THESIS STUDIES ... 62

CHAPTER 2. COMPLEX SLEEP IN A PARROT SPECIES ... 64

INTRODUCTION ... 64
RESULTS ... 66
Characteristics of budgerigar sleep behavior ... *66*
Electrophysiological characteristics of budgerigar sleep ... *69*
Sleep architecture across day and night ... *71*
Effects of constant light ... *74*
Characteristics of sleep states ... *76*
Slow waves and eye movements ... *79*
Ultradian rhythms and sleep cycles ... *81*
DISCUSSION ... 82
Budgerigars exhibit large amounts of REM sleep ... *83*
Evidence for SWS homeostasis ... *84*
Intermediate sleep is analogous to human stage 2 ... *85*
A long-period sleep cycle ... *86*
Constant light as a confounding factor ... *86*
Evolution of sleep ... *87*
METHODS ... 88
Animals ... *88*
Surgery ... *89*

Data acquisition ... *90*
Behavioral video scoring ... *91*
Manual PSG sleep scoring ... *95*
Constant light ... *98*
Motion detection ... *99*
Spectral analysis ... *100*
Event detection: slow waves, eye movements, and eye movement artifacts ... *100*
Ultradian rhythms ... *102*
Experimental design and statistical analyses ... *102*
Code accessibility ... *103*

CHAPTER 3. SLEEP STRUCTURE OF ADULT MALE ZEBRA FINCHES ... 104

INTRODUCTION ... 104
MATERIALS ... 105
Animals ... *105*
Surgery ... *106*
Data collection ... *108*
Preprocessing ... *108*
Behavioral characterization ... *109*
Comparison to budgerigar methods ... *111*
Automated sleep/wake scoring ... *112*
Spectral analysis ... *116*
Ultradian rhythms ... *117*
Statistical analyses ... *117*
RESULTS ... 117
Sleep/wake behavior ... *117*
State dependence and time course of spectral measures ... *121*
Ultradian rhythms at multiple timescales ... *123*
DISCUSSION ... 125

CHAPTER 4. A METHOD FOR LONG-TERM, HIGH-DENSITY MULTICHANNEL RECORDING IN FREELY-MOVING BIRDS ... 129

INTRODUCTION ... 129
IMPLANT CONSTRUCTION ... 132
Lightweight custom headstage ... *132*
Microdrive ... *135*
Microdrive holder ... *137*
Attaching the array to the microdrive ... *138*

Custom electrode array ... *139*
Preparing the headstage: metal legs ... *142*
Preparing the headstage: EEG-style ground ... *143*
Preparing the headstage: optional EEG/EOG electrodes ... *143*
PREPARATION FOR SURGERY ... 144
IMPLANTATION SURGERY ... 145
Anesthesia for long surgeries ... *145*
Food deprivation, injections, and bird jacket ... *147*
Surgical approach ... *148*
Making the craniotomy & the durotomy ... *151*
Lowering the array and microdrive ... *152*
Placing ground and other electrodes ... *154*
Attaching the headstage ... *155*
Protecting the implant ... *156*
Recovery from surgery ... *157*
Home cage setup ... *157*
Days following surgery ... *157*
RECORDING PROCEDURES ... 158
The recording setup ... *158*
Raising and lowering the array during recovery ... *159*
Acclimation to tether ... *160*
Lowering the array: speed, how often, raising and lowering repeatedly ... *161*
Software and impedances ... *162*
Common sources of noise ... *162*
SPIKESORTING ... 163
Preparing data for analysis ... *163*
MountainSort ... *164*
Converting back to bark ... *167*
ARRAY RECOVERY ... 167
Cleaning the array for reuse ... *168*
CONCLUSION ... 169

CHAPTER 5: SONG REPLAY IS RELATED TO LOCAL AND GLOBAL SLEEP STRUCTURE ... 174

ABSTRACT ... 174
INTRODUCTION ... 175
METHODS ... 179
Birds, polysomnography, and array implantations ... *179*
Implantation of single-unit Pt/Ir extracellular electrodes ... *180*

Data collection ... *181*
Preprocessing ... *182*
Song labeling and data visualization ... *182*
Spikesorting ... *183*
Replay identification ... *184*
Spectral analyses ... *191*
Eye movement index and detection of eye movements ... *191*
Dynamic time warping and spiketrain alignment ... *191*
Replay content ... *192*
Statistical analyses ... *193*
RESULTS ... 193
Replay identification and timescale ... *195*
Time-locked oscillations during replay ... *198*
Global sleep structure and replay frequency ... *202*
Replay content ... *204*
Compressed events ... *206*
Non-canonical replay ... *208*
Changes in burst structure during sleep ... *210*
DISCUSSION ... 212
CHAPTER 6. GENERAL DISCUSSION ... 216
OVERVIEW OF FINDINGS ... 216
FUTURE DIRECTIONS ... 218
Function of REM ... *218*
Tonic and phasic REM in birds ... *219*
Slow waves and evoked BOS responses ... *220*
Properties of slow waves in birds ... *220*
Adult neurogenesis ... *221*
Functional effects of sleep and sleep replay ... *222*
REFERENCES ... 226

LIST OF FIGURES

Figure 1.1. Vigilance states and sleep architecture……9

Figure 1.2. Stages of birdsong learning……19

Figure 1.3. The song system.……22

Figure 1.4. Cladogram of amniote evolution……58

Figure 2.1. Examples of video and polysomnography data.……67

Figure 2.2. Sleep architecture and rhythms over 24 hours……72

Figure 2.3. The effect of constant light on sleep/wake behavior…..……75

Figure 2.4. Time-varying and spectral characteristics of sleep states……77

Figure 2.5. Automated detection of slow waves, eye movements, and eye movement artifacts...80

Figure 2.6. Ultradian rhythms in sleep.……82

Figure 3.1. Automated video scoring……115

Figure 3.2. Hypnograms of all datasets.……119

Figure 3.3. Summary of vigilance states during night and day……120

Figure 3.4. Comparison of EEG distribution across vigilance states……122

Figure 3.5. Time course of EEG/LFP features across the night……123

Figure 3.6. Ultradian rhythms...……124

Figure 4.1. Comparison of headstages……..……..133

Figure 4.2. Components of microdrive.……135

Figure 4.3. Diagram of microdrive and electrode assembly.……136

Figure 4.4. Microdrive holder.……138

Figure 4.5. The tip of a lab-made electrode.……..140

Figure 4.6. Attachment of metal legs to headstage……142

Figure 4.7. Placement of scalp incisions and electrodes.……149

Figure 4.8. Placement of implant components.……155

Figure 4.9. A fully acclimated tethered bird……161

Figure 4.10. Population RA response to stimulus playback during sleep.…….……..170

Figure 4.11. Chronic recording of a single RA neuron over 5 days……171

Figure 5.1. Replay identification method……187

Figure 5.2. Examples of replay events and simultaneous LFP……194

Figure 5.3. Replay identification at different timescales.……196

Figure 5.4. Timescale distribution found with a correlation-based method.……...197

Figure 5.5. Replay events and event-triggered averages of LFP, EEG, and EOG..……199

Figure 5.6. Replay-triggered EEG and LFP……..…201

Figure 5.7. Spectral characteristics of epochs containing replay……..…202

Figure 5.8. Sleep structure vs replay frequency across the night…….……203

Figure 5.9. Replay content……...……205

Figure 5.10. Compressed events and event-triggered averages of LFP, EEG, and EOG……207

Figure 5.11. Timescale of replay events vs amplitude of LFP……...….208

Figure 5.12. Motor coding across multiple sleep-wake cycles: whole-motif activity.……209

Figure 5.13. Motor coding across multiple sleep-wake cycles: individual bursts.……..211

LIST OF TABLES

Table 2.1. Sleep stage proportions……69

Table 2.2. Behavioral scoring criteria..……..…93

Table 2.3. Sleep scoring and vigilance state characteristics..……96

Table 3.1. Animals and datasets..…….106

Table 3.2. Summary of vigilance states during night and day……..121

Table 5.1. Animals and datasets……..179

ACKNOWLEDGMENTS

Like many others I tend to use the pronoun “we” for scientific writing. I think this comes not from latent inclinations toward royalty, but from an instinctive understanding of how many people have contributed to the work of any one individual.

I need to first thank Peter Morgan for his mentorship, thoughtfulness and compassion. He introduced me to sleep research and to medicine, and he epitomizes the type of physician-scientist I wish to become. Peter, I hope to live up to your example.

Thank you to my thesis committee, David Freedman, Jason MacLean, and Murray Sherman, for your insight, advice, and support over the years, and for letting me occasionally show up in your labs and follow your students around. Thanks to Wim van Drongelen for teaching me an unbelievable amount in a short five weeks.

I also want to thank Kate Hosford, whose collection of poems captures the whimsical and beautiful nature of sleep across the animal kingdom. During grad school, I had the honor of providing scientific feedback on her book. I hope many children are inspired by it, as I was.

I owe my deepest gratitude to Dan Margoliash, the best mentor I could have possibly asked for. I first met Dan at my admissions interview. We talked an hour longer than scheduled; we came up with the initial idea for the budgie project; and we watched a David Attenborough video about lyrebirds. Joining Dan’s lab was one of the best decisions of my life. Dan — thank you for your contagious enthusiasm, your mentorship, and your unmatched integrity and commitment to your students. I feel excited about science every time I walk out of your office. Most of all, thank you for your endless support and understanding, which have sustained me through the many ups and downs of the years.

This lab has been a haven for me, a place of not only learning but friendship. I thank Daniel Baleckaitis for his endless patience, guidance, help, pumpkin spice lattes, and many early-morning conversations. Thanks to Tim Brawn and Kyler Brown, who also helped train me and guide me over the steep learning curve that was my first few years in the lab. Thanks to Graham Fetterman, my unflappable fellow adventurer; together we traversed the wilds of multielectrode arrays, headstages, and databases. To all of the aforementioned and Arij Daou, Peter Malonis, Nelson Medina, and Daniel Lam: Thank you all for creating a warm, engaging, and welcoming lab culture, where we can enthusiastically discuss anything from science to tea to the surface area of sperm whales. I must also thank the smallest and noisiest members of the lab, Professor Grey and Dr Patches, for being excellent officemates.

My MSTP class has become like family; I never would have made it without you. Thank you to Alex Guzzetta, Ben Casterline, Dan Camacho, and Eliza Frost; to my neuroscience co-conspirators Tahra Eissa and Sophia Uddin, and to our extended MSTP family, Deanna Arsala, Regina Casterline, Chanie Howard, and Gabriel Riccio. An especially important thanks goes to my classmate Victoria Lee, who lived with me through the first two years of grad school and all the accompanying adventures and tribulations. We both made it through. I also thank Heather Lemire for her unbroken emotional support since freshman year of high school.

Thank you to my entire family, who raised me with love and chaos. My parents instilled me with curiosity and drive, which turned out to be pretty important. Thank you for supporting all of my various eccentric interests; eventually they led to science, right? My mother Valentina has been for many years the only female professor of mathematics in her department. She imbued me with the confidence that a woman could succeed in the most technical and male-dominated of fields. My father Ed has been a science role model for me. He was the one who taught me that

creativity is an integral part of science. Although as a physicist, he sees biology as an extended form of taxonomy, he nevertheless helped me every step of the way.

To my sister Kalina, you are the eye of the storm and the electrical ground of our family. Thank you for always being my reality check, for always making me laugh, for never letting me take things too seriously.

Thank you to Spas and Viktorija, who always believed in me. If they were with us today I know they would be incredibly happy, but unsurprised, to see this moment.

My fiancé Jeffrey Bunker has supported me through every day of this five year journey. Thank you for everything. You have stood by me and lifted me up through the darkest times, and you have brought about the brightest times of my life. Your hard work, curiosity, and clarity of mind inspire me as a scientist and a person.

ABSTRACT

Birds, like mammals, have multiple forms of sleep including rapid eye movement sleep (REM) and slow wave sleep (SWS). It is not known why or how these specialized stages of sleep evolved. For many decades, the overwhelming consensus was that avian sleep was more primitive. This led to the conclusion that complex sleep evolved independently in mammals and birds.

Recently, songbirds were found to have surprisingly mammalian-like sleep architecture as well as sleep replay of song, a learned motor skill. In mammals, sleep replay in hippocampal place cells is thought to be a central mechanism for the function of sleep in learning and memory. The well-established co-occurrence of hippocampal replay with slow waves demonstrates the link between global sleep architecture and circuit-level mediators of sleep function. However, sleep has profound effects not only on hippocampal-dependent declarative memory, but also on procedural memory. Song replay, as the only other confirmed exemplar of sleep replay, thus offers a chance to study a similar mechanism within a procedural memory system. I sought to better understand how sleep architecture is expressed across multiple bird species, and how song replay is related to sleep structure.

I characterized sleep architecture in budgerigars (*Melopsittacus undulatus*), finding multiple signs of complex, highly structured, and mammalian-like sleep. These traits included patterns of REM increase and SWS decrease, a stage of intermediate sleep that remained consistent over the night, a 34-minute sleep cycle, and the largest amount of REM found in adults of any bird species to date (26.5%). Furthermore, I demonstrated that a major source of error in earlier studies was the use of constant light, which I found to abolish the circadian rhythm, decrease total sleep, and fragment sleep episodes.

Using automated techniques, I went on to confirm recent results on sleep architecture in zebra finches (*Taeniopygia guttata*) and characterized the sleep/wake cycle over 24 hours. The findings are consistent with mammalian-like patterns of REM increase and SWS decrease, contradicting older reports of songbird sleep. I also observed a 38-minute sleep cycle in zebra finches. These results indicate that complex sleep structure is most likely to includes the majority of extant species of birds (songbirds and parrots), and promotes re-evaluation of the evolutionary history of complex sleep in birds and in mammals.

As part of the work on sleep replay, I was involved in an effort to develop techniques for chronic multielectrode array recordings in zebra finches. These methods are described here in detail to facilitate replication of this technique, including implant construction, surgery, recording, and spikesorting. I used this technique to record from the nucleus robustus of the arcopallium (RA), the motor cortex analogue of the song system. By combining chronic recordings of RA activity with polysomnography over multiple sleep/wake cycles, I was able to examine the relationship between song replay and sleep structure. Song replay was most strongly linked to non-REM, occurred during periods of higher slow wave activity, and often co-occurred with local slow waves. Replay events most often occurred at or near real-time, in contrast with the highly compressed replay of the hippocampus. These results establish for the first time similarities and differences in sleep replay comparing declarative and procedural memories.

In sum these results show that highly complex sleep traits manifest across songbirds and parrots, and that complex sleep architecture is linked to song replay. This supports the hypothesis that shared attributes of avian and mammalian sleep are derived from a common precursor, and helps to illuminate underlying mechanisms by which complex sleep can affect procedural memory.

CHAPTER 1. INTRODUCTION

The question of sleep

Unlike other daily activities such as eating, drinking, or breathing, the contribution of sleep to adaptive fitness – that is, its basic function – remains a mystery. To address such a broad issue, this thesis investigates sleep from evolutionary, behavioral, and systems neuroscience perspectives. The importance of sleep is abundantly clear, as witnessed by clinical pathologies and experimental manipulations of sleep. Yet on its surface, sleep does not make sense for survival — why would animals spend many hours of the day in a state in which they cannot respond quickly to threats, in which they cannot forage or care for young? Despite these apparent disadvantages, the ubiquity of sleep across the animal kingdom has been known since classical times:

> "Almost all other animals are clearly observed to partake in sleep, whether they are aquatic, aerial, or terrestrial, since fishes of all kinds, and molluscs, as well as all others which have eyes, have been seen sleeping. 'Hard-eyed' creatures and insects manifestly assume the posture of sleep."
>
> *— Aristotle, On Sleep and Sleeplessness (Aristotle, 350BCa)*

Why would such a state evolve in the first place? What is the selective pressure underlying its prevalence in our lives? Why have so few species, perhaps none, evolved a way to escape it? Whatever it is that sleep does, it must be highly important to any organism with a nervous system.

Sleep drive and sleep deprivation

Not only has sleep evolved across the animal kingdom, but within the individual this behavior is enforced by a powerful drive. Sleep deprivation is so unpleasant that it has been used as an interrogation tool and a form of torture for more than a thousand years, going back at least to the ancient Romans7 (Linden, 2012). People who have survived this describe the overwhelming ferocity of the sleep drive:

> "The interrogated prisoner… has one sole desire: to sleep… Anyone who has experienced this desire knows that not even hunger and thirst are comparable with it."
>
> *— Menachem Begin, White Nights (Begin, 1979)*

Why is the drive for sleep so strong? There is a good reason: the consequences of not sleeping are dire, possibly life-and-death. Rats deprived of sleep die in 11-32 days (Everson et al., 1989) and flies die after 60-70 hours (Shaw et al., 2002). History indicates this may extend to humans:

> "According to legend, King Perseus of Macedonia was put to death by being prevented from sleeping when held prisoner in Rome."
>
> *— Paul Martin, Counting Sheep (Martin, 2004)*

> "Records of Nazi death camp experiments during World War II as well as reports of executions by sleep deprivation in China in the nineteenth century… suggest that 3-4 weeks of sleep deprivation will kill humans as well."
>
> *— David J. Linden, The Accidental Mind (Linden, 2012)*

The mechanisms whereby sleep deprivation causes death remain under active investigation. Sleep deprived rats develop sores, their body temperature fluctuates wildly, and they shed weight despite actively increasing their caloric intake (Rechtschaffen et al., 1983; Bergmann et al., 1989). The immune defenses become compromised (Bergmann et al., 1996), a finding that has

been inadvertently replicated in birds (Snyder et al., 2013). Flies with knockouts of heat shock proteins die more quickly from sleep deprivation, implicating the cellular stress response (Shaw et al., 2002). This multifaceted involvement of sleep in basic physiological functions across the animal kingdom makes it that much harder to explore its other roles — any experiment that uses sleep deprivation in any species is expected to introduce a number of confounds.

But the long-term consequences of total sleep deprivation do not necessarily explain why animals are driven to sleep so often or so much. Most people are severely impaired by even 24 – 72 hours of sleep deprivation, experiencing cognitive impairments, memory deficits and even hallucinations (Morris et al., 1960).

> "Finally, from so little sleeping and so much reading, his brain dried up and he went completely out of his mind."
>
> — *Miguel de Cervantes Saavedra, Don Quixote (de Cervantes Saavedra, 1949)*

The longest that a person has been able to voluntarily sleep deprive themselves is 11 days (Gulevich et al., 1966), nowhere close to the 3-4 weeks described above. Some species have developed the unusual ability to periodically sleep less: for example, during the breeding season male sandpipers reduce their sleep to as little as 5% of total time over three weeks; in this context not sleeping was directly correlated with number of offspring (Lesku et al., 2012). During the migration season, white-crowned sparrows reduce their sleep by over 60%, even when confined to the laboratory, but they retain cognitive abilities that normally deteriorate after sleep deprivation outside of the migration season (Rattenborg et al., 2004). However, even in extreme cases sleep is not completely jettisoned: great frigatebirds, who fly continuously for up to 10 days while migrating over the Pacific, are able to sleep on the wing (although their sleep is reduced to about 7% of their normal amount (Rattenborg et al., 2016). If animals needed sleep

only to stave off death, why would they not evolve a reduced amount of sleep and regularly go for a week or so with needing it at all?

Instead, daily sleep is underwritten by two interacting systems. The homeostatic drive builds up sleep pressure during wake: the longer an animal spends awake, the more it is driven to sleep.

> "No small art is it to sleep: it is necessary for that purpose to keep awake all day."
>
> — *Friedrich Nietzsche, Thus Spake Zarathustra (Nietzsche, 1909)*

The circadian system uses environmental cues, primarily light, to track the 24-hour rhythm (Aschoff, 1965) and step up the drive for sleep at specific times (Sterman et al., 1965). In nocturnal animals this time is during the day; in diurnal animals, it is at night. In humans and probably some other diurnal animals, sleep need also peaks to a lesser extent in the mid-afternoon (Dijk and Franken, 2005). Both the homeostatic and circadian drives therefore ensure that sleep occurs every day, at an optimal time, and in proportion to the amount of wakefulness.

Sleep and memory

The question of what sleep is "for" is commonly posed but poorly considered, because it presumes a unitary function for sleep that belies the complexity and multifaceted role of sleep in many or most animals. A better posed question is what about sleep justifies its daily occurrence, the strength of its underlying drives, and its universality among animals? Whatever sleep originally evolved for, it has clearly taken on many functions.

> "Blessings on the one who invented sleep, the cloak that covers all human thoughts, the food that relieves hunger, the water that quenches thirst… and that puts the fool on an equal footing with the wise man."
>
> — *Miguel de Cervantes Saavedra, Don Quixote (de Cervantes Saavedra, 1949)*

An emerging consensus suggests that one of sleep's chief roles is in the domain of learning and memory — arguably a central purpose for which nervous systems elaborated following basic stimulus/response behavior.

Multiple forms of memory benefit from and require sleep. This holds true of declarative memories (Gais and Born, 2004), emotional memories (Walker and van Der Helm, 2009), and procedural memories (Walker and Stickgold, 2006) — including motor learning (Smith and Macneill, 1994; Walker et al., 2002; Brawn et al., 2010), which this thesis will focus on.

An extensively studied mechanism that contributes to sleep-dependent learning and memory is sleep replay, in which neurons recapitulate patterns of activity associated with a learned behavior or experience (O'Neill et al., 2010). This mechanism was discovered in rodent hippocampus (Skaggs and McNaughton, 1996), where it has been studied almost exclusively in the context of initial memory consolidation. Another form of replay appears in the song system of zebra finches, during active maintenance of motor memory (Dave and Margoliash, 2000).

Like sleep itself, the importance of sleep to memory has been demonstrated across many species, from insects (Donlea et al., 2011; Beyaert et al., 2012) to mammals (Smith, 1985; Walker and Stickgold, 2004) to birds (Solodkin et al., 1985; Derégnaucourt et al., 2005; Jackson et al., 2008; Brawn et al., 2013). This raises the question whether memory is an ancestral function of sleep or alternatively sleep-dependent memory formation (consolidation; see below) emerged independently in multiple evolutionary lineages. Related, it remains unclear whether sleep plays a similar role in all these lineages, or whether it has become more specialized to support a different capacity for learning in some. If the latter is the case, then it would point towards a yet–unidentified basal condition of the interaction of sleep and memory.

Passive hypotheses of sleep

The link between sleep and learning is not without controversy (Vertes, 2004). Some theories of sleep have suggested instead that its function is relatively passive — it exists as the absence of waking, the absence of movement, the absence of energy expenditure. These theories are unbounded, that is they posit the absence of structure (in this case, the function of sleep) is the defining feature (in this case, of the function of sleep). This can lead to unfettered speculation. For example, by one hypothesis sleep may function merely to prevent the animal from moving around and encountering predators during a non-optimal time of day (Rial et al., 2007b):

> "It is conceivable that animals who are too stupid to be quiet on their own initiative are, during periods of high risk, immobilized by the implacable arm of sleep."
>
> — *Carl Sagan, The Dragons of Eden (Sagan, 1977)*

By this account, animals are evolutionarily poorly adapted but saved from their own limitations by sleep, which somehow exists as a separate (or independent) evolutionary process. Furthermore, this description would include humans, who too are immobilized by sleep and tend to be more active during nighttime awakenings.

Some have even posited that sleep is an evolutionary spandrel, an unimportant byproduct of the evolution of conscious wakefulness (Rial et al., 2007a). This too is a remarkable suggestion, given the potential impact of sleep for survival, and given the breadth of sleep in the animal kingdom.

Neither of these hypotheses explain the heightened arousal threshold, a defining feature of sleep that is also one of its most dangerous. In a way these ideas mirror very early conceptions of sleep, in which it was viewed as an unconscious state akin to death:

> "In ancient Greek mythology... the goddess of Night had twin sons called Hypnos

(Sleep) and Thanatos (Death)."

— Paul Martin, Counting Sheep (Martin, 2004)

"For between a sleeping man and a dead one there is very little difference."

— Miguel de Cervantes Saavedra, Don Quixote (de Cervantes Saavedra, 1949)

A related but more credible hypothesis suggests that sleep exists to conserve energy — the brain, which consumes disproportionate amounts of energy (Niven and Laughlin, 2008), essentially shuts off in a state analogous to light hibernation but with more ability to monitor the environment and respond to threats (Schmidt, 2014). After all, learning is not the most universal function of the nervous system; the first nervous systems may have evolved to allow for movement and control of musculature (Keijzer et al., 2013), which is closely linked to energy usage. But at least from a passive standpoint, sleep saves very little energy compared to quiet wakefulness, perhaps 10 – 15 %. As Allan Rechtschaffen put it, "from the standpoint of energy savings, a night of sleep for a 200-pound person is worth a cup of milk." Given the modest savings in energy consumption one might expect various specializations in species where animals fail to sleep but conserve energy utilizing other methods, but no such examples are known. This idea is brought further into question by the specialized and complex sleep that has evolved in a subset of animal species.

Specialized sleep

In mammals and birds, the multifunctionality of sleep has seemingly come to be reflected in the heterogeneity of sleep structure. Mammals and birds have developed several types of sleep, which include rapid eye movement sleep (REM), slow wave sleep (SWS), and various types of intermediate sleep. First discovered in humans (Blake and Gerard, 1937; Aserinsky and Kleitman, 1953; Rechtschaffen and Kales, 1968) and cats (Derbyshire et al., 1936; Dement,

1958; Jouvet et al., 1959), these sleep stages were soon found in other mammals (Weitzmann, 1961; Swisher, 1962) as well as birds (Klein et al., 1964; Ookawa and Gotoh, 1964).

Each sleep stage is characterized by a specific neuromodulatory milieu (Lee and Dan, 2012), a set of autonomic effects (Schulz and Salzarulo, 2012), and specific regulatory drives. In contrast to the idea of sleep as a passive torpor-like state, the sleeping brain stays busy, deliberately generating unique oscillations and other patterns of activity (Ancoli-Israel et al., 2007). These multiple forms of sleep presumably carry out mutually exclusive roles which have evolved in only a subset of animals. Notably, both birds and mammals happen to also share highly developed neural circuity and cognitive abilities (Emery and Clayton, 2004; Rattenborg, 2006; Ditz and Nieder, 2015; Nieder, 2018). Understanding why these separate stages evolved, and how they carry out their functions, is central to understanding how sleep works.

Sleep architecture: a brief introduction

Sleep states can be measured through the use of polysomnography (PSG), a combination of recording techniques which can include measuring brain activity with electroencephalography (EEG), eye movements with electrooculography (EOG), muscle activity with electromyography (EMG), as well as measurements of respiration and heart rate. What follows is a brief summary of the characteristics of these stages as defined in mammals (Ancoli-Israel et al., 2007) (**Figure 1.1**). The most common distinctions are between rapid eye movement (REM) sleep and non-REM (NREM) sleep. NREM is further subdivided into slow wave sleep (SWS) and various forms of intermediate sleep.

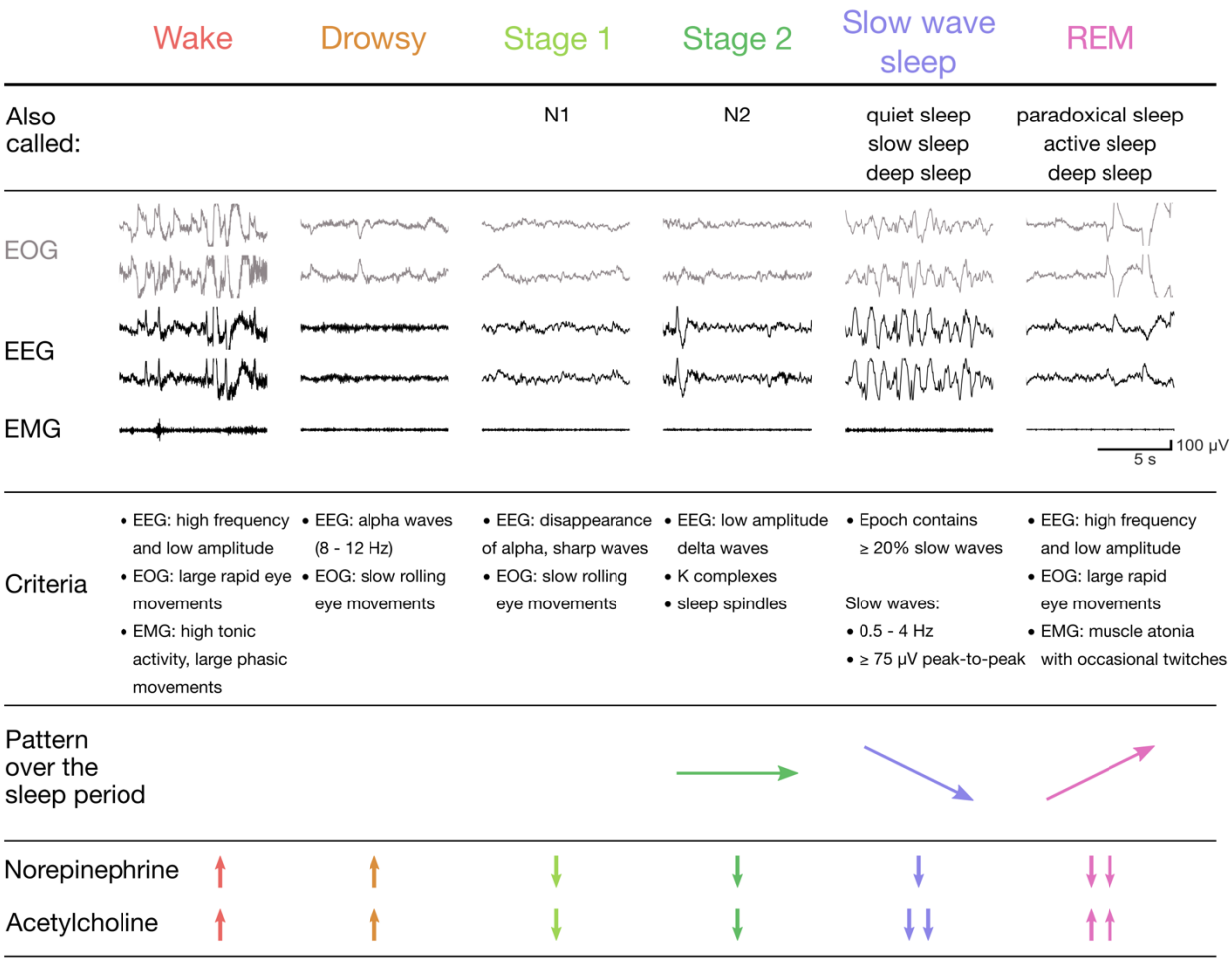

Figure 1.1. Vigilance states and sleep architecture. Each vigilance state is defined by characteristics of the polysomnogram, a combination of EEG, EOG, and EMG recordings. Example polysomnographic traces are from a 20-year-old human female (the author). Criteria and characteristics are as defined in humans by current clinical guidelines (Ancoli-Israel et al., 2007).

REM

REM was once called "paradoxical sleep" because the REM EEG so strikingly resembled wakefulness, but it is also paradoxical in the sense of the non-veridical representation of daytime reality. During REM humans experience vivid hallucinations, i.e. dreams, which can sometimes lead to confusion upon waking and even false memories. Anyone who has woken up disturbed by upsetting dreams can attest to this, as can anyone who's remembered doing something, only

to realize later that it only happened in a dream. Other species almost certainly experience dreams, as Aristotle noted in 350 B.C.E:

> "it would appear that not only do men dream, but horses also, and dogs, and oxen…sheep, and goats, and all viviparous quadrupeds; and dogs show their dreaming by barking in their sleep."
>
> *— Aristotle, The History of Animals (Aristotle, 350BCb)*

Thus, it is likely that the mental states that REM induces in humans are broadly represented at least in mammals and birds.

The outward signs of REM, discovered long before REM was recognized as a distinct sleep state (Schulz and Salzarulo, 2012), are no less disadvantageous. Animals in REM twitch frequently, which would increase their visibility to predators. Michel de Montaigne, writing in the late 1500s, observed this: "even brute beasts are subject to the force of imagination as well as we; witness dogs… bark and tremble and start in their sleep; so horses will kick and whinny in their sleep" (Montaigne, 1877). Other than these intermittent twitches, the muscles dwindle into complete atonia. Most people will at least once experience a phenomenon called sleep paralysis, in which they wake up unable to move; this is the muscle block imposed by REM bleeding over into the waking state (Schiappa et al., 2018). This paralysis can be accompanied by the feeling of a weight on the chest, intense fear, and hallucinations: additional elements of REM carrying over into wake. Sleep paralysis has been hypothesized as the explanation behind the incubus myth and reports of alien abductions (Sagan, 1996).

Superficially, muscle atonia is disadvantageous, but it is well-established (at least in mammals) that if this muscle block is eroded the organism will act out its dreams. This condition is known as REM behavior disorder. The arousal threshold during REM is variable but can become even higher than during NREM (Carskadon and Dement, 2011). Obstructive sleep

apnea, a common sleep disorder in which patients are unable to breathe, tends to be at its worst during REM (Findley et al., 1985). A number of other bodily changes appear during REM, notably the loss of thermoregulatory control and irregular breathing and heart rate (Carskadon and Dement, 2011).

The EEG during REM takes on an appearance that is strikingly similar to wake: relatively flat or low-amplitude and containing higher frequencies than during other states of sleep. In rodents, the hippocampus produces almost continuous theta waves (4-8 Hz) which also appears during active exploration (Vanderwolf, 1969; Fox et al., 1986). In humans, REM hippocampal activity appears to fall instead within the delta range with only intermittent bursts of theta (Cantero et al., 2003; Ferrara, 2012). Depth recordings reveal ponto-geniculo-occipital (PGO) waves that start in the brainstem and travel throughout the visual system (Hobson, 1965). These tend to accompany the characteristic large rapid eye movements, which appear on the EOG and typically come in clusters. REM which contains eye movements is referred to as "phasic REM," and is associated with a very high arousal threshold, while REM without eye movements is known as "tonic REM" (Wehrle et al., 2007).

REM usually occurs after some period of non-REM sleep has passed; the exception is in narcolepsy, a disorder of REM regulation (Carskadon and Dement, 2011; Leschziner, 2014). Sudden-onset REM can also be induced by REM-depriving organisms, suggesting a homeostatic element of regulation (Morden et al., 1967). REM tends to occur at low levels at the beginning of the sleep period and increase towards the end (Agnew and Webb, 1973), suggesting it is also regulated by circadian processes or by a process occurring during NREM (Peever and Fuller, 2017).

The neurotransmitter acetylcholine is released at high levels during REM, sometimes even exceeding levels during wakefulness (Vazquez and Baghdoyan, 2001). In contrast, norepinephrine is released at its lowest levels (Hobson et al., 1975) and this seems to be crucial to the normal functioning of REM (van der Helm et al., 2011; Swift et al., 2018). Many brain areas are highly active, but others such as the dorsolateral prefrontal cortex exhibit very low activity (Maquet et al., 1996). This may contribute to the dreamer's subjective lack of executive control, their acceptance of abnormal events and the inability to recognize they are dreaming (Voss et al., 2013; Dresler et al., 2014).

Juveniles of most mammalian species exhibit higher amounts of REM than adults (Peever and Fuller, 2017). This has led to theories of REM's involvement in early life. The muscle twitches, for example, are thought to help with motor system development, perhaps by linking motor commands to proprioceptive processes (Blumberg et al., 2013). In mammals, REM is associated with precociality/altriciality of a species: if juveniles of a species are born less developed, the adults of that species will have more REM (Lesku et al., 2008).

SWS

During SWS — the deepest form of NREM sleep —the arousal threshold is consistently very high. Awakening from SWS can be an extremely slow process and even once awake, humans experience cognitive disruption (or "fog") that can take tens of minutes to wear off (Bonnet, 1983; Tassi and Muzet, 2000). Humans woken during SWS, especially during periods of slow wave activity, often recall nothing and may not be aware they had slept (Cicogna et al., 2000; Chellappa et al., 2011). SWS is also the stage during which common arousal parasomnias such as sleepwalking, sleep talking, and night terrors are expressed. These are especially prevalent in children (Mahowald and Bornemann, 2005). From the perspective of adaptive fitness, SWS must

confer advantages that outweigh its effects in younger children – for example, night terrors afflict up to 17% of children under the age of 5, causing them to periodically arise from bed screaming and confused (Ekambaram and Maski, 2017).

Physiological changes during NREM include slow and regular respiratory and heart rates, which are at their slowest during SWS (Aldredge and Welch, 1973; Krieger, 2005). Muscle tone is low but not abolished, and eye movements can occur but are small and rare. In the EEG, the defining characteristic of SWS is the slow wave — a delta wave (0.5 – 4 Hz) of high amplitude (defined as 75 μV peak-to-peak). To be classified as SWS using standard criteria for humans, at least 20% of a given epoch must contain slow waves. Originally a distinction was made between stage 3 (>20% slow waves) and stage 4 (>50% slow waves) (Rechtschaffen and Kales, 1968) but decades of research found little functional difference and so both stages were folded into SWS, also called stage 3 (Ancoli-Israel et al., 2007; Schulz, 2008).

The slow wave reflects widespread synchronization across the cortex (Steriade, 1997). Its source is the intracellular slow oscillation (0.1 – 1 Hz) expressed in the membrane voltage of most cortical cells (Steriade et al., 1993c). During the UP state of the slow oscillation, cells fire or burst robustly; during the DOWN state, cells fall almost completely silent (Steriade et al., 1993c). While the thalamus can modulate them, slow oscillations are primarily generated by cortex (Steriade et al., 1993d). Although NREM is globally regulated by a network of brainstem nuclei (Schwartz and Roth, 2008), individual cortical slices can exhibit slow waves *in vitro* (Sanchez-Vives and McCormick, 2000). These slice recordings reveal that cortical slow waves arise in layer 5 and propagate both vertically and horizontally (Sanchez-Vives and McCormick, 2000). Such massive synchronization is likely to preclude much active or continuous processing, which may explain why sleepers report so little mentation during SWA (Chellappa et al., 2011).

Slow waves travel in two dimensions across the cortical sheet, usually originating in an anterior region and moving posteriorly (Massimini et al., 2004).

At the very beginning of the sleep period, NREM gradually builds up to SWS; the animal then goes into REM or has a brief awakening. This pattern of intermediate NREM to SWS to REM is called a sleep cycle and lasts 90 minutes in the human, who will go through 4 – 5 sleep cycles in a night (Carskadon and Dement, 2011). The amount of SWS is highest at the beginning of the night and decreases in subsequent sleep cycles (Ohayon et al., 2004). It is very clearly regulated by a homeostatic process and rebounds after sleep deprivation (Borbély and Achermann, 2005). An objective estimate of SWS depth can be obtained from slow wave activity (SWA), usually defined as total delta power in each epoch. SWA is often used as a proxy for sleep depth or quality in humans; arousal threshold scales with SWA activity (Blake and Gerard, 1937), and the amount of SWA can predict how refreshed a person feels after a night of sleep (Keklund and Akerstedt, 1997). SWA can also serve as a measure of sleep need, reflecting the amount of time spent awake (Webb and Agnew, 1971). Of all the sleep stages, SWS seems to be the most highly prioritized by the various competing drives. When people are restricted to very small amounts of sleep, the body will get the maximum amount of SWS first at the expense of other stages (Van Dongen and Maislin, 2003).

NREM and particularly SWS is marked by low acetylcholine and low norepinephrine (Lee and Dan, 2012). SWS is high in infants and tends to decrease steadily with age (Ohayon et al., 2004), although not as dramatically as REM. Of all the sleep stages, SWS is the most likely to enact any sort of energy savings; it is known to regulate metabolism and circulatory function, although slow waves appear to exert additional proactive effects on these systems (Zepelin et al., 2005; Tasali et al., 2008; Grimaldi et al., 2019). SWS is also most closely linked with restorative

functions such as protein synthesis (Ramm and Smith, 1990), glymphatic clearance of waste (Xie et al., 2013; Varga et al., 2016), and secretion of growth hormone (Van Cauter et al., 2008).

Intermediate sleep: stage 2 and transition to REM

The best studied form of intermediate sleep is NREM stage 2 in humans. Stage 2 is a less deep form of NREM sleep (i.e. lower arousal thresholds) than SWS and constitutes about 50% of sleep (Ohayon et al., 2004). During K-complexes and sleep spindles (see below) it is more likely for people to have no recollection of any mentation (Chellappa et al., 2011). Otherwise, mentation from early-night stage 2 commonly involves slow trains of thought (McNamara et al., 2010):

> "It was that sort of sleep in which you wake every hour and think to yourself that you have not been sleeping at all; you can remember dreams that are like reflections, daytime thinking slightly warped."
>
> — *Kim Stanley Robinson, Icehenge (Robinson, 2014)*

Throughout the night, delta activity in stage 2 sleep continuously decreases. Concomitantly, the dreams experienced during stage 2 sleep become more like REM dreams, although less bizarre, emotional, and vivid (Antrobus et al., 1995), and involving more familiar settings and characters (McNamara et al., 2010).

The hallmarks of stage 2 are K-complexes, sleep spindles, and relatively low SWA (i.e. under the 20% threshold for SWS, although the EEG is not as flat as it is during REM). K-complexes consist of large positive deflections in the EEG followed by negative deflections. They can be triggered by external stimuli such as loud noises (Riedner et al., 2011), and may in part function to prevent awakening (Halász, 2016). They strongly resemble single slow waves and are likely generated by similar mechanisms (Amzica and Steriade, 1998).

Sleep spindles are bursts of 12-16 Hz waves lasting 0.5 – 3 seconds. The amplitude of the waves within each burst typically waxes and wanes, creating the "spindle" shape. They come into two forms, fast spindles (14-16 Hz) predominating in parietal areas and slow spindles (12-14 Hz) predominating in frontal areas (Schabus et al., 2007). Spindles are generated by intrinsic oscillations within the thalamic reticular nucleus. This inhibitory nucleus modulates the rest of the thalamus (Steriade et al., 1987). During stage 2 it interacts with other thalamic nuclei to create the characteristic spindle burst, which is then propagated to cortex via thalamocortical neurons (Steriade, 2003). Both spindles and K-complexes can appear during SWS as well, and so stage 2 is primarily distinguished from SWS by a lack of SWA.

The amount of stage 2 does not change across the night. Spindle expression, however, is slightly suppressed during SWS (Uchida et al., 1991; Himanen et al., 2002), and is highest in the first 1-2 sleep cycles. Stage 2 may be involved in motor learning (Walker et al., 2002), a role that is particularly associated with fast spindles in motor cortex (Schabus et al., 2007; Tamaki et al., 2008). The function of the slow spindles in frontal cortex is less clear, nor is any specific function associated with the general non-REM low-SWA brain activity that makes up most of stage 2.

The relative amount of stage 2 increases with age, as REM and SWS decrease (Ohayon et al., 2004). Spindles have been observed in most mammalian species and never in birds. Because stage 2 is almost never characterized outside of humans, its evolutionary origins remain a mystery.

Another form of intermediate sleep called transition to REM (TR) has been characterized in rats and cats (Gottesmann, 1996). It comprises a combination of spindle activity, mixed REM- and NREM-like EEG, and a REM-like decrease in muscle activity. TR occurs in relatively small

amounts, always immediately before or after REM episodes. Its regulation and function appear tightly linked to REM: as the amount of REM increases so does the amount of TR (Watts et al., 2012; Swift et al., 2018).

Intermediate sleep: other forms

The last form of NREM in humans is stage 1. This stage makes up very little of the night, about 5% (Carskadon and Dement, 2011). It is characterized primarily by its occurrence immediately after sleep onset, and by its lack of spindles, K-complexes, or slow waves. In humans, awake drowsiness is marked by a very distinct alpha rhythm (8 – 12 Hz) predominating in the occipital lobe. The disappearance of alpha marks the onset of stage 1. This stage is often accompanied by slow rolling eye movements in the EOG (distinct from saccadic-like rapid eye movements), and low amplitude sawtooth-shaped waves in the EEG.

People commonly report hypnagogic dreams during this period; these consist of repetitive motor or sensory experiences (McKellar and Simpson, 1954). For example, after playing Tetris for several hours a day over 60% of people reported hypnagogic imagery and music from the game (Stickgold et al., 2000b). These stage 1 dreams can be accompanied by hypnogogic muscle jerks (Weiss, 2013); it is common to experience drifting off to sleep only to be awakened by a sudden movement of one's own leg.

Sleep architecture outside of mammals: initial comments

Most nonhuman sleep studies do not differentiate between stages of NREM and, confusingly, often use the terms NREM and SWS interchangeably. This has led to a relative dearth of information on intermediate sleep, especially on features beyond spindle activity. In birds, who

do not have spindles, this terminology resulted in the impression of NREM as a homogeneous state exclusively characterized by slow wave activity. As will be shown later, this is not accurate.

Songbirds as a model organism

> "The sounds uttered by birds offer in several respects the nearest analogy to language, for all members of the same species utter the same instinctive cries expressive of their emotions… but the actual song, and even the call-notes, are learnt from their parents or foster-parents."
>
> *— Charles Darwin, The Descent of Man p 86 (Darwin, 1882)*

Songbirds are experts in vocal learning. This is a relatively common skill in birds that is shared with parrots and the dull-colored hummingbirds (Nottebohm, 1972), but in mammals outside of humans is generally considered to be well-established only in cetaceans (Janik, 2014), with some evidence for vocal learning in pinnipeds (Reichmuth and Casey, 2014), bats (Knörnschild, 2014), mice (Portfors and Perkel, 2014) and elephants (Stoeger and Manger, 2014). There are no known vocal learners outside of higher vertebrates. Accordingly, songbirds have evolved brains that are highly devoted to song. Song learning is therefore an ethologically relevant behavior, one that is complex and woven into development. It bears many parallels to human language learning (Doupe and Kuhl, 1999). Young birds must first memorize the song of their adult tutor and then learn to produce it themselves (Marler and Tamura, 1964; Nottebohm, 1970) during two critical periods (**Figure 1.2**).

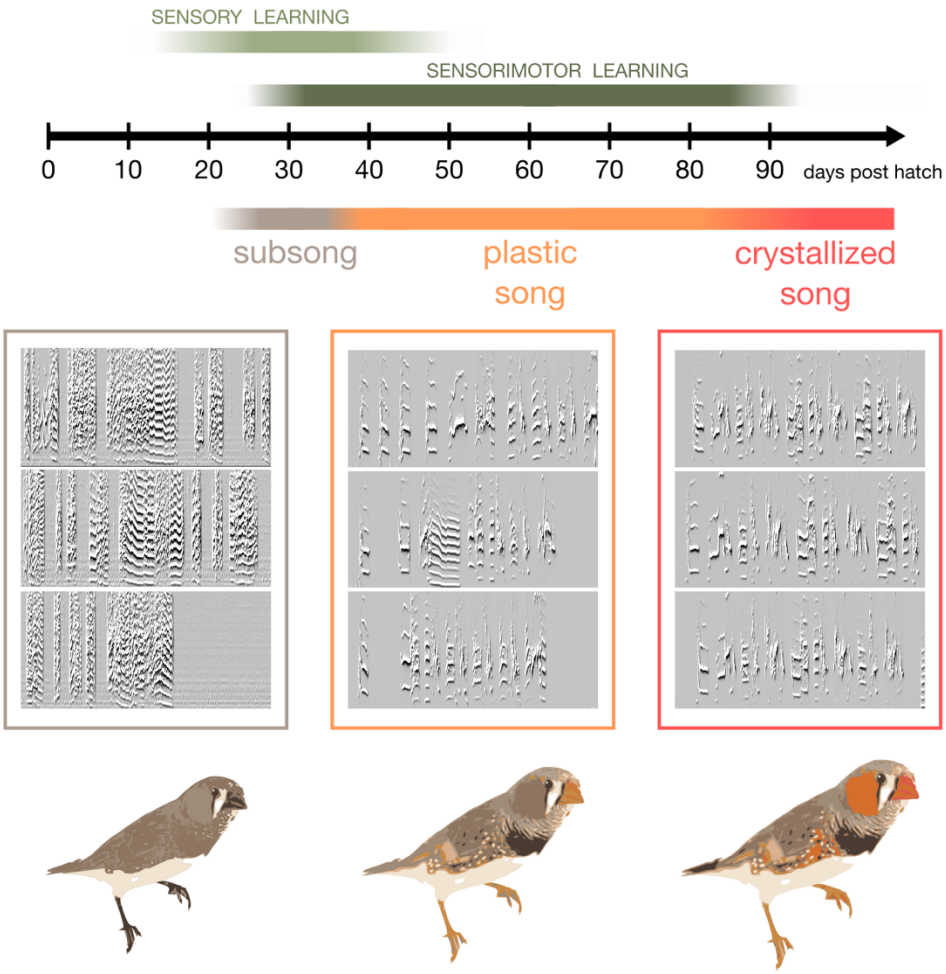

Figure 1.2. Stages of birdsong learning in zebra finches. Top: green bars indicate ages of the critical periods for the two phases of learning. Brown/orange/red bar indicates progression of the song. By 90 days post hatch, the male zebra finch song has crystallized and birds are sexually mature adults. Bottom: Three examples each of subsong, plastic song, and crystallized song from the same bird are shown as spectrograms.

In zebra finches, the songbird species most commonly studied in the lab, these critical periods overlap (Böhner, 1990). The phases of behavior include first subsong, a babbling phase (Thorpe, 1958).

> "The first attempts to sing 'may be compared to the imperfect endeavor in a child to babble.'"
>
> *— Charles Darwin, The Descent of Man p 86 (Darwin, 1882)*

Juvenile birds then progress to plastic song, a phase of imitation, rehearsal, and gradual improvement requiring auditory feedback (Konishi, 1965; Tchernichovski, 2001).

> "The young males continue practicing… for ten or eleven months. Their first essays show hardly a rudiment of the future song; but as they grow older we can perceive what they are aiming at."
>
> *— Charles Darwin, The Descent of Man p 86 (Darwin, 1882)*

Finally birds achieve crystallized song, a phase involving active maintenance using auditory feedback (Nordeen and Nordeen, 1992; Leonardo and Konishi, 1999). Deafened juveniles cannot learn to sing, and deafened adults will eventually start to exhibit deterioration of their song. It was originally thought many adult species do not require feedback to maintain adult song (Konishi, 1963) but this may be less common than originally presumed.

Some bird species such as mockingbirds, starlings and many more continue to learn into their adulthood, and imitate new songs as well as other sounds in their environment (Hindmarsh, 1984). Others, such as canaries, go through seasonal cycles of learning, adding new syllables to their repertoire in time for each breeding season (Nottebohm et al., 1986). Species such as zebra finches, in contrast, are closed-ended learners, forming their repertoire as juveniles and maintaining it via active auditory feedback throughout adulthood (Immelmann, 1969) . Older adult zebra finches are less sensitive to disruption of auditory feedback than are younger adult zebra finches (Lombardino and Nottebohm, 2000). Zebra finch males learn only one song, which they use primarily for courtship (Morris, 1954). Along with their ease of captive housing, breeding, and strong proclivity to sing in response to females even under laboratory conditions, this makes zebra finches a convenient model organism, albeit like any songbird species only reflecting a limited range of the breadth and complexity of birdsong learning.

The songbird brain

The song system, a network of brain regions that support singing and song learning (**Figure 1.3**), is highly developed and well characterized, a set of specialized and cytoarchitectonically distinct structures and pathways that arise from a general reptile-bird plan of forebrain organization (Ulinski and Margoliash, 1990). Some of its components resemble specializations that have formed in the human brain but are not present even in nonhuman primates. One example is the nucleus robustus of the arcopallium (RA), which will be of particular importance going forward.

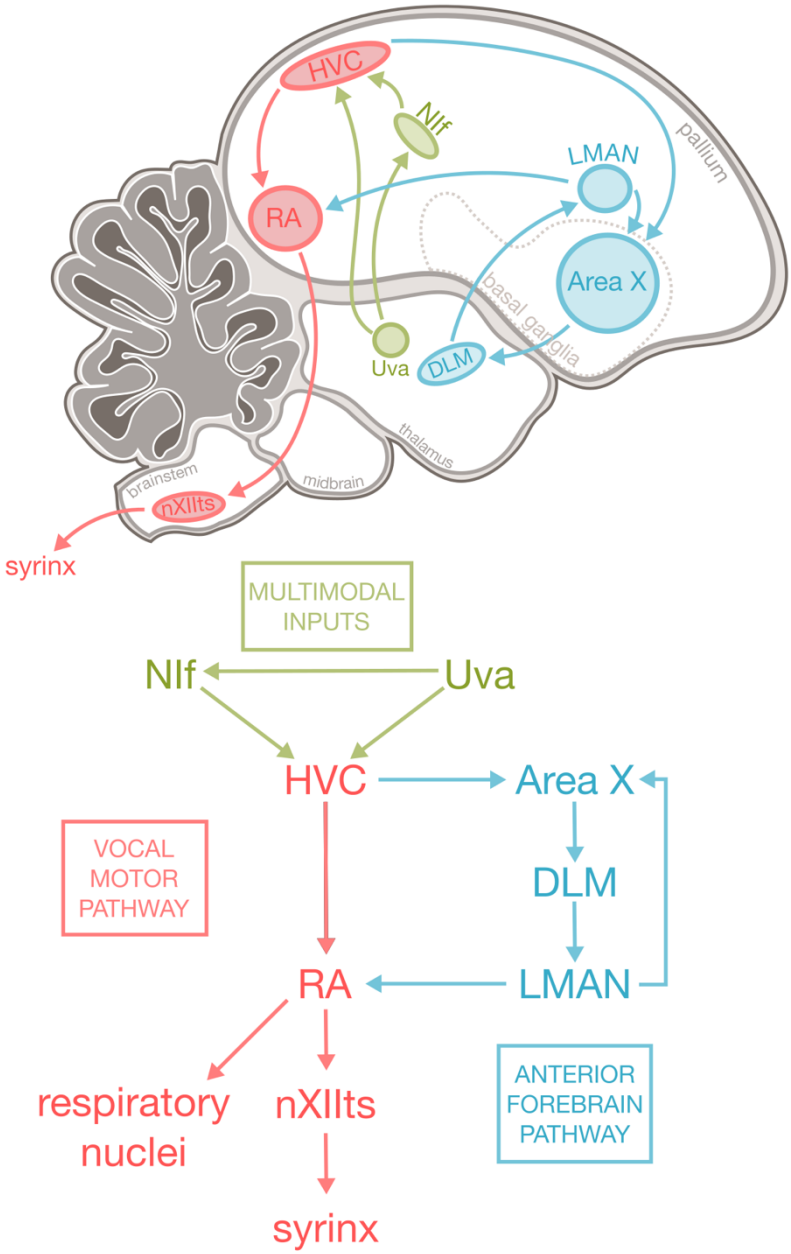

Figure 1.3. The song system. Top, diagram of key song nuclei. The vocal motor pathway is indicated in red, the anterior forebrain pathway in blue, and multimodal input and brainstem feedback to HVC in green. General brain regions are indicated in grey. Bottom, circuit diagram.

RA, itself a pallial structure, receives input from other telencephalic song nuclei, is necessary for singing, and projects directly to brainstem motor neurons (Nottebohm et al., 1976; Wild, 1993), making it analogous to the layer 5 neurons of the mammalian motor cortex (Simonyan,

2014). These outputs carry instructions destined for the respiratory muscles and the syringeal muscles controlling the song (Wild, 1993). In the ventral subdivision of RA, the projection neurons synapse directly onto motor neurons in the tracheosyringeal nucleus (Nottebohm et al., 1976; Vicario, 1991). Such a monosynaptic connection from primary motor cortex to motor neurons is rare, developing only when extraordinary dexterity, control, and speed is required (Shapovalov, 1970). The human laryngeal motor cortex is one of the few examples: it projects monosynaptically onto brainstem motor neurons that control the larynx (Wild, 1993). More than that, laryngeal motor cortex and RA share specific patterns of gene expression which are not present in the closest brain areas of either nonhuman primates or non-songbird birds (Pfenning et al., 2014). In the dorsal subdivision of RA, the projection neurons synapse directly onto brainstem respiratory nuclei. These brainstem nuclei control respiration and also give rise to feedback projections via a projection to Uva (**Figure 1.3**).

RA's projection neurons have a uniquely stereotyped pattern of activity. Zebra finch songs vary over multiple temporal scales of analysis, but most compelling are motifs, comprising sequences of syllables (distinct continuous vocalizations separated by 10-50 ms of silence), with syllables comprising sequences of notes. During song, each RA neuron fires a series of bursts, each precisely timed to a note of the song (Yu and Margoliash, 1996) – on average 12 bursts per neuron per motif (Leonardo and Fee, 2005). In adults with a crystallized song, both the firing pattern and the resultant behavior are almost exactly the same every time the bird sings; any fluctuations are on a submillisecond time scale (Chi and Margoliash, 2001). When the bird is not singing, RA neurons fall back into a tonic mode, firing at a highly consistent rate somewhere between 20 and 40 Hz. Both in advance of singing and following its termination, there are periods of transition with distinct characteristics (Yu and Margoliash, 1996). On an audio

monitor the rhythmic spikes of an RA neuron sound like the blades of a helicopter spinning. This tonic firing is probably a result of intrinsic oscillations in the membrane voltage (Mooney, 1992; Liao et al., 2011) and resembles patterns found in mammalian layer 5 motor cortex (Stafstrom et al., 1984). For unknown reasons it is faster when the bird is awake and slower when he is asleep (Dave et al., 1998).

Why study sleep in birds?

Birds provide an important test case for many of the hypotheses generated by the sleep field. Sleep and memory have been extensively studied in mammals, but sleep is evolutionary ancient and its proposed functions should be broadly distributed. Conversely, if there are features of sleep that are specific to mammals, these are valuable to identify, which can only be achieved by comparative studies. Moreover, birds possess a dramatically different gross forebrain organization (Reiner et al., 2004) and yet they resemble mammals in the specialized nature of their sleep (Klein et al., 1964; Low et al., 2008; Rattenborg et al., 2009), their higher-order cognitive abilities (Emery and Clayton, 2004; Gentner et al., 2006; Spierings and Cate, 2016; Kabadayi and Osvath, 2017), and the underlying circuitry of their brains (Reiner et al., 2005; Dugas-Ford et al., 2012; Dugas-Ford and Ragsdale, 2015). Are there qualities of complex sleep that are necessary for the learning of complex skills? Is the evolution of specialized sleep related to the evolution of neural circuitry and learning capacity? Or is this relationship in some ways unique to mammals?

Within mammals, approaches to this question have diverged to some extent. Many of the early studies on sleep function involved total or REM-only sleep deprivation, both of which induce large amounts of stress especially in nonhuman subjects who are not voluntarily sleep

depriving themselves (Maquet, 2001). The behavioral studies that have been conducted on rodents tended to focus extensively on REM, finding few effects of NREM (Smith, 1985), and often used appetitive/avoidance conditioning tasks (Horne and McGrath, 1984; Smith, 2011). Therefore, studies of what sleep actually does has arguably been most carefully examined in humans (Maquet, 2001). While very early human studies used declarative memory tasks (Jenkins and Dallenbach, 1924), much of the recent behavioral literature has focused on motor learning (Smith and Macneill, 1994; Walker et al., 2002; 2003; Kuriyama et al., 2004; Morin et al., 2008) or other forms of hippocampal-independent memory (Karni et al., 1994; Smith, 1995; Stickgold et al., 2000a; Gomez et al., 2006).

On the other hand, mechanistic studies – how sleep carries out its functions — tend to concentrate on the hippocampus and its role in spatial learning (Pavlides and Winson, 1989; Wilson and McNaughton, 1994; Skaggs and McNaughton, 1996; Poe et al., 2000; Louie and Wilson, 2001). The songbird model provides a way to further understand the contribution of sleep to motor learning, linking brain and behavior. Finally, the zebra finch model exhibits compelling examples of sleep and memory phenomena, and with evolutionary implications, also motivating this as a model species.

In the sections following I will discuss what is known about the functional impacts of sleep on memory, first in birds and then in mammals. I will then focus on sleep replay as a key potential mechanism undergirding these effects.

Functional effects of sleep on memory: songbirds

Memory encoding and initial learning

Juveniles: Sleep-dependent deterioration

In many experiments, access to the tutor song is delayed until birds have entered the critical period for sensorimotor learning. This means that the bird is simultaneously memorizing the tutor song and attempting to copy it; thus, any learning is reflected in measurable behavior (Derégnaucourt et al., 2005; Shank and Margoliash, 2009).

Each day as juveniles practice, their song becomes slightly better (Tchernichovski, 2001). One useful measure to capture this behavior is entropy variance (EV). Entropy measures of the complexity of a given power spectrum, and EV as used here quantifies how this metric fluctuates over the course of a single syllable (O and P, 2002). For many song syllables, EV goes up as they become more adult-like and complex (Derégnaucourt et al., 2005). Accordingly, EV of certain syllables was found to increase over the entire course of development as well as over the course of a single day. But a compelling observation was that EV decreased significantly over nights of sleep, especially in younger birds. Although this seems like a form of regression, it was ultimately beneficial: birds with the most dramatic overnight drops in EV also grew up to form the best copies of tutor song (Derégnaucourt et al., 2005). Thus, song development is characterized by daily increases in song complexity that is lost following nighttime sleep.

What causes the overnight deterioration in song? Through a series of control experiments researchers showed that the cause was sleep itself (Derégnaucourt et al., 2005). Deterioration was not the result of sleep inertia: if birds were prevented from singing for several hours after they woke up, the first songs they sang after that had still deteriorated. Deterioration did not

result from lack of practice for a prolonged amount of time: if birds were prevented from singing or sleeping for long periods in the middle of the day, the deterioration did not re-emerge. Deterioration was not a strictly time-of-day (circadian) effect: if birds were given melatonin in the middle of the day to induce napping, upon wakening the deteriorated songs re-appeared. (As melatonin is a powerful circadian hormone in birds (Cassone, 2014), this experiment may not completely rule out circadian effects; a further control would be to administer melatonin but keep birds awake, but this was not reported.) Thus, it appeared that sleep specifically led to overnight "worsening" of song, which was advantageous to the bird's overall learning. Thus, song learning does not proceed in a monotonic increase towards a final target. We will refer to this overnight worsening as sleep-dependent deterioration (SDD). It remains to be seen if such extensive structured variation in learning is observed during development of other learned sensorimotor tasks, and whether this is limited to sensorimotor tasks.

Reciprocal interactions of experience, behavior, and sleep

Further examination of the initiation of song learning also revealed a curious interesting first-night effect of sleep (Shank and Margoliash, 2009). On the first day the juveniles heard the tutor song, they showed only small amounts of change in their own singing behavior. But the next day saw a sudden shift in behavior, reflecting as a jump in EV, as the young bird began to imitate adult song in earnest. During this first night, neurons in RA began to exhibit spontaneous bursting for the first time. The structure of bursting appeared to depend on which tutor song the bird learned. Removing auditory feedback, either through muting or temporary deafening, prevented both the sleep bursting and the change in song behavior (Shank and Margoliash, 2009). This suggests that initial plastic song is facilitated by a combination of tutor song access, auditory feedback, and sleep. Spontaneous bursting in RA, plausibly the juvenile form of replay,

could be a systems-level manifestation driving this sleep-dependent developmental change in behavior.

Song maintenance

So far we have discussed sleep effects during the early phases of learning and consolidating memories. What about adult songbirds, who have learned and crystallized their song?

Adults: ultradian changes in song

In adult birds, the song changes very little overall and overt SDD is not apparent (Derégnaucourt et al., 2005). However, adult song does undergo subtle changes over the course of the day. Individual RA neurons, which fire bursts that are precisely correlated with the song, exhibited an increase in inter-burst intervals over the day. This neuronal drift was reflected in temporal drift in the song (Chi and Margoliash, 2001; Glaze and Troyer, 2006). Because the song is stable over long time periods, these daily changes are presumably reversed overnight. Another daily pattern was found at the level of individual harmonic syllables. The pitch and amplitude both increased over the morning, peaked at midday, and decreased over the afternoon (Wood et al., 2013). Across the morning, pitch increased faster if the day's starting pitch was especially different from the weekly average. This study did not assess overnight changes, but this would imply that after sleep periods, the syllable's pitch tends to differ from its normal value (Wood et al., 2013). Alternatively, the evening decrease in pitch may simply be sustained until the next morning. The circadian system acting via melatonin is almost certainly involved in some of these daily changes (Derégnaucourt et al., 2012; Wang et al., 2012), although it should be pointed out that the effects of sleep and melatonin are particularly difficult to disentangle in birds. Manipulations such as pinealectomy or constant light will affect both melatonin (Derégnaucourt

et al., 2012) and sleep (Berger and Phillips, 1994), while administering melatonin will induce sleep (Phillips and Berger, 1992) while also carrying circadian signals (Cassone, 2014).

Adults: sleep-dependent changes in motor coding

Single RA neurons were recorded during singing before and after sleep periods (Rauske et al., 2010). The overall structure of a neuron's song activity stayed very stable, but sleep caused subtle alterations. Individual bursts changed structure slightly, sometimes gaining spikes but most often losing spikes. These changes appeared in about half of the neurons and 20% of the total bursts recorded. Far fewer changes were found across periods of wakefulness. The source and timing of when spikes are added to overall RA activity remains unresolved. Given that the population of RA-projecting HVC neurons is undergoing significant neurogenesis in the adult (Goldman and Nottebohm, 1983), there may be specialized mechanisms related to neurogenesis for how spikes are added to RA, and these may vary by species depending on learning strategies (Walton et al., 2012).

Consolidation and reconsolidation

Perceptual learning

Sleep also has powerful effects on the perception of song in birds; this was demonstrated most thoroughly in starlings. In this paradigm starlings are first trained on a baseline go-no-go task, then presented with novel sets of conspecific song which they had to learn to categorize (Brawn et al., 2013). In the wild, this might be analogous to birds learning which member of their flock sings which songs.

Consolidation and interference

If trained on a single set of new stimuli and retested, either later the same day or the following morning, starlings maintained high performance across both wake and sleep. But when starlings had to learn two different sets in one day, upon retest in the evening they became markedly worse at both tasks. This indicated interference between competing memories. However, if retested on either set the next morning, starlings completely recovered their performance. Sleep therefore reversed the effects of both proactive and retroactive interference (Brawn et al., 2013). This pattern closely resembles one found in human studies of motor (Brawn et al., 2010) and speech perceptual learning (Fenn et al., 2013).

Cycles of reconsolidation

After sleep, a memory learned on a previous day was also resistant to the effects of further interference and did not benefit from additional nights of sleep (Brawn et al., 2018). But retesting of the memory could make it labile again and therefore susceptible to interference from other task learned the same day. Another night of sleep would reconsolidate the memory. Multiple cycles of reconsolidation were found to slowly improve performance over many nights (Brawn et al., 2018).

Summary

Birdsong learning and sleep interact at several points. In young zebra finches who are learning to sing, sleep benefits song learning by causing their song to deteriorate, possibly increasing motor exploration. Likewise, learning experience affects brain activity during sleep. In adult starlings who are learning to associate actions with particular song stimuli, sleep reinforces memory consolidation and reconsolidation, reversing the effects of interference. Even

in adult zebra finches, who have already learned their song, sleep causes subtle changes in their singing and the motor activity associated with their song.

How does this compare with functional effects of sleep in mammals? Some of the songbird results are remarkably similar, such as the starling experiments on perceptual learning (Brawn et al., 2013; 2018). In these experiments starlings are capable of learning a new set of stimuli within a single day, which closely resembles the paradigms used in human and rodent studies. In contrast, the zebra finch findings engage with a long-term, complex type of learning rarely studied outside of songbirds. Anecdotal observations in humans are germane here, however: it is a common experience for an athlete or musician to practice a difficult move or passage with limited success in one session and experience sudden improvement by the next session. Such changes are likely to result from offline learning mechanisms.

Sleep and memory in mammals

Studies in mammals have made central contributions to our understanding of sleep in memory. This is an exceedingly large body of work that has tested a vast breadth of types of memory and for a few tasks there have been many different populations and task variants examined. In general, these studies confirm an overall pattern of sleep dependent effects on memories. But in addition, the well-established characterization of sleep in mammals has been leveraged to tie behavioral effects to specific stages of sleep and in some case, specific oscillations and neural events therein.

The distinction between declarative and procedural memory will become highly relevant in this field. Declarative memory – that pertaining to specific events, facts, objects and locations – depends on the hippocampus. In contrast, procedural or nondeclarative memory includes motor

skills, perceptual learning, and generally "how" to do something; this type of learning relies on circuits largely independent of the hippocampus. While the distinction is not absolute, it was demonstrated in dramatic fashion. This view was promoted by studies of the famous patient H.M., who underwent bilateral hippocampus removal to treat his epilepsy, retained old memories of his experiences, but could not remember the few years preceding his surgery and could not form new declarative memories (Milner et al., 1968). However, he could learn new procedural skills perfectly well, leading to strange situations in which he had mastered a difficult ability such as mirror tracing but could not recall having ever learned it (Corkin, 1968). One wonders what his sleep looked like, and how it affected his capacity for procedural learning.

Functional effects

In 1924 researchers set out to resolve a mystery discrepancy in the findings of Hermann Ebbinghaus, the pioneer in the field of learning and forgetting. Ebbinghaus reported in 1885 that the rate of forgetting was very fast at first and then slowed down as a function of time (Ebbinghaus, 1912). But between the intervals of 8.8 hours and 24 hours, forgetting seemed to halt almost completely. Ebbinghaus considered, but dismissed, the idea of sleep as an explanation; he assumed he had made a mistake with his experimental methods. But as it turned out, Ebbinghaus had underestimated himself. Jenkins and Dallenbach (Jenkins and Dallenbach, 1924) had two beleaguered college students memorize series of nonsense syllables, and then at random intervals — day and night — had them repeat back the syllables from memory. For several months the students and the first author lived in a makeshift dormitory next to the lab. Either in the morning or just before bed, the students memorized a new list. At night, every few hours the first author woke up to his alarm clock and went to shake the students awake to recall the syllables. The routine became harrowing: "After a few experiments [he] found it difficult to

arouse the [students] and difficult to know when they were awake. [They] would leave their beds, go into the next room, give their reproductions, and the next morning say they remembered nothing of it." But it paid off: despite the midnight awakenings, the students remembered far more over intervals of sleep than of wake — during sleep, the rate of forgetting leveled off almost completely. These differences fully explained the variation in the results of Ebbinghaus, bringing together the fields of sleep and memory.

REM and sleep deprivation

After the discovery of REM in 1953 (Aserinsky and Kleitman, 1953), fascination with this new stage of sleep abounded and the question of memory resurfaced. Selective sleep deprivation became one of the most popular techniques for examining this question. For example, study participants were deprived of either REM or stage 4 and tested on lists of words, sentences or stories (Empson and Clarke, 1970; Tilley and Empson, 1978). In most of these experiments, REM emerged as the critical stage for learning. A large number of studies in rats tested the effects of sleep deprivation on fear conditioning and various operant tasks (Smith, 1985) and almost invariably found effects of REM; conversely, the experience of learning seemed to increase the amount of REM afterward (Smith, 1995). However, more recent studies employing selective sleep deprivation (Plihal and Born, 1997) have found SWS to be far more important and have questioned any role of REM in declarative memory per se.

In the 1990s, most experiments on sleep and learning focused specifically on procedural memory. For example, REM deprivation impairs visual texture discrimination, a form of perceptual learning wherein participants have to quickly pick out a visual pattern that differed from a field of other patterns (Karni et al., 1994; Stickgold et al., 2000a). Sleep deprivation also negatively impacts motor learning, such as a rotor pursuit task in which participants followed a

moving light with a stylus in their non-dominant hand (Smith and Macneill, 1994). Another decrement was found for mirror tracing (Plihal and Born, 1997). Both rotor pursuit and mirror tracing rely on procedural learning abilities that remained intact in H.M. (Corkin, 1968) and other patients with removed or damaged hippocampi (Gabrieli et al., 1993).

The sleep deprivation technique, while powerful, is also a messy one. Total sleep deprivation introduces a number of physiological stressors and cognitive disturbances. REM deprivation, which in animals involves falling into water multiple times throughout the sleep period, is likewise imprecise. And there is no good equivalent of REM deprivation for NREM. Stage 4 deprivation leaves large amounts of SWS (stage 3) intact as well as plenty of covert SWA during stage 2. Moreover, the body seems to prioritize SWS homeostasis so highly that any attempts at total SWA deprivation without affecting other types of sleep will inevitably become futile as the SWS drive ramps up. Thus, it is difficult to make any firm conclusions on the basis of sleep deprivation alone.

The Motor Sequence Task

Later studies began to dispense with sleep deprivation, instead showing a direct benefit of normal sleep on learning. One of the most widely used tasks is known as the finger tapping task or Motor Sequence Task (MST). Participants must learn to quickly type a sequence of numbers with their non-dominant hand. In the original landmark MST study, researchers found that a night of sleep improved participants' typing speed without compromising accuracy (Walker et al., 2002). An equivalent 12-hour period of wake had no such benefit, and circadian effects were also ruled out by administering training and test sessions at various times of day. This effect has been confirmed multiple times, and has been shown to interact with age, initial performance (Wilhelm et al., 2012), and task complexity (Kuriyama et al., 2004).

This result came under fire when another lab showed a fatigue effect — if participants were allowed longer rest periods between trials, performance was greatly improved by the end of training compared to the original MST studies (Rickard et al., 2008). This improved post-training performance was now concomitant with performance the next morning, abolishing the apparent performance enhancement and leading to the conclusion that sleep had no effect on motor memory. Curiously, however, Rickard et al. did not test for a sleep effect. The discrepancy was resolved by a study that employed careful controls (Brawn et al., 2010). The original training block was used alongside a retest five minutes later to assess the effects of fatigue within-subjects. Relative to the end of the training block, performance increased at this retest. But when participants were tested again in the evening, their performance declined again (the test missing from the Rickard et al. study). Then in the morning, they rebounded to the original retest levels. Finally, after this night of sleep, performance became immune to further erosion by daytime wakefulness. Thus, sleep was not enhancing the motor memory, but it was stabilizing it and restoring it to original post-training levels.

Language learning

Sleep affects multiple types of memory related to language learning. After a nap, infants were better able to recall abstract patterns of an artificial language both immediately afterward (Gomez et al., 2006) and 24 hours later (Hupbach et al., 2009). In toddlers with Down syndrome, poor sleep quality was associated with deficits in language abilities (Edgin et al., 2015). Sleep-disordered breathing, which worsens sleep quality, was also shown to negatively impact language abilities in older children (Honaker et al., 2009). In adults, sleep led to consolidation of speech recognition learning, including generalization wherein participants were better able to recognize new words they had never encountered during training (Fenn et al., 2013).

Does sleep affect learning independent of the hippocampus?

The link between sleep and declarative learning, now well established, is often tested with word-pair association tasks in which participants memorize unrelated pairs of words (Plihal and Born, 1997). A variant involves memorizing an association between a word or picture and a specific location on a computer screen (Shanahan et al., 2018). So strong are these results that some have ascribed sleep effects on procedural learning to concomitant hippocampal-dependent processes (Song et al., 2007; Vorster and Born, 2015). For example, during the MST participants could improve their performance by memorizing the sequence of numbers they are typing (although during the task, the sequence is continuously displayed on the screen).

There is some evidence that the hippocampus does participate in procedural tasks. For example, overnight consolidation on an oculomotor sequence task was related to BOLD responses in both the hippocampus and the striatum (Albouy et al., 2008). However, most of the evidence for hippocampal participation comes from a procedural task known as the serial reaction time task (SRTT) which has both an implicit and an explicit version. Several studies have found a sleep benefit for the explicit but not the implicit version of the task, in which the participant is not aware of the sequence being learned (Robertson et al., 2004; Spencer et al., 2006; Song et al., 2007; Nemeth et al., 2010). This has been used to argue that any sleep benefits on procedural memory can be entirely ascribed to hippocampal effects.

But this seems outweighed by the preponderance of evidence for sleep effects on many other forms of procedural learning, the ability of persons who entirely lack a hippocampus to learn such tasks, and the double dissociation between sleep effects on declarative versus procedural tasks (Dresler et al., 2011a). Furthermore, it has been shown that overnight improvement on the MST is inversely related to participant's ability to recall the sequence (Galea et al., 2010).

Sleep correlates of procedural memory

It was recognized early on that different types of sleep might have different roles when it comes to memory. This seems to have been affirmed, for example in patient populations in whom sleep-dependent effects are selectively impaired for procedural memory but not declarative memory (Dresler et al., 2011a).

An early hypothesis held that SWS consolidated declarative memory, while REM consolidated procedural memory (Plihal and Born, 1997). But since then a more complicated picture has emerged. For example, perceptual learning was correlated with both early-night SWS and late-night REM (Stickgold et al., 2000a). Administering SSRIs to suppress REM in healthy volunteers caused an increase in sleep-dependent benefits of skill learning (Rasch et al., 2009). Conversely, in rodents, suppressing the hippocampal theta rhythm during REM led to an impairment in declarative memory consolidation (Boyce et al., 2016).

Sleep spindles

A few overall conclusions have emerged after decades of study. One of the more secure associations is between motor learning and spindles. The original MST study reported a correlation of overnight improvement with the amount of stage 2 (Walker et al., 2002). Learning the MST caused an increase in spindle density over the contralateral hemisphere (Nishida and Walker, 2007). When patients learned to selectively increase activity at one ECoG electrode in M1, sleep spindling later intensified at that electrode (Johnson et al., 2012). Patients with schizophrenia, who have far fewer spindles than controls (Ferrarelli et al., 2007; Wamsley et al., 2012), also lack overnight improvement on the MST (Manoach et al., 2004) and this deficit was correlated with late-night stage 2 (Manoach et al., 2010). Increasing spindle activity with transcranial alternating current stimulation enhanced overnight improvement on the MST

(Lustenberger et al., 2016). Such results cast suspicion on studies that use SSRIs or SNRIs to suppress REM; in one such study these compounds increased stage 2 and fast spindles (Rasch et al., 2009) which could explain the intact or improved procedural memory effects, independent of any REM-related effects.

REM

An association between REM and emotional memory consolidation has become well-established (Nishida et al., 2009; Walker and van Der Helm, 2009; Gujar et al., 2011; van der Helm et al., 2011). But the evidence for the involvement of either REM or SWS in procedural memory is less consistent.

The structure of REM muscle twitches may play an important role in motor learning during development (Blumberg et al., 2013). In rats, learning an avoidance task causes an increase in the characteristic PGO waves of REM; this task, however, is difficult to classify as it relies on both hippocampal and non-hippocampal regions (Datta, 2000). If rats are deprived of REM their performance worsens, but this is rescued by activation of the PGO wave generator in the pons (Datta et al., 2004). Cueing of a motor task during SWS improves performance on the cued (but not the uncued) version of the task. The performance gain was associated with an increased BOLD response to the cued sequence in cerebellum and cortex – but the magnitude of this change was associated with time in REM (Cousins et al., 2016).

Slow waves

Slow wave activity is broadly thought to be an important mechanistic component of declarative and spatial learning, both processes which are strongly hippocampus dependent (Marshall et al., 2006; Rasch et al., 2007). But the case for motor learning and SWS is perhaps

least clear. The cueing study described above also found that task performance scaled with an increased BOLD response in the hippocampus and caudate, which was correlated with time in SWS and in N2 (Cousins et al., 2016). But given that the cueing was performed during SWS, it is difficult to draw any definitive conclusion from this. A pharmacologic study in rats used SNRIs to suppress both REM and the spindle-rich stage of transition to REM (TR). This increased rats' performance on a procedural learning task, and this increase correlated with SWS (Watts et al., 2012). But as noted before, spindles are key for procedural learning, the stage of TR is extremely short, and the amount of TR is more related to the number of REM episodes than it is to spindle activity (Gottesmann, 1996). Thus, most spindle activity in rats still occurs during SWS, suggesting the correlation with SWS can be ascribed to spindles.

Some of the strongest evidence for SWS involvement came from a study where participants learned to adapt to rotational forces while reaching – an implicit learning task with a sleep dependent effect and with a control version that involves similar movements but no learning (Huber et al., 2004). Because this task is both motor and implicit, it is particularly likely to be hippocampal-independent. Learning the task resulted in an increase in local SWA in multimodal parietal areas known to be active during learning but not during the non-learning version of the task. However, the study used high density EEG, which is uncomfortable enough that the cap is removed after the first 2 hours of sleep (Huber et al., 2004). Very little REM occurs in the first 2 hours of the night (Agnew and Webb, 1973) and so REM was not examined as part of the experiment. Therefore this study supports a role for SWS in a hippocampal-independent task, but does not exclude a role of REM.

By what mechanism do specific stages of sleep affect memory?

The two leading hypotheses of how sleep affects memory both invoke slow waves. The first is the synaptic homeostasis hypothesis (Tononi and Cirelli, 2003). This posits that most synapses are potentiated during wakefulness. Sleep, and specifically slow wave activity, are thought to universally downscale synaptic strength, leading to pruning of weak synapses. Strong synapses would remain, and thereby the overall signal to noise ratio for the contribution of these synapses would increase. Much work in a multitude of systems has gone into proving this hypothesis (Cirelli and Tononi, 2015; de Vivo et al., 2017; Diering et al., 2017), although the idea has not gone unchallenged (Frank, 2012), and much of the direct structural evidence comes from flies, who do not exhibit slow waves.

Another leading idea — which is by no means mutually exclusive with synaptic homeostasis — is the systems consolidation hypothesis (Diekelmann and Born, 2010). This holds that sleep selectively potentiates important synapses and circuits. The main focus of this hypothesis is the transference of memories from the hippocampus to more permanent storage in the cortex. The key mechanism in this hypothesis is sleep replay, which I will discuss next.

Sleep replay in mammals

Hippocampal sleep replay

Discovery of hippocampal reactivation

When a rat encounters a new environment, neurons in CA1 quickly map the space by developing "place fields," or specific locations within the environment that activate particular cells. These neurons are known as place cells (reviewed in (Moser et al., 2015)). When

researchers continued to record from the same cells as the rat fell asleep, they saw something remarkable. Cells that had been active in the new environment increased their activity during sleep (Pavlides and Winson, 1989). Cells that represented similar locations in space – whose place fields overlapped in the new environment – began to fire simultaneously (Wilson and McNaughton, 1994). This was not a preexisting pattern: these cells did not fire together when the rat slept before encountering the new environment. Given that it appeared that place cells formed their receptive fields randomly, this means that during sleep the place cells' reactivations were specifically reflecting the rat's most recent experience. If there was an underlying logic hidden to researchers as to how place cells remap new environments, for example a group of cells that is selected as an already interconnected assembly to represent a new region of space, then this conclusion might need to be re-evaluated.

Sequential replay

Further study revealed that not only did cells reactivate together, they were actually replaying specific trajectories through the new environment (Skaggs and McNaughton, 1996). To see this, researchers introduced the rat into a linear track, using treats to cause him to run from one end to the other. As the rat moved through each place field on the track, a different place cell fired. This creates a stereotyped sequence of neurons firing one after another. When the rat slept, the place cells replayed this stereotyped sequence over and over. But during sleep, the sequence was usually compressed in time (Nádasdy et al., 1999), as much as 20 times faster than it took the rat to run the track in real life (Lee and Wilson, 2002). Researchers called this phenomenon sleep replay.

Replay and sleep structure

Since its discovery, the relationship of hippocampal replay to sleep structure has been extensively studied. It tends to occur during NREM (Kudrimoti et al., 1999), although one study found REM replay which, unlike the NREM replay, played out in real time (Louie and Wilson, 2001). Replay is usually time-locked to a layered set of oscillations, some local to the hippocampus and some more global. Within the hippocampus, the replay sequences appear during sharp-wave ripples (SWRs) (Kudrimoti et al., 1999; Nádasdy et al., 1999; Girardeau and Zugaro, 2011). These consist of a sharp, high-amplitude spike, or sharp wave, with a high-gamma ripple occurring at the peak. SWRs in turn are time-locked to sleep spindles (Latchoumane et al., 2017). In turn, sleep spindles tend to occur nested in the negative peaks (or UP states) of slow waves in cortex (Mölle et al., 2002; 2006; Klinzing et al., 2016). This strongly suggests that slow waves, spindles, and SWS all contribute to generating replay.

Functional effects of replay

This discovery of the many manifestations of hippocampal and cortical replay facilitated direct tests of replay's effects. Two separate groups performed an experiment to detect SWRs in real time and quickly trigger a burst of electrical stimulation to the input pathway of the hippocampus (Girardeau et al., 2009; Ego-Stengel and Wilson, 2010). This disrupted neuronal activity occurring in the hippocampus, presumably including replay events. As expected, animals suffered a decrement in their spatial learning abilities on nights following the treatments (Girardeau et al., 2009; Ego-Stengel and Wilson, 2010). This showed replay to be necessary for consolidating spatial memories.

Simultaneous extrahippocampal reactivation

As predicted by the systems consolidation hypothesis, hippocampal replay was also shown to work in concert with cortex and other extrahippocampal areas. To show this, paired recordings were combined with altered versions of the standard track-running task. For example, striking visual stimuli were placed along certain sections of the track. During sleep, hippocampal replay of those sections occurred simultaneously with increased activity in visual cortex (Ji and Wilson, 2007). In another experiment, animals ran a circular track and encountered a reward at a specific location. During sleep replay, as the place cells representing that location fired, basal ganglia neurons fired alongside them (Lansink et al., 2009). Similar experiments have been conducted in the prefrontal cortex (Peyrache et al., 2009; Wierzynski et al., 2009), in parietal cortex (Qin et al., 1997), and in association cortices (Khodagholy et al., 2017). Replay was also discovered among multiple neocortical sites in a primate model (Hoffman and McNaughton, 2002). Not only do these experiments support replay outside the hippocampus, they point to replay as carrying out a major stage of hippocampal memory consolidation: transference of memories out of the hippocampus.

Systems consolidation hypothesis

The hippocampus is heavily involved in the initial formation of declarative memories; it then stores them in the short term and slowly, over weeks, months, or even years, it transfers these memories to distributed networks across the cortex. This view was first promoted by studies of H.M. (Milner et al., 1968); since then extensive animal studies have extended this hypothesis (Marshall and Born, 2007). The systems consolidation hypothesis links the hippocampal transfer of memories to cortex occurs via sleep replay events coordinated across both areas (Diekelmann and Born, 2010). In turn, the dependence of hippocampal replay on slow waves could mean that

slow waves serve as a global signal, triggering replay events that are coordinated across disparate areas. The systems consolidation concept has also been proposed to explain sleep-development effects in memory systems outside the hippocampus, and outside mammals, e.g. navigational memory in honeybees, imprinting in chicks, and song learning in songbirds (Vorster and Born, 2015).

Reactivation in humans and cued replay

Although it is not feasible to record directly from large numbers of human place cells, the results in rodents have been more or less confirmed in humans. Sleep exerts a beneficial effect on spatial learning (Peigneux et al., 2004) and other forms of hippocampal-dependent learning, and many of these are tied specifically to SWS (Gais and Born, 2004). Imaging studies have found increased hippocampal activity in sleeping humans following virtual navigation tasks (Peigneux et al., 2004). The pattern of hippocampal SWRs, nestled in spindles, nestled in cortical slow waves, has been confirmed in depth recordings in epilepsy patients (Clemens et al., 2007). SWRs are associated with memory consolidation in humans (Axmacher et al., 2008). Enhancing slow waves with timed auditory stimulation can lead to improved sleep-dependent memory consolidation (Ngo et al., 2013).

Perhaps most interestingly, sensory cues appear to directly trigger replay events, leading to memory improvement (O'Neill et al., 2010). In sleep cueing studies, participants learn a task such as matching pictures to specific locations on a screen (Rasch et al., 2007; Rudoy et al., 2009). During the task, each stimulus is accompanied by a cue, usually a sound (Rudoy et al., 2009) or a smell (Rasch et al., 2007). For example, every time a picture of a cat appears, a meowing sound might be played. These cues are unrelated to the task at hand. When the participants went to sleep, researchers then played the cues during SWS corresponding to half of

the task stimuli. In the morning, participants had greatly improved their memories for the cued elements of the task. Importantly, cueing during quiet wakefulness had no such effect. A cueing experiment in rodents showed that the sound cues trigger replay events in the hippocampus (Bendor and Wilson, 2012). The memory benefit conferred by sleep cueing therefore seems to work by triggering replay during NREM.

Cueing during REM, however, does not appear to be effective. The efficacy of cueing might depend on the type of learning: for example, one group reported that cueing boosted "hippocampus-dependent declarative memories" but not "hippocampus-independent procedural memories" (Rasch et al., 2007). But other studies have found cueing to benefit a vast number of memory types (Batterink et al., 2017; Johnson et al., 2019), including motor memories (Schönauer et al., 2013; Cousins et al., 2016).

Other forms of replay

Are there memories that do not require the hippocampus and are those memories also expressed as replay events during sleep? Is there replay independent of hippocampal replay? This question is difficult to answer because measuring replay requires an activity pattern that is highly reproducible, stereotyped, and directly related to a specific experience or behavior. Reactivation is slightly less onerous to show, as it "only" requires an experience-dependent change in firing rate and/or correlations between multiple neurons.

A few experiments have successfully found reactivation in mammalian motor systems. One group created a neuroprosthetic paradigm allowing a task to be linked to specific cells in the motor cortex (Gulati et al., 2014). A few cells in M1 (usually four at a time) are recorded. Two of these cells are assigned as "task-related". When the animal increases the firing rate of these cells above a certain threshold, a spout is lowered and the animal has access to water. After

learning, as the rat slept, these task-related cells began to fire together, and locked their firing to slow waves. This was not true of non-task-related cells that did not increase their firing during the task. This also did not occur while the rat was awake, or in rats that were exposed to the task but had not learned it as well.

In another paradigm, rats were trained on a reach-to-grasp task using their forelimb (Ramanathan et al., 2015). This activated subsets of neurons in M1 of the corresponding forelimb, which researchers identified with principal component analysis. After learning, these M1 ensembles began to fire synchronously during sleep in a form of reactivation. Analysis of temporal patterns suggests the neurons were replay sequences of movements. In turn, sleep benefited performance on the task by increasing the rats' speed without compromising accuracy. Sleep also led to temporal shifts in the task-related neural activity: neurons more closely coupled their activity to the onset of the reaching motion. Like in the neuroprosthetic experiment, the M1 reactivations tended to time-lock with slow waves; in this case they locked to spindles as well.

However, studies in humans have implicated REM for what – unclear sentence. Participants who had learned a motor task showed increased BOLD responses during REM in task-related brain areas (Maquet et al., 2000). One ECoG study found that during phasic REM, the motor cortex activates in a pattern resembling a voluntary movement from wakefulness (De Carli et al., 2016). Studies of lucid dreamers have shown that when dreamers make hand movements during REM, the corresponding part of motor cortex activates, suggesting that motions in dreams are accompanied by a form of motor replay (Dresler et al., 2011b). Several studies of patients with sleep disorders have investigated replay in humans. One REM behavior disorder patient incorporated learned material into their sleep talking during REM (Uguccioni et al., 2013). A sleepwalking patient, after being trained on a complex sequence of hand and arm movements,

was recorded repeating part of the sequence during NREM (Oudiette et al., 2011). Therefore, a concluding sentence…

Summary: mammalian sleep replay

In conclusion, reactivation and possibly replay occurs in the motor system of mammals. Most human studies have found this to occur during REM. In contrast, rat studies found that like hippocampal replay, motor reactivation appears to be locked to slow waves and possibly spindles. Motor activity is difficult to decode in this system (perhaps resulting from lack of behavior stereotypy), making it challenging to study this replay in great detail. What motions are being replayed? How fast? What effect is replay having on behavior? What effect on neural coding? The answers may come from a different source: replay of song activity in birds.

Sleep replay in songbirds

Evoked replay

The BOS response

The song system nucleus HVC is one of two major sources of input to RA and is thought to be premotor in function. Lesioning it will completely abolish singing, even as the bird "assume[s] the posture and movements typical of song" (Nottebohm et al., 1976).

But under urethane anesthesia (Margoliash, 1983; Margoliash and Konishi, 1985) and then in awake sparrows (Margoliash, 1986), neurons in the HVC of white-crowned sparrows were found to respond to auditory stimuli, specifically the sound of the bird's own song (BOS) . The auditory responses were extremely specific for the sound of the bird's own song; HVC would not respond to the song of other birds or even the song of the bird's original tutor. BOS-selective

responses were subsequently observed in anesthetized zebra finches (Margoliash and Fortune, 1992; Margoliash et al., 1994). In 1998 this result was extended to natural sleep in zebra finches, implicating both BOS responses and complex bursting patterns of spontaneous activity that are observed in RA neurons during sleep (Dave et al., 1998).This study was the first to implicate sleep as a possible mediator of birdsong learning.

Mirror neurons?

An experiment in swamp sparrows and Bengalese finches found HVC neurons that responded to conspecific songs while birds were awake (Prather et al., 2008). These "mirror" neurons fired both when a bird sings a specific syllable type, and also when that same syllable is played back. Other syllables yielded no responses. Given that in many species examined, HVC has auditory responses in awake birds (e.g. white-crowned sparrows (Margoliash and Konishi, 1985), Bengalese finch, swamp sparrows (Prather et al., 2008)and canaries (Prather, 2013)) this mirror neuron result may obtain generally. However, obtaining positive results demonstrating the mirroring effect requires difficult recordings, and these have not been attempted in other species.

HVC wake vs sleep responses

Zebra finches are characterized by having a strong suppression of auditory responses in HVC while birds are awake — unusual among songbirds. This could be considered a puzzling result, given that the situation of the bird hearing its own song while asleep would never occur in the real world. Firstly, however, the effect is not universal. Some subtypes of HVC interneurons in zebra finches continue to respond during wake — however, the wake response is weaker and less specific to BOS than the sleep response (Rauske et al., 2003). In sleeping juvenile zebra finches, HVC was most responsive to the most recent variant of a bird's own rapidly changing song

(Nick and Konishi, 2005a). This was found as early as 35 days post hatch, which predates even the beginning of the plastic phase of song development (Nick and Konishi, 2005b). But during wake, juvenile HVC neurons responded most vigorously to the tutor song. This tutor song response peaked during the plastic song phase and diminished as the juveniles grew older and crystallized their song (Nick and Konishi, 2005b).

Evoked replay in RA

The sleep response to BOS also appears in areas downstream of HVC. The nucleus RA (Dave et al., 1998) and even the muscles of the syrinx (Young and Goller, 2012) respond, also highly selectively, to BOS. These areas completely lose auditory responsiveness during wakefulness (Dave and Margoliash, 2000). This is consistent with the finding that the projection neurons in HVC, including those that target RA, do not respond during wake (Rauske et al., 2003).

Results from RA recordings during sleep help to clarify the significance of these auditory responses, in that individual neurons show the same pattern of response to playback of the individual bird's own song as the pattern they exhibit during singing (Dave and Margoliash, 2000). Hence, the RA neurons, and presumptively the auditory response in sleeping birds throughout the zebra finch song system, can exhibit a form of fictive singing during sleep. Thus, the sleep auditory responses appear to be a unique state, distinct from wake responses. It is perhaps best described not as mirror neuron activity, but as a form of evoked replay perhaps similar to sleep cueing.

Spontaneous replay

In 2000, researchers observed spontaneously replay of song activity in single RA neurons (Dave and Margoliash, 2000). During sleep, firing in RA takes on unique characteristics. It expresses rhythmic tonic firing (but not a precisely tonic as in awake birds), with the rate of firing slowing down from its 30-40 Hz wake rhythm to 15-20 Hz during sleep. At fairly frequent intervals, RA spontaneously expresses trains of spike bursts interspersed with long silences. About 15% of this bursting activity was found to constitute song replay; the rest was not related to anything that occurred during wakefulness (Dave and Margoliash, 2000). This latter conclusion is weak, however, since in the initial study (Dave and Margoliash, 2000), analysis of replay was confined to spike activity associated with individual syllables. There are also replay events across multiple syllables (Dave and Margoliash, 2000). If one or more syllables in such a sequence had an incomplete replay "signature" then those syllables would not have been counted as replay using the measures of (Dave and Margoliash, 2000), whereas a more global analysis may have associated the entire sequence as associated with replay. By these considerations, the 15% of bursting activity that represented song replay is likely to be a lower bound.

The replay seldom covered the entire song, and sometimes bursts were replaced with a single or a few spikes. The replay could also appear slightly compressed or slightly expanded in time. But otherwise, this sleep activity bore striking resemblance to the burst patterns that these same cells fired during singing to drive the song (Yu and Margoliash, 1996; Dave and Margoliash, 2000). Simultaneous recordings of pairs of RA neurons showed that multiple cells were replaying the song at the same time (Dave and Margoliash, 2000). Thus, there is at least some coordination across the RA network during spontaneous replay, although the spatial extent, frequency, and fidelity of that coordination remains unknown.

The studies of RA replay also gained insight into the functional significance of song system BOS responses in sleeping birds (Dave and Margoliash, 2000). It was observed that BOS reliably triggered activity that was very similar to activity of the same neurons during singing — much more so than spontaneous replay itself. This suggests that playing back BOS is artificially triggering a process that occurs naturally during sleep. This has several functional implications, but a practical one is that BOS playback during sleep elicits fictive singing activity.

What is the extent of spontaneous song replay?

Replay has been directly recorded in HVC by comparing BOS-evoked activity patterns to spontaneous ones (Chi et al., 2003a; 2003b). Paired recordings of sleep bursting show that spontaneous sleep activity in RA is highly correlated with HVC as well as LMAN, the other major input to RA (Hahnloser et al., 2006). If HVC activity is inhibited the bursting disappears in both RA and LMAN.

This suggests activity is propagating from HVC to the auditory forebrain pathway (AFP), as well as to RA. The AFP consists of a pathway traveling from HVC —> Area X —> DLM —> LMAN —> RA, forming a basal ganglia-thalamo-cortical loop that is critical for learning during development and for maintaining variability in the song (Scharff and Nottebohm, 1991; Kao et al., 2005; Garst-Orozco et al., 2015; Hisey et al., 2018). Area X neurons exhibited spontaneous sleep firing that shared properties with song activity (Yanagihara and Hessler, 2011a; 2011b). Downstream of RA, the muscles in the syrinx also contract and relax in ways identical to singing behavior, again with an approximately 15% ratio of replay to non-replay activity (Young et al., 2017).

Where does the replay come from?

Researchers have examined two of HVC's inputs to look for sources of signals driving replay: the telencephalic nucleus NIf and the thalamic nucleus Uva. When NIf was inhibited during sleep, bursts in HVC interneurons were suppressed. Paired recordings showed that NIf projection neurons fired bursts just before HVC interneurons fired (Hahnloser and Fee, 2007). The Uva findings were less straightforward. Two cell types and two firing modes appeared to modulate HVC in opposite directions. When Uva neurons projecting to NIf fired in a burst mode, this enhanced bursting in HVC and RA. On the other hand, when Uva neurons projecting to HVC fired in a tonic mode, this suppressed HVC bursting. Pharmacological manipulations of Uva showed that the inhibitory effect seemed to override the excitatory one. This was true of both spontaneous bursting and BOS-evoked bursting (Hahnloser et al., 2008).

What can we conclude from this, assuming we accept sleep bursting as a proxy for sleep replay? Spontaneous song replay seems to extend throughout the song system. Modulated by Uva, it emerges as far upstream as the auditory area NIf and travels to the premotor nucleus HVC. The replay then propagates to both of HVC's targets, the aforementioned RA and to Area X in the basal ganglia. From Area X, replay travels to the thalamic DLM and from there to LMAN, which also targets RA and likely modulates the replay firing therein. RA then transmits some of this information to the syrinx muscles, causing them to contract during sleep.

Why does the bird not sing in his sleep, if the syrinx is moving? To produce sound, the bird must normally engage the respiratory muscles to push air through the syrinx in a specific pattern (Wild et al., 1998; Alonso et al., 2015). The respiratory muscles do not do this during sleep, at least not with sufficient force, although they may twitch slightly in a very subtle version of replay (Young and Goller, 2012).

What is the function of song replay?

Evidence so far

Thus far there have been no demonstrations of a direct effect of replay on either brain or behavior. Preliminary evidence in adults hints at a role of replay in changing motor coding: namely, that RA replay is actually preplay, expressing changes in burst structure that would appear once the bird wakes up and begins to sing (Rauske et al., 2010). As mentioned earlier, when juveniles are exposed to a tutor song for the first time, RA suddenly develops sleep bursting. Only after a night of sleep, during which this possible proto-replay in RA begins, does the juvenile start to dramatically change his song (Shank and Margoliash, 2009). In older juveniles, HVC bursting — again a possible form of replay — declined overnight; this decline was correlated with lower HVC activity during song the next morning, and with sleep-dependent deterioration of the song (Day et al., 2009).

Does replay have a function at all?

In all of these studies it remains unclear whether the replay is an agent of change, or merely a passive reflection of changes in the circuit mediated by other elements of sleep. For instance, (Day et al., 2009) hypothesize that sleep replay "represents a trace of synaptic enhancement that occurred during waking" and that the HVC activity decrease during and after sleep "may reflect nonspecific synaptic downscaling." But replay, especially in HVC and RA, involves very high-frequency bursting which consumes energy. Perhaps more compellingly, there is a clear role of sleep in juvenile song learning (Derégnaucourt et al., 2005), evidence that juvenile RA proto-replay bursts at night help drive changes in singing during the following day (Shank and Margoliash, 2009), evidence for a role of sleep in operantly-driven adaptive changes in adult

song (Andalman and Fee, 2009), as well as a presumptive role for sleep in normal adult song maintenance. These results do not directly address the role of replay in sleep-dependent learning, but they motivate that hypothesis, not the null hypothesis.

Why do adults have replay?

Why does replay occur in adult zebra finches, who have already learned and crystallized their song? Perhaps replay is merely a holdover from active song learning in juveniles. However, a study of HVC sleep bursting found that "putative sleep replay activity [bursting] is significantly less in juveniles when compared with adults" (Crandall et al., 2007). It seems unlikely that replay would increase in the group in which it had ceased to serve a function. The alternative is that replay is involved in maintenance of the song memory. Juvenile RA bursting could be involved in this process, as the bursting emerges just after song tutoring, but is suppressed if the bird cannot hear himself sing (Shank and Margoliash, 2009).

Replay and song maintenance

Just as a professional athlete or musician must practice constantly to maintain peak performance, an adult zebra finch sings his song hundreds of times per day even in the absence of other birds. He must practice, and he must have access to auditory feedback as he does so. If an adult zebra finch is deafened, his song does not immediately change, but slowly degrades over weeks or months (Nordeen and Nordeen, 1992). The exact amount of time this takes increases as the bird gets older (Lombardino and Nottebohm, 2000). Interestingly, this strongly resembles the effects of deafening on human speech (Waldstein, 1990).

An adult bird also undergoes song deterioration in response to certain forms of feedback. Delayed auditory feedback (DAF), a condition that causes human speakers to stutter (Lee, 1950),

first induces subtle changes to song structure (G. Fetterman, personal communication). Over days, the bird develops large-scale alterations in song syntax, including repetition of syllables (Leonardo and Konishi, 1999; Fukushima and Margoliash, 2015). In the paradigm of conditional disruptive auditory feedback, birds can be driven to shift the pitch of a single syllable (Tumer and Brainard, 2007). Once the altered feedback is stopped, birds can recover their original song, a slow process taking days. The exception to recovery may be long-term DAF; in some cases birds were never seen to fully recover their song (Leonardo, Fukushima, G. Fetterman, personal communication). Normal adult birds also exhibit small daily variations in the song itself (Chi and Margoliash, 2001; Wood et al., 2013); neither the purpose nor the cause of this is known.

Is song replay related to sleep structure?

What are the conditions that create song replay? How does sleep, a global brain state, give rise to this altered mode of firing? A few hints have emerged. HVC and RA begin to respond to BOS very quickly after the bird falls asleep (Dave et al., 1998; Dave and Margoliash, 2000). Spontaneous bursting also develops around the same time (Dave and Margoliash, 2000). This implicates NREM, as transitions from wake directly to REM are unusual.

Another group successfully found HVC responses when they defined sleep as periods with increased delta activity in the EEG (Nick and Konishi, 2001; 2005a). This lead them to conclude that "HVC response to auditory stimuli is greatest during slow-wave sleep" (Nick and Konishi, 2001); however, the study does not define or identify any type of sleep other than SWS, suggesting they mean that BOS responses are greater in SWS than during wake. In a later study, this group found no difference in spontaneous HVC firing properties between all nighttime epochs and the 16% of epochs with the highest 1 – 4 Hz activity (Day et al., 2009). This would seem to suggest that replay occurs during both SWS and other stages. Finally, a study in young

juveniles found RA bursting during both NREM and REM, with a small but significant increase in bursting during REM (Shank and Margoliash, 2009).

Thus, studies of song replay in the past have variously implicated SWS, NREM, REM, or all of the above. Further insight into this question could help connect specialized sleep states directly to circuit-level mechanisms. Alternatively, replay may dependent on mechanisms that are shared across sleep states. For example, in rats hippocampal replay can occur during either NREM or quiet wake (Foster and Wilson, 2006). Another alternative is that replay takes different forms or serves different functions depending on the sleep stage; one hippocampus study found real-time replay during REM, distinct from the highly compressed replay that occurs during NREM (Louie and Wilson, 2001).

Summary

In sum most of the work on song replay is limited to zebra finches. Song replay in zebra finches appears spontaneously but can also be evoked by the sound of the bird's own song. Perhaps only for technical reasons, it is most easily recorded in RA but it seems to reverberate throughout the song system, originating somewhere upstream of HVC. It most likely appears first in juveniles once they begin to attempt imitating a tutor song; but it continues robustly throughout adult life.

Adult birds with crystallized song must maintain that song, via an active process involving practice and sensory feedback. It seems very likely that sleep replay helps to implement this process — an exciting prospect, as maintenance is a stage of memory not commonly studied with respect to sleep. What exactly sleep replay does for song maintenance, however, is up in the air. One possibility is that it is somehow related to the overnight changes in motor coding found in RA cells (Rauske et al., 2010), although the function of these changes are likewise unknown.

Replay could drive or enhance these changes, perhaps resulting from the relatively noisy and fragmentary nature of replay and the fact that it necessarily occurs without auditory feedback (Derégnaucourt et al., 2005; Young et al., 2017). Alternatively, replay could strengthen existing circuits and actively counteract overnight changes. This would align with the hypothesized role of hippocampal replay, which is thought to selectively potentiate circuits, perhaps preserving them in the face of widespread synaptic downscaling. A third possibility is that replay could strengthen some circuits and weaken others – the song system has be shown to be capable of selectively varying certain parts of the song while keeping the rest stable (Tumer and Brainard, 2007; Ravbar et al., 2012).

The mechanisms of sleep that drive song replay have only begun to be explored, and progress here could greatly inform our understanding of sleep. As I will discuss next, birds and mammals have evolved many sleep traits in common. There are many theories of what these sleep traits do in mammals, but practically none in birds. This is partially because of a three-pronged traditional view that birds were more primitive in behavior, in brain structure, and in sleep architecture. Recent studies have overturned the first two assumptions. I will examine the evidence for the third claim, and for the related hypothesis that birds and mammals independently evolved sleep with only superficial similarities. I will then draw from more recent literature to build the case against this hypothesis.

Evolution of sleep in birds

As early as 1871 Darwin effectively predicted both REM and complex cognitive abilities in birds:

> "As dogs, cats, horses, and probably all the higher animals, **even birds have vivid dreams, and this is shown by their movements and the sounds uttered**, we must

admit that they possess some power of imagination."

— Charles Darwin, p 74 (Darwin, 1882)

Confirmation of this remarkable insight would have to wait until after the discovery of REM itself (Aserinsky and Kleitman, 1953).

The traditional view: rudimentary REM

The very first study of avian sleep architecture found something remarkable: birds have REM and SWS much like mammals (Klein et al., 1964), despite being separated by over 300 million years of evolution (**Figure 1.4**).

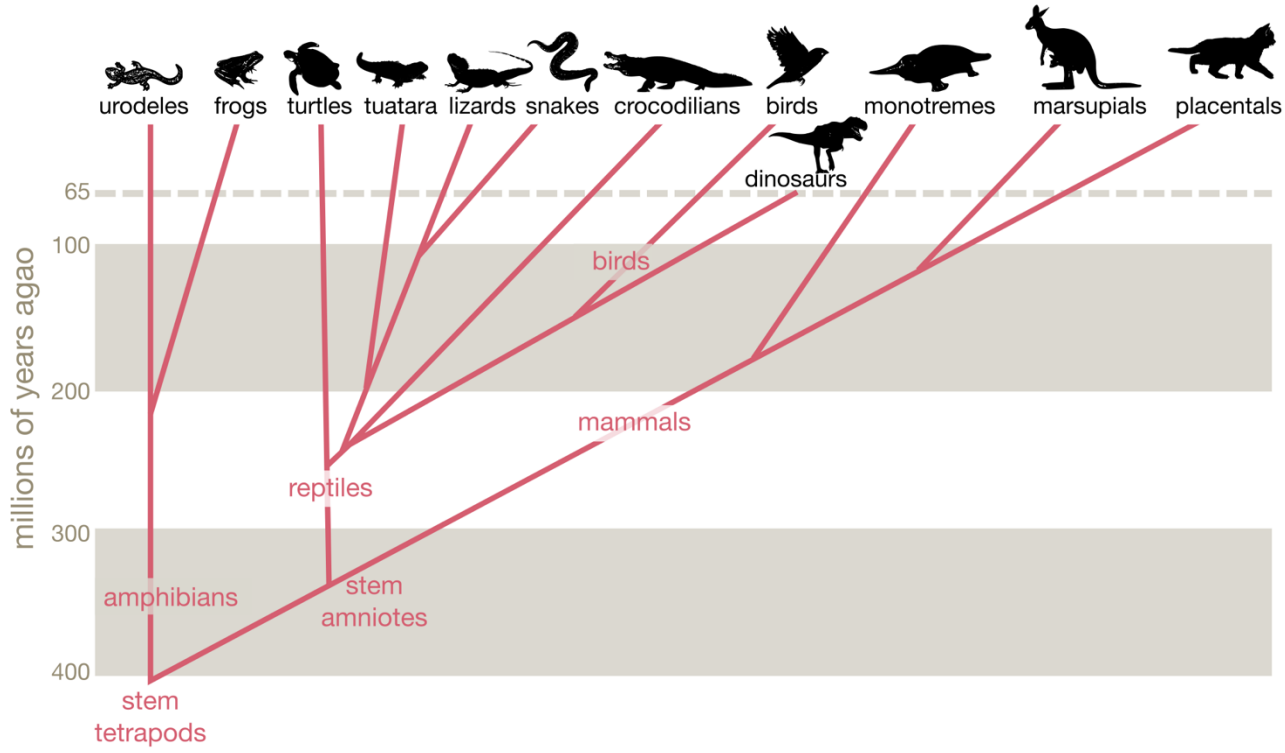

Figure 1.4. Cladogram of amniote evolution. At left is shown approximate dates at which branching occurred. Note the derivation of birds from the reptilian lineage. Based on Figure 5 from (Reiner et al., 2005).

However, in the chickens and the lone pigeon of this study, the amounts of REM found were very small, ranging from 0.3% - 0.6% of total sleep. The episodes of REM were short, only 5 – 8

s, and they did not seem to occur in any clear pattern. The EMG during REM showed muscle hypotonia but no clear atonia. The authors concluded:

> "the paradoxical phase of sleep [REM] exists only in a 'rudimentary state' in birds, yet their 'slow' sleep [SWS] is similar to that of mammals. This result is thus in favor of the existence of difference mechanisms underlying the two states of sleep." *
>
> —*Klein et al, 1964 (Klein et al., 1964).*

The argument here is that birds have 'highly evolved' SWS similar to mammals, but 'less evolved' REM that is dissimilar to mammals, supporting this group's overall hypothesis that REM and SWS are generated by distinct mechanisms (Jouvet, 1965). This implies an interpretation that was picked up by subsequent studies: avian and mammalian sleep is fundamentally different, and SWS has converged across the two groups more than REM has.

The hypothesis of convergent evolution

Over the following decades, these results were confirmed over and over, in species including songbirds, parrots, ducks, geese, birds of prey, penguins, and doves. Although the accepted total estimate of REM in birds rose to about 2 – 7%, birds were still considered to have far less REM than mammals (Van Twyver and Allison, 1972; Szymczak, 1986a; 1987; Ayala-Guerrero et al., 1988; Ayala-Guerrero, 1989; Szymczak, 1989; Mexicano et al., 2014).

Birds also lacked sleep spindles, had "less developed" slow wave activity (Tobler and Borbély, 1988), and did not consistently exhibit a SWS increase and REM decrease. These differences from mammals supported a hypothesis that sleep structure evolved independently in birds (Rattenborg and Martinez-Gonzalez, 2015). In this case, surface similarities between sleep stages are not necessarily expected to reflect similarities in the generation, regulation, or functions of these stages.

Early experimental limitations

However, several of these earlier studies had a number of severe limitations, especially related to the choice of lighting conditions. Before the advent of widely available infrared video recording, constant light was a not uncommon experimental condition in sleep studies not only of birds (Ayala-Guerrero et al., 1988; Ayala-Guerrero, 1989; Ayala-Guerrero et al., 2003), but also mammals (Campbell and Tobler, 1984) as well as amphibians and reptiles (Libourel and Herrel, 2016). Other common lighting conditions included nighttime dim blue light (van Luijtelaar et al., 1987) or nighttime dim red light (Van Twyver and Allison, 1972; Szymczak, 1987; Ayala-Guerrero and Vasconcelos-Dueñas, 1988). Unfortunately constant light is a very strong stimulus capable of abolishing circadian rhythms in a diurnal animal. Birds, with their complex circadian systems and multiple deep brain photoreceptors (Cassone, 2014), may be susceptible to even dim light.

Other studies avoided this by forgoing any illumination at night. This had the consequence that researchers could not directly observe nighttime behavior. Instead, daytime behavioral observations were used to infer the bird's behavioral states directly from the EEG at night (Šušić and Kovačević, 1973; Dewasmes et al., 1985; Tobler and Borbély, 1988). Unlike humans, birds do not appear to have an alpha rhythm that clearly demarcates quiet wake and sleep, nor is the EMG a reliable indicator of REM. The PSG characteristics of quiet wake and REM are often extremely similar, and daytime behavior contains far more wake than it does REM. Thus, both constant lighting conditions and the lack of nighttime behavioral observation may have led to inaccurate measurements of sleep, especially REM.

Recent studies in songbirds: unexpected similarities

The hypothesis of convergent evolution has started to be re-evaluated in light of recent evidence demonstrating unanticipated and striking similarity to mammalian sleep in multiple species of songbirds. Larger amounts of REM were found, in the range of 15 – 25% of total sleep (Szymczak et al., 1993; Rattenborg et al., 2004; Low et al., 2008; Lesku et al., 2011a; Brawn et al., 2018). Furthermore, several of these studies found overnight increases in REM and decreases in SWS similar to patterns in mammals. One study also identified a stage of intermediate sleep that resembled human stage 2 (Low et al., 2008).

Basal birds

The evolutionary origin of these patterns remains to be resolved. One approach is to study the most basal bird lineage, the Palaeognathae, who are the most distantly related to all other living birds. In ostriches, which are a species of ratites, a hybrid REM state which combined features of SWS and REM was observed (Lesku et al., 2011a). This is a primitive condition that is also observed in monotremes, basal mammals such the echidna and the platypus (Siegel et al., 1998). Yet in a species of tinamous, another clade within the paleognath basal bird lineage, distinct SWS and REM were observed (Tisdale et al., 2017). Thus, it is possible that the evolutionary origins of complex sleep patterns extend to and arose from the basal bird lineage, perhaps involving more than just songbirds. Furthermore, paleognath birds are derived, that is not closely resembling ancestral (stem) birds, so that the structure of sleep in paleognath is not necessarily reflective of the primitive condition.

The hypothesis of common ancestry

The degree of similarity between sleep in mammals and songbirds challenges the hypothesis that complex sleep structure emerged independently. Alternatively, birds and mammals may share features that reflect a common ancestral condition, giving rise to similar sleep patterns through evolutionary and functional constraints acting on homologous mechanisms. Similarities comparing the avian and mammalian neuraxis have been strengthened by recent studies reporting homologies between cell types and circuit organization in avian forebrain regions and layer-specific neocortical cells and circuits (Reiner et al., 2004; Jarvis et al., 2005; Reiner et al., 2005; Dugas-Ford et al., 2012; Dugas-Ford and Ragsdale, 2015).

The thesis studies

Overall, birds and mammals share 1) aspects of global sleep structure, 2) circuit-level mechanistic mediators in the form of replay, and 3) functional impacts of sleep on learning. While the relationship between sleep structure, replay, learning behavior, and has been somewhat resolved in the mammalian hippocampus, it is unclear whether this relationship holds outside of mammals, outside of the hippocampus, or outside of declarative learning. In this dissertation I take a comparative approach to examine the evolution of sleep and its role in motor learning. In Chapter 2, I extend the recent findings on songbird sleep complexity by examining the sleep architecture of budgerigars, a species of parrot. To resolve discrepancies between older and modern avian sleep literature, I also test the effect of experimental conditions used in many studies pre-1995. In Chapter 3, I confirm prior findings on sleep structure in zebra finches and demonstrate a set of nested ultradian rhythms similar to those in budgerigars. In Chapter 5, I record motor replay in conjunction with global sleep structure and changes in motor coding over

multiple sleep/wake cycles. During the course of data collection for Chapter 5, I was involved in efforts to develop new techniques for recording multisite, long-term neuronal activity in the song system. These methods are described in detail in Chapter 4.

CHAPTER 2. COMPLEX SLEEP IN A PARROT SPECIES

Introduction

Although sleep is broadly expressed (Campbell and Tobler, 1984; Kavanau, 1998), a subset of species have developed specialized forms of sleep. Rapid eye movement sleep (REM) and slow wave sleep (SWS), with their associated changes in cortical activation, are found only in mammals and birds (Hartse, 1994; Tobler, 2005; Roth et al., 2006; Lesku et al., 2008; Rattenborg and Martinez-Gonzalez, 2015; Libourel and Herrel, 2016). Many hypotheses of sleep in mammals ascribe specific functions to REM, SWS and features thereof (Karni et al., 1994; Ficca et al., 2000; Poe et al., 2000; Walker et al., 2002; Tononi and Cirelli, 2003; Peigneux et al., 2004). Understanding how and why complex sleep architecture evolved in birds may inform how we understand sleep evolution as a whole (Rattenborg, 2006; Rattenborg et al., 2011; Margoliash and Brawn, 2012) and will constrain hypotheses on the role of sleep that have focused on mammals and neocortex.

While the structure of sleep in mammals is extensively studied – especially in humans (Rechtschaffen and Kales, 1968) – and conforms to a broadly accepted general pattern, the description of sleep in birds is undergoing rapid revision. A wealth of older studies in birds found only 2-7% REM (reviewed in (Siegel, 1995; Tobler, 2005; Roth et al., 2006), inconsistent ultradian regulation (Rojas-Ramírez and Tauber, 1970; Szymczak, 1986b; 1987; Ayala-Guerrero et al., 1988; Ayala-Guerrero, 1989), and no SWS rebound after sleep deprivation (Tobler and Borbély, 1988). This has promoted the hypothesis that sleep evolved independently in birds and mammals and shares few functional similarities.

More recently, complex mammalian-like sleep with abundant REM has been observed in multiple songbird species (Szymczak et al., 1996; Rattenborg et al., 2004; Low et al., 2008), and may even extend to certain species of basal birds (Lesku et al., 2011a; Tisdale et al., 2017). Ostriches, basal ratites of the avian clade Palaeognathae, exhibit a hybrid REM state (Lesku et al., 2011a) that combines some attributes of SWS and strongly resembles hybrid REM in monotremes (Siegel et al., 1996; 1999), the most basal group of mammals. In contrast, tinamous, another paleognath species, have typical REM (Tisdale et al., 2017) like that of neognaths. Therefore, it remains unresolved whether hybrid REM evolved independently in ostriches and monotremes, and whether "normal" REM dates back to the common ancestor of all living birds.

This gives rise to several questions: how to reconcile the old and new findings, how broadly distributed in birds is the mammalian-like sleep structure, and how this impacts theories of sleep mechanisms and evolution. The role of sleep in birdsong learning (Derégnaucourt et al., 2005; Shank and Margoliash, 2009), in adult birds acquiring perceptual memories (Brawn et al., 2013) and in maintaining memories through cycles of reconsolidation (Brawn et al., 2018), all share striking similarities with observations in mammals (Brawn et al., 2010). This further motivates interest in understanding how similarities in sleep arose.

Here, we investigated sleep architecture in a parrot species, budgerigars (*Melopsittacus undulatus*). Parrots (Psittaciformes) are the sister taxon to songbirds (Hackett et al., 2008; Zhang et al., 2014) and like songbirds, are one of three orders of birds that possess vocal learning abilities (Nottebohm, 1972; Petkov and Jarvis, 2012). We found that budgerigars have abundant REM, a distinct N2-like state of intermediate sleep, and circadian and ultradian rhythms in sleep structure which mirror those found in songbirds and mammals. We showed that the budgerigar sleep/wake cycle is significantly altered by constant light, which was used to facilitate

observations of sleeping birds in several early sleep studies, including the only previous study of budgerigar sleep (Ayala-Guerrero, 1989). This led to considerable disruption of sleep in budgerigars, and probably in other species. Finally, our results help define an emerging framework for scoring sleep in birds, taking into account the newer sets of observations. A standard for defining sleep architecture in birds may provide benefits comparable to what has been enjoyed in mammalian studies (Rechtschaffen and Kales, 1968; Ancoli-Israel et al., 2007).

Results

Characteristics of budgerigar sleep behavior

We first sought to describe the sleeping behavior of the budgerigars. All birds exhibited the expected diurnal pattern of activity. Lights off was invariably followed by 10-20 minutes of vigorous activity as birds moved around the enclosure, sometimes circling the perimeter several times before settling into their preferred spot. The birds frequently climbed up the sides and sometimes onto the ceilings of their enclosures. One bird [Bird 5] was observed sleeping for several hours while hanging upside down from the ceiling (**Figure 2.1A**). During the day, climbing was much less common; although birds napped often, they usually remained perched near the floor of the enclosure.

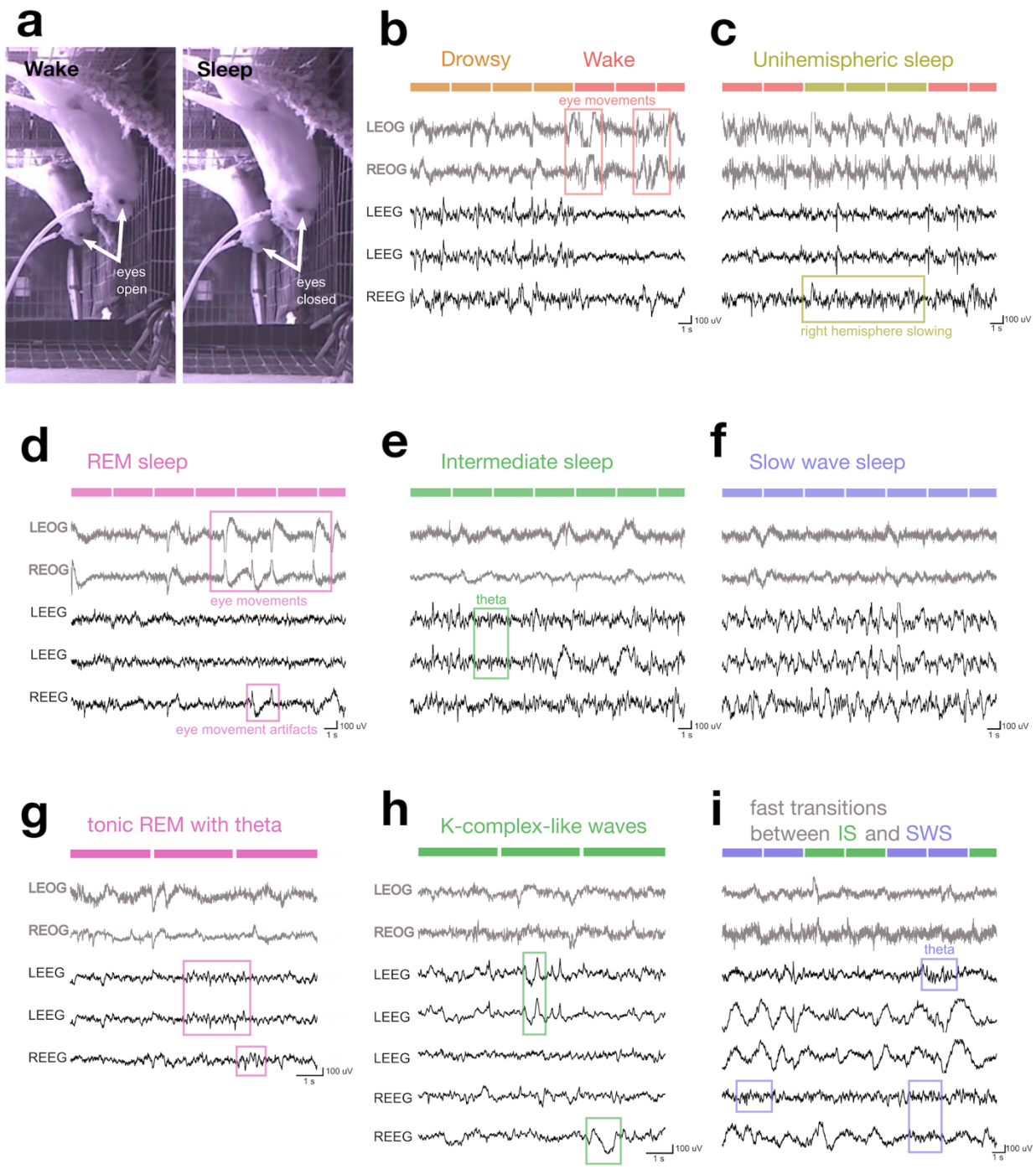

Figure 2.1. Examples of video and polysomnography (PSG) data. A) Infrared image of Bird 4 falling asleep at night while hanging from the ceiling of the enclosure. The bird is facing the cage wall on the right of the picture. A mirror on the back wall reveals the eye contralateral to the camera. During the brief awakening (left) both eyes were open; contrast with closed eyes (right) during sleep (two images separated by approximately 6 min). B-H) Example PSG recordings. Panels B-G are from Bird 1. Panels h-i are from Bird 4. The upper two EOG traces are gray; the lower three EEG traces are black. Vertical scale bars, 100 μV. Horizontal scale bars, 1 s. In panels B-F and I, a total of 20 s (about seven epochs) is shown. In panels G-H, a total of 9 s (three epochs) is shown to highlight details of the EEG recording. Within each hemisphere, EEG

Figure 2.1, continued
channels are arranged from most anterior at the top to most posterior at the bottom. B) A transition from drowsiness to full wakefulness. During drowsiness, note the occasional (every 1 – 2 s) slow, medium amplitude oscillations occurring along with higher frequency elements. As the bird transitioned back to alert wakefulness, the EEG became low amplitude and high frequency. Frequent eye movements appeared on the EOG throughout both states, but especially during wake. C) Unihemispheric sleep. Medium amplitude delta activity (0.5 – 4 Hz) appeared in the right hemisphere, while the left hemisphere maintained a flat, wake-like EEG. The left eye was closed and the right eye was open (not shown). D) REM. Note wake-like EEG with bursts of fast eye movements. Two eye movement artifacts are identified in the right EEG channel. E) Intermediate sleep (IS). Low-frequency, medium-amplitude oscillations appeared in the EEGs of both hemispheres. These were larger than either REM or wake EEGs (cf. 1b, 1d), but only infrequently reached an amplitude sufficient to be classified as slow waves. An example of theta (4 – 8 Hz) is highlighted. F) Slow wave sleep (SWS). The EEG contained numerous slow waves (0.5 – 4 Hz, >4 times wake amplitude). G) A long period of tonic REM with few eye movements and a particularly clear example of theta. H) An example of K-complex-like waves observed during IS. I) Using the amount of slow wave activity to distinguish between SWS and IS. The first IS epoch in this example contained one slow wave in the last channel, preventing this epoch from being scored as REM. This example also includes instances of theta during SWS.

At night birds engaged in long bouts of deep behavioral sleep (deep rhythmic breathing, muscle twitches, and head drooping) punctuated by brief awakenings of a few seconds. Most birds also exhibited a few longer nighttime awakenings during which they either climbed to a new sleeping position or made their way to the food dish for a nighttime meal. In contrast, behaviorally apparent deep sleep with noticeable breathing occurred very infrequently during the day. Most daytime naps occurred as brief sleep episodes amid long periods of drowsiness. Overall birds slept far more at night (82.9% ± 6.9% of time) than during the day (17.4% ± 11.9% of time) (**Table 2.1**).

Table 2.1. Sleep stage proportions.

NIGHTTIME				
Stage	**% of Recording Time**		**% of TST**	
	Mean	**SD**	**Mean**	**SD**
Wake	11.97	6.33	-	
Drowsy	5.09	1.62	-	
Unihemispheric sleep	0.023	0.019	0.029	0.023
Intermediate sleep	42.24	11.19	50.44	10.22
Slow wave sleep	15.71	5.10	18.86	5.66
REM sleep	24.96	7.94	30.66	11.51
Total sleep time	82.94	6.87	-	
DAYTIME				
Stage	**% of Recording Time**		**% of TST**	
	Mean	**SD**	**Mean**	**SD**
Wake	49.82	15.29	-	
Drowsy	32.80	14.76	-	
Unihemispheric sleep	3.27	2.35	29.33	21.88
Intermediate sleep	9.32	7.30	51.66	6.84
Slow wave sleep	3.12	3.81	13.00	10.40
REM sleep	1.67	2.44	6.01	6.96
Total sleep time	17.37	11.89	-	
24 HOURS				
Stage	**% of Recording Time**		**% of TST**	
	Mean	**SD**	**Mean**	**SD**
Wake	32.56	10.44	-	
Drowsy	20.09	7.56	-	
Unihemispheric sleep	1.77	1.21	3.83	2.43
Intermediate sleep	24.42	5.29	51.48	7.46
Slow wave sleep	8.91	3.95	18.18	5.82
REM sleep	12.26	3.55	26.51	8.97
Total sleep time	47.35	6.68	-	

Electrophysiological characteristics of budgerigar sleep

To further characterize budgerigar sleep, we examined the PSG data. Active wake contained large bouts of movement artifacts as expected. Quiet wakefulness revealed a low-amplitude and high-frequency EEG with frequent eye movements in the EOG (**Figure 2.1b**, Wake). Eye movements sometimes caused large artifacts in the EEG which could resemble delta waves

(**Figure 2.1b**, Wake). During drowsiness, it was common for slower and higher amplitude elements to appear in the EEG, while the EOG reflected frequent slow eye movements and blinking (**Figure 2.1b**, Drowsy).

Unihemispheric sleep was observed wherein the hemisphere contralateral to the closed eye exhibited low-frequency EEG activity, while the other hemisphere continued to show wake-like activity (**Figure 2.1c**). Notably, birds exhibited more unihemispheric sleep during the day (**Table 2.1, Figure 2.2e-f**).

Strikingly, budgerigars had large amounts of REM, characterized by fast-frequency low-amplitude EEG activity and large rapid eye movements appearing in the EOG (**Figure 2.1d**). We observed both phasic REM with frequent eye movements (**Figure 2.1d**) and tonic REM with few eye movements. We were sometimes able to capture instances of head drooping as the budgerigars slept. Upon reviewing the behavioral notes, we found that the majority of these instances occurred during REM. The head drooping appeared similar to the description of slow, controlled dropping of the head observed during REM muscle hypotonia in geese (Dewasmes et al., 1985).

We also identified large amounts of intermediate sleep (IS), a non-REM non-SWS state (**Figure 2.1e**). Consistent with prior work, we observed SWS episodes with long continuous trains of slow waves (**Figure 2.1f**). In contrast with SWS, IS typically contained a mix of low-amplitude delta, high-amplitude, K-complex-like waves (**Figure 2.1h**), and higher-frequency elements such as theta (**Figure 2.1e**). Birds often alternated quickly between IS and SWS as slow wave content fluctuated (**Figure 2.1i**). We did not identify sleep spindles in budgerigars (see Discussion).

In mice and rats, hippocampal theta (4 – 8 Hz) is prominent in the EEG during REM and wake. In humans, theta waves are less apparent on the surface EEG, but can appear as bursts of sawtooth waves during REM. While we did observe occasional REM theta in the budgerigars (**Figure 2.1g**), theta bursts could also appear during IS (**Figure 2.1e**) or during SWS (**Figure 2.1i**). Thus, we did not find theta to be a useful indicator of sleep stage in budgerigars. This is consistent with findings from depth recordings from chicken hippocampus (Sugihara and Gotoh, 1973).

Sleep architecture across day and night

We next considered how budgerigar sleep architecture was modulated over 24 hours. Individual hypnograms revealed considerate fast fluctuations between vigilance states (**Figure 2.2a**), but several consistent patterns emerged (**Figure 2.2b**). During the day, birds tended to remain either awake or drowsy, with frequent but short bouts of IS and unihemispheric sleep (**Figure 2.2a-b**). Napping was most common in the early afternoon, resulting in a small dip in wakefulness around 7 hours after lights on (**Figure 2.2a-b**). After lights off, birds fell asleep during the first hour and slept largely in a consolidated block until shortly before lights on (**Figure 2.2b**).

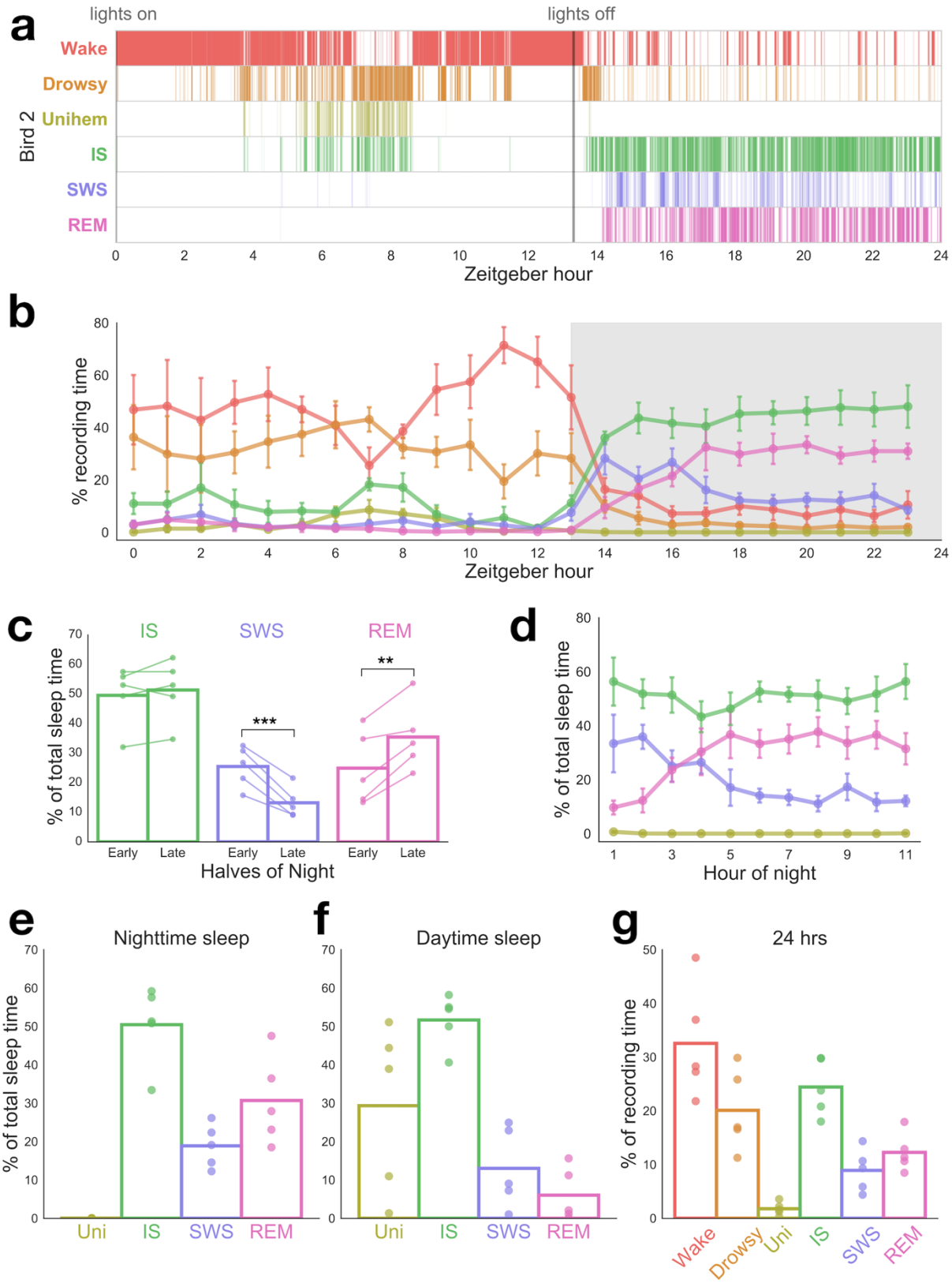

Figure 2.2. Sleep architecture and rhythms over 24 hours. A) An example hypnogram showing sleep scored across 24 hours in a single bird (Bird 2). Each tick represents one 3-second epoch with rows

Figure 2.2, continued
corresponding to vigilance states. Time of lights on and lights off are indicated by grey vertical lines. B) The mean of vigilance states across the 24-hour recording period in all birds. Lights off is shaded in grey. Error bars indicate SEM. C) Comparison across the two halves of the night. Sleep states are shown as a percentage of TST. Paired t tests: **p<0.01, ***p<0.005. d) Hour-by-hour patterns of sleep states as a percentage of TST. E-f) Total amounts of each sleep state as a percentage of TST during the night and day. G) Total amounts of each vigilance state across 24 hours. In e-g each point represents one bird and bars show the mean.

To look for patterns of changes across the night, we divided the night in half and examined each stage of sleep as a percentage of total sleep time (TST) (**Figure 2.2c**). From the first to the second half of the night, REM significantly increased ($t(4) = -5.14$, $p = 0.007$), SWS significantly decreased ($t(4) = 7.12$, $p = 0.002$), and IS did not change significantly ($t(4) = -1.06$, $p = 0.35$) (**Figure 2.2c**).

When we considered sleep stages across the night on an hour-by-hour basis (**Figure 2.2d**), the same pattern was observed wherein REM increased (regression with hour of night: slope = 2.27% TST/hour, $r^2 = 0.588$, $p = 0.006$), SWS decreased (slope = -2.37% TST/hour, $r^2 = 0.769$, $p = 0.0004$), and IS remained the same (slope = 0.13% TST/hour, $r^2 = 0.012$, $p = 0.74$). Results were similar when sleep stages were regressed not with time but with hour of total sleep (REM: slope = 2.71%, $r^2 = 0.673$, $p = 0.007$; SWS: slope = -2.67%, $r^2 = 0.673$, $p = 0.007$; IS: slope = -0.027, $r^2 = 0.000346$, $p = 0.96$). These patterns appeared in all individual birds (**Figure 2.2c**), including those for whom sleep was scored blind to hour of night.

The total amounts of sleep stages expressed by a given species are thought to provide important clues as to how sleep co-evolved with other species characteristics (Ball and Amlaner, 1983; Capellini et al., 2008; Lesku et al., 2008). Comparative studies of sleep in animal species typically consider sleep across a 24-hr recording period. In contrast, human sleep statistics are typically reported for nighttime sleep only. To facilitate comparison we report both measures here (**Table 2.1**, **Figure 2.2e-g**). Nighttime sleep was composed of 50.4% ± 10.2% IS, 18.9% ± 5.7% SWS, and 30.7% ± 11.5% REM (**Table 2.1**, **Figure 2.2e**).

Sleep architecture during the day (**Figure 2.2f**) was markedly different from nighttime sleep. Most of this limited daytime sleep consisted of either IS (51.7% ± 6.8% of daytime TST) or unihemispheric sleep (29.3% ± 21.9%). REM made up the smallest share of daytime TST at only 6.0% ± 7.0%. In total across a 24-hr period, animals spent 11.4 ± 1.6 hours asleep.

Effects of constant light

We sought to understand why the amounts of TST and REM we observed greatly exceeded that found previously. In many early sleep studies of birds, direct observation of behavior in the dark was not possible with available technology. In the case of both previous parrot studies, including a budgerigar study, birds were placed in constant light (LL) and given 7 days to acclimate prior to recording (Ayala-Guerrero et al., 1988; Ayala-Guerrero, 1989). We predicted that LL was responsible for some of the differences in our results.

We replicated these conditions with 3 of our birds (2 males, 1 female). Behavior after 7 days of LL was highly disrupted relative to baseline light-dark (LD) conditions in all three birds. For the one bird (a male) where we conducted manual video scoring (**Figure 2.3a**), this revealed 14.6% TST in LL; this bird had 38.8% TST at baseline. This is consistent with the difference in TST between previous work in LL (25.15% of time) (Ayala-Guerrero, 1989) and our study in LD (47.35% ± 6.68% of recording time).

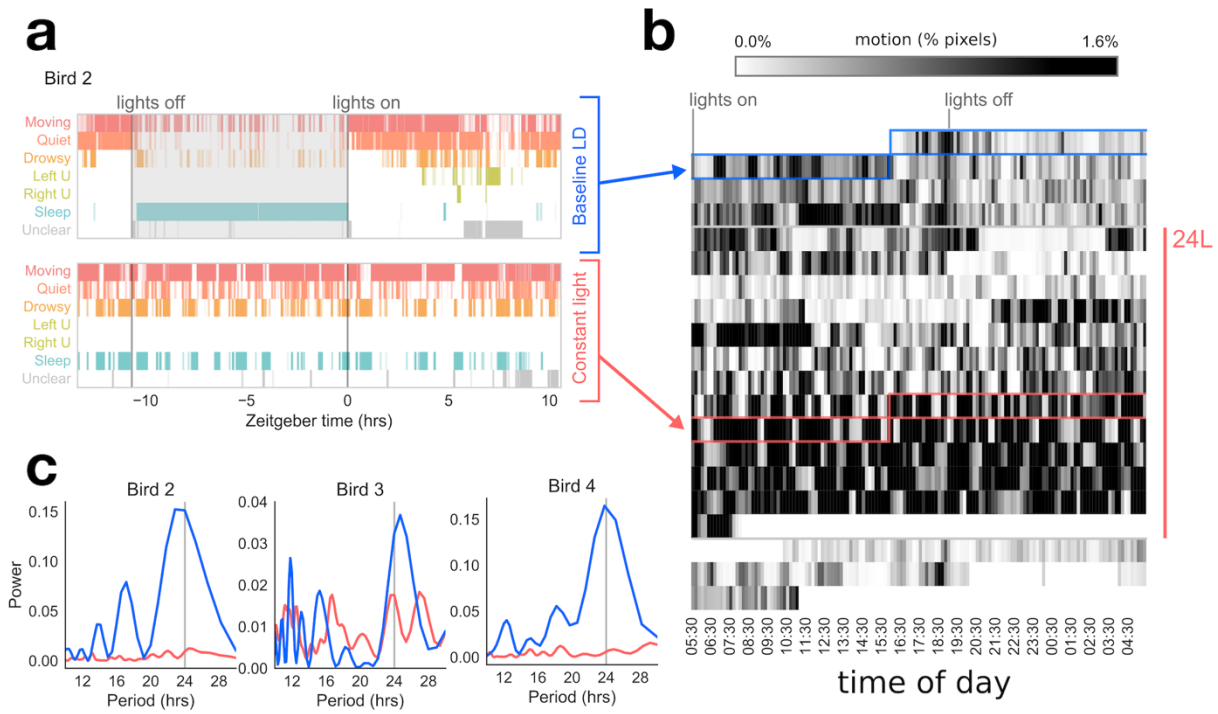

Figure 2.3. The effect of constant light on sleep/wake behavior. A) Video scores of one bird (Bird 2) across 24 hours. U, possible unihemispheric sleep, scored when the contralateral eye was closed and the ipsilateral eye was open. Each tick represents one 3-second epoch with rows corresponding to behavioral states. Lights off is shaded in grey. Top: Baseline light/dark cycle. Bottom: Constant light, day 8. Sleep is distributed across the 24 period in the constant light condition. B) Actigram of motion detected from video spanning baseline light/dark conditions, constant light, and return to baseline light/dark. Each row represents 24 hours. Each vertical segment in a row represents average motion in a 10-min bin, where darker indicates more motion. Boxed sections indicate days plotted in a). White area at the end of the LL period indicates missing data. C) Lomb-Scargle periodograms of motion data during constant light (red) and during normal 13L:11D (blue) for each bird. Vertical grey line indicates a 24-hour period. In LD all birds had close to a 24 hr period, which was lost under LL.

This bird's sleep was also highly fragmented. The average duration of the bird's sleep episodes in LD was 178.7 s, but this dropped to 23.0 s in LL. Across 24 hours in LD the bird exhibited 177 total sleep episodes, whereas in LL this went up to 547 sleep episodes. This fragmented behavior and lack of consolidated sleep periods greatly increased the difficulty of already laborious manual scoring. For this reason, we chose to analyze the other LL birds with automated methods.

Massive disruption of sleep/wake behavior was confirmed in all 3 birds by automated motion detection of continuous video over baseline LD, 8-12 days of LL, and subsequent recovery in LD

(**Figure 2.3b**). Moreover, in LL, birds almost never engaged in the climbing behavior that they exhibited at the beginning of the dark period. Instead, they slept on the ground or a low perch, similar to LD daytime napping.

The response to constant light was somewhat individualized; for example, one bird (Bird 3) showed signs of free-running during the first few days of LL. By day 8, which corresponds to the day of sleep recording in prior studies, all three birds appeared arrhythmic, which was confirmed by periodogram analysis (**Figure 2.3c**). This agrees with the prior budgerigar sleep study, which reported that, although sleep was increased significantly during subjective night, budgerigars were "polyphasic…. [S]leep episodes were distributed irregularly throughout the 24-hr period without showing a clear periodicity" (Ayala-Guerrero, 1989). We conclude that exposure to constant light has dramatic effects on budgerigar sleep that have obscured interpretation of previous studies.

Characteristics of sleep states

Many previous studies have described avian REM as particularly unstable, occurring in very short episodes. We therefore examined the continuity of each sleep state. Across the night, REM episodes became longer in duration while SWS episodes became slightly shorter (**Figure 2.4a**). All three sleep stages were relatively brief in duration: REM episodes were the longest and most variable (11.3 ± 5.0 s), IS episodes were shorter (9.3 ± 1.3 s), and SWS episodes were the shortest (5.1 ± 0.8 s). A one-way ANOVA indicated significant differences in the duration of the different sleep stages ($F(4) = 4.26$, $p = 0.04$), which resulted from SWS episodes being significantly shorter than IS episodes ($t(4) = -4.6$, $p = 0.01$) and trending shorter than REM ($t(4) = -2.62$, $p = 0.059$). The duration of IS and REM episodes did not differ ($t(4) = -0.703$, $p = 0.52$).

These observations underscore that all the sleep stages in budgerigars tended to occur in short episodes.

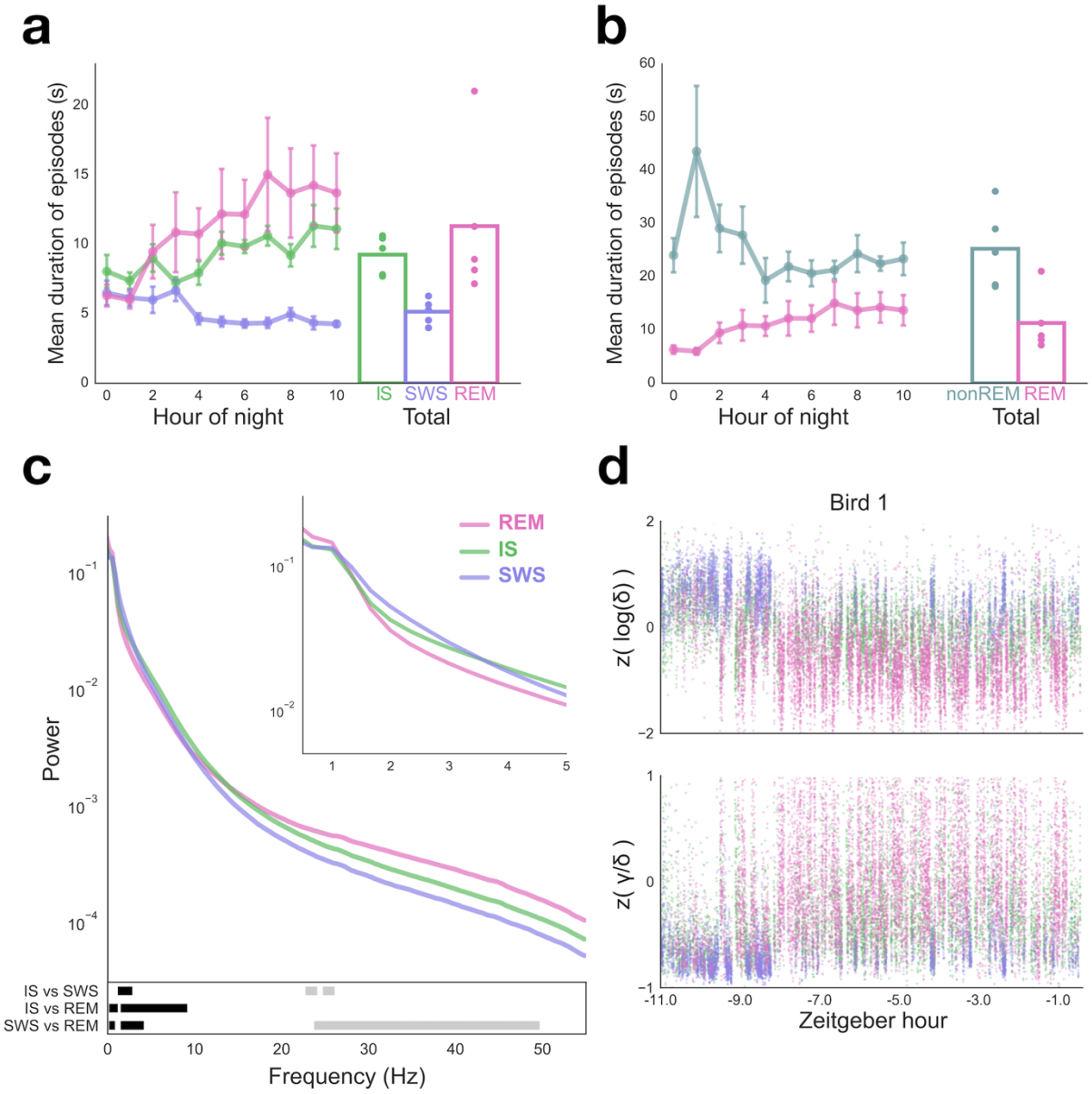

Figure 2.4. Time-varying and spectral characteristics of sleep states. A) Durations of each sleep state. Left: durations per hour of night. Right: mean durations across the entire night. B) Durations of sleep states with IS and SWS combined into a single NREM state. C) Average power spectra of sleep states. Bottom, statistical comparisons between pairs of spectra. Black indicates significant differences (Rüger's areas; see text); gray indicates trends (consecutive bins with $p<0.05$). Inset, closer view of the delta band. D) An example of time-varying spectral characteristics of single-channel EEG data across the night. Dots represent epochs spaced 1s apart. Colors indicate sleep stage. Top: Z-scored log of delta per epoch. Bottom: Z-scored gamma/delta ratio per epoch. Delta was defined as 0.5 – 4 Hz and gamma as 30 – 55 Hz.

Because sleep studies in animal models often do not divide NREM into SWS and IS, we also examined NREM as a whole. The duration of NREM episodes reached a peak in the second hour of the night and then fell sharply, reaching a plateau after 4 hours (**Figure 2.3b**). On average, NREM episodes (25.2 ± 6.7 s), were longer than REM episodes (11.3 ± 5.0 s) (**Figure 2.4b**) although this difference did not quite achieve significance (paired t-test, $t(4) = 2.55$, $p = 0.06$). In this regard, we note that one animal (Bird 1) exhibited approximately twice the average REM duration of the other four (**Figure 2.4b**).

We computed power spectra to characterize frequency content and Rüger's areas to assess significance of differences between sleep states (**Figure 2.4c**). This confirmed the manual scoring, which relied largely on delta content, and revealed additional differences in higher frequency bands less visible to the manual scorer. Compared to other vigilance states, SWS exhibited the highest amount of low-frequency power with a broad peak encompassing the delta band (**Figure 2.4c** inset). SWS significantly exceeded REM in the frequency range 1.66 – 4 Hz, which spans most of the delta range. In contrast, IS fell between SWS and REM in the delta band (**Figure 2.4c** inset). IS was significantly lower than SWS in the band 1.33 – 2.66 Hz and significantly exceeded REM between 1.66 and 9 Hz, which includes both delta and theta power. REM had significantly more power in very low frequencies than both SWS (in the range 0.33 – 0.66 Hz) and IS (0.33 – 1 Hz), which we speculate is due to eye movement or twitch artifact we were not able to filter out.

In the range of 25 – 55 Hz (which includes both beta and gamma frequencies), REM appeared to contain more high frequency power than other sleep states while SWS had low power and IS contained an intermediate amount of power in this range; however, these differences did not reach significance. REM trended higher than SWS in the 24 – 49.5 Hz range,

while IS trended higher than SWS in a few high-beta/low-gamma ranges (23 – 24 and 25 – 26 Hz) (**Figure 2.4c**).

Because budgerigar sleep stages alternate rapidly, we examined individual 1 s epochs of EEG during sleep. Delta and gamma activity exhibited oscillations throughout the night (**Figure 2.4d**) that broadly correlated with manual sleep scores. As expected, individual SWS epochs tended to contain high delta and a low gamma/delta ratio; REM epochs occurred during periods of low delta and high gamma/delta; and IS epochs fell in between, with average delta and relatively low gamma/delta.

We conclude that budgerigars exhibit extensive REM episodes characterized by a prevalence of high frequency peaks. Spectral analyses confirm our manual classification of mixed-frequency IS interspersed with low-frequency SWS.

Slow waves and eye movements

To extend manual sleep scores to unbiased characterization of a larger dataset, we carried out automated detection of slow waves, eye movements, and eye movement artifacts.

Slow wave detection were detected using an adapted version of the zero-crossing method (**Figure 2.5a**) (Mölle et al., 2002; Massimini et al., 2004; Mensen et al., 2016). As expected, the slow waves occupied the highest amount of time during SWS epochs and the lowest during REM epochs (**Figure 2.5b**). The mean seconds/epoch of slow waves identified with this method typically fell below 50% of the 3-s epoch, the criterion for manual scoring of SWS. Whereas manual scoring typically counts continuous "runs" of slow waves, the automated procedure imposes strict cutoff points between half-waves; this results in a more conservative estimate.

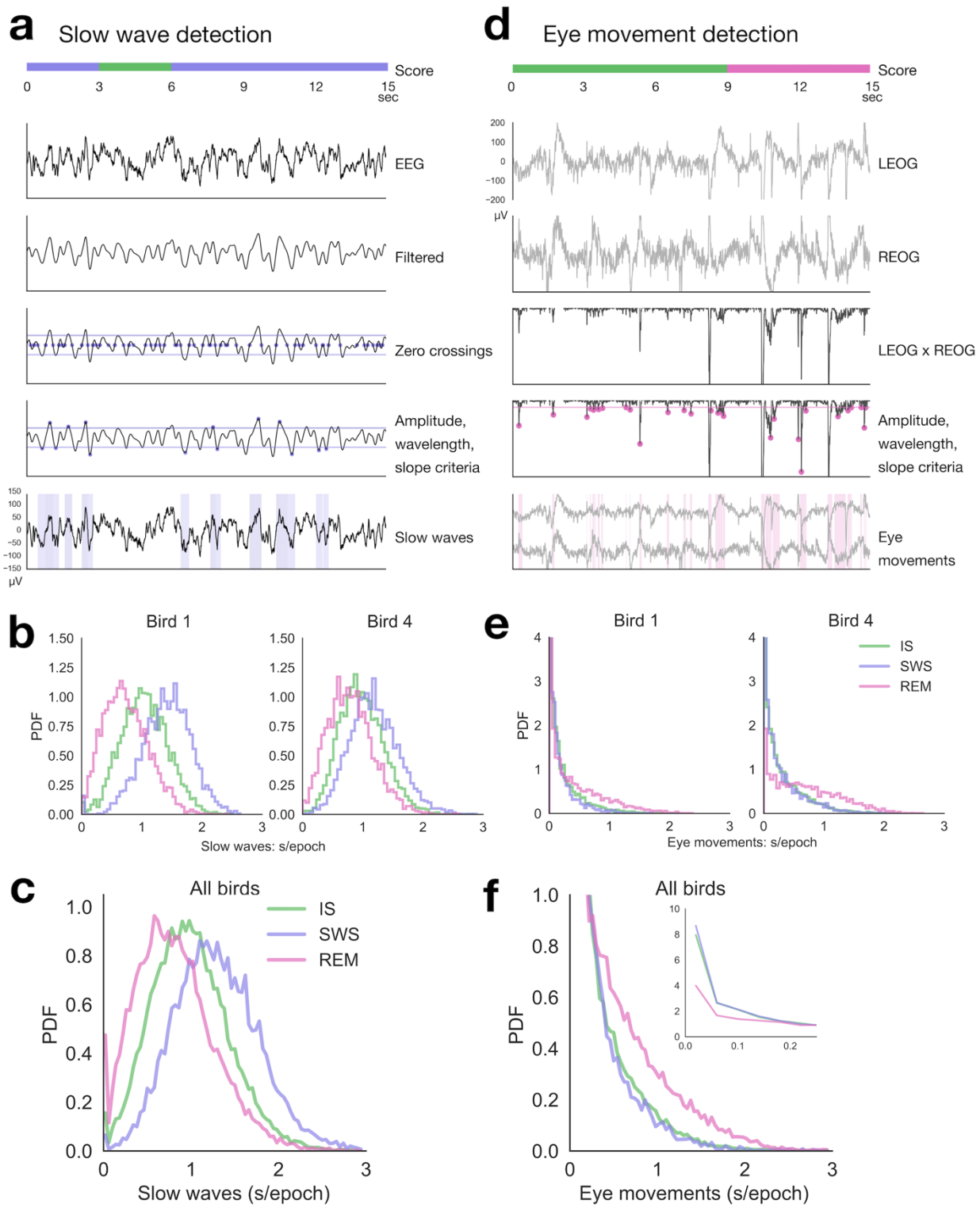

Figure 2.5. **Automated detection of slow waves, eye movements, and eye movement artifacts.** A) An example of slow wave detection. The EEG is filtered between 0.5 – 4 Hz, zero crossings are identified, and each resulting half-wave is evaluated for amplitude, wavelength, and slope criteria. Eye movement artifacts were also excluded from the pool of candidate slow waves (see text). B) In two representative birds, the

Figure 2.5, continued
normalized distributions of slow wave content per epoch in each sleep stage. C) Average of slow waves per epoch across all birds. D) Example of eye movement detection. Eye movements appear as opposing deflections in the two EOG channels. The left EOG is multiplied with the right EOG, and large negative half-waves in this correlation are identified as eye movements. Eye movement artifacts in the EEG (not shown) were detected with a similar process applied to the EEG x EOG product. E) In two representative birds, the normalized distribution of the number of seconds of eye movements per epoch, for each of the stages of sleep. F) Average of eye movements per epoch across all birds. Inset, close up of distributions near zero eye movements/epoch. The number of zero-eye movement epochs during SWS and IS greatly exceeded those during REM.

Eye movements were detected as the anticorrelation of the left and right EOGs (**Figure 2.5c**). The two NREM stages differed from REM in eye movement content (**Figure 2.5d**): In all birds, NREM epochs were heavily skewed toward 0, while REM epochs formed a much broader distribution with one large peak near 0 and a long tail spanning the 0.25 s – 2 s range. This may indicate two subtypes of REM that correspond to tonic REM (no eye movements) and phasic REM. In summary, automated sleep analyses supported our manual scoring and further highlighted a preponderance of REM, both tonic and phasic, in budgerigars.

Ultradian rhythms and sleep cycles

We examined oscillations in the gamma/delta ratio at several timescales (**Figure 2.6a**). We identified two rhythms with a highly consistent period across birds: a 65-s rhythm (65.37 ± 13.04 s) and a 34-min rhythm (33.82 ± 5.18 min) (**Figure 2.6b**). These data suggest that budgerigars undergo both a short ultradian rhythm similar to that reported in some other animals (Shein-Idelson et al., 2016; Libourel et al., 2018), and a long ultradian rhythm on the order of the human 90-minute sleep cycle.

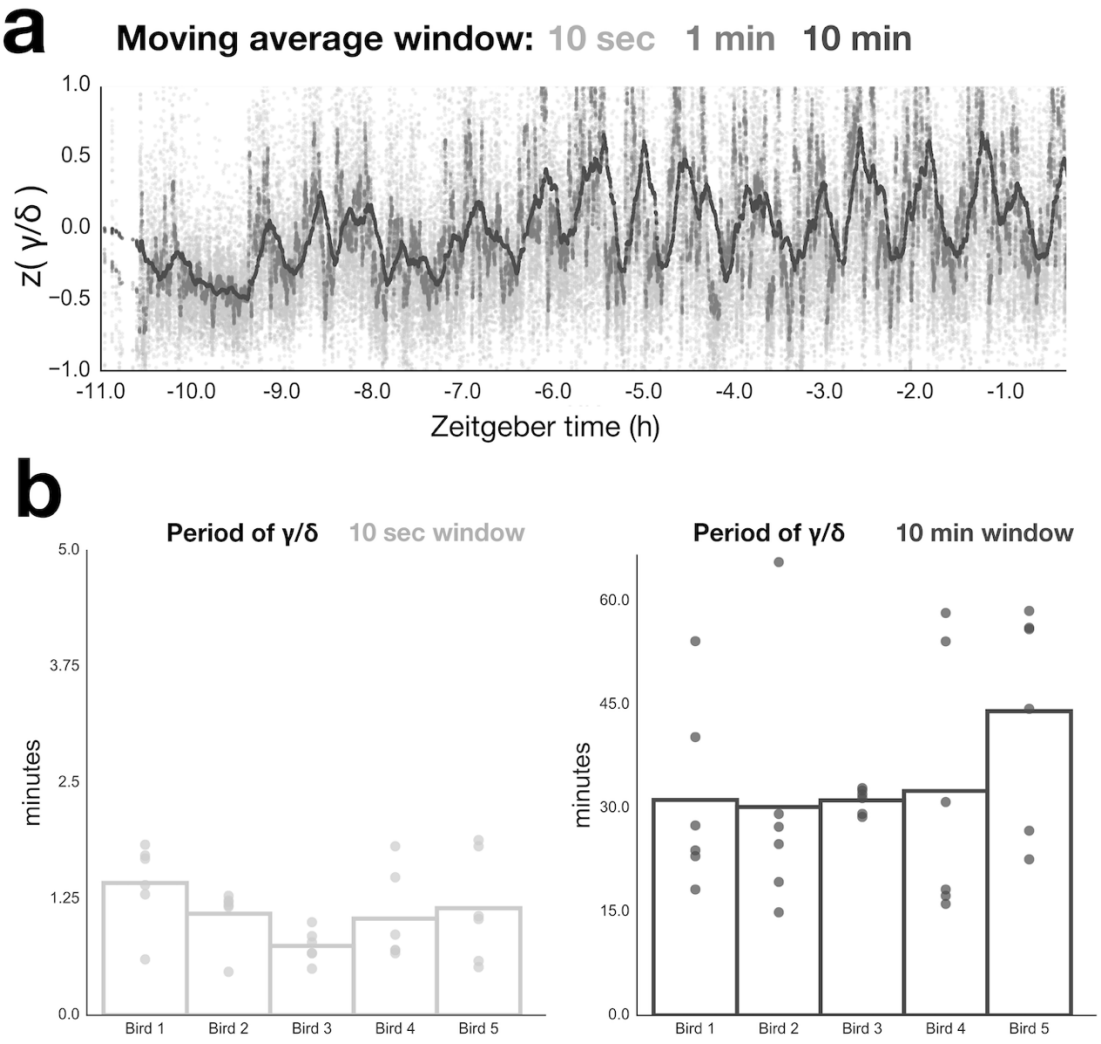

Figure 2.6 Ultradian rhythms in sleep. A) The gamma/delta ratio across the night (Bird 3). Moving averages with three different window lengths revealed underlying oscillations in the gamma/delta ratio. B) The period of the 10 s and 10 min moving averages, which had the most consistent peaks across birds. Each dot represents a single EEG channel. Each bar represents an individual bird.

Discussion

We have demonstrated that budgerigar sleep exhibits numerous complex characteristics not previously described. Budgerigars have large amounts of REM, and their NREM is partitioned into SWS and IS. These classifications based on manual scoring were supported by spectral characteristics and by automated detection of slow waves and eye movements. We also observed

a SWS decrease, a REM increase, and a 34-minute ultradian rhythm over the night, similar to the human sleep cycle.

Budgerigars exhibit large amounts of REM sleep

We found that budgerigars spent over 30% of nighttime TST in REM (26.5% of 24-hour TST). This amount is higher than that of most mammals (Lesku et al., 2008) and any bird species reported to date (Roth et al., 2006; Low et al., 2008; Lesku et al., 2011a). It is comparable to the 20 – 25% REM in humans (Ohayon et al., 2004) and to the 26.3% REM in ostriches (Lesku et al., 2011a). This diverges from a prior study of budgerigars (Ayala-Guerrero, 1989) along with many older studies of birds in which REM was likely underestimated (Klein et al., 1964; Szymczak, 1985; Schmidt, 1994).

Eye movement content during REM was distributed broadly with a pronounced peak at 0. This may indicate distinct tonic and phasic REM, categories often applied to mammalian REM that may have functional differences. The eye movements of phasic REM co-occur with ponto-geniculo-occipital waves, which facilitate sleep consolidation of learning (Datta et al., 2004); one study has found similar waves in the avian tectum (Sugihara and Gotoh, 1973). Phasic REM may correspond to periods of more intense dream experience (De Carli et al., 2016; Usami et al., 2017). In contrast, tonic REM, not typically described in birds, is a state of heightened environmental processing (Wehrle et al., 2007) with long-range synchrony across cortical areas (Simor et al., 2018).

Moreover, REM increased across the sleep period, as occurs in mammals with consolidated sleep patterns and in songbirds (Szymczak et al., 1993; 1996; Rattenborg et al., 2004; Low et al., 2008). These findings sharply contrast the traditional view that avian REM is “rudimentary” (Klein et al., 1964), comprises about 7% of total sleep, and has no consistent pattern across the

night (Szymczak, 1986a; 1987; Ayala-Guerrero, 1989; Mexicano et al., 2014). These differences likely arise from technical limitations of the older studies (see below).

Why might budgerigars have such an abundance of REM? In humans, REM is associated with procedural and emotional memory consolidation (Karni et al., 1994; van der Helm et al., 2011; Boyce et al., 2016). REM may be important for brain development and learning during early life (Solodkin et al., 1985; Marks et al., 1995), particularly during critical periods (Aton et al., 2009) and with regards to motor development (Blumberg et al., 2013). More REM appears in juveniles in many species: humans (Ohayon et al., 2004), other mammals (Shimizu and Himwich, 1968; Jouvet Mounier et al., 1969), and some birds (Saucier and Astic, 1975; Scriba et al., 2013). Comparative analyses of mammalian sleep have found higher REM in more altricial species, which are born in a less developed state (Lesku et al., 2006; Capellini et al., 2008; Lesku et al., 2008). Thus, an interesting possible explanation for large amounts of REM in budgerigars (and songbirds) is that it supports the persistence of vocal learning abilities into adulthood (Hile et al., 2005; Gallup et al., 2015; Spierings and Cate, 2016; d'Antonio-Bertagnolli and Anderson, 2017) or more generally, their sophisticated social and cognitive abilities (Miller et al., 2012; Buckley et al., 2017). Further studies are needed on the interplay of learning and sleep within budgerigars and other advanced bird species.

Evidence for SWS homeostasis

Budgerigars spent 18.9% of nighttime TST in SWS, similar to the proportion in humans (Ohayon et al., 2004). We also found a SWS decrease over the night. This pattern appears in mammals (Sinha et al., 1972; Agnew and Webb, 1973) and reflects the homeostatic regulation of SWS (Dijk et al., 1990). This is consistent with a growing number of recent studies in birds. SWA decreased in blackbirds (Szymczak et al., 1993; 1996), white-crowned sparrows

(Rattenborg et al., 2004), zebra finches (Low et al., 2008), and starlings (T. Brawn, personal communication). SWA rebounds after sleep deprivation in pigeons (Martinez-Gonzalez et al., 2008). Exposing one eye to increased visual stimulation caused a local SWA enhancement in the corresponding hemisphere (Lesku et al., 2011b). Thus, our data support the interpretation that like mammals, birds regulate SWA in a homeostatic manner.

Intermediate sleep is analogous to human stage 2

Few avian sleep studies have differentiated NREM into SWS and IS, due to precedent and the lack of spindles (Šušić and Kovačević, 1973; Dewasmes et al., 1985; Szymczak, 1987; Ayala-Guerrero, 1989; Szymczak et al., 1993). Indeed, spindles are a hallmark of human N2. However, N2 is primarily distinguished from SWS by lack of slow wave content (Ancoli-Israel et al., 2007). Motivated by previous work finding IS in zebra finches in the absence of spindles (Low et al., 2008), we adapted human scoring guidelines to distinguish IS from SWS.

We found that budgerigars spent approximately 50% of nighttime TST in IS, and this amount remained steady over the sleep period. This closely resembles the amount and time course of IS in zebra finches (Low et al., 2008) and of N2 (Carskadon and Dement, 2011). N2 is associated with procedural memory consolidation (Walker et al., 2002; Manoach et al., 2010), although much of this work has focused on sleep spindles (Johnson et al., 2012; Wamsley et al., 2012). It is an open question whether IS in birds shares a similar function despite an apparent absence of spindles. Given that spindles are propagated from the thalamus to the cortex, and that thalamorecipient areas of the pallium are not superficial structures in birds, this may preclude detecting spindles with surface EEG recordings in birds.

A long-period sleep cycle

Humans alternate between NREM and REM in a 90-minute sleep cycle. Studies in other animals have often identified shorter sleep rhythms, for example a 90 s cycle in lizards (Shein-Idelson et al., 2016). Ultradian rhythms in avian sleep architecture have rarely been examined. REM was found to recur with a period of 1.1 min in pigeons (Walker and Berger, 1972) and 8.2 min in burrowing owls (Berger and Walker, 1972). Other studies reported aperiodicity of SWA and/or REM (Van Twyver and Allison, 1972; Szymczak et al., 1996). We found that budgerigars exhibit a 65 s cycle, similarly to pigeons and lizards, and a 34 min cycle with remarkably consistent periods across individuals. The repeated alternation between NREM and REM has been proposed as a key mechanism of sleep-dependent memory consolidation (Ficca et al., 2000). The existence of similar cycles in budgerigars could support similarities in sleep regulation and function.

Constant light as a confounding factor

Previous studies of budgerigars (Ayala-Guerrero, 1989) and of orange-fronted parakeets (*Aratinga canicularis*) (Ayala-Guerrero et al., 1988) found significant differences in parrot sleep as compared with mammals. Those studies examined birds in constant light. Other early studies likewise employed dim red or blue light at night, or chose to forgo nighttime behavioral observation, as infrared video was not widely available. Additional confounding factors in many early studies (but not in the prior parrot studies) include a) the use of long scoring epochs for NREM and short epochs for REM, and b) the lack of eye movement measures like EOG, possibly resulting in eye movement artifacts being classified as slow waves.

We found that constant light strongly disrupted the sleep/wake cycle in budgerigars, fracturing their normal diurnal pattern of behavior. This renders the prior results unreliable and

likely explains the discrepancies with the current results. Indeed, we found that during the day REM comprised 6.0% of TST (normal LD), similar to the previous report of 5% REM in budgerigars (LL) (Ayala-Guerrero, 1989). Interestingly, orange-fronted parakeets in the same LL conditions had 14.8% REM, a possible underlying species difference (Ayala-Guerrero et al., 1988). Perhaps under normal LD, parrots on average exhibit a great deal of REM.

These observations motivate revisiting phylogenetic analyses of avian sleep, which have thus far found little correlation between sleep architecture and species traits (Roth et al., 2006). In contrast, a nearly identical meta-analysis in mammals yielded a wealth of associations, for example between REM and encephalization (Lesku et al., 2008). Our findings suggest that suboptimal experimental conditions may have masked analogous links in birds.

Evolution of sleep

An emerging body of work points to many similarities across mammalian and avian brains and behavior. Our findings extend recent evidence that avian sleep exhibits more REM, more features, and more complexity than were historically recognized. We confirm complex sleep in a species of parrots (Psittaciformes), the sister taxon of songbirds (Passeriformes). The consensus result in songbirds and parrots indicates strong similarities to the structure of mammalian sleep (Low et al., 2008). Additional similarities between birds and mammals arise considering the role of sleep in learning and memory. Behavioral developmental studies demonstrate a relation between sleep and zebra finch song learning (Derégnaucourt et al., 2005; Shank and Margoliash, 2009), studies in adult starlings demonstrate a role of sleep in memory (re)consolidation (Brawn et. Al. 2013, 2018), and zebra finch electrophysiological studies demonstrate neuronal bursting (Hahnloser et al., 2006) and song replay (Dave and Margoliash, 2000; Hahnloser et al., 2006; Shank and Margoliash, 2009; Rauske et al., 2010) during sleep.

How did these extensive similarities arise in birds and mammals? One hypothesis is that sleep in birds results from convergence of similar traits through independent evolutionary processes (Siegel et al., 1998; Rattenborg, 2006; Rattenborg et al., 2009). The difference in sleep structure comparing ostriches (Lesku et al., 2011a) and tinamous (Tisdale et al., 2018), and a recent study in a lizard (*Pogona vitticeps*) (Shein-Idelson et al., 2016; Libourel et al., 2018) give question to those predictions, although many more sleep studies in reptiles are required. The present results motivate an alternate hypothesis, that the similarities arose by parallel evolution acting through processes of deep homology – shared across some reptilian taxa and including birds and mammals. In this hypothesis, attributes of complex sleep patterns appeared during evolution at multiple loci. How would such deep homology be expressed in brain functional anatomy? Recent studies identify similar cell types and circuits in a canonical forebrain pattern of connections in reptiles, birds, and mammals, providing a mechanistic focus for such a hypothesis (Dugas-Ford et al., 2012). It remains unresolved whether such constraints of connectivity could give rise to the similar patterns of behaviors and physiological properties in birds and mammals.

Methods

Animals

Adult budgerigars (*Melopsittacus undulatus*) (n = 5; 3 female, 2 male) were obtained from Magnolia Bird Farm (CA). In what follows, birds 1, 3, and 5 were the female birds. Birds were housed in large group cages in a 13L:11D photoperiod and allowed to acclimate to the lab environment for at least 3 months before recordings began. Parakeet seed mix, water, and

cuttlebone were provided *ad libitum*. Starting 1-5 days before surgery, birds were transferred to an individual recording cage in an acoustically and electrically shielded enclosure (18" w, 10" h, 14'' d). Perches were placed close to the floor to avoid tether wrapping. The temperature was maintained at 20-22 °C. All procedures were approved by the Institutional Animal Care and Use Committee at the University of Chicago.

Surgery

Following transfer to the recording cage, birds were implanted with polysomnography (PSG) electrodes which consisted of 6 electroencephalogram (EEG) electrodes, 3 electrooculogram (EOG) electrodes, and 2 subcutaneous ground electrodes.

Birds were anesthetized with isoflurane gas, placed in a stereotaxic apparatus, and head-fixed via custom-sized ear bars. After removal of the feathers on the top of the head, the skin was sterilized with iodine and lidocaine cream was applied. A Y-shaped incision was made in the skin, exposing an area of skull approximately 1 cm in diameter. During this process, blunt dissection was used to create the subcutaneous channels that would later accommodate the EOG electrodes. The upper layer of the skull was removed over both hemispheres.

All PSG electrodes consisted of flattened segments of silver-plated 32 AWG copper wire; the final size of each flat electrode was approximately 1 mm x 2 mm in size. These electrodes typically had an impedance of 2-10 kΩ *in vivo*.

To implant EEG electrodes, the trabeculae were shaved down over each of the desired sites and a small incision was made in the lower layer of the skull. The electrode was then positioned parallel to the surface of the head and slipped into the incision to rest between the skull and the dura. Three EEG electrodes were implanted over each hemisphere (approximate coordinates relative to the center of the Y-sinus): a frontal electrode (3 mm lateral, 6 mm rostral), a central

electrode (3.5 mm lateral, 2 mm rostral), and a posterior electrode (4 mm lateral, 2 mm caudal). In choosing electrode locations we prioritized avoiding large blood vessels and spacing the electrodes as far apart from each other as possible. To minimize risk, we left intact the upper layer of skull over the Y-sinus itself. Therefore, electrode placement varied somewhat from bird to bird, and the coordinates listed above are approximate. We observed that within each bird, the EEG signals were markedly similar between the three electrodes on each hemisphere – the main difference being that eye movement artifacts were more prominent on more frontal channels – suggesting that exact location does not strongly affect EEG recording with this type of electrode.

Three EOG electrodes for measuring eye movements were implanted under the skin: one electrode 3-4 mm lateral to each eye and one at the midline (approximately 6 mm medial to each eye). Each of the lateral EOG electrodes were later referenced to the central EOG, similar to the AASM sleep montage in which lateral EOG electrodes are each referenced to a contralateral mastoid electrode (Ancoli-Israel et al., 2007).

Ground was connected to two electrodes implanted under the posterior skin over each side of the cerebellum. All PSG electrodes were wired to a connector (Omnetics, Minneapolis, MN). Electrodes and connector were affixed to the skull with dental acrylic reinforced with cyanoacrylate glue.

Data acquisition

Birds were allowed to recover from surgery for 3-5 days before being fitted with a lightweight cable that attached to a 12-channel mercury commutator (Dragonfly Inc.) on top of the cage. This allowed birds to freely move about the enclosure. After at least 4 days of acclimation to the cable, baseline sleep recordings were collected.

Video from a webcam (Logitech) with its IR filter removed was captured to disk, for the first bird using the software guvcview (MKV file format, 640x360 resolution, 10 frames per second), and for the other four birds using the software Mencoder (AVI file format, 640x480 resolution, 30 frames per second). We found the latter approach more reliable. Several mirrors were placed on the walls to facilitate visualization (especially of both eyes), and an IR light provided illumination during the night. Video recordings were reviewed daily to determine each bird's habitual sleeping location and the camera was moved accordingly. A sheet of Plexiglas was attached to the cage wall in front of the camera to prevent birds from climbing directly on this wall and obstructing the camera view.

After passing through the commutator, EEG and EOG signals were amplified, bandpass filtered (0.1 – 200 Hz), digitized at 2000 Hz with a 16-bit converter and recorded to disk using an amplifier board (model RHD2132; Intan Technologies, Los Angeles, CA) connected to an RHD2000 USB interface board (Intan). Offline, data were bandpass filtered between 0.5 – 55 Hz, digitally referenced, and downsampled to 200 Hz. Right and left EOG signal were each referenced to the central EOG electrode. EEG signals were each referenced to more posterior electrodes on the ipsilateral hemisphere, resulting in a total of 3 possible EEG derivations on each hemisphere (frontal-central, frontal-posterior, and central-posterior).

Behavioral video scoring

One continuous 24-hr recording was analyzed per bird. Climbing behavior at night resulted in unexpected difficulty in capturing continuous behavior and an adequate view of the bird's eyes with a single camera, despite the use of mirrors. Nights chosen for scoring were captured after multiple days of experimenting with camera placement. Usually, each bird slept in one of a

few preferred locations unique to each individual. This could include a preference to sleep upside down.

Prior to scoring, the video and PSG data were extensively reviewed to establish a scoring system. Some avian species exhibit non-REM (NREM) with their eyes open, for example pigeons (Martinez-Gonzalez et al., 2008), ostriches (Lesku et al., 2011a) and tinamous (Tisdale et al., 2017). We did not find evidence for this in the budgerigars. Although drowsiness often included mixed EEG activity with delta content (0.5 – 4 Hz), this coincided with wake-like behaviors: slow eye movements, blinking, head movements, and fluffing of the feathers. We concluded that sleep can be determined behaviorally by eye closure, as in most birds (Ookawa and Gotoh, 1965; Amlaner and McFarland, 1981). Therefore, we proceeded as follows, and later examined epochs of behavioral drowsiness for potential re-classification as sleep (see "Manual PSG sleep scoring" below).

We used a 2-step scoring process to determine vigilance states: behavioral video scoring (**Table 2.2**) followed by PSG scoring. We choose to use 3-second epochs because sleep states could fluctuate rapidly in the budgerigars, as in most birds including songbirds (Low et al., 2008; T. Brawn, personal communication).

Table 2.2. Behavioral scoring criteria

Stage	Posture/behavior: criteria	Eyes: criteria	Other notes
Active wake	Overt movements	Eyes fully open with infrequent, fast blinks	Can include climbing, eating, grooming, vocalizing, flying, etc.
Quiet wake	No overt movements		Body held still with an upright posture
Drowsy	No overt movements	Frequent slow blinking and partial closure of eyes	• Body may lean forward slowly • Head may tilt back or to one side
Possible unihemispheric sleep	Similar to either drowsiness or to full sleep	One eye closed and one eye open	• This stage is difficult to detect, as simultaneous observation of both eyes is usually required • Typically occurs during long periods of drowsiness • The open eye often appears drowsy with frequent blinking
Sleep	• Relaxed body posture • Deep rhythmic breathing, often causing the body to rock slightly	Both eyes closed	• At night, prior to falling asleep budgerigars often climb to a position high on the walls or ceiling of the enclosure • The transition out of sleep is often accompanied by abrupt movement, fast head shaking • Occasional muscle twitches and head drooping • Less frequently, rhythmic movements can occur e.g. fast beak movements resembling vocalizing

Video recordings of behavior were reviewed and each epoch was scored as active wake, quiet wake, drowsy, possible unihemispheric sleep, or (bihemispheric) sleep (**Table 2.2**). Active wake included any overt movements such as climbing, eating, flying, or grooming. During quiet wake, birds remained alert but became still, with an upright posture and infrequent, quick eyeblinks. As birds became drowsy, they began to blink slowly and close their eyes more frequently, and would often lean forward or tilt to one side. During sleep, birds fully closed both eyes; the head and body relaxed into a more horizontal posture, sometimes leaning against a nearby wall; and breathing become slow and deep. Breathing often caused noticeable rhythmic rocking movements that were not apparent when birds were awake. Sleep was not scored unless

both eyes were completely closed for the entire epoch. If one eye was observed to be closed and the other open, the epoch was marked as potential unihemispheric sleep. This was mostly observed in otherwise drowsy birds.

The deep breathing activity and concomitant whole-body rocking were particularly reliable indicators of behavioral sleep. This facilitated identifying awakenings, which were typically sudden and accompanied by abrupt movement, fast head shakes, and raising of the head. This distinction was not absolute, however. A few birds were sometimes seen to wake up without moving, opening their eyes suddenly and then falling asleep again after a few seconds.

We occasionally saw twitching, eye movements, or drooping of the head; epochs that contained these behaviors were annotated. Muscle twitches were usually of the head and beak, and sometimes involved the wings or the whole body. Twitches often occurred in clusters and appeared involuntary compared to movements during wake; for example, even during particularly violent twitches, sleeping birds often showed no sign of righting themselves despite coming close to falling off their perch. Twitches could sometimes trigger an awakening during which the bird righted itself and changed posture. Most commonly, twitches were small and relatively subtle, but it was not unusual to see larger twitches, sometimes occurring in long trains of repetitive movements. These features of twitches were observed in both sexes.

Eye movements during sleep were visible in some birds, but difficult to observe reliably given the variability in sleeping position and location between birds. Likewise, drooping of the head was sometimes observed, but birds often slept with their head resting against a wall, precluding consistent observation of this behavior.

Manual PSG sleep scoring

After behavioral scoring, EEG and EOG signals were visualized and sleep architecture was manually scored using a custom GUI written in Python. **Table 2.3** summarizes criteria used for scoring, along with additional PSG characteristics of each vigilance state.

Wake epochs were examined qualitatively but never re-classified as sleep based on the EEG alone. Drowsy epochs were reviewed and occasionally re-classified as sleep after examination of the PSG and video together. This tended to happen immediately following or preceding periods of wake. On average across birds, 2.88% ± 0.57% of epochs originally marked as drowsy were re-scored as sleep. In a similar fashion, behavioral sleep epochs were sometimes reclassified as drowsy (2.64% ± 0.51% of epochs originally marked as sleep).

Epochs marked as potential unihemispheric sleep was scored as such if the hemisphere contralateral to the closed eye exhibited signs of NREM sleep while the ipsilateral hemisphere showed signs of wake. If the EEG did not meet these criteria, the epoch was marked as drowsy.

Epochs marked as behavioral sleep were classified as SWS, REM, or IS with a scoring system (**Table 2.3**) adapted from current American Academy of Sleep Medicine guidelines for human sleep (Ancoli-Israel et al., 2007).

Table 2.3. Sleep scoring and vigilance state characteristics

	EEG	EOG	Transitions
Wake	• Active wake: Nearly constant movement artifacts • Quiet wake: "flat" EEG (low-amplitude, high-frequency) approx. 25 μV peak-to-peak	• Frequent eye movements, usually large and rapid	
Drowsy	• Mixed EEG: Wake-like "flat" activity interspersed with slower, higher-amplitude elements that begin to resemble sleep	• Eye movements not uncommon, often slower than during full wakefulness	• Drowsiness can include sleep-like behavior with a wake-like EEG that immediately precedes or follows clear behavior wake
Unihemispheric sleep	• Contralateral to closed eye: slower, higher amplitude activity • Contralateral to open eye, typically wake-like activity		
Intermediate sleep	• Slower and higher amplitude than wake or REM • Less than 50% of epoch contains slow waves • Delta activity (0.5-4 Hz) that does not meet amplitude criteria for SWS • K-complex-like events, resembling a single slow wave, can occur	• Infrequent eye movements; usually slow and low amplitude	• Transitions back and forth between IS and SWS are very frequent, as the slow wave activity of each epoch varies • Transitions from REM: Appearance of delta activity or K-complex with amplitudes exceeding that of typical wake or REM
Slow wave sleep	• At least 50% of the epoch must contain slow waves • Slow waves: delta frequency (0.5-4 Hz), amplitude at least 4 times that of typical quiet wake activity • Must rule out eye movement artifacts, which can resemble slow waves and are more prominent in frontal channels		
REM	• Low amplitude, high frequency EEG similar to wake • Theta waves (4-8 Hz) possible; these can be slightly higher in amplitude than typical wake activity • Eye movement artifacts are common and can have the appearance of slow waves, masking an otherwise "flat" EEG	• Large rapid eye movements are typically observed but are not required • Eye movements often start out small and become larger and more frequent as the REM episode progresses	• Transitioning into REM: Eye movements can appear in the EOG shortly before the EEG transitions to REM-like activity; in this case, the EEG is used to score REM onset

SWS was scored when at least 50% of the epoch contained slow waves on one or more channels. Slow waves were defined as delta waves (0.5 – 4 Hz) with an amplitude at least 4

times the typical artifact-free waking amplitudes; for most birds, this was ~125 μV. For Bird 1, who had unusually high amplitude EEG throughout the recording, a criterion of 250 μV was used. The criteria of 50% slow waves, rather than 20% as in human sleep scoring, was adopted due to the short length of the epochs. Small eye movements could appear in the EOG during this stage but were typically not present. In addition to slow waves, the EEG during non-REM sometimes exhibited other low-frequency elements, including artifacts from eye movements and very low frequency baseline fluctuations ~0.5 Hz. These artifacts were identifiable as excessively synchronous events across multiple channels.

REM was scored when at least 50% of the epoch consisted of low amplitude high frequency EEG similar to wake. This EEG pattern was often, but not always, accompanied by rapid eye movements in the EOG, which were almost never visible on the video. This is distinct from our prior report of sleep staging in zebra finches, where visible eye movements during sleep were commonly observed and in fact were one requirement for scoring REM (Low et al., 2008). However, the budgerigars had a much larger enclosure, chose far more varied sleeping locations and positions, and so were difficult to film. We surmise that these technical differences accounts for our failure to reliably observe on-camera eye movements during budgerigar REM. We were able to compensate for this with the use of two EOG channels (two lateral electrodes each referenced to a central electrode); the EOG measures the dipole formed by the positively charged cornea and the negatively charged retina. Concordant bilateral eye movements appear as diverging waves in the two EOG channels, which helps to distinguish true eye movements from artifacts caused by the eyelids and the nictitating membranes (Hartse, 1994; Tisdale et al., 2017). Observations during wake confirmed good correspondence of the EOG channels to eye movements.

REM epochs were not required to contain eye movements, but these were often detected shortly before or after the onset of REM-like EEG and were used to distinguish borderline REM from IS. Any occurrences of delta waves marked a transition out of REM, either to SWS or IS. Importantly, eye movements often contaminated the EEG, especially more frontal channels, and could resemble slow waves. Such artifacts would likely complicate the scoring of REM based on EEG alone.

IS was scored when at least 50% of the epoch consisted of non-REM sleep without sufficient slow wave activity to meet criteria for SWS. We approached the scoring of IS as analogous to human stages 1 and 2. Spindles were not observed in the EEG, so these could not be used to identify transitions from REM to IS. Instead, these transitions were delineated by the appearance of delta activity that was not of sufficient amplitude or quantity for the epoch to be marked as SWS.

Two scoring controls were used to evaluate order-of-scoring effects. For Bird 3, each hour of the night was scored in a randomized order. For Birds 4 and 5, each hour was scored in a randomized order and the scorer was blind as to time of night. The results of the blinded scoring are reported below.

Constant light

Three budgerigars (male Bird 2, female Bird 3, and male Bird 4) underwent a constant light manipulation. After 1-3 nights of baseline sleep were collected (6, 8, and 10 days after initial tethering, for each respective bird), the light cycle was switched to continuous 24-hr light lasting 8 days. This mimics the experimental conditions of a prior study of budgerigar sleep (Ayala-Guerrero, 1989).

On days 1, 4, and 8 of constant light, birds were tethered for 24 hr starting at or before 16:00 in order to collect PSG. Video recordings were collected throughout the entire period of constant light. The camera was not moved throughout the period of constant light and subsequent recovery.

After 8-12 days of constant light (12, 11, and 8 days for each respective bird), birds were returned to their normal 13L:11D light cycle. PSG and video recordings were continued for 1-3 days of recovery.

Motion detection

Motion was detected in grayscale video frames by determining the number of pixels with frame-to-frame change over a threshold, which we set to 10% of the maximum possible grayscale value for a pixel. This threshold was effective in capturing the animal's movement while filtering out slight fluctuations in lighting and other minor sources of frame-to-frame change.

For each of the three birds who underwent the constant light experiment, motion values were extracted from continuous video, starting at the time of baseline sleep recording and spanning all 8-12 days of constant light and the subsequent return to normal light/dark conditions. Data were averaged across 10-minute bins for visualization and periodogram analysis.

To examine the periodicity of the animals' movement patterns, we computed the Lomb-Scargle periodogram (Lomb, 1976; Scargle, 1982) in Python using the AstroPy library (VanderPlas et al., 2012; VanderPlas and Ivezic, 2015). For each bird, periodograms were calculated over the constant light period and over one continuous light/dark period, either baseline or recovery depending on which lasted longer for a given bird. For Bird 2, the baseline light/dark period was used (4 days). For Birds 3 and 4, the recovery light/dark period was used (7

and 4 days respectively). Periodograms were calculated over the range of periods from 10 to 30 hr. A large peak at or near 24 hr indicates an intact circadian rhythm.

Spectral analysis

The channels marked as the highest quality during manual scoring were used for spectral analysis (2 channels per bird, from opposite hemispheres for 3 birds). Epochs containing large artifacts (mean ± 4 SD) were excluded from analysis, as were periods scored as active wake and epochs with more than 0.5 s of eye movement artifact (see "Event detection" below). Multitaper spectrograms were calculated for each 3 s epoch with no overlap (custom-written Python library "resin" (see "Code Accessibility" below); NW = 3, number of tapers 4) across the entire 24-hr period and averaged across all epochs of each stage. The choice of non-overlapping windows was made to maximize frequency resolution and to include as many exemplars of each sleep stage as possible, including episodes lasting only 1 epoch. The frequency range examined was 0.33 – 55 Hz with a resolution of 0.33 Hz. Significance testing is described below (Experimental Design and Statistical Analyses).

To visualize changes in spectra across time, we averaged the mean activity in the frequency bands of delta (0.5 – 4 Hz) and gamma (30 – 55 Hz) for each 3 s window sliding by 1 s, based on previously published analyses (Low et al., 2008). From these we calculated 1) the log-transformed delta, and 2) the gamma/delta ratio. These values were z-scored to allow visual comparisons across channels and birds.

Event detection: slow waves, eye movements, and eye movement artifacts

To validate our manual scoring and further characterize budgerigar sleep, we applied several automated analyses to periods of sleep. Slow wave detection was carried out using the zero-

crossing method (**Figure 2.5a**) (Mölle et al., 2002; Massimini et al., 2004; Mensen et al., 2016); EEG signals from periods of behaviorally defined sleep were first filtered in the delta range (0.5 – 4 Hz). Individual half-waves between two adjacent zero-crossings were extracted and rectified. A series of criteria were then applied to determine which half-waves qualified as slow waves. Two inclusion criteria were applied: 1) a wavelength corresponding to delta and 2) an amplitude >75 μV peak-to-peak (37.5 μV for a half-wave). We applied three exclusion criteria: 1) waves with a peak >300 μV were excluded as large-amplitude artifacts; 2) waves with 50% or more overlap with detected eye movement artifacts (see below) were excluded; and 3) waves with multiple peaks were discarded if any of the troughs between peaks were <150 μV; this was done to exclude larger fast waves occurring on a small fluctuating baseline. For each bird, time spent in slow waves was collapsed across channels to obtain the total amount of time during which a slow wave was occurring in any channel.

Eye movements appear in the EOG as large rapid fluctuations with opposite polarities in the left and right channels. To detect these periods of anticorrelation, we took the product of the left and right EOGs and searched for periods where this correlation crossed a negative amplitude threshold. A zero-crossing analysis similar to the slow wave detection method was applied (**Figure 2.5d**). Negative half-waves in the anticorrelation were considered eye movements if they had: 1) a peak between -5000 and -500000 μV^2 in amplitude, 2) a wavelength corresponding to 0.2 – 60 Hz, and 3) a maximum negative slope in at least the 75th percentile of slopes for that dataset. In one bird (Bird 5) the right EOG was very low amplitude, so the anticorrelation amplitude criterion from step 1 was set to -250 μV^2.

Eye movement artifacts for each EEG channel were detected by applying a nearly identical procedure. The product of the EEG channel and its ipsilateral EOG was calculated. Eye

movement artifacts were defined as either positive or negative waves of any amplitude with 1) a wavelength corresponding to 0.2 – 60 Hz and 2) a maximum absolute slope in at least the 10^{th} percentile. For Bird 5, the left EOG was used to calculate eye movement artifacts for all channels.

Ultradian rhythms

We quantified ultradian rhythms in the gamma/delta ratio using a procedure similar to that of (Shein-Idelson et al., 2016). To capture the different frequencies of oscillations we observed, we calculated the rolling mean (one-sample step size) using three different window sizes: 10 s, 1 min, and 10 min. We obtained the autocorrelation at each time scale and took the first nonzero peak as the dominant period of that oscillation. Values of a period were averaged across all channels for a given bird.

Experimental design and statistical analyses

Statistical analyses were carried out in Python. We analyzed changes in sleep composition over the two halves of the night with two-tailed paired t-tests on IS, SWS, and REM. To look at hour-by-hour changes in sleep structure we calculated Pearson's correlation coefficient between hour and sleep stage proportion. Durations of episodes of each sleep stage were compared with a one-way ANOVA, followed by planned paired t-tests. Significance was set at 0.05. Throughout this paper, we report variance as mean ± SD unless otherwise noted.

To address the problem of multiple comparisons when assessing spectral differences between IS, SWS, and REM, we used Rüger's areas (Abt, 1987; Duffy et al., 1990), following the method described in Kis et al. (2014). For each pair of sleep stages, a set of paired t-tests were computed over the whole frequency range from 0.33 – 55 Hz, for each bin of 0.33 Hz. Then, starting from

the lower frequencies, all ranges of neighboring, consecutive frequency bins with $p > 0.05$ were identified. To qualify as a significant Rüger's area, a range must meet the following criteria: 1) 100% of bins are significant at the $\alpha = 0.05$ significance level; 2) at least 50% of bins are significant at the $\alpha = 0.025$ level (i.e. half of the standard significance threshold); and 3) at least 33% of bins at significant at the $\alpha = 0.0167$ level (i.e. one third of the standard significance threshold). If these criteria were met, the entire frequency range was considered significant. For completeness we also noted trends, i.e. Rüger's areas that met the first criterion but not all three (Simor et al., 2013).

Code accessibility

PSG scoring was performed in the custom-written GUI arfview, available at https://github.com/margoliashlab/arfview. An updated PSG scoring GUI compatible with binary files is available at https://github.com/margoliashlab/bark. The Python library resin, which was used for multitaper spectral analyses, is available at https://github.com/margoliashlab/resin. Custom code used for event detection and quantification of circadian and ultradian rhythms will be made available on https://github.com/margoliashlab.

CHAPTER 3. SLEEP STRUCTURE OF ADULT MALE ZEBRA FINCHES

Introduction

Despite the importance of zebra finches as a model for sensorimotor learning, and the numerous links between sleep and song learning in zebra finches (Dave and Margoliash, 2000; Derégnaucourt et al., 2005; Shank and Margoliash, 2009; Rauske et al., 2010), there has only been one published study on sleep architecture in this species (Low et al., 2008). Prior to that study, the only information came from a thesis (Schmidt, 1994), which was used as a source in the most recent meta-analysis of avian sleep (Roth et al., 2006).

These two reports directly contradicted each other in several respects. While Schmidt reported a value of 1.5% for nighttime REM, "consistent with the few studies reported for passerines" at the time (Schmidt, 1994), Low et al found REM to make up 25.4% of nighttime sleep. Moreover, Low et al reported a distinct SWS decrease and REM increase across the night, one of the first such reports in a bird (Szymczak et al., 1993; Jones et al., 2008) and in opposition to songbird studies that found the reverse trends (Szymczak, 1986b; 1989). These discrepancies are puzzling, and not explained by the issue of lighting conditions as with the older budgerigar studies (see Chapter 2): Schmidt recorded the finches in a standard 12:12 light:dark cycle and in fact specifically studied the effects of lighting manipulations on sleep (Schmidt, 1994). However, few details of the experimental procedures of this study are available, as it was never published.

In light of the results on complex sleep in budgerigars and the potential for links between learning and sleep structure in zebra finches (Shank, 2008), and the electrophysiological sleep studies to follow, I sought to confirm and extend the recent findings in this species. To this end I

recorded simultaneous EEG, EOG, and LFP; developed a method for automated behavioral scoring; and examined the spectral characteristics, time course, and periodicity of global brain activity during sleep. All birds in this study also participated in electrophysiological recordings, reported in Chapter 5. Hence, these birds carried more headgear than usual in a sleep study. To some degree this must have disrupted their sleep, although our results (see below) suggest that this was a minimal effect.

Materials

Animals

The five birds used in this study were adult male zebra finches (at least 120 days post hatch), either bred in-house or purchased from a commercial breeder (Magnolia Bird Farms, Anaheim, CA). Before surgery, the bird was moved to a recording enclosure in a sound attenuation chamber to acclimate, typically for at least several days. Birds were either kept on the colony's 13:11 light:dark cycle, or shifted to a 12:12 cycle. Ad libitum seed, water, grit, and cuttlebone were provided along with occasional millet spray. All enclosures were furnished with at least two sizes of wooden perches, and a portion of the wire floors were covered with cage liner to increase the bird's comfort.

The recording enclosures were 8'' square with perches placed on the bottom of the cage to accommodate tethered recording. Two walls were lined with mirrors to facilitate video recording of the bird's behavioral state. A female bird familiar to the subject was present, on the other side of a clear Plexiglas divider, for all recording sessions.

A webcam (Logitech) with the infrared filter removed was mounted on a perch and positioned with its face against the divider, allowing an unobstructed view of the male bird during recordings.

	Bird tag	Extracellular recording type	Dataset	Hours of recording	Complete nights recorded	Age at recording start (days)
Bird 3	orange257	Pt/Ir	22	16.02	1	258
Bird 6	orange253	Pt/Ir	8	44.03	2	318
			16	12.14	1	389
Bird 11	black 442	Pt/Ir	1	52.34	2	293
Bird 2	black 484	array	7	100.41	4	Unknown
Bird 5	lilac12	array	3	98.00	4	316

Table 3.1. Animals and datasets. For one bird (Bird 6), two datasets were included. The start dates of these datasets were 71 days apart. Bird 5 was obtained from a breeder; age is calculated based on the assumption that the animal was 120 days old upon arrival.

Surgery

Polysomnographic electrodes, headstages, and extracellular RA electrodes (either Pt/Ir or silicone arrays; see **Table 3.1**) were implanted as described in Chapter 3. A summary of the procedure is provided here for convenience. Details of the extracellular electrodes implanted will be provided in Chapter 5.

Approximately one hour prior to surgery, birds were food deprived with continued access to water. Anesthesia was initiated with an initial dose of 2.25 – 2.5% isoflurane in compressed room air at an airflow rate of 2 LPM; this dose was quickly lowered to 1.75% after a few minutes and gradually lowered over the course of the surgery. After approximately one hour, most birds could be maintained at 0.5 – 1.0% isoflurane. At the start of surgery birds were given intramuscular injections of 30 μL meloxicam analgesia and 4 μL enrofloxacin antibiotic, and 2-3 subcutaneous injections of 50 μL sterile saline for hydration. Birds were then wrapped in a cloth

jacket and placed in the surgery apparatus, where the head was fixed in place with ear bars and a beak bar at a 45º angle.

After removing the feathers on the top of the head, sanitizing the skin, and applying lidocaine cream, a Y-shaped incision was made in the scalp. Birds have a double-layered skull with a honeycomb of trabeculae between the layers; this top layer of skull was removed. Trabeculae were removed around the bifurcation of the Y-sinus to allow visualization of this landmark.

A ground and a reference electrode were inserted under the skin on either side of the head approximately 1 mm caudal to the Y sinus. Ground and reference were soldered together on the headstage.

A series of polysomnographic (PSG) electrodes were then implanted. PSG electrodes were constructed by flattening silver-plated copper wire for a final size of approximately 1 mm x 1 mm. Typical impendences in tissue were 2-10 kΩ. Two subcranial electroencephalogram (EEG) electrodes were placed ipsilateral to the extracellular electrodes, approximately 2mm and 4mm rostral to the Y sinus, both 2-3 mm lateral. Three subcutaneous electrooculogram (EOG) electrodes were placed: one midway between the eyes approximately 1cm rostral to the Y sinus, and two lateral to each eye.

A connector wired to both the extracellular and PSG electrodes was then lowered onto the head and affixed with dental acrylic, reinforced with cyanoacrylate glue. Finally, the whole implant was wrapped in surgical tape, reinforced with additional dental acrylic and cyanoacrylate, and wound edges were treated with antibiotic cream.

Following surgery, birds were allowed to recover under a heat lamp for 1-2 hours before being returned to their home cage. On days following surgery, birds were monitored and given additional doses of meloxicam as needed (no more than 1 dose per day).

Data collection

Electrophysiological data were captured via an interface board (RHD 2000 amplifier evaluation system, Intan Technologies, Los Angeles, CA) with a sampling rate of 30,000 Hz and a 16-bit ADC. Data from one bird, Bird 2, was collected with a sampling rate of 20,000 Hz due to the large volume of data from the 64-channel array. Data were visualized and recorded on a Linux computer with either Open Ephys (Siegle et al., 2017) (Birds 3 and 6) or the native Intan Interface software (Birds 2, 5, and 11). (For the latter three birds we used the default highpass filter settings (resulting in a 1 Hz, 1-pole filter) to minimize DC fluctuations in the recordings. The actual cutoff frequency of this filter varied by recording, and was 0.78 Hz for Bird 2 and 1.16 Hz for Birds 5 and 11). Sound was captured with a microphone connected to an M-Audio Fast Track Ultra audio interface (M-Audio, Cumberland, RI) and routed through a custom circuit board (designed by Kyler Brown and built by Daniel Baleckaitis; schematics available at https://github.com/kylerbrown/jill-in-a-box) before passing to one of the analog inputs on the evaluation board. The purpose of the custom circuit board was to apply an anti-aliasing filter while converting the bipolar voltage signal from the microphone amplifier to a unipolar (positive) signal compatible with the Intan evaluation board.

Video recordings were collected with Mencoder and filenames were automatically time-stamped to allow synchronization with electrophysiological data later. Cron was used to restart the video recording every 1 or 4 hours to ensure accuracy of timestamps.

Preprocessing

Data were preprocessed using Bark, a suite of software tools created by Kyler Brown and Graham Fetterman and written in Python (available on Github at https://github.com/margoliashlab/bark). Bark commands were run via GNU Make.

PSG and LFP data were bandpass filtered (zero-phase second order Butterworth filter) between 0.3 – 55 Hz for Birds 3, 6, and 11, and between 0.3 – 100 Hz for Birds 2 and 5 (the subset of birds implanted with 64-channel arrays). The larger band for the latter two birds was chosen to include high-gamma frequencies that may appear locally on different pads of the array. The results reported in this chapter concern only frequency bands below 55 Hz.

The frontal EEG was then referenced to the central EEG to yield one final EEG channel. The left and right EOG channels were each referenced to the central EOG channel, yielding two final EOG channels. Finally, data were downsampled by a factor of 100 using the bark command dat-decimate.

Behavioral characterization

Video recordings were saved as 640x480 pixel .avi files and converted to .mov with SmartConverter. Videos were manually scored in ELAN in a continuous fashion (i.e. without splitting the data into epochs). Behavior was classified into the following categories:

1. Preening: The bird used his beak to groom his feathers, usually with eyes closed. Preening was scored as a separate state due to reports of EEG slow waves appearing during preening episodes; recent work has suggested that these slow waves are not a consequence of movement artifact (Rattenborg et al., 2015).

2. Singing: Initially scored based on visual cues only. Later, labeled vocalizations from acoustic recordings were used to rescore any instances of singing or calling.

3. Active wake: Any other form of wake in which the bird was moving. This state included eating, scratching or grooming with the feet, stretching, flying, hopping, interacting with the female bird or the mirrors, etc.

4. Quiet wake: Wakefulness likely to be free of movement artifact. The eyes were open and the bird appeared alert with minimal blinking. Zebra finches spent only short periods of time in this state.

5. Drowsy: This state included frequent and slow blinking of the eyes along with drooping or tilting of the head.

6. Probable unihemispheric sleep: One eye was closed while the other eye remained open, often with a drowsy appearance. The hemisphere contralateral to the closed eye was indicated as the sleeping hemisphere. As this study did not specifically focus on detecting unihemispheric sleep (which would require the use of multiple cameras), we have likely underestimated the total amount especially during the day.

7. Sleep: The bird adopted a relaxed posture closer to the ground, with both eyes closed. During long episodes of sleep the bird typically puffed up its feathers. Two of the most reliable postural signs of sleep were: a) deep, regular, visible breathing that slightly rocked the whole body, and b) small, rapid episodes of repeated twitching, often in the head, that appeared involuntary. These episodes of twitching were easily distinguishable from arousal from sleep, in which the bird would rapidly shake its head and move in a more irregular and unpredictable manner.

8. Unclear or out of frame: Only an average of 0.17 % of time per dataset were labeled as such (range: 0 – 0.96%). Video recordings were only labeled “unclear” when all signs of behavioral state were not accessible, e.g. eyes, posture, and breathing. If one of these indicators was visible, an effort was made to classify behavior.

Comparison to budgerigar methods

Although these procedures were as close as possible to the methods used in Chapter 2, some improvements were made along with some necessary adjustments to allow simultaneous extracellular recording.

Here, the headstage was mounted on the head, whereas in the budgerigar study the analogous hardware was located between the commutator and eval board. This should benefit recording quality by reducing analog noise from the movement of the tether and commutator.

Due to space constraints only one EEG channel (differential recording from two electrodes) was recorded. This was augmented by deep-brain LFP recordings, which were not collected in budgerigars. Both EEG and LFP were collected from the same hemisphere. This prevents us from characterizing unihemispheric sleep on an electrophysiological basis. In addition, this could actually result in a slightly underestimation of total SWA; following human scoring guidelines, slow waves from any electrode location contribute to the total slow wave content of a given epoch.

Because zebra finches do not require as large an enclosure as budgerigars do, video recordings afforded a much better view of the entire space. Zebra finches, unlike budgerigars, did not climb; thus, the location of the video camera did not require adjustment for individual birds. The smaller space requirements also meant that the zebra finches could be provided a cagemate.

Behavioral scoring was conducted with essentially identical procedures, with the addition of two subcategories of active wake, preening and singing.

Automated sleep/wake scoring

The combined video and sound recordings were used to predict behavioral state (either wake or sleep; **Figure 3.1**) for Birds 2 and 5. Videos were analyzed using the Python library scikit-image. The video was first converted to greyscale. Motion was detected across frames as the number of pixels that changed above a certain threshold. The threshold was chosen to capture movement of the animal as opposed to slight frame-to-frame noise and motion caused by breathing. The sound waveform during each video frame was rectified and the mean amplitude was calculated.

Both motion and sound data were then smoothed by convolving with a cropped-Hamming window. This window K_{mixed} is constructed from a conventional Hamming window, where M is the number of points in the window:

$$K_{Hamming}(t) = 0.54 - 0.46\cos(\frac{2\pi t}{M-1})$$

The central 50% of the window is then kept while the rest is set to 0:

$$K_{mixed}(t) = \begin{cases} K_{Hamming}(t), & if\ \frac{M}{4} \leq t < \frac{3M}{4} \\ 0, & otherwise \end{cases}$$

Here, a 32 s Hamming window was first created, resulting in an effective final window size of 16 s. This combination of a Hamming and a square window was chosen to preserve relatively abrupt state transitions while still eliminating momentary noise.

Behavioral state was then predicted for each epoch of 3 s. To qualify as sleep, an epoch had to fall below a threshold for mean sound levels, mean motion, and SD of motion. For all three measures the threshold was set to -0.1, measured in standard deviations relative to the mean of the dataset. Birds usually take at least a few seconds to fall asleep. Therefore, the first epoch of each sleep episode was set to wake, also eliminating sleep episodes only 1 epoch long.

The automated scoring procedure was validated and the parameters were chosen by testing on the longest manually scored dataset of 44.03 hours (Bird 6, dataset 8) which spanned two full nights of sleep (**Figure 3.1**). A brute force search was conducted on the following parameters: Hamming window size, epoch length, sound threshold, motion threshold, motion SD threshold, and minimum number of epochs per sleep episode. Performance was evaluated from several metrics calculated from *n*, the number of epochs; *TP*, true positives or sleep epochs correctly predicted as sleep; *TN*, true negatives; *FP*, false positives; and *FN*, false negatives. Accuracy captures the proportion of scores that were correctly predicted:

$$accuracy = \frac{TP + TN}{n}$$

Sensitivity, in this case, indicates how well the algorithm did at correctly identifying sleep epochs.

$$sensitivity = \frac{TP}{TP + FP}$$

Specificity indicates how well the algorithm avoided labeling non-sleep epochs as sleep – in other words, how well it identified wake:

$$specificity = \frac{TN}{TN + FN}$$

The F1 score was used as the primary indicator of performance. It falls between 0 and 1, with 1 being the best score. It is a useful indicator of both sensitivity and specificity:

$$F1 = \frac{2\,TP}{(2\,TP) + FP + FN}$$

Manual scores were converted to wake/sleep scores for comparison with the predicted scores. "Sleep" included only manual scores of bihemispheric or unihemispheric sleep. Scores of

“unclear” or “out of frame” were not included. All other scores, included “drowsy”, were designated as wake.

The parameters generated by the blind search were used as an anchor point. Slight adjustments were then made by comparing video and predicted scores for the unscored datasets.

Using the initial set of parameters optimized for Bird 6, a maximum F1 score was reached of 0.933 (accuracy 93.0%). After adjustments, the algorithm predicted sleep in this dataset with an F1 score of 0.924, accuracy of 91.9%, sensitivity of 98.7%, and specificity of 84.9%.

In one bird (Bird 3) video was not recorded due to a technical error for a four-hour period starting at 4:00 am. The rest of the dataset was scored manually. The sound recording was used to automatically score this four-hour period with a procedure identical to the above, except no motion data could be used and the sound threshold was calibrated based on the manually scored portion of this bird’s data.

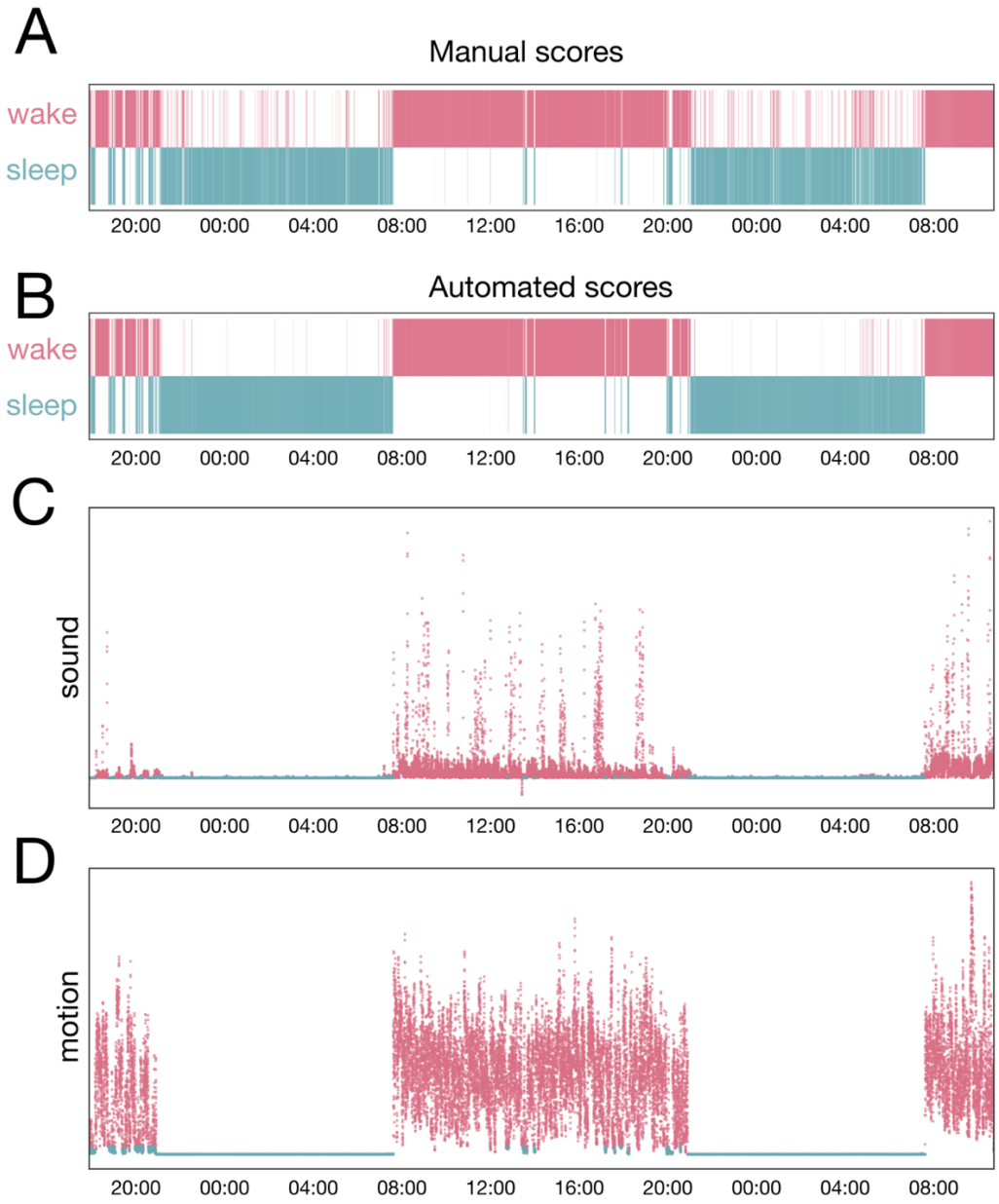

Figure 3.1. Automated video scoring. Data are from Bird 6, dataset 8; this recording spanned two full nights and one full day. Wake scores are indicated in red and sleep in blue. A) Hypnogram of manually scored behavioral state with wake on the top row and sleep on the bottom row. The width of each vertical line corresponds to the duration of the score. The bird slept in a largely consolidated block during both nights. B) Hypnogram of automatically scored behavior in 3-second epochs. Most epochs were scored accurately with the exception of some of the very brief awakenings at night. Compared to the manual scores, these scores had an accuracy of 91.9% and an F1 score of 0.92. C-D) Mean sound I and motion (D) amplitude in each 3-second epoch (arbitrary units). Colors correspond to automatic scores.

Spectral analysis

Spectral analysis was carried out on EEG and LFP signals for the stages of sleep, drowsiness, and quiet wakefulness. For each stage, all episodes lasting longer than 3 s were identified, then divided into 3 s epochs. The number of peaks per epoch was calculated by obtaining the local maxima. This measure reflects the prevailing frequencies in a given stretch of time.

A multitaper spectrogram of each epoch was then calculated in 3-s windows sliding by 1-s, using the Python library "resin" (available at https://github.com/kylerbrown/resin). The results were averaged to yield a single power spectrum for each epoch. Power was averaged in the following frequency bands: delta (0.5 – 4 Hz), theta (4 – 8 Hz), beta (8 – 30 Hz), and gamma (30 – 55 Hz).

To compare across birds a single channel was chosen for each bird. This was the EEG channel in the single-electrode birds (Birds 3, 6, and 11). In the array birds an LFP channel, positioned close to the neuron of interest, was used; importantly this LFP was not median-referenced, but instead effectively referenced to the surface ground. (EEG was not collected in Bird 2, while in Bird 5, the EEG was placed too far lateral due to space constrictions on the head and therefore contained excessive eye movement artifact.)

For measuring change across the night, the logarithm of delta power was taken. Other frequency bands were normalized by delta power. The EEG power spectrum scales by 1/frequency; thus, raw power in all frequency bands is highly correlated (Bédard et al., 2006). Thus, a ratio is more informative for comparing frequency changes over time and across animals than total power. Delta was chosen both for consistency with earlier work (Low et al., 2008; Shein-Idelson et al., 2016) and because, given its importance for sleep structure, a ratio such as gamma/delta provides more information than either gamma or delta alone.

Ultradian rhythms

For each night, the gamma/delta and nPeaks/s were analyzed for ultradian rhythms during sleep, using a procedure adapted from a recent reptile sleep study (Shein-Idelson et al., 2016). A rolling mean (one-sample step size) was calculated for three different bin sizes in order to capture rhythms at different scales: 10 seconds, 1 minute, and 10 minutes. For each of these rolling means, the period was calculated as the first peak of the autocorrelation.

Statistical analyses

Analyses were carried out in Python. All variables were z-scored to allow comparison across birds. Two-tailed paired t-tests were used to compare spectral measures across the two halves of the night.

Results

Sleep/wake behavior

Zebra finches slept through most of the night in a relatively consolidated block, waking often but briefly (**Figure 3.2, Figure 3.3, Table 3.2**). These awakenings were usually spent preening, stretching, or in drowsiness. Birds only rarely changed position or moved to a different location. Most individuals appeared to have a preferred sleeping location, where they slept on multiple nights; for example, Bird 6 slept in the same spot during two recordings over two months apart. In all five birds, the preferred location was in a corner adjacent to the divider, i.e. as close as possible to the conspecific cagemate.

The usual sleeping posture was with the beak pointing forward and the head slightly lowered. Alternatively, the bird slept with the head tilted back, to one side or drooping downward –

possibly due to the weight of the implant combined with relaxation of the neck muscles. Also observed, usually only at night, was a posture with the beak pointing back and the head tucked between the wings. This is a commonly adopted sleep posture in zebra finches and indicates that the birds were relatively comfortable even carrying the headgear.

Twitching of the head and body was common during nighttime sleep, sometimes in long trains. As most of the birds favored a corner for their sleeping location, it was not possible to directly visualize eye movements despite the relatively complete view of the enclosure. However, distinct and frequency eye movements were observed on the EOG.

The majority of the day was spent awake, with frequent periods of drowsiness punctuated by brief naps (**Figure 3.2, Figure 3.3, Table 3.2**). Napping was especially common in the late afternoon, although the amount and timing of daytime naps varied greatly on an individual basis (**Figure 3.2**). Between naps, birds were highly active, in almost constant motion, and spent their time feeding, interacting with the female bird and the mirrors, hopping around the enclosure, and preening.

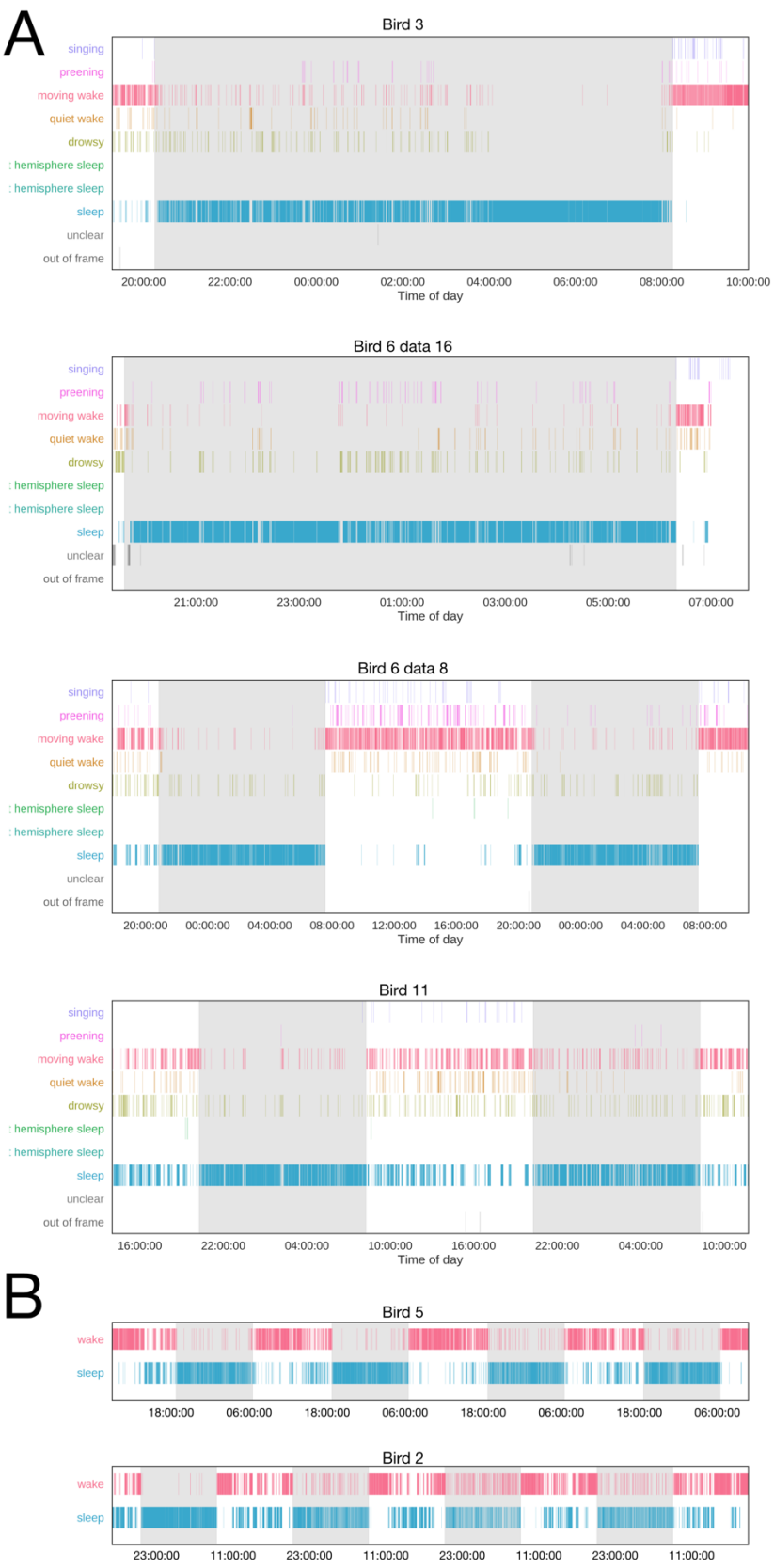

Figure 3.2 Hypnograms of all datasets. Different rows and colors correspond to different behavioral or sleep states. Width of each line indicates duration of that state. Grey shading indicates lights off. A) Manually scored datasets. Note the middle two datasets are from the same bird. In bird 3, the hours between 04:00 and 08:00 were automatically scored using the sound recording due to a technical error in the video recording. B) Automatically scored datasets.

What little unihemispheric sleep was observed was invariably seen during the day; however, this study was not specifically designed to detect it. The amount was likely underestimated, because to verify unihemispheric sleep both eyes must be visible. When only one eye is visible, behavioral state is determined from that eye alone i.e. wake, drowsiness, or sleep. Even with a good view of the enclosure and the mirror, clear view of both eyes was rare in this study.

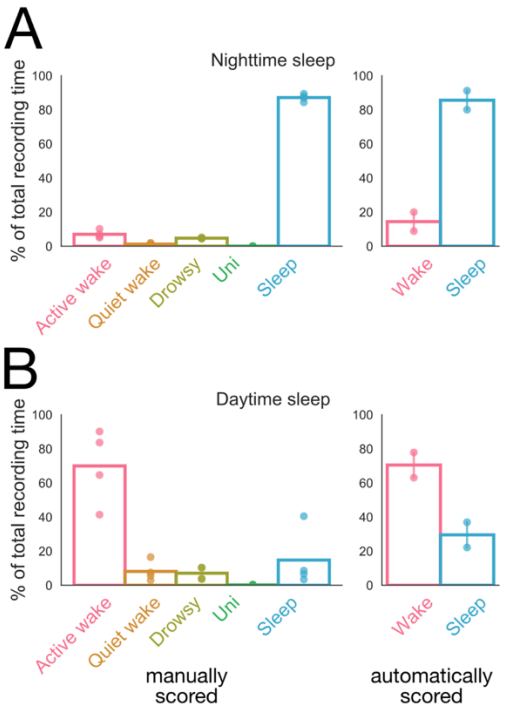

Figure 3.3. Summary of vigilance states during night and day. Each point represents the mean across all nights for an individual bird. Bar represents grand mean across all birds. Left, manually scored birds. Right, automatically scored birds. A) Sleep and wake during lights off. B) Sleep and wake during lights on.

Manual scores and automatic scores yielded similar proportions of wake and sleep (**Figure 3.3, Table 3.2**), especially of nighttime sleep and daytime active wake. The largest difference was in daytime sleep, of which the automatically scored has twice as much as manually scored birds (**Figure 3.3, Table 3.2**). It seems likely that automatic scoring tended to misclassify drowsiness and possibly quiet wake as sleep, especially during the day when sleep is highly fragmented (**Figure 3.2**).

		Recording time per bird (hrs)	Sleep (%)	Unihemispheric (%)	Drowsy (%)	All wake (%)	Active wake (%)	Quiet wake (%)	Preening (%)	Unclear/out of frame (%)
NIGHT										
Manual scores	Mean	17.24	87.13	0.00	4.70	8.17	6.97	1.20	1.11	0.16
	SD	6.84	2.11	0.00	0.34	2.24	2.29	0.74	1.04	0.24
Automatic scores	Mean	47.57	85.60	-	-	14.40	-	-	-	-
	SD	0.41	7.89	-	-	7.89	-	-	-	-
DAY										
Manual scores	Mean	13.89	14.75	0.17	7.03	78.05	69.95	8.10	3.01	1.22
	SD	13.21	17.28	0.20	3.79	20.14	21.92	5.90	4.10	2.43
Automatic scores	Mean	51.64	29.54	-	-	70.46	-	-	-	-
	SD	1.30	10.46	-	-	10.46	-	-	-	-

Table 3.2. Summary of vigilance states during night and day. Means and standard deviations are calculated on a per-bird basis. Manual scores, n = 3 birds and a total of 6 nights. Automatic scores, n = 2 birds and a total of 8 nights. For manually scored birds, "sleep" includes bihemispheric sleep only, and "all wake" excludes drowsiness, as this can sometimes be considered a hybrid state between wake and sleep.

State dependence and time course of spectral measures

To better understand how sleep structure changed across the night, we further analyzed the EEG and LFP data. As a validation step, we first compared the vigilance states of sleep, drowsiness, and quiet wake, in the manually scored datasets (**Figure 3.4**). Of the measures used nPeaks/s (number of peaks per second) was found to vary especially reliably with vigilance state (other measures examined were the log of delta and the ratios theta/delta, beta/delta, and gamma/delta). This measure can be thought of as capturing the prevailing high frequency in a given epoch. The distribution of nPeaks/s was distinct and with more peaks per second during wake than in sleep in all four datasets (Kolmogorov-Smirnov test between wake and sleep distributions, $p << 0.001$ for all datasets; paired t-test between medians of sleep vs wake, $t(3) = -3.99$, $p = 0.03$) (**Figure 3.4**). Drowsiness (a small proportion of the entire recordings) was more variable than sleep or wake with some tendency for it to be intermediate between sleep and wake (**Figure 3.4**).

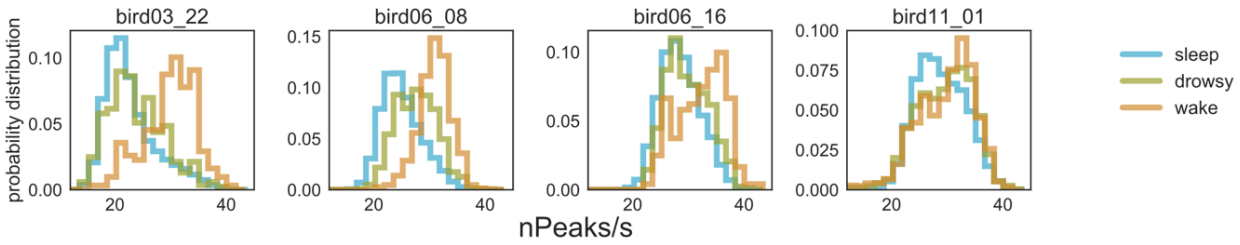

Figure 3.4. Comparison of EEG distribution across vigilance states. The probability density function of the number of peaks/second in the EEG for each dataset. Three vigilance states are compared: sleep (blue), drowsiness (yellow), and quiet wake (orange). Active wake and automatically scored datasets were not included due to movement artifact. The measure nPeaks/s can be thought of as the approximate prevailing frequency in a given epoch of EEG. Note the middle two datasets are from the same bird.

We then focused on the EEG during nighttime sleep, comparing early-night sleep with late-night sleep (**Figure 3.5**). Confirming the results of (Low et al., 2008), we found that log(delta) was highest in the first half of the night and decreased thereafter (paired t-tests: $t(4) = 11.86$, $p = 0.0003$) (**Figure 3.5A**). Conversely, nPeaks/s increased throughout the night ($t(4) = -5.58$, $p = 0.005$). While the ratio theta/delta increased slightly but nonsignificantly ($t(4) = -2.57$, p- = 0.06), the ratios beta/delta and gamma/delta both increased significantly across the night (beta/delta $t(4) = -4.8$, $p = 0.009$; gamma/delta $t(4) = -3.21$, $p = 0.03$). This pattern of a decrease in low-frequency activity and an increase in high-frequency activity held true over most individual nights (**Figure 3.5B**) (paired t-tests, treating nights as independent: log(delta) $t(13) = 15.35$, $p = 10^{-9}$; theta/delta $t(13) = -3.19$, $p = 0.007$; beta/delta $t(13) = -4.92$, $p = 0.0003$; gamma/delta $t(13) = -3.76$, $p = 0.002$; nPeaks/s $t(13) = -6.49$, $p = .00002$)

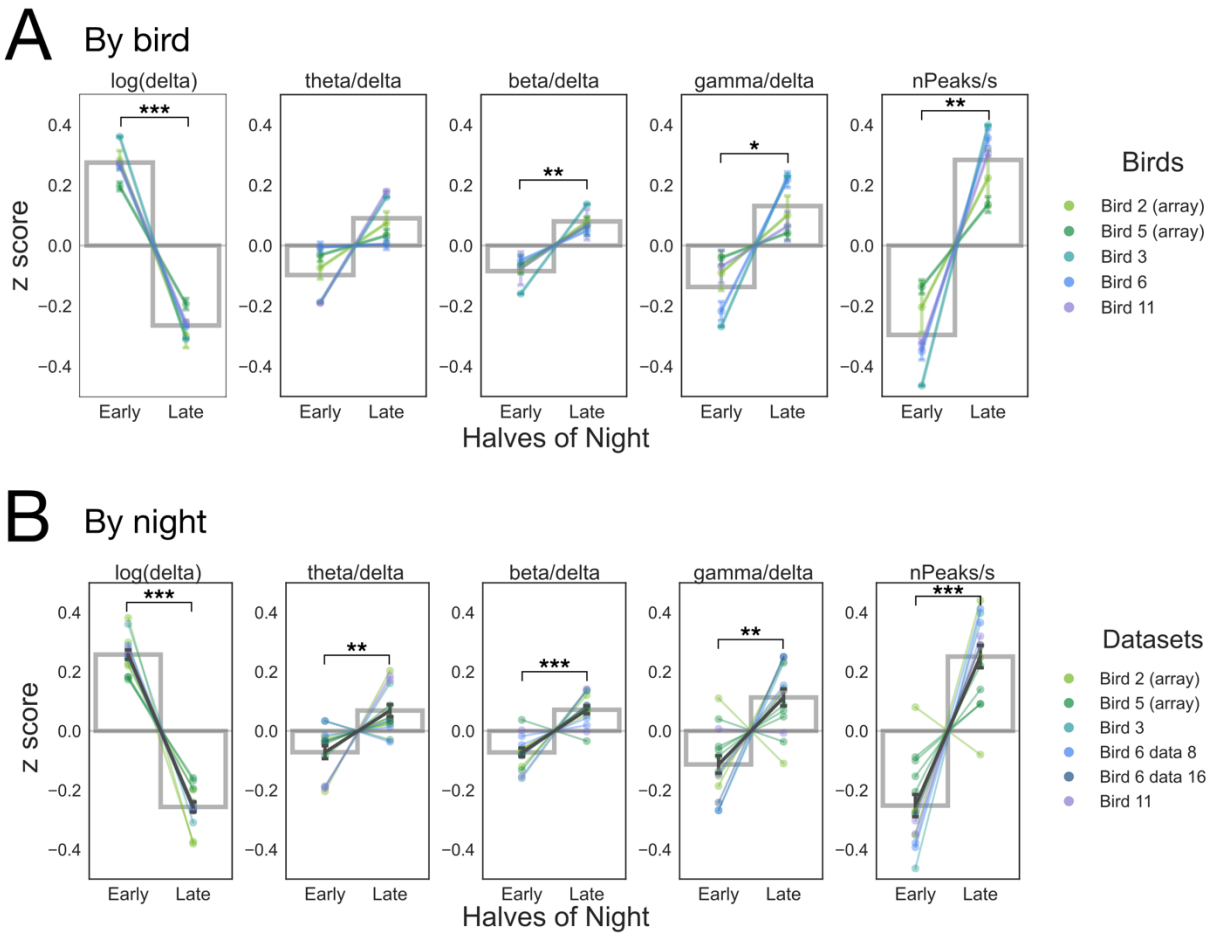

Figure 3.5. Time course of EEG/LFP features across the night. The z-score of five different measures are plotted for each half of the night. Note Birds 2 and 5 were scored automatically, and for these birds the measures shown here were calculated from the LFP in RA, collected from a multichannel array. For all other birds, the surface EEG was used. A) Each point corresponds to the mean across all nights for each bird. Error bars, SEM. Gray bars show the grand mean across all birds. B) Each point corresponds to a single night. Mean and SEM for all nights is plotted in black. Grey bars show the mean across all nights. * $p < .05$; ** $p < .01$; *** $p < .001$.

Ultradian rhythms at multiple timescales

We observed rhythmicity at several scales in plots of spectral measures of most nights of data (**Figure 3.6A**) and the autocorrelation thereof (**Figure 3.6B**). To explore this, we further analyzed the gamma/delta ratio both as a check for consistency with past work (Low et al., 2008; Shein-Idelson et al., 2016) and because the gamma/delta ratio seemed to capture these rhythms most robustly. For gamma/delta (**Figure 3.6C**), in the 10-second, 1-minute, and 10-minute

rolling means respectively, the mean periods found were 90.45 ± 39.12 seconds, 5.09 ± 0.75 minutes, and 37.75 ± 8.34 minutes. These ultradian rhythms were markedly similar across datasets, although variation occurred both within and between birds (**Figure 3.6C**) and could also vary during the course of a given night (**Figure 3.6A**). In several birds, the ~38-min rhythm appeared to start out more slowly and speed up over the course of the night.

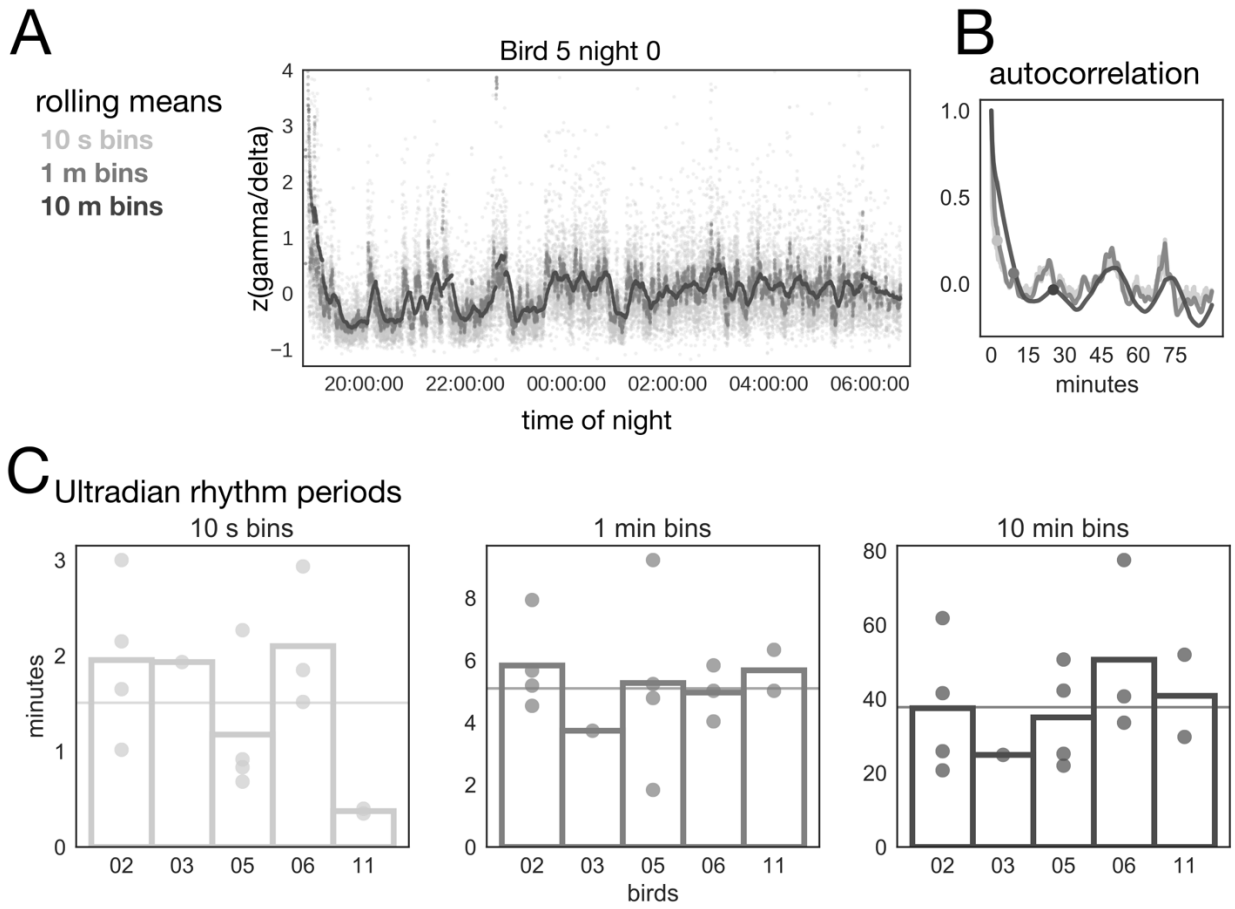

Figure 3.6. Ultradian rhythms. The z-score of the LFP gamma/delta ratio during sleep, plotted for one night from Bird 5. Each point corresponds to a 3-second epoch, smoothed over fine to coarse resolution with rolling means taken over 10 seconds (light grey), 1 minute (medium gray), and 10 minutes (dark grey). B) Autocorrelation of the data from panel A. Points indicate the leftmost peak for each of the three rolling means. C) Summary across all birds. Each bar corresponds to one bird, with points indicating individual nights. The horizontal line shows the mean across all birds.

Discussion

These findings confirm previous work on sleep/wake patterns and spectral characteristics of sleep in zebra finches. Here we show that finches sleep in a consolidated block over the night; that slow-wave activity (delta power) is highest at the beginning of the night while high-frequency activity (associated with REM) is highest at the end; and that finches' sleep is structured by a set of consistent nested ultradian rhythms.

The amount of sleep at night (87.1%) was remarkably similar to previous reports of 91.3% (Shank, 2008) and 88.3% (Schmidt, 1994). However, during the day, manual behavioral scoring showed that birds slept far less during the day (14.8%) than had been previously found (33.8%) (Schmidt, 1994). One possibility is that this previous study misclassified drowsiness and/or quiet wakefulness as sleep, which is plausible given the rapid and frequent transitions between sleep and drowsiness during the day. The automated scoring algorithm, which found results very close to manual scores in most other respects, returned an amount of daytime sleep (29.5%) close to this previous report. An alternative explanation is that the birds in this study were more active, which could result both from the presence of a conspecific and from the high degree of acclimation. Due to the nature of the coupled extracellular experiments, birds were given an unusually long time to become accustomed to carrying the implant and the tether – in most cases at least several months had passed between surgery and recordings.

Spectral analyses supported previous findings that, like mammals, birds have more SWS early in the night and more REM later in the night. Delta power, often used as a measure of slow wave activity, was highest in the first half of the night and declined thereafter. Total slow wave activity may be slightly underestimated here, due to the use of fewer EEG electrodes than is typical, and the default 1-Hz filter imposed by our recording software. While this may diminish

some of the amplitude in the delta band (0.5 – 4 Hz), studies of avian slow waves have been successfully conducted using highpass filters as high as 1.5 Hz (van der Meij et al., 2019).

In contrast to the delta pattern, higher frequencies, particularly beta (here defined as 8-20 Hz) and gamma (30-55 Hz), increased across the night. These frequencies have been associated with REM in zebra finches (Low et al., 2008; Shank, 2008), and therefore the increase likely reflects the increase in REM over the course of the night.

These results also validate the use of nPeaks/s as a robust measure for differentiating between vigilance and sleep states. Furthermore, at least for the global assessment of sleep state conducted here, the LFP from deep in the brain (RA, 2.1 – 2.5 mm deep) produced results indistinguishable from the surface EEG patterns. This is consistent with the discovery that slow waves travel throughout the avian pallium in three-dimensional "plumes" (Beckers et al., 2014; van der Meij et al., 2018). Global sleep structure appears to be relatively unaffected by small differences in the timing of slow waves as they travel between deep and superficial locations. This supports the use of LFPs for tracking sleep state, which opens the door to analyzing sleep in extracellular data not specifically collected with this purpose in mind.

Ultradian rhythmicity was observed at several frequencies, echoing the "fractal" nature of multiple nested ultradian rhythms observed in other systems such as the locomotor behavior of quails (Guzmán et al., 2017). The 5-minute period resembles the interdigitation of high and low frequencies observable in a previous report on zebra finch sleep (Low et al., 2008). The 38-minute period is remarkably similar to the longer ultradian rhythm found in the budgerigars (34 minutes) and to a 27-minute rhythm previously reported in zebra finches, in a population that included both head-fixed juveniles and freely moving adults (Shank, 2008).

Such a rhythm has not been reported in other avian sleep studies, many of which were conducted without spectral analyses of EEG signals. This includes previous studies of both budgerigars (Ayala-Guerrero, 1989) and zebra finches (Schmidt, 1994). One study in starlings (a songbird) reported a 3-hour rhythm in sleep/wake cycles at night and commented that "this rhythm, if it exists in starling, can be considered as vestigial" (Szymczak, 1986b). This dismissal may reflect the prevailing notion at the time that most birds slept in a fragmentary and unstructured fashion. For example, a report on pigeon sleep specifically described REM as occurring "aperiodically" (Van Twyver and Allison, 1972). However, the present findings add to a body of data that suggest otherwise. The significance of finding strong ultradian rhythms in avian sleep is twofold. First, it supports the emerging hypothesis that sleep in birds is regulated in a fashion similar to that in mammals. Second, it extends a key hypothesis of sleep function to include birds: namely, that alternating NREM and REM cycles work reciprocally to consolidate memory (Ficca et al., 2000; Yang et al., 2014; Li et al., 2017).

One key difference between this study and most avian sleep experiments was the presence of a conspecific. In a few previous studies, birds had auditory contact with conspecifics in the same room (Szymczak, 1985), or in exceptional studies the birds roamed free in the wild (Lesku et al., 2011a; Tisdale et al., 2017), but more typically birds are isolated. The presence of a cagemate may have resulted in more natural sleep patterns, given that zebra finches are a gregarious species (Morris, 1954) and would rarely sleep alone in the wild. It is also possible that the birds could disrupt each other's sleep, for example by causing noise during nighttime awakenings. However, the benefits of providing a familiar cagemate likely outweigh any disadvantages. There is evidence in ducks, for example, that birds switch from unihemispheric sleep to deeper

bihemispheric sleep when conspecifics are in a position to guard against threats (Rattenborg et al., 1999).

One limitation of the present findings is that the population under study was exclusively male. In mammals, sleep architecture can vary with gender: for example, in humans, women have more SWS (Armitage et al., 1997; Hume et al., 1998) and possibly more REM (Kobayashi et al., 1998). Thus far, gender differences in sleep have not been reported in birds, except for total sleep amounts during the breeding season. During this period, males of two species (sandpipers and herring gulls) have been found to spend more time awake, either displaying (Lesku et al., 2012) or guarding the nest (Amlaner and McFarland, 1981). The extensive nighttime singing of many species of diurnal songbirds (Walk et al., 2000; Van T La, 2012; Celis-Murillo et al., 2016) suggests that gender differences in sleep in breeding songbirds may be a fruitful avenue of future research. It would be interesting to know if more general gender differences manifest in sleep structure itself, and whether such differences might be related to song learning, which in zebra finches is restricted to males.

CHAPTER 4. A METHOD FOR LONG-TERM, HIGH-DENSITY MULTICHANNEL RECORDING IN FREELY-MOVING BIRDS

Introduction

The ability to record from large populations of neurons over long periods of time has yielded much insight into brain mechanisms. Long-term population recordings have been thoroughly developed in small mammalian model organisms such as rats and mice, with techniques ranging from electrophysiological to optical (Nicolelis and Ribeiro, 2002; Stosiek et al., 2003; Grewe et al., 2010; Patel et al., 2016). These techniques are beginning to be extended to small songbird model organisms, such as zebra finches and Bengalese finches, used to study forms of complex skill learning, motor critical periods. And vocal communication abilities not present in lab rodents. In particular, calcium imaging techniques have been used to record population activity in the nucleus HVC which is located near the dorsal surface hence providing technical advantage (Peh et al., 2015; Picardo et al., 2016; Daliparthi et al., 2019).

The song system includes many other regions of interest, but due to the nuclear structure of the avian brain many of these lie deep below the surface, which gives rise to additional challenges for optical imaging. Furthermore, the temporal resolution available with current imaging techniques such as intracellular calcium imaging is relatively coarse as compared to the timing resolution of individual spikes or spike bursts observed in some systems. In the song system, fine temporal resolution is critical for resolving the timing of neural activity driving the song (Hahnloser et al., 2002). Additionally, electrophysiological recordings provide simultaneous information from the local field potentials (LFP) which can inform numerous

research questions, including the role of sleep (Dave and Margoliash, 2000; Nick and Konishi, 2001; Derégnaucourt et al., 2005; Shank and Margoliash, 2009) and for studying oscillations involved in song production (Day and Nick, 2013; Markowitz et al., 2015; Lynch et al., 2016). All these considerations promote the use of extracellular recordings simultaneously from multiple sites in the songbird song system.

To record extracellularly from multiple cells in songbirds, studies have used tetrodes (Yanagihara and Hessler, 2011a; 2011b), microwire arrays (Markowitz et al., 2015), carbon fiber arrays (Guitchounts et al., 2013), and fixed silicone arrays (Beckers et al., 2014; van der Meij et al., 2018). But depending on experimental goals, in songbirds the behavior of interest often takes place across long periods of time — for example, juvenile learning (Tchernichovski, 2001; Ravbar et al., 2012), manipulation of auditory feedback (Lombardino and Nottebohm, 2000; Fukushima and Margoliash, 2015), conditional pitch shifting (Tumer and Brainard, 2007), and adult maintenance of song over days (Chi and Margoliash, 2001; Rauske et al., 2010; Wood et al., 2013). Thus, it is highly desirable to record from the same cells over long periods of time (e.g. > 1 day). While each of the electrophysiological techniques already developed have shown promise, carbon fibers and fixed arrays rarely yield single unit activity (although see (Markowitz et al., 2015)) and have primarily been used to obtain multiunit and LFP recordings. Tetrodes, on the other hand, have been used to record single units in Area X and NCM for up to several hours, but recordings lasting more than a few hours have not been reported (Yanagihara and Hessler, 2011a; Yanagihara and Yazaki-Sugiyama, 2016).

Several difficulties arise when trying to incorporate techniques established in mammalian systems. The small size of the zebra finch, which makes it a convenient lab organism, also imposes a significant weight constraint. A typical zebra finch weighs 12-15 g and can carry no

more than 1.5 – 2 g on its head. Very long recordings from single cells are challenging due to finches' quick movements and flight abilities. Finally, the cytoarchitecture of the avian brain is distinct in terms of organization and neuronal density (Reiner et al., 2004; Olkowicz et al., 2016) from the far more studied mammalian cortex. The small cells, high density, and in some cases robust population activity yield poor signal to noise (SNR) using traditional multisite arrays such as NeuroNexus arrays. We anticipate a similar result using Utah arrays but have not investigated those. This further contributes additional challenges when implementing multichannel spikesorting techniques developed for use in very different systems (Pachitariu et al., 2016; Chung et al., 2017; Yger et al., 2018).

During the research for this thesis, a significant effort was directed towards development and testing of new methodologies to facilitate long term recordings of single neurons from zebra finches. This work was conducted in collaboration with another graduate student, Graham Fetterman. Here we describe in detail a method for using high-density multielectrode arrays mounted on screw microdrives with an on-head headstage, including fabrication steps and surgical procedures. We will also briefly describe the use of these techniques with small assemblies of 3-4 metal electrodes. The steps illustrated include the construction of the implant; surgical implantation of the array; recording techniques; and analysis, including a suggested protocol for multichannel spikesorting (Chung et al., 2017). In addition, it was necessary to develop a lighter headstage than was available. The development of the headstage was a team effort (myself, Fetterman, and Margoliash). Our efforts were spurred by experience we gained in collaboration with Kyler Brown, using an approach developed by Hamish Mehaffey in the laboratory of Michael Brainard. We are grateful for the unfailing generosity of Dr. Mehaffey to

help us in those initial steps. The following is written with extensive detail, to serve as a manual to help train future students in these techniques.

Implant construction

Lightweight custom headstage

The advent of integrated circuits from Intan Technologies for making population extracellular electrophysiological recordings has revolutionized the field. One advantage of this miniaturized hardware is the ability to mount the amplifier board (carrying the Intan chip, I/O connectors, and ancillary hardware) on the head of the animal. Intan chips provide for digitization of multiple electrophysiological channels and multiplexing them onto a Serial Peripheral Interface (SPI) bus requiring between 6 and 12 wires, depending on configuration, effectively addressing the wiring issue presented by multiple channels. Furthermore, by digitizing the signal at this early point in the chain, artifact can be greatly reduced. Intan amplifier boards, however, are presumably built for mammalian (rodent) research animals. In any case, considered as devices to be surgically mounted on an animal's head (i.e. a headstage), the Intan amplifier boards are too large for making recordings in freely moving zebra finches. For example, the 32-channel Intan headstage is 24 x 15 mm and 0.94 g (**Figure 4.1, left**), and is thus physically too large for a zebra finch to comfortably carry on its head; the weight of the entire assembly (including Microdrive) would surpass the 2 g weight a bird could carry. Even the smallest, most recently developed 16-channel Intan amplifier board is too large for recording from small songbirds and would not support many channels.

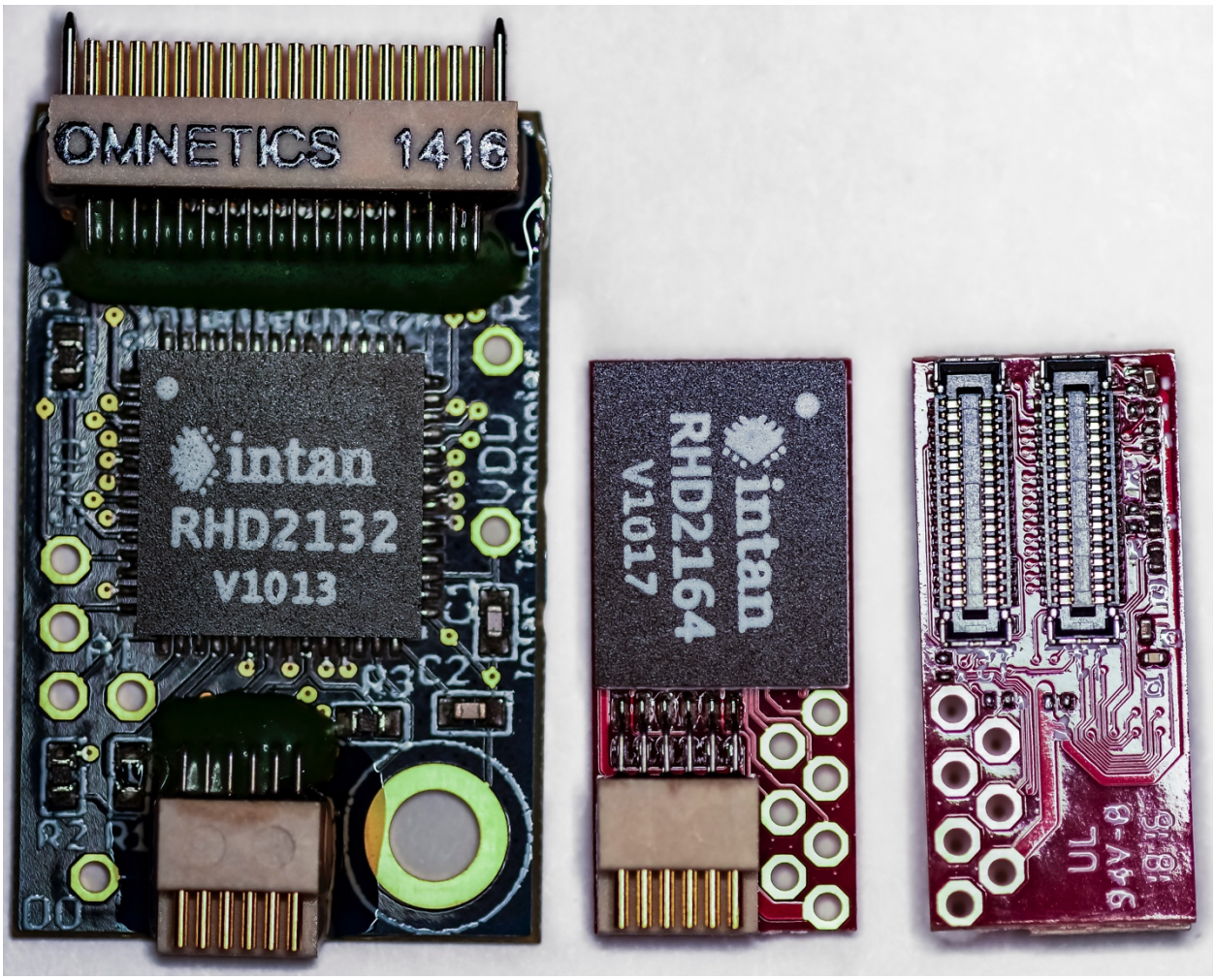

Figure 4.1. Comparison of headstages. Left, commercial 32-channel Intan headstage. Center, front of 64-channel custom lightweight headstage, on which the Intan chip and Omnetics connector for SPI bus are mounted. Right, back of custom headstage with two 32-channel Slimstack connectors. Photograph by Daniel Baleckaitis.

Spurred by our limited success using NeuroNexus probes, and the size of Omnetics Nanoconnectors (which were at the size limit for zebra finches even for the 32 channel headstage developed by Dr. Mehaffey) we explored a range of professional contacts to identify an alternative strategy. Initial contacts with Dr. Timothy D. Harris (Janelia Research Campus) identified a promising new electrode array technology. We confirmed the utility of these arrays with acute recordings in the forebrain nuclei HVC and RA using prototype arrays generously provided by Dr. Harris. We then developed contacts with Tahl Holtzman, President of

Cambridge Neurotech, who was commercializing the arrays, and Bruce Kimmel, President of Vidrio Technologies, the company which provided expertise to develop a new headstage based on our specifications. The Cambridge Neurotech probes offer improved SNR and smaller and higher density recording pads. A limitation of the CNT probes is that they are expensive, and they were not designed to be recovered from an animal and re-used (but see below). Importantly, the CNT probes can be ordered with Molex SlimStack connectors having 0.025" spacing, double the density of Nanoconnectors. A potential limitation of SlimStack connectors is that they have a life expectancy of only 30 connect/disconnect cycles. In practice, to date we have not found that to be a practical limitation.

With these considerations in mind, the collaborative team designed a minimally-sized headstage using the 64–channel Intan BGA chip (**Figure 3.1, center and right**). The core capability of each Intan chip includes fixed gain (20x) amplification per channel, programmable low and high pass filtering, 16–bit digitization at 30kHz/sample, and multiplexing onto a reduced 8–wire SPI bus (each of four SPI channels requiring two wires for low-voltage differential signaling, and with master/slave wires for controlling a second chip eliminated) with two additional wires for power and ground. For 64 channels (unipolar amplifiers), the chip is 7 x 9 mm, with 104 contacts arranged in a ball grid array (BGA). The assembled board has two SlimStack I/O connectors on its back (to minimize the surface area of the headstage) (**Figure 3.1, right**), and a single Omnetics polarized PZN-12-AA connector (**Figure 3.1, center**) to carry the SPI bus signals. Compared to the Intan 32-channel headstage, the surface area of the custom board (7 x 16 mm) is 31%, the weight (0.38 g) is 40%, and yet the board offers double the channel count. Our experience to date has been promising, although the SNR is low enough to make spike processing challenging, and at a given depth (recording site) in the brain we typically

identify only a single site (contiguous set of neighboring recording pads) that contains useful data (see Chapter 5).

Microdrive

The microdrive was created using the specifications provided in (Vandecasteele et al., 2012), which utilize a set of common and inexpensive components (**Figure 4.2**). To fabricate taller microdrives the nut can be placed below the top plate.

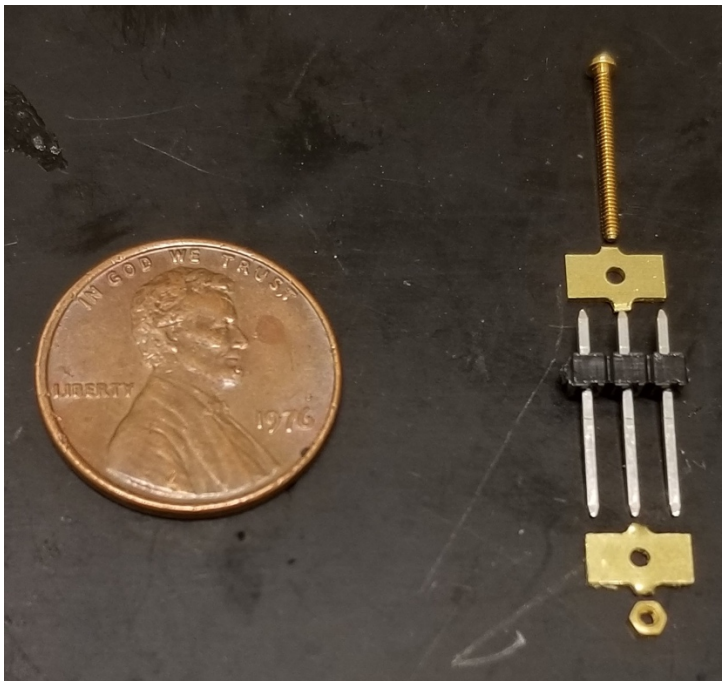

Figure 4.2. Components of microdrive. From top to bottom: brass screw, brass top plate, pin headers, brass bottom plate, brass nut. Photograph by Graham Fetterman.

The electrodes or array are attached to the microdrive's shuttle, which can move up and down along two rails constructed from pin headers (**Figure 4.3**). The rails are supported by a base plate and top plate. The shuttle is moved by turning a screw, which runs through a threaded hole in its center and is secured by a nut beneath the base plate. Due to the length of the arrays, the microdrive should be made as tall as possible. We use 0.5" (13 mm) long 00-90 screws

(McMaster-Carr, Elmhurst, IL) and 16 mm headers for a final microdrive height of about 12 mm from base plate to top plate. With these screws, 1/8 of a turn counterclockwise will move the shuttle down 35 μm.

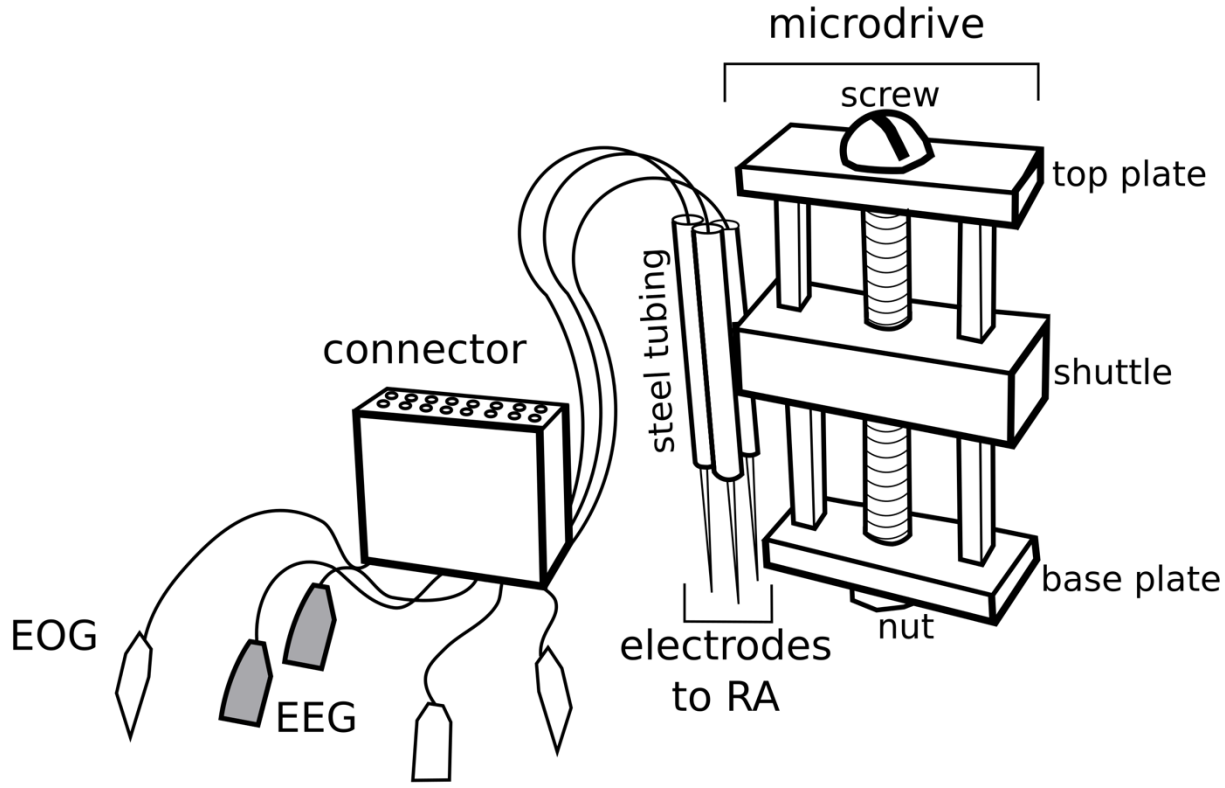

Figure 4.3. Diagram of microdrive and electrode assembly. Shown here: the custom-made electrode array and additional polysomnographic electrodes.

Prior to attaching the array, move the shuttle to the desired position, usually between one-half and two-thirds of the way up the rails. This allows for more than sufficient downwards throw but ensures the array can be raised out of the brain during recovery, which lowers the chances of damaging the array.

At this point the microdrive can be placed in a microdrive holder (itself custom-built by Daniel Baleckaitis), and bone wax applied to the screw to prevent dental acrylic from binding it. Completing these steps before attaching the array to the holder minimizes risk to the array. Bone

wax is applied with a clean syringe tip attached to a long cotton swab. Liberally apply the bone wax around the nut and the bottom of the screw, ensuring there are no gaps that acrylic could flow into. Do not apply bone wax to the remainder of the bottom plate; this is where the acrylic will adhere in order to secure the microdrive to the skull.

Microdrive holder

To attach the microdrive to the stereotax, hold it securely, and remove it easily during surgery, a holder (**Figure 4.4A**) was designed and built by Daniel Baleckaitis.

The microdrive holder is made up of two sections. The top section is made of a plastic (Amerilok HSS-86) CPVC spacer. These spacers come in two shapes: rounds and hexagons. The important measurement is the internal opening: the one used here was chosen to fit the piston on a Narishige MO-8 hydraulic drive. The spacer had two holes drilled and tapped: the first, near the top, is tapped to accept a ⅛" fine thread machine screw, which attaches the microdrive holder to the Narishige piston. A second hole can be tapped to accommodate a 1/72" screw which will run through both pieces of the bottom section (not shown; see below).

The bottom section is made up of two layered pieces of metal connected by a screw. The two metal pieces are constructed from small sheets of brass or aluminum (~ 5/16" wide x ¾" long x ⅛" thick each). The bottom layer will slide under the microdrive's top plate and support it, while the top layer will press down on the microdrive's top plate to secure it in place.

The bottom piece has one 90° bend, ¼" from the end. Three slots are cut into this bent portion (done with a small file) to accept the central screw and the two rails of the microdrive. On the opposite end of the bottom piece, one hole is made to accommodate than a 1/72" screw. The bottom layer is then epoxied to the spacer. If a corresponding 1/72" hole was tapped in the spacer, it should be lined up with the hole in the brass piece.

The top piece of metal has two 90° bends, each of roughly ¼" length: one to hold the microdrive and another as a tab to push down on. A long slot is cut through the central portion, allowing this layer to slide up and down the screw. In the bent portion, another slot to fit around the screwhead on top of the microdrive. The 1/72" screw is then inserted to pass through the slot in the top piece and screw into the tapped hole in the spacer.

When secured, the holder sandwiches the top plate of the microdrive (**Figure 4.4B**). It requires a small amount of downward pressure and the tightening the screw to hold the microdrive securely in place between the metal pieces. A small pocket for the headstage can be constructed out of tape and attached to the side of the microdrive holder (**Figure 4.4A,B**).

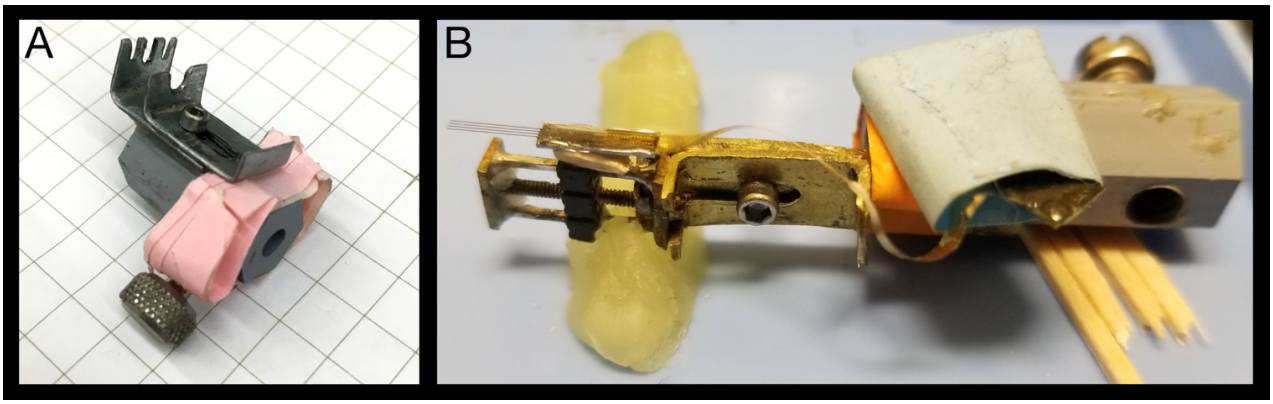

Figure 4.4. Microdrive holder. A) Empty microdrive holder, with slots for microdrive toward the top left and spacer opening for attaching to stereotax toward the bottom right. Grid is ¼" squares. B) Microdrive (at far left, oriented horizontally) in microdrive holder with array attached to the shuttle. This microdrive holder is of a slightly earlier design; the bottom piece of metal, rather than the spacer, is tapped to accommodate the central screw. Also shown (at right) is the small pocket for the circuit board and headstage, connected to the array by a ribbon cable. Photograph by Graham Fetterman.

Attaching the array to the microdrive

The array will now be attached to the side of the shuttle with non-sag epoxy (Hardman Double Bubble Red Epoxy2, Royal Adhesives & Sealants, Wilmington, CA).

1. Trim the red and white wires (ground and reference) to the desired length. They will eventually be trimmed completely, but at this step leaving them around 1 cm long can make handling the array easier.
2. Secure the microdrive by pressing a small blob of wax onto a glass slide. Push the microdrive into the wax with the desired side of the shuttle facing up.
3. Prep the side of the shuttle by scoring it in a cross hatched pattern with a scalpel or razor blade.
4. Clean the side of the shuttle with a drop of isopropyl alcohol.
5. With a toothpick or a needle, place a small blob of epoxy on the scored surface.
6. Remove the array from the packaging. This can be accomplished safely by pressing one finger to the small circuit board from which the shanks protrude. (Be careful not to touch or brush the shanks. They should be pointing away from the tip of the finger, with the finger parallel to the ribbon cable.) Then, keeping the finger firmly pressed against the small circuit board, flip the packaging upside down and allow the ribbon cable and attached connector to fall into the palm of the hand.
7. The array can now be handled by picking up the small circuit board with two fingers. Forceps are not recommended as the circuit board is slick, and can easily slip out. Position the array on the epoxy, pressing the small circuit board onto the side of the shuttle. Be sure to avoid getting epoxy on the shanks of the array. Generally, the array should be placed as high as possible on the shuttle. Use a syringe tip to spread epoxy on top of the board and down the adjacent sides of the shuttle. Then, using fingers or a needle to tap the small circuit board, adjust the alignment of the array such that the shanks are parallel to the microdrive screw in all three axes.
8. Let the epoxy dry overnight. Allowing the epoxy less time to set risks detachment during surgery, likely leading to damage to the array.

Custom electrode array

A small custom-made array of single electrodes can be constructed for use in place of the silicone array. The electrodes used for this technique can be of any type as long as they are sufficiently short. The length needed will depend on the depth of the target brain area; for superficial nuclei such as HVC, the insulated portion of the electrode should be ~5 mm. We typically use lab-made platinum-iridium electrodes insulated with melted powder glass (Dow-Corning #7570), allowing the length to be easily customized while hand-crafting the recording tip (**Figure 4.5**).

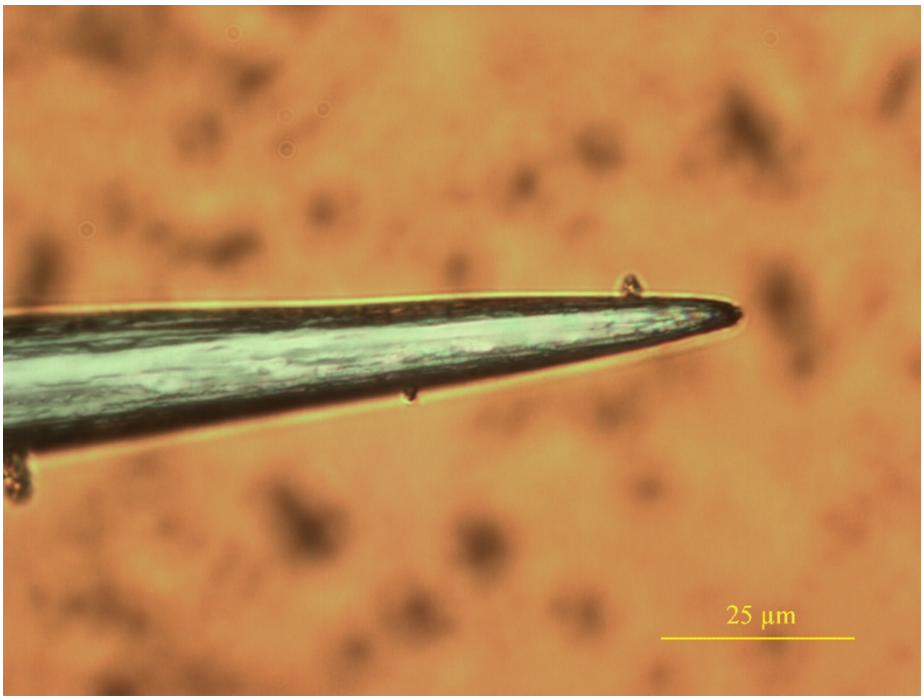

Figure 4.5. The tip of a lab-made electrode. This electrode had an impedance of 1.5 MΩ, typical of those used for single unit recordings in RA. The glass coating is slightly transparent, allowing visualization of the thinness of the coating and the smooth transition from exposed to insulated portion. Small dots protruding from the sides of the electrode are pieces of debris or dust. Note the very small surface area of the exposed portion at the tip, comparable to 5 MΩ commercial electrodes (MicroProbes; personal communication, Philip Troyk). Image courtesy of Philip Troyk.

1. To construct holders for the electrodes:
    a. Cut ~8 mm segments of 27-gauge stainless steel needle (or tube) with sharp wire cutters.
    b. Sand the cut ends down to remove the portion that has been crimped.
    c. Use a small (~30 gauge) needle or the point of a #11 scalpel blade to ream out each end.
2. Attach a wire to each holder; this wire will eventually run to the connector (**Figure 4.2**).
    a. Any insulated wire can be used, provided it is small enough to fit inside the 27-gauge needle. It can be helpful to use different colors of insulation for each electrode. This will make it easier to record the correspondence between pinout and implantation location during surgery.
    b. Cut a 0.5 - 1 cm length of wire and strip ~1 mm of both ends.
    c. Insert the wire into one end of the holder. (The electrode will later be inserted into the other end.)
    d. Solder in place — as it can be difficult to solder to stainless steel, use plenty of flux and supplement with silver paint or conductive epoxy if necessary.

3. Reinforce the solder joint with a small blob of non-sag epoxy and let dry, preferably overnight.
4. Secure the microdrive by pressing a small blob of wax onto a glass slide. Push the microdrive into the wax with the desired side of the shuttle facing up. Prep the side of the shuttle by scoring it in a cross hatched pattern with a scalpel or razor blade.
5. Attach the first electrode holder to the side of the shuttle (**Figure 4.2**):
    a. With a toothpick or a needle, paint the scored surface with no-sag epoxy.
    b. With the connecting wire toward the top of the microdrive, push one of the needle holders into the epoxy, keeping it parallel with the screw of the microdrive.
    c. Let dry for 10-15 minutes or until the epoxy "sets" and is no longer pliable.
6. To add more holders:
    a. Paint a small amount of epoxy over the exposed surface of the existing holder (attached in the previous step). This will serve as insulation to prevent the holders from making electrical contact. Be sure to avoid getting epoxy in the open end of the holder, where the electrode will sit.
    b. Push the new holder into the epoxy, positioning the open end as close as possible to the existing holder. Ideally the electrodes will be clustered in a tight area, allowing them to fit in the smallest possible craniotomy.
    c. Add as many holders as desired, typically 3-4. Let epoxy dry overnight.
7. Solder the free end of the connecting wires to the desired attachments on the connector. We typically use a 14-channel Omnetics nanoconnector with spaces for two guide posts (Omnetics Connector Corporation, Minneapolis, MN).
8. Coat solder joints with epoxy and let dry at least 10-15 minutes.
9. Before inserting the electrodes, attach the drive to the microdrive holder and apply bone wax to the screw as described above.
10. To insert the electrodes:
    a. Position the microdrive under a microscope such that the open ends of the holders are visible.
    b. Prepare a small amount of silver paint or conductive epoxy.
    c. With forceps, grasp the electrode just above the insulated portion and trim the bare end to a length of 1-2 mm.
    d. Dip the bare end into the silver paint/epoxy, and insert into one of the holders.
    e. Adjust the direction of the electrode to run parallel to the screw, by tapping gently at the base of the electrode with forceps.
11. Repeat for all electrodes, ensuring that excess silver paint or epoxy for each electrode does not overflow to avoid short-circuiting between electrodes.
    a. Let silver paint or conductive epoxy dry completely, then apply non-sag epoxy around the base of the electrodes and holders.

b. Let dry overnight.

12. Coat the ribbon cable in high vacuum grease (Dow-Corning 1597418, Midland, MI) using a toothpick. This step is critical as it will secure the ribbon cable to the side of the implant later, preventing the cable from vibrating and causing noise during movement.

Preparing the headstage: metal legs

The headstage will be secured to the bird's head with metal legs in order to prevent acrylic from contacting the Slimstack connectors (**Figure 4.6**).

The metal legs are made of 16-gauge steel wire. Cut two 8 mm lengths of wire. Alternatively, a single U-shaped section of wire can be created (as in **Figure 4.5**). Use pliers to bend the wires slightly at the middle into a 30-45° angle which will follow the curvature of the skull. Attach the straight section of the legs to the epoxied side of the headstage, using NoSag epoxy. Let dry overnight.

Figure 4.6. Attachment of metal legs to headstage. Left, bare headstage. Center, metal legs. Right, headstage with metal legs secured with epoxy. Photograph by Graham Fetterman.

Preparing the headstage: EEG-style ground

Prepare the ground wire. This can be done in several ways, but we have found that an EEG-style electrode works well.

1. To prepare the connecting wire, cut a 15 - 20 mm long piece of approx. 22 - 24 gauge insulated stranded wire. Strip about 1 mm of both ends, being careful not to cut or score the individual strands. The material used for this wire can be virtually anything with the properties that will best suit the experiment (e.g. stiffness, insulation color, etc).
2. For the EEG electrode itself, we use 32-gauge silver-plated copper wire, but other bio-compatible solid core conductive wire (e.g. gold) will work. Solder the EEG electrode material to one end of the connecting wire. Cut the EEG material to a length of 1-2 mm and flatten the end. (Note: flattening the wire before cutting it to length will result in a sharp edge and is not recommended.) The final uninsulated portion of the flattened electrode should be about 1mm square.
3. Coat the solder joint in a bead of NoSag epoxy, leaving only the flattened portion of the EEG material exposed.
4. Solder the other end of the connecting wire to the ground through-hole on the headstage. Trim any excess wire protruding from the circuit board.
5. Once all of the desired wires (including any EEG/EOG; see below) have been soldered to the headstage, coat the all solder joints to the headstage with silicone adhesive gel (732 Multi-Purpose Sealant, Dow-Corning, Midland, MI), to prevent breakage.
6. Let NoSag and silicone gel dry overnight.
7. Sterilize the ground, EEG, and EOG electrodes by placing in bleach for 5 minutes, then placing in a water rinse for at least 5 minutes.
8. If desired, the headstage can be connected to the array at this point.

Preparing the headstage: optional EEG/EOG electrodes

To add EEG wires, repeat the process used to construct the ground wire and solder to the extra through-holes on the headstage. As before, use several colors of insulation for the connecting wire; this will facilitate determining the correspondence between pinout and implantation location during surgery.

To add EOG wires, use an insulated form of the EEG material about 1 cm long. This extra length is needed to implant the electrode subcutaneously.

1. Strip about 1 mm of both ends, flatten one end, and solder the other end to the connecting wire.
2. Coat the solder joint in NoSag.
3. When implanting, the insulated portion of the EOG electrode will be slipped under the skin, while the solder joint will rest outside the skin and can be attached to the skull.

Preparation for surgery

1. Make one or two dura hooks.
    a. Secure a sterilized 30 gauge needle to a cotton bud or syringe.
    b. Push the needle tip perpendicularly against a clean glass slide.
    c. Check the needle tip under a microscope. Repeat the process until the tip is bent in a U-shaped hook; this should be barely visible to the naked eye. Be careful to keep the hook clean.
2. Make the plastic shield that will be used to protect the array once it is implanted.
    a. Cut a 12 mm length of 7 mm diameter plastic tubing. Then cut in half lengthwise to create two semicircular shields.
3. Clean and sterilize the surgical tools. I accomplished this in three steps. The first two steps will help to remove any debris that has adhered to tools, which an autoclave may not remove.
    a. First, scrub the tools under running water with a toothbrush and a drop of surgical detergent. Take care to scrub forceps from the handle to the tip and not vice versa to avoid bending the tips.
    b. Second, clean tools in a sonicator with a small amount of surgical detergent added to the water. Run for at least 20 minutes.
    c. Finally, dry off tools and sterilize in an autoclave.
4. Prepare a bird jacket.
    a. This can be made of either cloth or plastic-backed bench liner.
    b. Cut a 10 cm by 15 cm rectangle and cut two wing slits in one corner (4 cm long slits about 8 mm apart) perpendicular to the short edge of the rectangle (1 cm from the long edge and 2 cm from the short edge).
    c. If possible, adjust the heat in the surgery room to a warmer temperature (e.g. 22 - 24º C). Birds can lose heat quickly when anesthetized, but we find that birds do well with this combination of the bird jacket and the warm room, without the need for additional heat sources during surgery.
5. Prepare other tools and reagents as needed. Any small steps that can be completed in advance will help to reduce the duration of surgery.

Implantation surgery

Anesthesia for long surgeries

Good anesthetic technique is the most important factor in ensuring survival and recovery. Array implantation surgeries often ran 3-5 hours especially when additional electrodes were implanted. This section will go over best practices for initiating, monitoring, and maintaining anesthesia for multi-hour surgeries.

1. **Delivery of anesthetic.** We typically use isoflurane anesthesia delivered via compressed air at a rate of 2.5 LPM. Note that this rate assures proper metering by the vaporizer. The actual amount of gas delivered to the bird is vastly less. Two different types of disposable surgical masks are used, both made of inexpensive lab supplies:
    a. A large mask is used for initiation of anesthesia and administration of injections. This is constructed from a disposable 50 mL conical tube. An opening is made at the point of the cone and fitted with a small tube that can be connected to the gas flow. During surgery, the conical tube is laid on its side and secured to the bench top. The bird's entire head is placed inside the opening, allowing the surgeon access to the body.
    b. A small mask is used once the bird is placed in the surgical apparatus. This is constructed from of a 1 mL disposable transfer pipette bulb with a rectangular window cut into the side (1 cm by 1.5 cm). The narrow end of the pipette is trimmed and fitted to a tube connected to the gas flow. During surgery, the window is fitted over the beak and nostrils, and the mask is secured in place to the surgical apparatus.
4. **Reducing environmental stimuli.** Especially when first establishing a plane of anesthesia, it is important to minimize stimuli that can wake up the bird.
    a. Dim or turn off room lights.
    b. Keep loud noises and talking to a minimum.
    c. Handle the bird very gently.
    d. Birds are generally more comfortable lying on their front and will respond to anesthetic more quickly in this position.
    e. The bird's response to stimuli can be tested by gently pinching the toe.
5. **Initiation of anesthesia.** Begin at a rate of 2.25%. It should take about one minute for this to fully take effect; the eyes should close, and the breathing should slow down.
    a. If environmental stimuli have been reduced and the bird is not falling asleep, as a last resort the isoflurane can be turned up to 2.5%. It is not advisable to use a

setting higher than 2.5%; instead check for a problem in the delivery system, such as low airflow

b. In contrast, if the anesthetic is taking effect very quickly (such as very slow breathing or insensitivity to stimuli within the first minute), turn the isoflurane down to 2.0%.

c. Ideally the bird will spend the shortest possible time at the initial high level of isoflurane > 2.0%.

6. **Assessing depth of anesthesia.** At all times the anesthesia should be deep enough that no responses are apparent, the eyes are completely closed, and the breathing is around 2 Hz.

   a. If the breathing slows to around 1 Hz or becomes unusually shallow, the anesthesia may be too deep.

   b. Monitor breathing throughout the surgery every few minutes by visually inspecting the movement of the back and wings through the microscope if necessary.

7. Maintaining anesthesia.

   a. As a rule of thumb, decrease the isoflurane by 1 increment on the vaporizer if the breathing rate has settled around 2 Hz or less. (On the Ohio vaporizer I used, the increment is 0.25% between 3 and 1.5, and then 0.125% between 1.5 and 0.)

   b. If any sign of arousal is noted, including fast breathing > 3Hz, increase by 1 increment.

8. **Individual responses to anesthesia.** Some approximate numbers will be provided below, but these should be used as a guideline only. The most important deciding factor is the individual bird's response.

   a. The longer an animal is under anesthesia, the less isoflurane will be needed to maintain the surgical plane.

9. Approximate numbers throughout the surgery assuming an airflow of 2.5 Lpm.

   a. 1.75% - 2.0% until the scalp incision has been completed. The initial incision has the most potential to cause pain and to allay this, anesthesia will need to be at its deepest.

   b. 1.5 - 1.75% after the incision is completed.

   c. Continue to turn it down each time the breathing slows to 2 Hz, and turn it up each time at any sign of arousal or fast breathing.

   d. Many birds will require about 1.5% for the first 1-2 hours, and around 1.0% for the next hour.

   e. By the end of the surgery, most birds can be maintained at a rate of 0.5% - 0.75%.

10. Recovery from anesthesia.

a. Overall depth of anesthesia can be judged immediately after the isoflurane is turned off. Ideally, the bird will open their eyes or begin to respond within the first two minutes.

b. Once placed in the food dish of the recovery cage, the bird will remain awake but relatively still for a few minutes, and ideally should move to a perch within the first 10-15 minutes.

c. If the anesthesia was too deep, the bird will take longer to wake up, will spend more time sleeping, and will sit in the food dish or on the floor.

d. If the bird wakes up immediately (moving around, responding with quick movements within a few seconds) the anesthesia may have been too shallow.

Food deprivation, injections, and bird jacket

1. **Food deprive the bird for one hour** prior to surgery. This will reduce risk of regurgitation during surgery.
    a. Place the bird in the recovery cage (or simply remove the food dish in the home cage) and make water easily available.
    b. If the recovery cage is in a large room or a high-traffic area, place a cloth or towel over the cage to reduce stress.
2. **Begin the surgery.** Place the bird in the large mask and initiate anesthesia (see section on anesthesia above) using the large mask.
3. **Remove the feathers** on the head in a region ~1 - 1.5 cm in diameter.
4. **Administer subcutaneous saline**. Inject boluses of 50 µL in 2-3 locations for a total of 100-150 µL of saline.
    a. Do not inject more than 50 µL in any one site as this can lead to abscess formation. Place injections either over the lumbar muscles (easier) or in the inguinal region.
5. **Administer intramuscular (pectoral) injections** of analgesic (e.g. meloxicam) and an antibiotic (e.g. enrofloxacin).
    a. Dexamethasone can also be given especially if a large array (>= 4 shanks) is to be implanted. This will help prevent brain swelling.
6. Place the animal in the bird jacket.
    a. Gently push the wings through the wing slits and then wrap the bird in the jacket and secure with tape.
    b. The jacket should be snug but not tight. If the bird begins to open and close the beak with each breath (gasping) the jacket is too tight around the chest.
7. Place the bird in the surgical apparatus.
    a. Transfer the anesthesia to the small mask over the beak bar.
    b. Secure ear bars and the beak bar.

c. Make sure the head is centered on the beak bar, and that the bird's breathing is clearly visible. If it is not, the edge of the jacket can be trimmed back.

8. **Position the bird's body** so that it is not too close to the head.
    a. The skin on the back of the neck should be taut and not bunched; otherwise, there is a risk of making the initial incision too large and exposing the neck muscles.

Surgical approach

1. **Remove any remaining small feathers** on the scalp. If necessary, trim the feathers toward the front of the head.
2. Prepare the skin.
    a. Sterilize thoroughly with iodine.
    b. Apply topical analgesia such as lidocaine cream; wait for several minutes for this to take effect.
    c. Apply antibacterial gel around the perimeter of the area; this also helps to smooth down the feathers away from the incision site.
3. **Test depth of anesthesia**. With forceps, gently pinch a section of the scalp and monitor closely for any reaction.
    a. The isoflurane may need to be turned up temporarily while the incision is being made, or more lidocaine applied.
4. Make the scalp incision (**Figure 4.7A**).
    a. With forceps in one hand, gently pinch the scalp in the center. With microscissors (ophthalmic scissors) in the other hand, cut the section of scalp.
    b. Repeat this technique to create a Y-shaped incision. The stem of the Y should point toward the front of the head and the arms should point toward the neck. To avoid several larger blood vessels, do not make the arms of the Y too shallow (i.e. a T-shape).
    c. If EOG electrodes will be implanted, make two 2 mm incisions at the stem of the Y to create a triangular flap of skin. The frontal EOG electrode will be implanted here at a later step.
    d. Control any bleeding by pressing large paper points or Kimwipe twists against the source. If the paper point dries out and sticks to tissue, re-wet it with saline before removing.

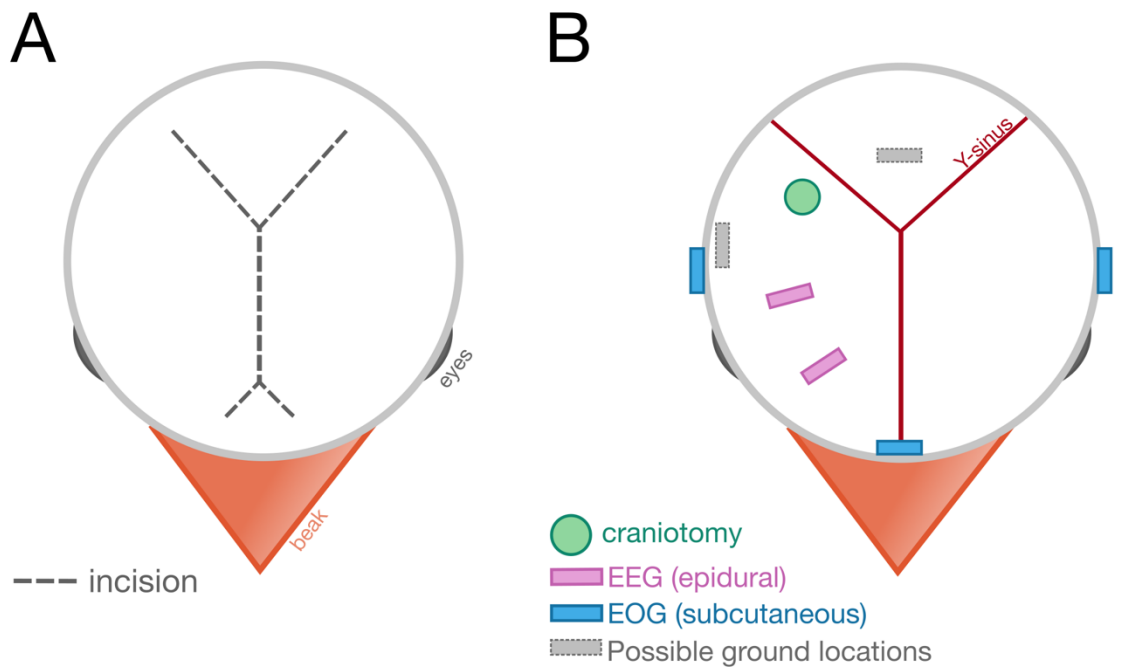

Figure 4.7. Placement of scalp incisions and electrodes. View of the bird's head from above, with the beak pointing down. A) Black dotted line indicates placement of main Y-shaped incision and small anterior flap. B) Placement of electrodes relative to Y-sinus and craniotomy. Green, craniotomy (exact location will depend on coordinates of target area). Purple, epidural EEG electrodes placed ipsilateral to craniotomy. Red, subcutaneous EOG electrodes. Grey, two possible locations for the ground (an EEG-style epidural electrode).

5. **Expose the skull**. With closed forceps, gently push the edges of the incision away from the center to expose a circular ~1 cm diameter region of the skull.
    a. Use the microscissors to trim any fascia between the scalp and the skull. Blunt dissection can also be used. Alternatively, push the fascia to the side, to minimize compromising the mechanical connection of the neck muscles.
    b. Any remaining fascia on the surface of the skull can be cleaned off with saline on a large paper point or cotton swab.
6. If EOG electrodes will be implanted, create subcutaneous channels for the two lateral EOG leads (**Figure 4.7B**).
    a. The channels will go on either side of the head, ~3-4 mm posterior to each eye. Usually this falls directly above the ears, so the ear bars can be used as a visual guide.
    b. With the forceps, pull the skin gently away from the side of the head. Then with the microscissors, blunt dissect or trim the fascia to create a channel ~2-3 mm long.
7. Begin removing the first layer of skull.

a. Use a surgical razor blade holder (also called a blade breaker) to grip the edge of a breakable razor blade and twist to snap off a small triangular piece, creating a small scalpel.

b. Hold the scalpel blade parallel to the surface of the skull and shave off the first layer, cutting through the trabeculae in between the two layers of skull.

c. When removing skull near delicate areas e.g. the posterior neck muscles, first score a line demarcating the desired area of skull to remove. When shaving off that area of skull, it should break off at the scored line.

8. **Remove the first layer of skull** over the center of the Y-sinus and the areas in which the array, the ground electrode, and any EEG electrodes will be implanted (**Figure 4.7B**).

    a. Typically the EEG electrodes should be implanted on the same side as the array. In birds, the EEG of the two hemispheres is asymmetric.

    b. The ground electrode can be implanted on either side, ideally as posteriorly as possible to avoid excessive contamination from eye movements.

    c. Another good location for the ground is the cerebellum, which has a relatively silent EEG. If using this option, the ground may need to be implanted before the array. Also make sure this site will not occlude access to more posterior recording sites such as RA.

9. **Create anchor points** by removing the skull over each arm of the Y-sinus as far posteriorly as possible.

    a. Stop just before reaching the posterior neck muscles.

    b. This should expose the two "cavities", corresponding to widened spaces between the two layers of skull on either side of the cerebellum. These cavities will act as an anchoring point for the dental acrylic later.

    c. If desired, create a few small 1-mm holes in the remaining top layer of skull; these can act as additional anchor points.

10. **If the center of the Y-sinus is difficult to visualize**, change the scalpel blade and carefully shave off the trabeculae in this area.

    a. Hold the scalpel blade parallel to the surface of the skull and cut through the struts of the trabeculae.

    b. Do not remove or nick the bottom layer of skull in this area. This sinus contains large amounts of venous blood and injuring it can be fatal.

11. Measure out the desired coordinates for the array implantation.

12. **Shave away the trabeculae in a 2-3 mm radius** around this area. If desired, use the tip of the scalpel to carefully score a small mark over the exact coordinates for implantation.

13. Shave away the trabeculae over the areas in which the ground electrode and any EEG electrodes will be implanted.

14. If the ground electrode is to be implanted over the cerebellum (**Figure 4.7B**), this should be done at this point; once the microdrive is attached this area will be occluded. See later section on implantation of EEG and ground electrodes.
15. Apply acrylic to the anchor points.
    a. Mix a thin liquid batch of dental acrylic; the consistency should be close to that of cooking oil.
    b. With a paper point, apply the acrylic to any small anchor holes that have been made in the top layer of skull.
        b.i. Use this step to test the acrylic.
        b.ii. If the acrylic is a thin enough consistency, it should easily flow into the spaces between the trabeculae.
    c. Finally, apply acrylic to completely fill the posterior cavities on either side of the cerebellum.

Making the craniotomy & the durotomy

1. During any step of this process, is important to not allow blood to pool on the surface of the brain as this can damage the brain.
    a. If there is any bleeding near or in the craniotomy, alternate flooding with saline and wicking away the saline with a large paper point or Kimwipe twist. Then flood with fresh saline.
    b. Repeat until bleeding has stopped. It may take several cycles of adding and wicking away saline.
    c. Flooding with warm saline (40 °C) and with dissolved $CaCl_2$ (Ca^{2+} is blood clotting factor IV) can facilitate clotting.
2. If bleeding is occurring outside of the craniotomy and not coming into contact with the brain, it is not necessary to fully wash it away. Instead, stop the bleeding by encouraging the blood to clot.
    a. Press a large paper point or Kimwipe twist against the location of the bleeding. The paper point can be left in place until bleeding stops.
    b. If the paper point dries and sticks to tissue at all, simply flood it with saline and it should be easy to remove with forceps.
    c. Warm saline will also encourage clotting.
3. If a blood clot forms over the area in which the array is to be implanted, it can be gently pushed aside with closed forceps.
    a. Although this may re-induce bleeding, it is important not to drive the array through a blood clot. Blood clots can hide bone chips or occlude the craniotomy edges, which can break the array.
4. **Mark the edges of the craniotomy** with a fresh scalpel blade, scoring the bottom layer of skull to outline the desired craniotomy.

a. Continue to re-score, running the blade lightly over these score marks, until it breaks through the skull.

b. Once this has been done for all (or all but one) of the sides, this will result in a trapdoor-like flap of bone resting over the desired area of brain.

5. Remove the flap of bone in one of two ways.

    a. The first is to turn the blade parallel to the surface of the skull, insert the tip under this flap of bone, and lever it up to expose the brain.

    b. The second way is to lightly press the tip of the blade into the center of the bone flap, then lift it off the brain.

6. Control any bleeding and then **apply a few drops of sterile saline** to the craniotomy. Periodically add more saline to keep the brain from drying out. Do not allow large amounts of excess saline to run onto the feathers; this can start to wake up the bird.

7. **Make the durotomy**. Use a durotomy hook (described earlier in "Preparation of tools").

    a. The fibers of the dura run in the anterior-posterior direction; the goal of the durotomy is to pull in a perpendicular direction and tear the dura along these natural lines of separation.

    b. Touch the hook to the surface of the dura and gently pull in the medial-lateral direction. It may take several passes to fully open a hole in the dura.

Lowering the array and microdrive

1. **Optional: Confirm the coordinates electrophysiologicall**y by lowering a conventional single electrode into the craniotomy

    a. This can be useful for structures such as RA, which has a readily identifiable pattern of tonic firing even under isoflurane.

    b. However, song system nuclei usually do not respond to BOS under isoflurane anesthesia so this cannot be used for localization.

2. **Check that the craniotomy is clear of bone** by gently touching the blunt end of the dura hook to the surface.

3. **Lower the microdrive and attached array** until the tips of the shanks are just touching the exposed brain. Position the microdrive in either of the orientations shown in **Figure 4.8**, depending on whether the craniotomy is more posterior (**Figure 4.8A**) or anterior (**Figure 4.8B**).

4. **Lower the array slowly into the brain** to the desired depth using a stereotaxic or hydraulic micromanipulator/microdrive.

    a. The correct depth will usually be 100-200 μm superficial to the target area. By not implanting directly in the target area this will help avoid scarring in the area of interest.

5. **If the shanks of the array bend** as they are lowered, this means they are encountering resistance and are not descending into the brain.

a. This may indicate that the dura has not been fully removed.
b. Try raising and lowering the array a few times.
c. If this does not work, retract the array and remove more dura.

6. **Seal the craniotomy** once the array has been fully lowered into the brain
    a. Flood with saline and wick away excess saline.
    b. Apply a few drops of artificial dura (Dura-Gel, Cambridge NeuroTech, Cambridge, UK) to form a thin layer (an overly thick layer can impede the movement of the shanks).
    c. If artificial dura is not available, a thick layer of viscous liquid silicone (Dimethylpolysiloxane, Dow-Corning 200 fluid, custom mixed to viscosity ~30,000 cs) can be used instead. In this case, a small well of acrylic can be built around the craniotomy to contain the silicone.
7. Attach the microdrive.
    a. Mix dental acrylic of medium thickness, about the consistency of honey. Using too thin a mixture can risk the acrylic flowing into the craniotomy and contacting the surface of the brain, causing injury.
    b. Apply the acrylic under the base of the microdrive to secure it to the skull and to the anchors created earlier.
    c. The microdrive may stand off of the skull by a couple of millimeters. If so, simply build the acrylic up to meet it.
8. **Build the acrylic up** over the sides and top of the baseplate of the microdrive.
    a. Be careful not to get acrylic onto the screw - if necessary, add more bone wax to protect the screw.
    b. Make sure to apply acrylic to the back of the baseplate, which may not be visible through the microscope.
9. **Paint a thin layer of cyanoacrylate glue** over the acrylic. This will speed up drying and reinforce the acrylic.
10. Attach the plastic shield to protect the array from the bird's scratching and from physical damage (e.g. when struck by the bird against the side of the cage).
    a. Test the size and shape of the shield; it may require trimming. It should fit around at least the sides and back of the array.
    b. Another critical purpose of the shield is to prevent the array from being crushed when the experimenter holds the array steady, i.e. while attaching a tether or turning the microdrive screw.
    c. Use thick dental acrylic and cyanoacrylate glue to secure the shield in place.
11. After the acrylic under the microdrive has fully dried, detach and remove the microdrive holder, leaving the microdrive and array in place.

Placing ground and other electrodes

1. If the headstage and the array have not been connected before the surgery, connect them now.
2. **Attach the headstage to a holder** (such as an alligator clip with flat or cushioned jaws). The metal legs can face either anteriorly or posteriorly.
3. **Lower the headstage** until the attached electrodes are sufficiently close. The ground/EEG/EOG electrodes will be implanted first, and then the headstage will be positioned on top and fixed into place.
4. **Implant all ground and EEG electrodes** (**Figure 4.7B).** To implant one electrode of this style:
    a. Clear the trabeculae from the desired area of implantation.
    b. Bend the electrode and its connecting wire into place so that it is close to where it will be implanted. This will prevent strain.
    c. The uninsulated electrode tip itself should be parallel to the surface of the brain.
    d. With a scalpel, score a line into the bottom layer of skull, perpendicular to the direction the electrode is pointing in. Retrace the line with the blade until it has broken through.
    e. Push down gently on one side of the line; the skull should separate. Slide the electrode through this gap, settling it just under the skull so it is resting on the surface of the brain.
    f. If there is any bleeding, flush repeatedly with saline. Too much blood on the surface of the electrode can damage the brain and may also compromise the quality of recording.
    g. Mix a batch of very thick dental acrylic with a consistency close to peanut butter. Acrylic that is too thin can flow into the incision in the skull and settle on the surface of the brain or coat the electrode.
    h. Apply a large bead of acrylic where the electrode meets the skull to secure it in place.
    i. Paint a thin layer of cyanoacrylate glue over the dental acrylic.
5. Optionally, implant subcutaneous EOG electrodes (**Figure 4.7B**).
    a. The lateral EOGs will be implanted under the skin lateral/posterior to each eye, in the channels created earlier. The central EOG will be implanted over the beak, equidistant to each eye, under the small flap of skin created earlier. If either the channels or the flap of skin needs to be created or expanded at this point, apply more lidocaine cream before doing so.
    b. The skin at the edges of the incision may have dried out, adhering to the skull. If so, apply a few drops of saline.

c. Bend the insulated portion of the electrode slightly to follow the curvature of the skull. Bend the uninsulated tip slightly inward so that it will not protrude through the skin.

d. Adjust the connecting wire so that the electrode is resting close to the implantation site, so that the strain on the skin will be reduced after implanting.

e. Slide the electrode under the skin about 2-3 mm keeping close to the side of the skull.

f. Use a small amount of cyanoacrylate glue to secure the skin over the electrode and prevent gapping.

g. Using very thick acrylic, secure the epoxied bead of the electrode to the skull. As much as possible, avoid placing acrylic directly on the skin.

h. Paint a thin layer of cyanoacrylate glue over the acrylic.

Attaching the headstage

1. **Lower the headstage** as close to the head as possible without putting pressure on the skull. Place in either of the orientation shown in **Figure 4.8**. Metal legs can face either direction depending on available space.

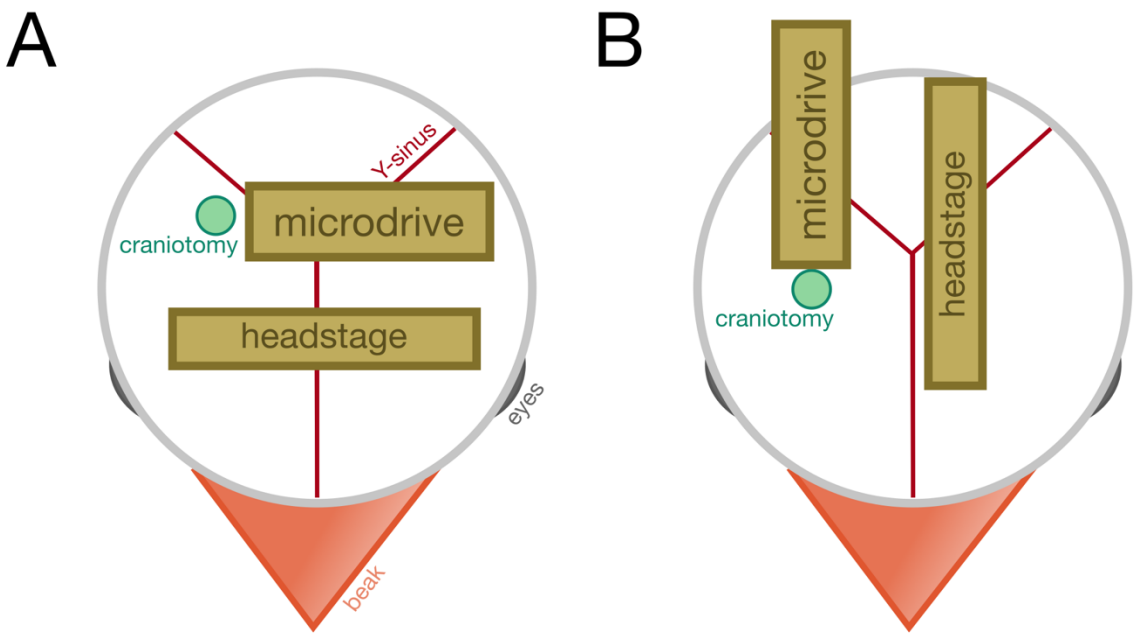

Figure 4.8. Placement of implant components. A) This arrangement is most suited to more posterior target areas (e.g. RA) but can be used in most cases. B) This arrangement is best for more anterior target areas (e.g. HVC) and may offer improved balance for the bird.

2. **Secure the metal legs to the skull** with dental acrylic. Use thin acrylic to fill in small gaps. Wrap thicker acrylic over the tops of the metal legs. Be careful not to get acrylic into the connector of the headstage itself.
3. Paint a thin layer of cyanoacrylate glue over the acrylic.
4. While waiting for the acrylic to dry, move on to the next steps.
5. Once the acrylic is dry, unclip the headstage from its holder.

Protecting the implant

1. **Seal the top of the plastic shield** to protect the craniotomy from any seeds or other debris.
    a. Cut several strips of surgical tape in halves or thirds lengthwise.
    b. Place one of these thin strips to form a "roof" over the plastic shield around the array.
    c. Secure to the shield with cyanoacrylate glue.
2. Construct the protective "hat" around the sides of the implant.
    a. Cut a large piece of surgical tape long enough to wrap around the entire implant. Check the width of the tape against the height of the implant. Trim any excess width.
    b. Cut a ~2 cm piece of surgical tape of the same width. Attach to the larger piece with the adhesive sides facing together. This will protect the ribbon cable from adhering to the inside of the hat.
    c. **Apply medium-thick acrylic** around the base of the implant. Place a small bead of acrylic on the ground wire so that it will stick to the tape shield; this will help reduce noise from vibration.
    d. **Position the large piece of surgical tap**e so that the ribbon cable will contact only the non-adhesive portion.
    e. Wrap the large piece of surgical tape around the implant to form a cylinder. Push the bottom edge into the acrylic at the base of the implant.
    f. Seal the seam of the tape with cyanoacrylate glue.
3. **Seal the top of the hat** with several long thin strips of tape.
    a. Leave only the microdrive screw and the headstage connector exposed.
    b. These strips should extend all the way to the base of the cylinder. Seal to the sides with cyanoacrylate glue and if necessary, thin acrylic.
4. If there is any gapping, use forceps to pinch sections of tape together.
5. Wrap a thin strip of tape around the base of the cylinder, sealing any gaps at the bottom of the hat.
    a. Seal the seam with cyanoacrylate glue.

6. Apply more lidocaine cream and/or antibiotic cream to the wound edges.
7. **Turn off the anesthesia** and transfer the bird to the food dish in the recovery cage.

Recovery from surgery

1. Allow the bird several hours in the recovery cage under the heat lamp.
    a. Provide plenty of food and easily accessible water.
    b. The recovery cage should be furnished with perches both low to the ground and higher up.
    c. Cover the cage with a towel (without blocking the heat lamp) to reduce stress from outside noise.
2. Check on the bird about every 30 minutes to monitor recovery.
3. The bird can be returned to the home cage either several hours after surgery, or the following day.
    a. Make sure that lights off does not occur for at least 3 hours post surgery so that the bird has ample time to eat.

Home cage setup

1. Cover the floor of the cage with cage liner. Birds recovering from a long surgery are often very drowsy and can easily get their wings or head stuck in even closely spaced cage material.
2. Provide low perches and shallow food dishes so that the bird can access food by walking. If available, add an open water feeder to encourage the bird to drink.
3. Place a sprig of millet spray in an easily accessible spot, in the food dish or low to the ground.
4. If the home cage is a divided enclosure, it can be helpful to place another bird on the other side of the cage to encourage socialization and activity.
    a. Wait 1 or 2 days after the surgery before introducing a new bird to avoid causing stress. Often the day after surgery, birds spend a lot of time sleeping and an unfamiliar conspecific can be more disruptive than helpful.
    b. However, if there is already a familiar cagemate, there may not be a need to move them during this period. This is a judgment call.

Days following surgery

1. The day after surgery, check the bird 2 - 3 times, preferably without opening the enclosure so that normal behavior can be observed.
2. Signs of good recovery include eating, drinking, and perching. The bird spending time sitting in the food dish is also normal.

3. It is normal for the bird to puff up the feathers and to spend long periods sleeping. The posture of the bird is a critical indicator. A bird with puffed up feathers standing with straight legs is severely distressed. A bird with puffed up feathers resting against a perch is comfortable.
4. Additional signs of poorer recovery include lying in the food dish, sitting or lying on the floor, not changing positions for long periods of time, and not responding quickly when the door of the enclosure is opened.
5. If recovery is average or poor, administer meloxicam. For poor recovery consider also giving antibiotic.
6. If recovery is good, it is not necessary to administer injections; it may be better to minimize any stress caused by handling.
7. For at least four to five days following surgery, repeat these daily checks and administer meloxicam (and antibiotic) as needed. Most birds will only need these additional injections on the first 1-2 days.

Recording procedures

The recording setup

The exact specifications will depend on the available equipment and the experimental goals. For the sake of completeness we will briefly describe a typical setup used to record from these arrays.

The bird's home cage measured 42 x 30 x 22 cm, split in half with a divider, and placed in a sound attenuation chamber (Acoustics Corporation, New York, AC-1). A female bird was typically housed in one half of the cage.

Once the bird was tether acclimated, the divider was replaced with an opaque Plexiglas divider. Upon finding a neuron, the divider could be swapped out for a clear Plexiglas divider, revealing the female and encouraging the male to sing.

An additional divider was built into the male's portion of the cage to make the enclosure square (a square or circular enclosure is best for use with a commutator). This made the final

dimensions 21 x 21 x 22 cm. At least two perches were placed in the enclosure, low to the ground so that there was no chance of the bird wrapping the tether around a perch.

For the tether, we used a lightweight 0.3 m cable (RHD2000 Ultra Thin SPI cable, Intan Technologies, Los Angeles, CA). This was connected to a custom-built 10-channel commutator (fabrication instructions available at https://voices.uchicago.edu/margoliashlab/tech_docs/). Depending on the cage height it was sometimes necessary to shorten the tether by creating a loop close to the commuter end of the tether.

A standard 0.9- or 1.8-m SPI cable (Intan Technologies, Los Angeles, CA) ran from the commutator to an Intan RHD2000 USB interface board (Intan Technologies, Los Angeles, CA). To ensure simultaneous recording of sound and neural activity, a microphone was secured to the ceiling of the bird's enclosure and was connected through an amplifier to one of the analog ports on the interface board.

The cage was insulated from the floor of the sound box with cage liner and then grounded to a single screw on the wall of the box. The evaluation board was likewise grounded to the sound box. A layer of copper mesh was used to shield noise from the fluorescent lights inside the box. Preferably, these would be replaced with DC-powered LED lighting.

Raising and lowering the array during recovery

Starting no later than 3 days after the surgery, it is important to raise and lower the array by a small amount daily. If the array is left is place for more than 4-5 days at a time, there is an increased chance of it adhering to the tissue and artificial dura.

Each day, first raise the array 35 - 70 µm and then lower it by the same amount; repeat this 3-4 times in a row and then release the bird. Given the 00-90 thread screw, an eighth of a turn is 35 µm. Importantly, note that turning the screw counterclockwise lowers the shuttle.

Acclimation to tether

1. Do not start tethering the bird until it has fully recovered from surgery, usually about 4-5 days.
2. Following recovery, the bird can be acclimated through gradually increasing sessions on the tether. Leave the bird untethered at least one day a week, or over weekends. This allows the bird a period of uninterrupted recovery and often seems to accelerate acclimation the following week. This schedule will depend on the strength of the bird and the speed of recovery from surgery.
3. Here are recommended times for how long to tether the bird each day:

    Day 1: 10 - 20 min

    Day 2: 30 - 40 min

    Day 3: 40 - 60 min

    Day 4: 60 - 80 min

    Day 5: 1 - 2 hours

    Day 6: 2 - 4 hours
4. Adjust these times based on how well the bird is carrying the tether.
    a. For the most accurate observations, check while the bird is unaware of experimenter presence.
    b. Signs of difficulty with carrying the tether include the head drooping or tilting to one side, excessive drowsiness, puffing the feathers, and any difficulty getting into and out of the food bowl.
    c. If these signs are present, untether the bird for the rest of the day.
    d. If these signs are especially pronounced, consider leaving the bird untethered for the next day or two.
5. Once the bird is able to carry the tether for at least 4 hours, tether overnight and untether in the morning. Repeat for at least 2 consecutive nights.
6. If the bird is carrying the tether well overnight, attempt tethering the bird for a full day; check every few hours and untether if signs of difficulty arise.
7. At this point, most birds will comfortably carry the tether for several days in a row (**Figure 4.9**). Check for singing while the bird is tethered; this is a good sign that the bird is fully acclimated. Continue to untether periodically (e.g. over the weekend) unless actively recording.

Figure 4.9. A fully acclimated tethered bird. The bird is balancing the head evenly without tilting to either side, and the posture is upright and alert. Note the copper shielding around the implant, which we tested in early versions of this procedure and found to be unnecessary for preventing noise. Photograph by Graham Fetterman.

Lowering the array: speed, how often, raising and lowering repeatedly

1. Once the bird is able to be tethered, the array can be lowered. Alternatively, if the array has been implanted very close to the target area, continue to raise and lower the array until the bird is acclimated to being tethered for the desired duration of recording.
2. Each time the array is lowered, it is best to first raise and lower it a few times to prevent adhesion to tissue.
3. The fastest the array should be lowered (i.e. if it is several hundred μm from the target area) is 2 times per day, 70 μm at a time.
4. Once the array is in the target area, move the array 1 - 2 times per day, 35 μm at a time, to search for neurons.
5. Monitor the recording for signs that the array is not moving. If this seems to be the case, it may be possible to remedy this through a short procedure:
    a. Anesthetize the bird and administer meloxicam.
    b. Remove enough of the surgical-tape shield to expose the top of the array and the plastic shield. Be careful not to damage the ribbon cable.
    c. If it is possible to visualize the array, look for bending. If there is no bending, try lowering the array slightly to see if bending occurs.

d. Load a syringe with sterile saline and apply a few drops to the inside of the shield, allowing it to flow down into the craniotomy. The saline will soften any tissue or clots that may have built up around the craniotomy.
e. Check for any other obstructions to the movement of the microdrive, such as a seed husk or piece of acrylic.
f. Turn the screw of the microdrive to move the array up and down a few times; repeat until the array is no longer bending when it is lowered. If possible, avoid lowering the array into the target area during this process.
g. Let the bird recover with no tethering for the next 2-3 days.

Software and impedances

Whenever the bird is tethered, it is a good idea to check the quality of recordings. We run the Intan Interface software provided at http://intantech.com/downloads.html.

Depending on the exact equipment and setup used, array channels can have impedances anywhere from 100 kΩ to 6 MΩ. On any given system these impedances should all be similar values. With our system 2-4 MΩ is typical, despite quoted impedances of 50 kΩ; we have corresponded with the manufacturer but have been unable to reconcile this divergence. Broken or unused array channels will have either a very low (<50kΩ) or very high (>10 MΩ) value.

EEG and EOG channels should ideally have impedances <10kΩ, but <50kΩ is acceptable.

Common sources of noise

1. **Constant rail-to-rail or harsh noise**: Check connections between all cables and connectors.
2. **Constant small angular noise waveforms**: Often related to the amplifiers on the headstage. Restart the evaluation board (which also power-cycles the headstage).
3. **Rail-to-rail noise that occurs in bursts**: Try swapping out the tether or commutator. When these components are faulty, they will introduce digital artifacts into the recording yielding waveforms that are angular in shape and which appear when the tether is at a specific angle or position.
4. **Very large movement artifacts**: This could be related to vibration of the ribbon cable or ground wire relative to the rest of the implant. A short procedure may be needed to secure these to the inside of the shield with Vaseline or grease (for the ribbon cable) or NoSag epoxy (for the ground wire). Another origin could be a faulty ground electrode or headstage.

5. **Constant or intermittent oscillatory noise** not related to the movement of the bird: Most likely not related to the tether or commutator. Check for standard noise sources e.g. ground loops (a very common culprit), AC sources inside the cage, lack of grounds, lack of shielding of AC sources, etc.

Spikesorting

Preparing data for analysis

1. Preprocess data.
    a. This includes removing any faulty channels, filtering and median-referencing.
    b. These steps can be carried out with the Bark library (available at https://github.com/margoliashlab/bark). An example Makefile containing the necessary commands is available at https://github.com/margoliashlab/analysis-scripts.
2. Split the file wherever shifts in spike waveform shapes are apparent.
    a. This can include a unit suddenly changing in amplitude, a unit disappearing or appearing, or a unit moving to a different channel.
    b. The software Neuroscope can be used to quickly scroll through the file in 5- or 10-minute increments to determine these timepoints. If the Bark format is used, Neuroscope can be easily accessed with the command bark-scope.
3. Split files into approximately 1-hour increments.
    a. This will help address the problem of spike drift. An example Makefile containing the Bark commands for splitting at specific timepoints is available at https://github.com/margoliashlab/analysis-scripts.
    b. If no split points were found in step 2, this step can instead be run in one line with the bark command dat-split.
4. Convert the file to mda format.
    a. The specifications of this format are available at https://mountainsort.readthedocs.io/en/latest/mda_file_format.html.
    b. Bark files can be converted to mda with the command dat-to-mda. A shell script to batch-convert all bark files in a folder is available at https://github.com/margoliashlab/analysis-scripts.
5. Create a geom.csv file.
    a. This file should include one row of *x, y* positions for each channel; more details are available at https://users.flatironinstitute.org/~magland/docs/mountainsort_dataset_format/.

b. Units of distance are not explicitly specified in the geom.csv file and should be the same units used for the adjacency radius parameter (see below). Instructions on creating a pinout for an Intan file are available at https://github.com/margoliashlab/array-mapping. (As of this writing, this Github repository needs to be updated to include information about geometry files for MountainSort, the spike sorting software we currently use. The repository is not yet available publicly.)

MountainSort

The MountainSort algorithm (Chung et al., 2017) first splits whitened data into "neighborhoods" of each channel with its surrounding neighbor channels. The "adjacency radius" parameter, set by the user, defines how large each of these neighborhoods are. For each neighborhood, candidate spike events are detected via thresholding. The user sets the threshold ("detect_threshold", in units of standard deviation from the mean) and the minimum time allowed between consecutive events on the same channel ("detect_interval," in units of timepoints).

The waveform of each event is then extracted and mapped onto a 10-dimensional PCA space. Clusters in PCA space are then sorted using the ISO-SPLIT nonparametric clustering procedure. This procedure uses an algorithm referred to as ISO-CUT, which determines whether a given cluster is unimodal and if not, what the optimal cut point is for splitting the cluster.

Once clusters have been defined for each neighborhood, the clusters are consolidated to eliminate redundant clusters across electrodes. Pairs of clusters on separate electrodes are compared for similar peak amplitudes and spike coincidences. Redundant clusters are then assigned to the electrode on which the spikes are largest. Finally, an iterative fitting step is used to detect any remaining redundant spikes.

Spikesorting in MountainSort

Running a spike sort in MountainSort takes three processing steps:

1. **Whitening** with ml-run-process ephys.whiten
2. **Sorting** with ml-run-process ms4alg.sort
3. **Computing templates** with ml-run-process ephys.compute_templates.

Documentation for using each of these commands can be accessed by running ml-spec.

First, decide on parameters for the sorting step. This can be done by running a parameter search on one file. The two parameters of interest are:

1. The "**detect_threshold**," in units of standard deviation from the mean, determining how large deflections must be to qualify as candidate events.
2. The "**detect_interval**" defines the minimum time allowed between consecutive events on the same channel. Note that because the sorting step does not incorporate sampling rate information, the interval is measuring in time points, which will depend on sampling rate.

An example script for running a parameter search on a single file is available at https://github.com/margoliashlab/analysis-scripts. The user can also set the "detect_sign," the "adjacency_radius," and the "clip_size."

1. The "**detect_sign**" parameter determines the sign of the events to be detected: -1 for negative spikes, 1 for positive spikes, and 0 for both.
2. The "**adjacency radius**" determines how many adjacent electrodes will be included in a neighborhood — in other words, how many channels are expected to detect the same neuron? The units are the same as the units in the geometry csv file.
3. The "**clip_size**" is a parameter for the last step of computing templates and will determine how long each template will be, again measured in time points.

After running the parameter search, use the automated Mountainview script (see below) to get an overview of the clusters found. If necessary, open a few of the best sorts in Mountainview manually and use the "All auto-correlograms" and "Timeseries" view to further examine the results. Choose the best parameters and run the sort on an entire dataset. The shell script used for sorting and viewing a folder full of hour-long data segments is available at https://github.com/margoliashlab/analysis-scripts.

Mountainview

To look at the MountainSort output, run Mountainview from the command line. When the program first opens, it will take some time to display the data. The first view opens automatically and shows each cluster found, its average waveform across channels, and its firing rate.

Usually each channel will have at least one noise cluster. Depending on parameters, these noise clusters will include varying numbers of spikes and may have merged with the neuronal clusters of interest. Thus, the first way to evaluate a sort is to look for more than one cluster per channel. A true neuronal cluster will usually have a waveform that appears across a small group of adjacent channels, and a markedly different firing rate from the noise clusters.

To further examine the clusters, use additional views in Mountainview by clicking on the buttons on the upper left panel. The "all auto-correlograms" view is useful for getting an overview. A single unit should have a clear refractory period, resulting in an autocorrelogram that dips close to zero lag.

Some of the views are specific to a single cluster. Click on a cluster of interest then select "Timeseries" to look at the raw data overlaid with the sorted events. The cross-correlogram view can be used to determine if a cluster should be merged with any of the other clusters.

To quickly get an overview of a large number of sorts, a batch script is included in the Appendix. This script runs through each file in a given folder, open it in Mountainview, waits for it to load, then saves a screenshot. The user can then quickly page through all of the screenshots and record potential clusters of interest and their firing rates.

Specific results using MountainSort and Mountainview for this thesis work are reported in Chapter 5.

Converting back to bark

The main output of MountainSort is the "firings" file, saved in mda format. To convert this to a .csv file in the bark format, use the command bark-convert-mountainsort. A batch script for this is available at https://github.com/margoliashlab/analysis-scripts.

Array recovery

1. Although the arrays were not necessarily designed for this, they can be recovered at the end of an experiment, cleaned, and re-used.
    a. For reuse after an acute experiment, see the section "Cleaning the array."
    b. For reuse after a chronic experiment, first follow these steps to extract the array.
2. Perfuse or euthanize the animal as normal.
    a. If perfusing, be sure to use proper ventilation for the rest of this procedure to minimize your exposure to formalin fumes.
3. Turn the microdrive screw to raise the array up as far as possible.
    a. Ideally, the shanks will be raised completely out of the brain at this point, but if the targeted area was very deep this may not be the case.
4. Wrap the bird in a protective cover.
    a. In the side of a ziplock bag, cut a slit large enough for the bird's head.
    b. Place the bird in the bag with its head through this slit, wrap the bag around the bird's body, and seal the ziplock opening. The bird should now be completely encased except for the head.
    c. This will both protect the surgical apparatus and reduce formalin fumes.
5. Place the bird in the surgical apparatus and secure the head with beak and ear bars.
    a. Secure the microdrive in its holder to further stabilize the array.
6. Remove the surgical tape shielding with forceps.
    a. Be careful to avoid the ribbon cable and other sensitive parts of the implant.
    b. Small scissors can also be used to cut away the surgical tape. Be especially careful of the ribbon cable if using scissors.
7. Use wire cutters to cut any EEG, EOG, and ground electrodes from where they are encased in the acrylic. Again, avoid the ribbon cable.
8. To remove dental acrylic:
    a. Use a small surgical scalpel to score lines in the acrylic.

b. Thoroughly soak a cotton bud or paper point in acetone. Before the acetone evaporates, quickly apply it to the acrylic, allowing the acetone to soak into the score marks.

c. Repeat these two steps until the acrylic becomes soft and/or begins to crack. This usually takes many repetitions.

d. As the top layer of acrylic softens, the scalpel can be used to scrape or cut it away.

e. Periodically apply back-and-forth pressure to the item encased in the acrylic to speed this process up.

9. Using the above steps, remove the headstage and the plastic shield. Be careful not to brush the array shanks, especially when removing the shield.

10. Once the array is visible, check the shanks.

    a. If they are still submerged in tissue or if they are visibly bending, apply warm water to the craniotomy with a syringe or Pasteur pipette. The water will soften any tissue adhered to the shanks.

11. Remove the acrylic encasing the base of the microdrive.

    a. Do not allow acetone to touch the shanks — this can damage them or cause material to adhere to them more firmly, making them difficult to clean later.

12. Incrementally lift the microdrive off of the head with the micromanipulator.

    a. This may have to be done in several cycles: lift a small amount, score and apply acetone to the acrylic, then lift again.

    b. As a last resort, if the acetone method is not sufficient to safely remove the microdrive, use a soldering iron on low heat to carefully melt the acrylic and/or the solder joints holding the sides of the microdrive to the base. This might require two people, one to apply the soldering iron to the microdrive base and one to simultaneously lift the array off. Be careful not to splash the array with melted acrylic or solder. (This technique is hard on the soldering iron tip. Be sure to tin it well afterwards.)

13. If the implant breaks off suddenly or falls, it may still be recoverable. Carefully replace the microdrive in the holder. Remove attached acrylic or tissue with forceps and the acetone method as above.

Cleaning the array for reuse

1. Place the array in a water bath overnight.
2. Repeatedly run the shanks through a block of 1% agar to mechanically remove large pieces of residue.
3. If visible pieces of tissue remain, repeat steps 1-2.
4. Place the array in a bath of trypsin (10X commercial stock diluted 1:10 in distilled water) with a magnetic stirrer overnight. (Do not heat.)

5. Rinse the array in distilled water for a few minutes.
6. If tissue or residue remains, repeats steps 1-5 as necessary, varying the order if desired. Typically, 1-2 passes will be sufficient.
7. Sterilize the shanks by immersing in isopropyl alcohol for 1-2 minutes.
    a. Be sure to only submerge the shanks, as the alcohol may damage the resin backing on the ribbon cable mounting.

Conclusion

In summary, we have described the use of high-density multielectrode arrays to record populations of neurons in freely behaving zebra finches. Current approaches in songbirds rely on either imaging techniques, which can capture many neurons with excellent spatial resolution over long timespans, or on techniques such as tetrodes or microwires, which can capture a few neurons with excellent temporal resolution over shorter time spans. Many lines of inquiry would benefit from the ability to simultaneously record from larger populations of neurons, with precise temporal resolution, over long periods of time.

This protocol builds on a set of techniques widely used and optimized in rodent models. The electrodes are spaced such that multichannel spikesorting can use information from several neighboring channels to extract overlapping single units. Especially in an acute (head-fixed) setting, a large number of neurons can be recorded simultaneously (**Figure 4.10**).

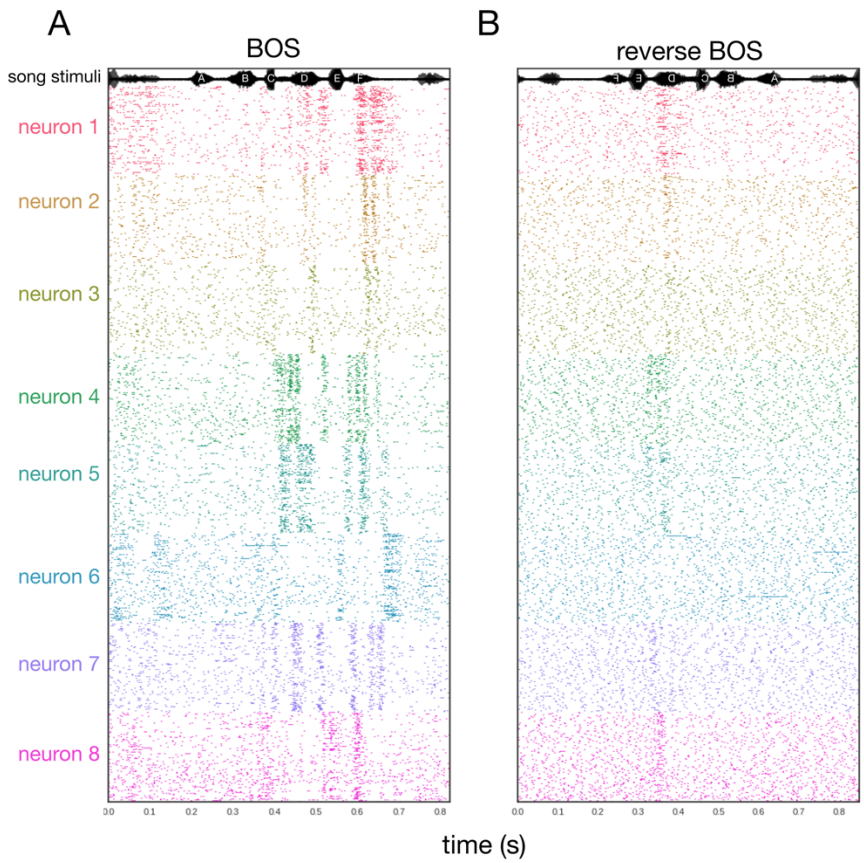

Figure 4.10. Population RA response to stimulus playback during sleep. These acute (head-fixed) data were collected with a single-shank 64 channel array; the lower ~32 channels were in RA during this recording. Spikesorting shown here was performed using SpyKING CIRCUS (Yger et al., 2018), one of several semi-automated approaches we tested. A-B) Oscillogram of stimulus amplitude is plotted at top. Each neuron is shown in a different color. The stimulus consisted of three introductory notes and five motifs. Both BOS and reverse BOS were played back 36 and 21 times, respectively, in randomized order with a jittered 30-second interval between stimuli. All motifs are shown here, for a total of 180 BOS trials and 105 REV trials. A) BOS playback. RA, like other song system nuclei, responds with motor-like activity. B) Reversed BOS playback. RA continues its baseline tonic firing throughout, except for a slight response during syllable D; this is likely due to a resemblance between syllable C and reversed E.

The implant incorporates a headstage on-head to greatly reduce noise. It does not require large or heavy components such as copper shielding, making it suitable for many small active vertebrates that can tolerate being caged. The multichannel approach allows single cells to be followed over many hours and potentially days (**Figure 4.11**).

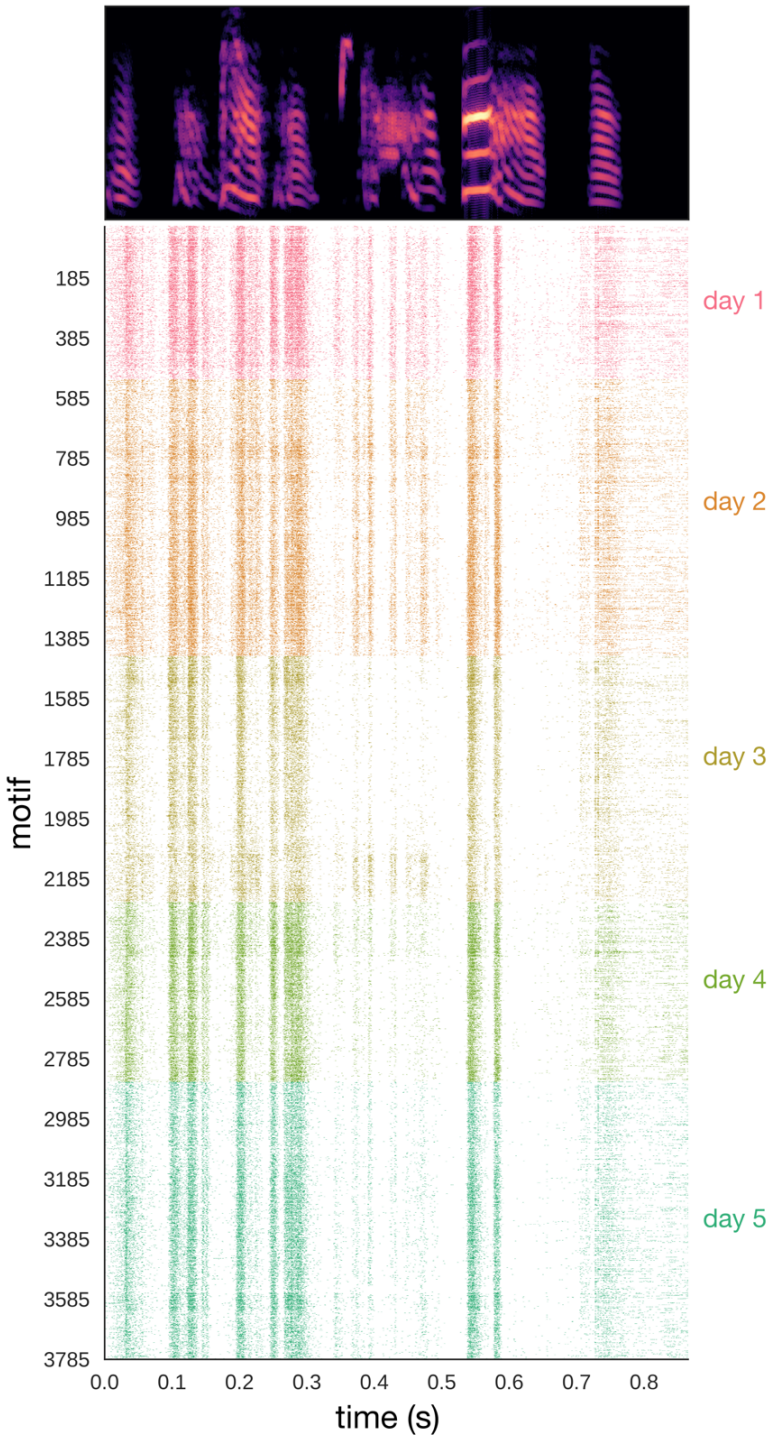

Figure 4.11. Chronic recording of a single RA neuron over 5 days. Top, spectrogram of the motif. Bottom, raster of song activity. Different days are indicated by different colors. Each row represents one motif sung. Spikes were sorted in MountainSort and aligned to song features with dynamic time warping (more details in Chapter 5).

The spikesorting program we have adapted for use in this system is largely automated and requires the least user intervention out of several approaches we tested (Chung et al., 2017). This approach is also long-lasting: once implanted, the array can continue to function over months. In several birds, multi-day recordings of good quality were obtained over 1 month from implantation (**Figure 4.11**; also see Chapter 5). While the arrays used here are not marketed for recovery and reuse, we have described a procedure for doing so with good success.

These procedures have in some cases yielded recordings with virtually zero movement artifact. Critical steps to achieve this quality of recording involve reducing the degree of vibration among components of the implant. All attachments should be of rigid material when possible; for example, epoxy is preferable to silicone gel when attaching the array to the microdrive. Conducting wires should be of sufficient stiffness to resist excess vibration, and should be secured to the implant when possible. The ribbon cable is a major source of movement artifact, and the steps to secure it should receive particular attention.

These recordings can easily be combined with auxiliary recordings such as EEG, EMG, EOG, etc. Most types of electrodes can be substituted in place of the silicon arrays depending on experimental goals and available resources, e.g. single electrodes, tetrodes, microwire array, or carbon fiber arrays. Further adaptations could include the use of multiple arrays to record simultaneously from several regions in the song system. This could be most achieved with two 32-channel arrays with slight modifications to the current headstage design, which currently accommodates one 64-channel array. Another advance would be to motorize the microdrive movement, allowing better cell isolation (at least for brief periods of time) without having to physically immobilize the animal while the array is advanced.

The songbird field has benefited greatly from existing insights gained by paired recordings, multielectrode recordings and calcium imaging of neural populations. We hope to provide a set of tools that will complement this work and further extend our understanding of motor learning.

CHAPTER 5: SONG REPLAY IS RELATED TO LOCAL AND GLOBAL SLEEP STRUCTURE

Abstract

Sleep replay is a central mechanism of the systems consolidation hypothesis, one of the major frameworks for understanding how sleep affects memory. The relationship of hippocampal replay to SWS is well established, with replay co-occurring with multiple stacked oscillations including slow waves. However, sleep is also thought to affect procedural memory, and these effects are distinct and dissociable from sleep effects on declarative memory. Moreover, much ambiguity remains around the question of what characteristics of sleep contribute to procedural memory. Songbirds exhibit one of the only known examples of true sequential replay, and the only known form of replay that occurs in a motor system. We therefore sought to further characterize song replay, and in particular to understand how this form of replay is related to sleep structure.

To address this question, we simultaneously recorded EEG, EOG, and single cell RA activity in adult male zebra finches (n = 5 neurons in 4 birds) during normal sleep and singing behavior. We obtained several continuous recordings over long periods spanning one or more sleep/wake cycles. We observed that replay was often time-locked to individual local slow waves, but not to global or surface slow waves. Replay tended to occur during periods with increased global slow wave activity, and the amount of replay fluctuated in tandem with the 38-min sleep cycle of slow wave activity. However, the overall time course of replay across the night did not follow the homeostatic decrease of slow wave activity, suggesting a possible connection to intermediate sleep or NREM in general. Supporting previous reports, the timescale of song replay was

centered around real time, varying from compression of 0.5x to expansion of 2.5x (n = 2 birds). While we found many apparent examples of highly compressed replay, most of these appear to be artifactual and do not coincide with local slow waves; however, true compressed replay events cannot be ruled out. We also examined motor coding during singing across multiple days (n = 3 birds over a total of 10 days). The structure of individual song-locked bursts remained remarkably stable, at least in this population of older adult birds. This suggests that any changes occurring over sleep periods do not build up over time but are corrected, possibly during subsequent sleep periods.

In sum, these findings point to an evolutionarily ancient role for SWS in which slow waves help to drive or coordinate sleep replay. This process appears to take place in a hippocampal-independent motor system as well as the hippocampus, and in the context of memory maintenance in addition to hippocampal-cortical transfer and consolidation of memories. The time course of replay occurrence also supports a role for intermediate sleep in motor replay. This is consistent with abundant evidence linking human stage 2 to procedural memory; however, most of the human literature has focused on sleep spindles, which birds are not known to have. This raises the possibility that replay is linked to another mechanism related to intermediate sleep, independent of spindles, or alternatively that birds have spindles which have not yet been detected.

Introduction

Sleep exerts a powerful effect on memory and learning. This has been observed across procedural learning (Walker et al., 2002; Brawn et al., 2010), perceptual learning (Karni et al., 1994; Fenn et al., 2003; Gomez et al., 2006), and declarative learning (Plihal and Born, 1997;

Borquez et al., 2013); across memory encoding (Morris et al., 1960; Harrison and Horne, 2000; Walker and Stickgold, 2006; Van Der Werf et al., 2009), consolidation (Jackson et al., 2008; Brawn et al., 2013), and reconsolidation (Brawn et al., 2018); and across species from humans to birds (Solodkin et al., 1985; Derégnaucourt et al., 2005; Jackson et al., 2008) to bees (Beyaert et al., 2012) and flies (Donlea et al., 2011). Studies in mammals have implicated REM, SWS, and N2 in various aspects of memory. For example, one hypothesis held that SWS consolidated declarative learning while REM consolidated non-declarative learning (Plihal and Born, 1997; Stickgold, 1998). More recent hypotheses attribute functions to specific features of a given sleep stage, such as the theta of REM (Nishida et al., 2009; Boyce et al., 2016), the slow waves of SWS (Marshall et al., 2006; Tasali et al., 2008; Ngo et al., 2013; Ong et al., 2018), or the spindles of N2 (Clemens et al., 2006; Nishida and Walker, 2007; Latchoumane et al., 2017). To understand how sleep affects memory, it is important to connect the global traits of a sleep state to specific circuit-level mechanisms that carry out the hypothesized function.

One such circuit-level mechanism is sleep replay, in which neurons spontaneously fire sequences of activity associated with a memory. Replay has been primarily studied in the rat hippocampus: populations of place cells spontaneously fire in order, re-creating spatial trajectories from recently experienced environments (Skaggs and McNaughton, 1996). This form of replay has been strongly linked to sleep structure and local oscillations. Replay events typically co-occur with hippocampal sharp-wave ripples (SWRs) (Lee and Wilson, 2002; O'Neill et al., 2017), which in turn are nested within thalamocortical sleep spindles (Siapas and Wilson, 1998), which occur during cortical slow waves (SWs) (Mölle et al., 2002; 2006; Maingret et al., 2016; Latchoumane et al., 2017). A similar form of replay is also observed during SWRs in quiet wakefulness, often when the rat is still in the maze (Foster and Wilson, 2006; Csicsvari et al.,

2007; Diba and Buzsáki, 2007). This association between SWRs and replay is powerful enough that the inhibition of SWRs during sleep is able to diminish spatial learning performance (Girardeau et al., 2009; Ego-Stengel and Wilson, 2010).

Hippocampal replay, at least during NREM and quiet wake, is highly time-compressed and can occur in both the forward and reverse directions. Most estimates put the compression at about 16-20x real time (Lee and Wilson, 2002; Davidson et al., 2009; Dragoi and Tonegawa, 2013). However, no evidence for compression or expansion was found in one report of NREM "reverberation" events measured across the hippocampus, barrel cortex, putamen, and thalamus (Ribeiro et al., 2004). REM hippocampal replay, of which there is only one study (Louie and Wilson, 2001), was found to occur near real-time i.e. centered around 1x. Finally, one report of possible replay in the prefrontal cortex measured a 7x speedup (Euston et al., 2007).

Outside of the hippocampus, the only other form of replay described in multiple reports exists in the motor system of zebra finches. Replay of singing activity is thought to take place throughout the song system (Dave and Margoliash, 2000; Chi et al., 2003a; 2003b; Hahnloser et al., 2006; Hahnloser and Fee, 2007; Hahnloser et al., 2008), and is typically recorded (including in this study) in single projection neurons of the robust nucleus of the arcopallium (RA) (Dave and Margoliash, 2000; Rauske et al., 2010); these neurons are analogous to layer 5 neurons in the primary motor cortex (M1) of mammals (Wild, 1993; Pfenning et al., 2014). During singing RA neurons fire an average of 12 bursts per motif (Leonardo and Fee, 2005) in an extremely stereotyped pattern (Yu and Margoliash, 1996), making it possible to capture replay on a single-neuron level. Replay in both RA and HVC appears to occur close to real-time, with only slight compression or expansion (Dave and Margoliash, 2000; Chi et al., 2003b) but the timescale has not been fully characterized, nor is it known whether song replay also occurs on highly

compressed or expanded timescales. Furthermore, the early studies of RA replay only analyzed short segments of bursting corresponding to single song syllables, although also showing exemplars of replay of entire motifs (Dave and Margoliash, 2000). This left unresolved the possible replay content of the majority of spike bursting events.

Since the discovery of song replay, it has been shown that zebra finch sleep resembles mammalian sleep much more closely than was previously known (Low et al., 2008). However, it is not known whether or how motor song replay is related to sleep architecture.

To address this question, we performed simultaneous recordings of song replay and global sleep architecture. While we had ample reason to believe that song replay would be associated with a specific stage of sleep, the literature gave rise to several contradicting predictions for what that sleep stage could be. Preliminary work suggested that song replay, or at least sleep bursting, tended to occur during REM (Shank, 2008). Behaviorally, REM (Karni et al., 1994; Smith, 1995; Plihal and Born, 1997) and stage 2 (Walker et al., 2002; Clemens et al., 2006; Nishida and Walker, 2007; Johnson et al., 2012; Wamsley et al., 2012) are strongly implicated in human studies of procedural learning. However, the circuit-level mechanisms behind this effect are not well understood. In contrast, hippocampal replay, has been strongly linked to SWS and slow waves (Wilson and McNaughton, 1994; Mölle et al., 2006; Girardeau et al., 2009; Ego-Stengel and Wilson, 2010). While this work has provided a foundation for understanding how sleep affects declarative memory, it is not known whether analogous mechanisms are at play outside of the hippocampus, for example in the case of hippocampal-independent motor learning. Finally, a few recent studies on motor learning in rodents also support a link between slow waves and sleep reactivation of M1 neurons (Gulati et al., 2014; Ramanathan et al., 2015). We sought to

understand whether song replay occurred during REM, SWS, or stage-2 like sleep, and whether sequences longer than individual syllables were commonly replayed.

Methods

Birds, polysomnography, and array implantations

The five adult male zebra finches and datasets in this study are those examined in Chapter 3 (see **Table 3.1**). Five of these datasets (all but Bird 5) were used for the studies on sleep replay. The dataset from Bird 5, which spans five days and over 3500 song motifs, is still undergoing analysis. Recordings from three birds (Bird 2, Bird 5, and Bird 6 cell 8) yielded longitudinal data suitable for the study on motor coding across days.

Arrays and polysomnography electrodes (EEG and EOG) were implanted as described in Chapter 4.

	Bird tag	Extracellular recording type	Dataset	Motifs	Days with singing	Means spikes/motif	Age at recording start (days)
Bird 3	orange257	Pt/Ir	22	51	2	28.4	258
Bird 6	orange253	Pt/Ir	8	1140	2	35.6	318
			16	5	1	27.2	389
Bird 11	black 442	Pt/Ir	1	5	2	22.8	293
Bird 2	black 484	array	7	394	3	25.9	Unknown
Bird 5	lilac12	array	3	3785	5	29.4	316

Table 5.1. Animals and datasets. "Days with singing" indicates the number of days on which the bird sang at least one motif. Bird 5 was obtained from a breeder; age is calculated based on the assumption that the animal was 120 days old upon arrival.

Implantation of single-unit Pt/Ir extracellular electrodes

The microelectrode component of the implant consisted of 3-4 platinum iridium electrodes spaced approximately 2.5 - 3.5 mm apart, mounted via sections of 27G hypodermic needle onto the side of a screw microdrive (Vandecasteele et al., 2012). All but one of the electrodes were coated in solder glass to an impedance of 1 - 2 MΩ; the uncoated electrode served as a reference.

A small craniotomy was made at coordinates targeting RA, measured relative to the Y-sinus (2.3 - 2.4 mm lateral and 1.0 - 1.1 mm caudal). The electrodes were lowered slowly into the brain to a depth of 1.5 - 1.9 mm; as these electrodes are capable of penetrating the dura, no dura removal was necessary. The brain was kept hydrated with sterile saline during insertion of the electrodes, then once electrode placement was finalized, several drops of viscous silicone were used to seal the craniotomy. In later surgeries, artificial dura (Cambridge NeuroTech, UK) was used in place of the silicone.

The mobile components of the screw microdrive were coated in bone wax to allow continued movement; the bottom plate of the microdrive was then cemented to the skull with dental acrylic. Acrylic was placed between the layers of skull to optimally anchor the microdrive.

Both the extracellular electrodes and the PSG leads were wired to a 14-channel Omnetics connector, which was lowered onto the head and attached will dental acrylic.

After 3-7 days of recovery from surgery, a small custom built headstage (15 mm wide by 17 mm tall, 0.7g, designed by Hamish Mehaffey; schematics available at https://github.com/kylerbrown/headstage_nano) was attached to the connector on the bird's head. After 1-2 days of acclimation to the headstage, acclimation to the tether began.

Data collection

Each day birds were tethered using a lightweight cable for increasing periods of time, starting at 10-20 minutes per day and ending once birds showed signs of difficulty carrying the tether. The cable was either custom built or purchased (RHD2000 Ultra Thin SPI interface cable, Intan Technologies, Los Angeles, CA). During each acclimation session, the extracellular electrodes were advanced 35-70 μm at a time, for a total of no more than 105 μm per day.

Recordings began once birds were able to comfortably remain tethered overnight and once the electrodes reached RA, typically at a depth of 2100 - 2400 μm. RA was identified by its characteristic tonic firing at a steady rate between 20-40 Hz; the firing rate increases with arousal and decreases with drowsiness or sleep. Other hallmarks of RA neurons include bursting during vocalizations or during sleep. This approach targets RA projection neurons, which generate this tonic firing pattern through intracellular oscillations (Mooney, 1992; Spiro et al., 1999). According to all available information, these properties are universally shared among RA projection neurons. This was corroborated by our experience: while lowering the electrode through RA in these recordings, it was never the case that RA-like tonic-firing neurons were interspersed with other types of neurons. However, this does not completely rule out the possibility of targeting bias.

An adult female bird was placed on the other side of a replaceable divider. Between recordings, a white opaque plastic divider was used, completely shielding the birds from each other's view. During recordings the opaque divider was replaced with a sheet of clear Plexiglas; revealing the female encouraged the male bird to sing shortly after the start of recordings, without the disruption involved in handling and placing the female bird into the cage.

This encouraged singing later in the evening, when recording sessions typically began. Thus, the song captured here should be considered a mix of directed and undirected song. Directed song is more stereotyped (Kao et al., 2005) and slightly faster (Sossinka and Böhner, 1980; Glaze and Troyer, 2006).

Preprocessing

Extracellular spike data were bandpass filtered between 300 and 10,000 Hz (zero-phase second order Bessel filter) and referenced using the command dat-ref in Bark (our data structure and signal processing environment, available at https://github.com/margoliashlab/bark). This function performs weighted median referencing with coefficients chosen to minimize total power.

In birds implanted with Pt/Ir electrodes, LFP channels were referenced to the uncoated Pt/Ir electrode. For bird 3, the LFP data collected from the high-impedance electrodes had large number of artifacts, and so the LFP of the uncoated electrode was used instead.

In birds implanted with arrays, LFPs from each channel were median-referenced. These LFPs were also analyzed in "unreferenced" form to capture global events, as median-referencing eliminated much of the large-scale LFP activity of interest.

Song labeling and data visualization

Sound data were highpass filtered at 300 Hz (zero-phase third order Bessel filter). The command dat-segment (based on Koumura and Okanoya, 2016)) was run to automatically detect vocalizations. Dat-segment parameters were adjusted based on the bird, but were approximately as follows: minimum syllable duration 75 ms, minimum gap duration 5 ms, threshold 8 (a.u.), step size 2 ms. This combination of parameters was used to quickly detect song occurrences. A

lower threshold (e.g. 6-7) and default parameters were used later for segmenting individual syllables and calls, in preparation for manual labeling into syllables and call types.

Electrophysiological and sound data were visualized in Neuroscope, using the command bark-scope. Segmented sound data were visualized and labeled in the program bark-label-view. Datasets were chosen based on the presence of song, song-related neuronal activity, clear video of behavior, and single RA units held over at least several hours of both wake and sleep.

Spikesorting

Spikesorting of the Pt/Ir data was carried out in Plexon Offline Sorter (Plexon Inc, Dallas, Texas). To accommodate drift in spike waveform shape, each dataset was first split into manually chosen segments, typically of a few hours or less. Spike sorting was performed in Plexon using a semi-automated method. First, a detection threshold was manually set and waveforms were extracted and aligned by the negative peak. Thresholds were then chosen to remove high amplitude artifacts. Remaining artifacts were identified and removed manually, primarily by examining the linear energy and nonlinear energy features in Plexon as well as principal components and raw waveforms. Principal component analysis was then rerun. Initial clustering of waveforms was performed using the template fit method in Plexon with user-defined template waveforms followed by manual adjustments of template tolerance. Clusters were then further hand-adjusted using multiple features including the first three principal components, peak and valley, and waveform amplitude at user-defined slices.

Spikesorting of the array data was carried out as described in Chapter 4.

Replay identification

A major focus of the analysis was to identify neuronal replay events in the "spontaneous" activity recorded during sleeping. The technique described in Chi (Chi et al., 2003b) was developed to identify replays using pattern filtering and local signal analysis, including timescale and significance testing. This is distinct from and complementary to the analysis of global spiking activity (Roxin et al., 2008; 2011). The Chi approach has been used to find replay in adult zebra finch HVC putative interneurons (Chi et al., 2003a; 2003b). The approach uses spike activity during singing as a template, which is then matched to sleep activity to find replay.

Implementation

The algorithm was parallelized and implemented on a high performance computing cluster. The most CPU intensive step by far were the initial filtering, which runs over all sleep periods in the dataset. For the longest datasets, filtering for a single template typically ran upwards 15 - 20 hours wall time.

Template selection

First, a set of template spiketrains was selected, where each template S consisted of spikes s during one motif of song:

$$S = \{s_1, \ldots, s_p\} \text{ on the interval } [0, \sigma]$$

Because RA neurons often have characteristic long periods of silence surrounding singing activity, template intervals $[0, \sigma]$ spanned the ISI immediately before s_1 to the ISI immediately after s_p. Motifs were excluded if they contained electrical artifacts or non-standard variants of the motif (e.g. omission of one or more syllables).

Filter construction

For each template s_n, a set of three filters F was constructed (**Figure 5.1A**). The template was discretized with resolution r, then convolved with a window function K. The function $K(x)$ is defined on the interval $(-\epsilon, \epsilon)$ where ϵ is the maximum allowable jitter of a target spike generated by a template spike. During silent periods, consisting of points outside of the interval around each spike $[s-\epsilon, s+\epsilon]$ the template was set to the background function B, where

$$B(x) = -\beta, \beta \geq 0$$

The first filter F_1 was relatively coarse, with the largest bin size r_1 and window size ϵ_1. A square window was used for K_1:

$$K_{square}(x) = \begin{cases} 1 & \text{if } x \in (-\epsilon, \epsilon), \\ -\beta & \text{otherwise} \end{cases}$$

The second and third filters were constructed using progressively finer bin and window sizes. The window function for F_2 was a Hamming window adjusted such that $K(-\epsilon) = K(\epsilon) = B(x)$, resulting in a smooth curve:

$$K_{Hamming}(x) = \begin{cases} \frac{1}{2}(1-\beta) + \frac{1}{2}(1+\beta)\cos\frac{\pi x}{\epsilon} & \text{if } x \in (-\epsilon, \epsilon), \\ -\beta & \text{otherwise} \end{cases}$$

The final filter F_3 used a mixture of a square window and a Hamming window:

$$K_{mixed}(x) = \min(0.5, K_{Hamming})$$

which is essentially a "cropped" Hamming window.

Threshold calculation

A threshold was selected for each filter F_n by training on a set of simulated background spike sequences and target spike sequences (**Figure 5.1B**). This yielded two possible thresholds, $\alpha(F)$

determined by training on the background sequences, and $\beta(F)$ determined by training on the target sequences. The final threshold was then selected as the highest of these two.

Background sequences were constructed as randomly generated Poisson sequences with the average firing rate f, which approximated normal tonic firing and was chosen by the process described below in "Parameter optimization". Any spikes violating the refractory period were identified by a preceding ISI $< \frac{1}{f_{max}}$ and removed sequentially (i.e. ISIs were recalculated after each spike was removed).

Target sequences were simulated by randomly modifying the template in 4 steps.

1. Each spike was shifted by a random distance $x \sim \text{Normal}(0, \delta)$.
2. Spikes were randomly deleted with a small probability.
3. Noise spikes were added from a Poisson process with low firing rate.
4. The entire sequence was scaled by $e^{-\xi}$ where $\xi \sim \text{Uniform}(-\epsilon, \epsilon)$.

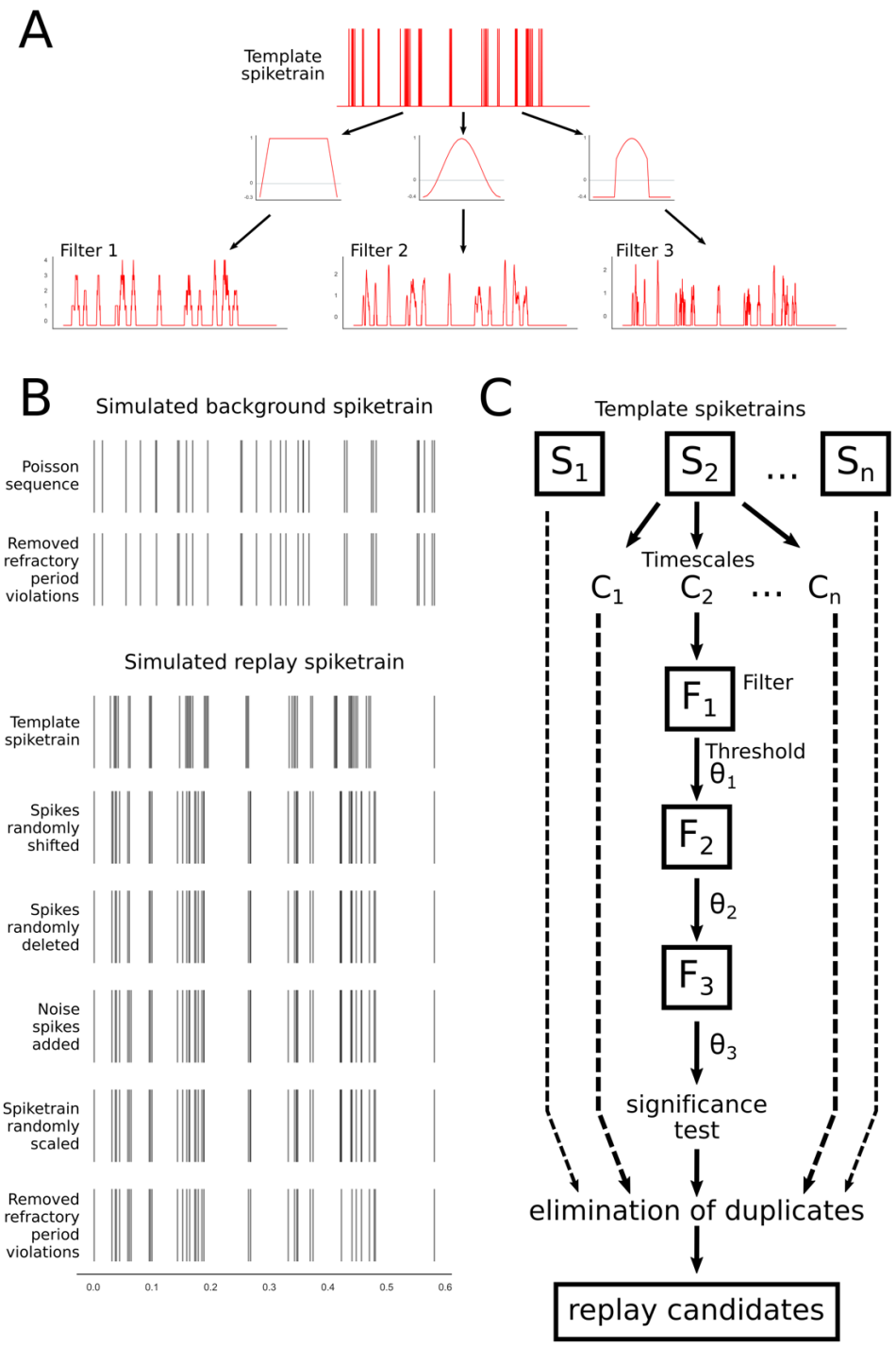

Figure 5.1. Replay identification method. A) Filter construction. The template spiketrain is binned and convolved with a window to create the filter. Three different filters are created by using increasingly narrow windows, and progressively decreasing the binning and window sizes. B) Simulation of background and target spiketrains, used to calculated the threshold for each filter. Top, steps for simulating one background sequence. Bottom, steps for simulating one target sequence. C) Overview of algorithm. For each template spiketrain S and each timescale c, a series of three filters F are created and applied to the data. For each filter, a threshold θ is calculated. Peaks in the filter response above the threshold are considered potential candidates and passed to the next filter. A significance test is run to calculate each candidate's p-value; the candidates from all templates and timescales are then pooled, and the p-values are used to eliminate duplicates.

Any spikes violating the refractory period were removed.

To identify the threshold, 1000 background sequences and 1000 target sequences were created, discretized at resolution r and convolved with the filter F. This convolution yielded a filter response R for each sequence, from which the peak response value $\max(R)$ was identified. From the background sequences, the threshold $\alpha(F)$ was set as the 99th percentile of the set of peak response values. From the target sequences, the threshold $\beta(F)$ was set as the πth percentile of the peak responses, where $\pi \geq 50$. Finally, the threshold $\theta(F)$ was set to $\max[\alpha(F), \beta(F)]$.

Filtering

Once filters and thresholds were created, replay identification was carried out as outlined in **Figure 5.1C**.

Spike data from each period of sleep were discretized with bins of duration r_1, identical to that used to construct filter F_1. Binned spike data were then convolved with the first filter F_1, yielding a filter response R_1. Targets in R_1 were detected at time points x_i which satisfied the criteria:

1. Local maximum within radius ρ:
$$R(x_i) \geq R(x), x \in (x_i - \rho, x_i + \rho)$$
2. Above threshold:
$$R(x_i) \geq \theta$$

The spiketrains in $[x_i, x_i + \sigma_n]$ were extracted as potential targets, where σ_n is the duration of the template S_n. These spiketrains were then discretized at finer resolution with bin sizes r_2 and r_3 and filtered with F_2 and F_3, respectively. At each step, spiketrains were discarded if no

peaks $> \theta(F)$ were detected in the filter responses, yielding a final set of candidate replay events that passed all three filtering steps.

Multiple timescales

To detect compressed or expanded replay, the filter was scaled by each timescale c in the set $\{c_1, \ldots, c_n\}$. At each timescale, c was also used to scale the bin size r used to discretize the spike data, the value ρ determining the radius in which local maxima were calculated, and the padding around the candidate spiketrain used in significance testing (see below).

Significance testing

For each replay candidate a p-value was calculated by taking the average firing rate f of the candidate spiketrain, padded on either side by 0.5 s (at timescale $c = 1$). A null distribution was created by generating N Poisson sequences with density f on an interval of duration σ. Any spikes violating the refractory period were removed, and then each of the Poisson sequences was run through the filtering procedure to detect potential targets. From this n was calculated as the number of Poisson sequences in which any targets were detected. The p-value was calculated as $p = n/N$, representing the probability of a target being detected in a spurious sequence of length σ and firing rate f.

Elimination of overlap

Overlaps were resolved across all candidate replay sequences resulting from all template sequences S. Any two replay candidates were counted as duplicates if the two intervals overlapped by 1 ms or more. The period of overlap was then assigned to the candidate with the lower p-value and deducted from the other candidate sequence. If the shortened candidate was less than 1 ms in duration, it was automatically discarded. The p-value of the remaining

shortened candidates were then recalculated. The goal of this procedure was to keeping intact any instances of partial or out-of-order replay.

Alignment

Finally, significant replay events were identified as those with a p-value of 0.05 or lower. Each replay event was then re-aligned to its origin template sequence using the spike synchronization measure from the PySpike library. The replay spiketrain was shifted relative to the template spiketrain at time steps of .05 ms, up to a maximum shift of 5 ms, until maximum spike synchronization between the sequences is obtained.

Parameter optimization

An optimization step was used to determine the following parameters: window sizes ϵ, radius ρ, average background-sequence firing rate f, the maximum target-sequence spike shift δ, and the firing rate of noise spikes used to simulate target sequences.

Each set of parameters was tested by choosing one motif as a template, and then running the filtering and thresholding steps on all wake periods containing song. Performance was evaluated based on how many of the bird's other motifs were detected, how many false positives were detected, and the average distance between the true motif starts and the starts of detected events.

The exact ranges of parameters tested was not exhaustive and varied between datasets, but typically a grid search was carried out across a series of values for ϵ_1 and ϵ_2. The other parameters were each sequentially tested, with the values of a single parameters being altered alongside each combination of ϵ_1 and ϵ_2. This optimization was sometimes carried out in 2-4 iterations: the starting values were set to the current best set of parameters, and the search carried out again in range centered on that set.

When detecting song for the optimization process, the following parameters were also varied: π (the percentile value used to calculate threshold β) and the probability of spike deletion used to simulate target sequences. However, sleep replay is more variable than song activity and also tends to occur in fragments. To account for this, when detecting replay these parameters were set to 50 and 0.5 respectively.

Spectral analyses

For epoch-by-epoch analysis of sleep, thresholds for firing rate and delta were applied to eliminate epochs with large EEG or LFP artifacts (log-transformed delta, 3 standard deviations above or below the mean) or epochs in which the neuron was not detected (firing rate, 1.5 standard deviations below the mean). Spectral content and number of peaks/s were calculated as described in Chapter 3.

Eye movement index and detection of eye movements

Eye movements appear as large deflections moving in opposing directions in the left and right EOGs, and are therefore measurable as the anticorrelation of the LEOG and REOG. Positive correlations between the two EOGs correspond to shared artifacts. Thus, the EOG product was used as a measure of eye movement activity. To calculate the "eye movement index," positive values were set to 0.

Eye movements were detected as large negative half-waves in the EOG product, using the method described in Chapter 2.

Dynamic time warping and spiketrain alignment

A dynamic time warping algorithm (implemented in Python with the ezdtw library, available at https://github.com/kylerbrown/ezdtw) was used to find the optimal warp path to align the

acoustic features within motifs. The template was chosen as the motif with duration closest to the 75th percentile, with no artifacts or other noise (e.g. female calls overlapping). The warp paths generated by this process were then applied to the spiketrains, correcting for any jitter that was a result of slight timing differences in song labeling or the song motifs themselves.

The warp path corresponding to a given motif was also applied to any replay events detected using that motif as a template.

To align two spiketrains, spiketrains were progressively shifted relative to each other in increments of 0.5 ms, up to a maximum of 10 ms. At each lag, the average spike synchronization was calculated, and the lag with the best spike synchronization value was used. Spike synchronization, an adapted and simplified version of event synchronization, is a measure between 0 and 1 with 1 corresponding to maximum synchrony; it was implemented using the Pyspike library (Kreuz et al., 2015; Mulansky and Kreuz, 2016). When calculated between two spiketrains, it is effectively a binary measure, with 1 indicating coincident spikes and 0 indicating non-coincident spikes.

Replay content

The spike synchronization profile was used to measure how often the different parts of the song were represented in replay events. To measure consistency of bursting in singing activity, the multivariate spike synchronization profile was calculated across all motif spiketrains. To measure bursting content of replay events, the spike synchronization profile was calculated between each replay event and its template, binned into 0.5 ms bins, and averaged across all replay-template pairs.

Statistical analyses

To compare epochs with and without replay, the Wilcoxon signed-rank test was used. Alpha was set to 0.05 for statistical tests and exclusion of replay candidates unless otherwise noted. Numerical values in the text are reported as mean ± SD.

Results

During singing, neurons in RA fired highly stereotyped trains of bursts. This can be seen in **Figure 5.2A** (top): this neuron's activity immediately before and after each motif is visible, and varied depending on what the bird sang in these periods (e.g. introductory notes, calls, additional motifs) but firing during the motif is precisely locked to the notes of the song.

The singing events gave rise to templates that were used in subsequent analyses. There were 1595 templates generated across five datasets, with 28.0 ± 4.2 spikes per template (**Table 5.1**). This singing activity is entirely consistent with what has been previously reported in RA (Yu and Margoliash, 1996; Leonardo and Fee, 2005).

Shortly after the start of recording in the afternoon, it was not uncommon for birds to resume their daytime napping. When this happened, most RA neurons began to start bursting soon after sleep onset (**Figure 5.2A**, bottom). Anecdotally, this often appeared to coincide with the appearance of slow waves in the EEG. REM was not reliably observed during these brief daytime naps, consistent with REM in most species occurring only after sustained NREM episodes.

As found previously, a subset of this sleep bursting recapitulated the song activity (**Figure 5.2A**). This spontaneous sleep replay usually did not span the entire song but rather a segment. In some cases, replay contained bursts with remarkably similar structure to singing activity (**Figure**

5.2A, bottom, first three sleeping examples). Conversely, bursts could also be substituted with a single spike or a few spikes (**Figure 5.2A**, bottom).

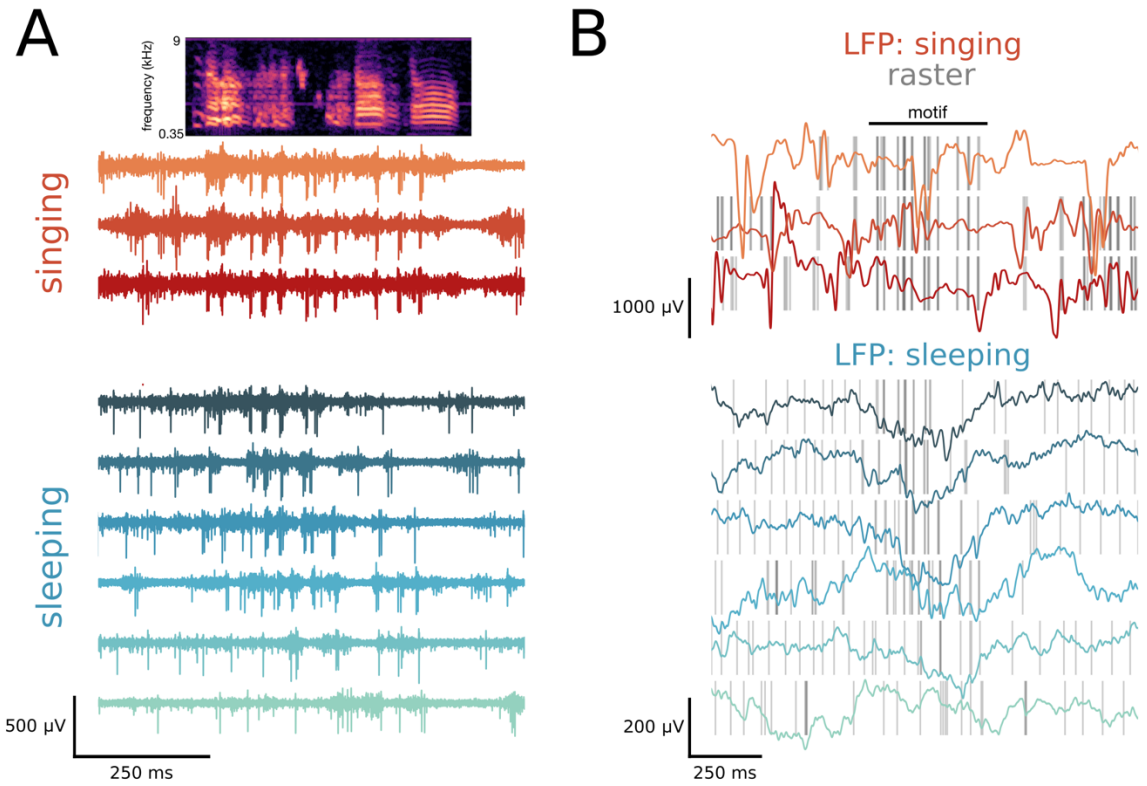

Figure 5.2. Examples of replay events and simultaneous LFP. A) Song spectrogram and extracellular recordings from a single neuron. Top, three examples of this neuron's activity during a motif. Bottom, six manually identified examples of spontaneous activity of this neuron during sleep. When aligned with the song activity, these events appear to recapitulate fragments of the bursting patterns seen during singing. Example events are shown in order of where they start in the song. B) Raster (gray vertical lines) of spike times from panel A, overlaid with the simultaneous LFP. Top, LFP during singing; rapid high amplitude fluctuations are typical of movement artifacts. Bottom, LFP during sleep replay events. (Data shown are from Bird 6, cell 16.)

We then examined the PSG during these manually identified examples of replay. All examples occurred near numerous EEG slow waves, with very few EOG deflections, but no specific time-locking was apparent. However, the LFPs showed a clear pattern of large negative half-waves which coincided with the start of each replay event (**Figure 5.2B**, bottom). These half-waves, 250-500 ms in duration and >100 µV in amplitude, met the criteria for slow waves. Nearly identical LFPs were seen on a nearby electrode (300-400 µm, approximately same depth),

on which no single unit activity was visible. This supports the interpretation that these waves are local oscillatory events, perhaps traveling in the region in and around RA (Beckers et al., 2014), and not a consequence of spike bleedthrough or other artifacts.

Replay identification and timescale

To rigorously identify replay events across the night, we applied a pattern-filtering algorithm (Chi et al., 2003a; 2003b) which is able to detect candidate replay events on multiple timescales and assess the significance of each event. Replay occurs at highly compressed speeds in the hippocampus (Lee and Wilson, 2002; Davidson et al., 2009; Dragoi and Tonegawa, 2013) and prefrontal cortex (Euston et al., 2007). Thus, to assess both the timescale of RA replay and the effectiveness of the algorithm, we applied this technique across a wide range of timescales (0.1 – 8x) in a subset of cells.

We also reversed the song templates and repeated this process. "Reverse" replay occurs in the hippocampus (Foster and Wilson, 2006; Csicsvari et al., 2007; Diba and Buzsáki, 2007). Whereas spatial trajectories are by nature a bidirectional process – the rat can run the same trajectory in either direction – rats mostly do not walk backwards. Similarly, birds do not sing the song backwards, and zebra finch song syntax is highly stereotyped with syllables almost invariably sung in the same order. Furthermore, while RA responds to playback of the forward song during sleep – possibly a form of evoked replay – it does not respond to the reversed song (Margoliash et al., 1994; Dave et al., 1998; Dave and Margoliash, 2000).

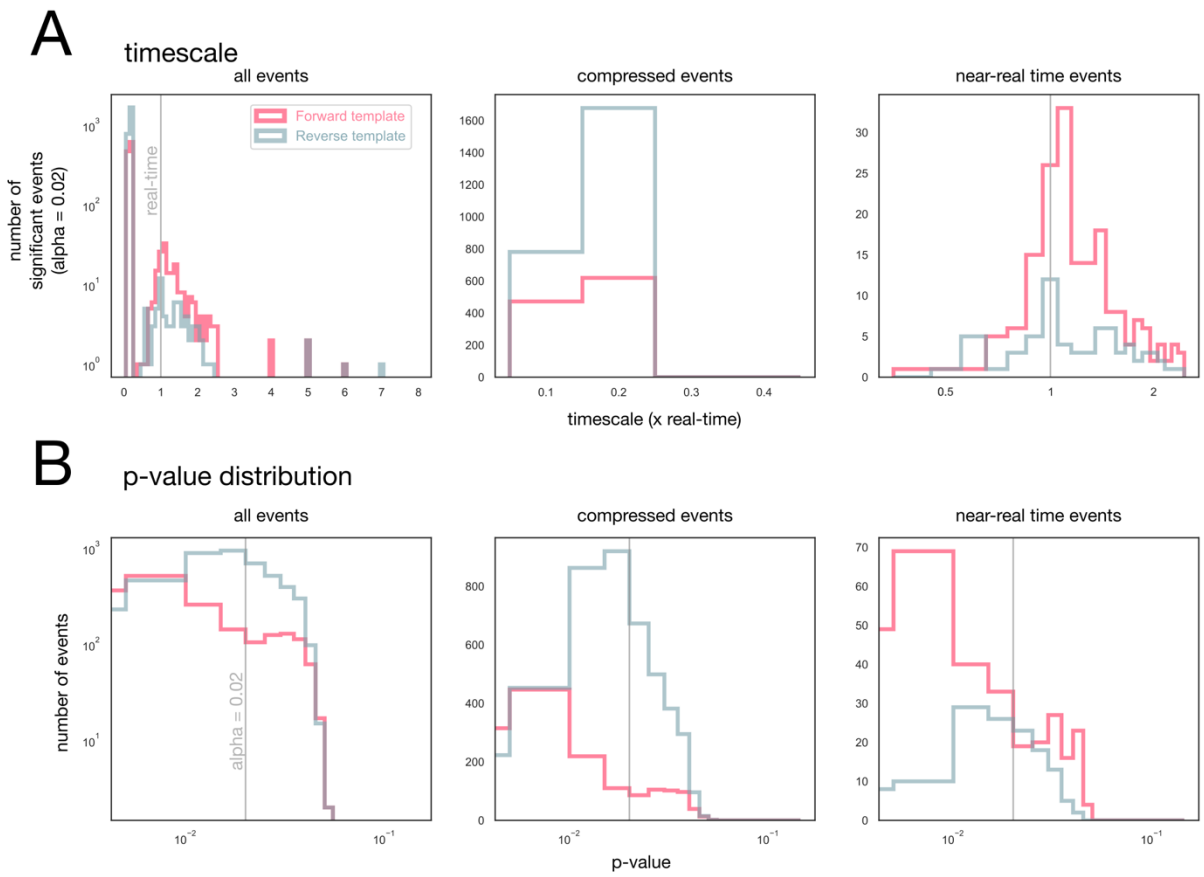

Figure 5.3. Replay identification at different timescales. The template matching algorithm was run with both the forward templates (red) and again with the reverse templates (blue) A) Distribution of timescale of significant replay events (alpha = 0.02) detected. Here, timescale is defined such that 1 (grey vertical line) indicates real time, timescales between 0 and 1 indicate time compression, and >1 indicates time expansion. Left: timescale distribution of all significant events; note log scale of y-axis. Center: compressed events (timescale < 0.4x). Right: events at timescales centered around real time (range, 0.4 – 2.5x); note log scale of x-axis. B) Distribution of p-values of all events detected, including both significant and nonsignificant events. The alpha value of 0.02 from panel A is indicated as the grey vertical line. Left, events of all timescales; note log scale of y-axis. Center, compressed events (timescale < 0.4x). Right: events at timescales centered around real time (range, 0.4 – 2.5x).

Both the forward and reverse templates found candidate replay events which formed a bimodal distribution, with one peak centered around 1x and a very large peak at 0.1 – 0.3x (**Figure 5.3A**, left). However, while similar numbers of forward and reverse events were found for the compressed peak (**Figure 5.3A**, center), very few reverse events were found near 1x (**Figure 5.3A**, right). This suggests events occurring at short timescales are an artifact of compression: as the template is compressed it increasingly resembles a single burst. At this scale,

the forward and reverse templates are indistinguishable and therefore both match a similarly large number of events.

The p-value distributions showed a rightward shift of reverse events as compared to forward events (**Figure 5.3B**, left): in other words, events found with the reverse template have a smaller significance value than events found with the forward template. Interestingly, this was true not only of the near-real-time events (**Figure 5.3B**, right) but also of the compressed events (**Figure 5.3B**, center).

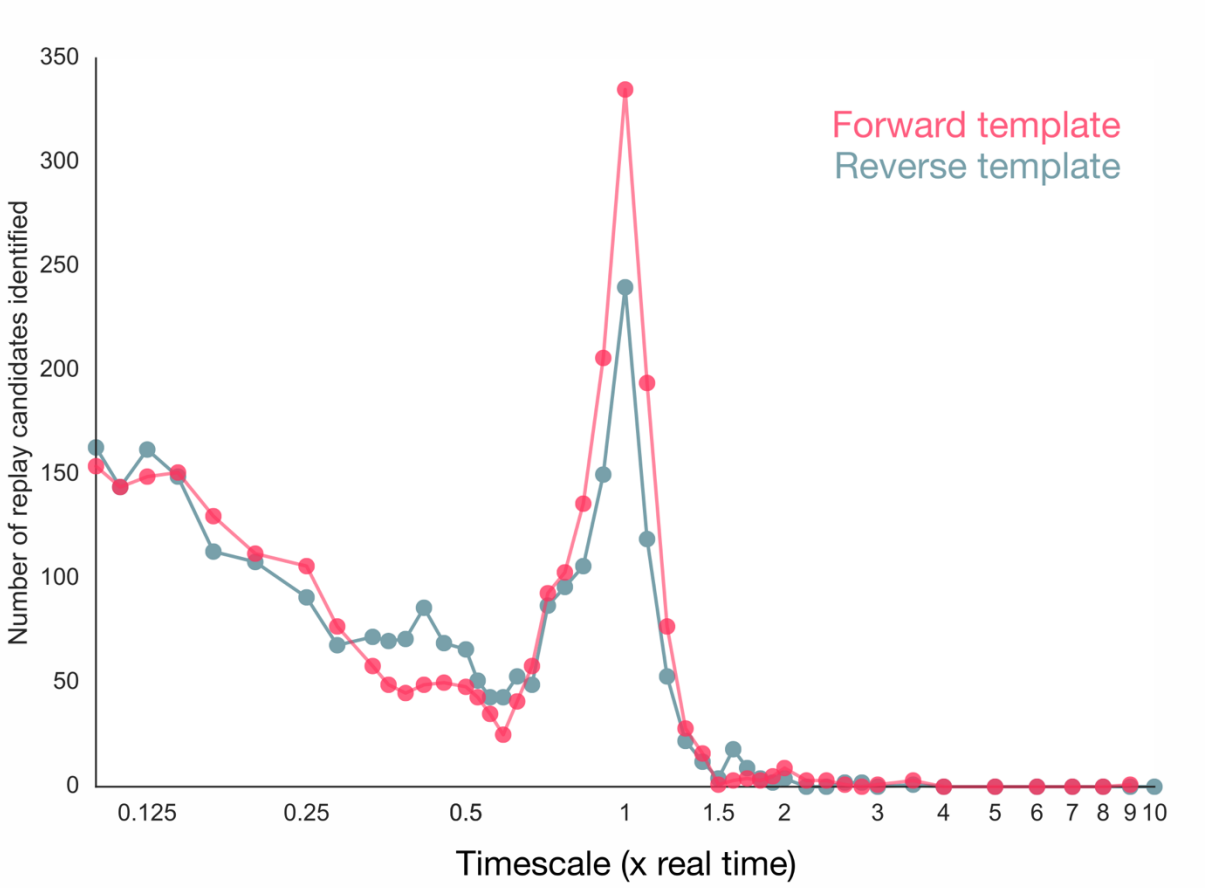

Figure 5.4. Timescale distribution found with a correlation-based method. This method can be thought of as a simplified variant of the pattern filtering approach. All spikes were discretized with bin sizes of 1 ms, and spikes during motifs were averaged to create a mean song template. The cross-correlation of the template and sleep spiketrains was taken, and then smoothed with a 2-point rolling mean. Replay candidates were identified as peaks in the correlation between the template and the data spikes which exceeded a threshold, chosen manually. Overlapping replay candidates were identified and the candidate with the shorter correlation peak discarded. To compress or expand the template, the interburst intervals of the spiketrain were multiplied by the timescale.

A similar pattern of replay timescales was seen using a correlation-based replay identification technique (**Figure 5.4**). In this example, compression and expansion was performed only on the interburst intervals, keeping intact the structure and timing of spikes within bursts. As in **Figure 5.3**, this yielded a large peak centered around 1 and another peak at highly compressed timescales; similarly, the real-time peak was much higher for forward events than reverse events, but similar numbers of compressed events were found for both forward and reverse templates. Unlike the approach in **Figure 5.3**, this technique found replay with a frequency that increased almost linearly with compression, forming a much shorter but broader peak at compressed timescales.

In both techniques, the peak centered on real time was relatively narrow, confirming a previous report that RA replay is largely close to real-time (Dave and Margoliash, 2000). Thus, going forward we restricted our analysis to events between 0.9 – 1.1x.

Time-locked oscillations during replay

We then examined whether the observations from individual, manually identified replay examples held true over all examples of replay. **Figure 5.5A** shows all 187 examples of replay from one cell identified over approximately six hours of sleep (the latter half of the night). The replay-triggered average of the LFP revealed a large negative half-wave followed by a smaller positive deflection (**Figure 5.5B**). This was also seen in the nearby quiet electrode (**Figure 5.5C**). In contrast, the mean surface EEG was flat, although large deflections are visible in most of the individual EEG traces (**Figure 5.5D**). This suggests that local slow waves are time-locked to replay events, while surface slow waves can appear during replay but are not time-locked.

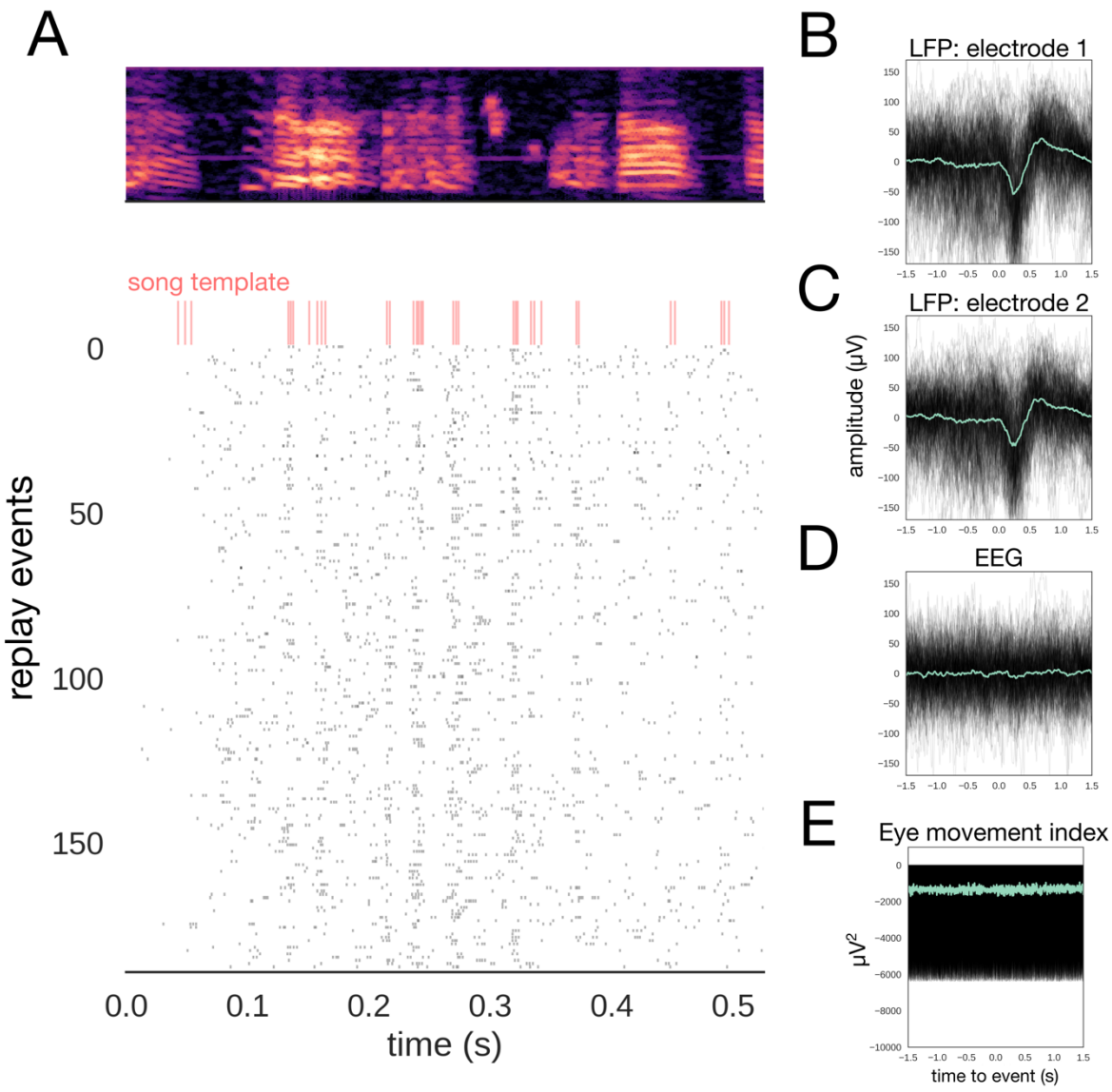

Figure 5.5. Replay events and event-triggered averages of LFP, EEG, and EOG. A) Raster of all replay events with $p < 0.02$. Top, motif spectrogram. Red, template spiketrain of activity during one motif. Black, replay events. All spiketrains are scaled and warped based on the template which with they were detected, as described in the Methods. B-E) Replay-triggered traces from the PSG, with 0 seconds corresponding to the start of each replay event. Thin black lines, individual traces. Thick green line, mean of all traces. In B-D, traces with artifacts > 500 μV were excluded. B) Replay-triggered LFP from electrode 1, the same electrode on which the RA neuron was recorded. C) Replay-triggered LFP from electrode 2, a nearby electrode of similar impedance with no visible single-unit activity at the time. D) Replay-triggered surface EEG. E) Replay-triggered eye movement index, calculated from the anticorrelation of the LEOG and REOG. Eye movements would appear on this index as negative deflections.

The average LEOG and REOG were likewise flat during replay, suggesting the LFP results cannot be ascribed to EOG artifact. To look for eye movements related to replay, we calculated the product of the LEOG and REOG; eye movements would appear as negative deflections, i.e. anticorrelation. Because the EOGs rest under the skin they are susceptible to various artifacts, which usually occur across both EOG channels and result in a positive correlation. Thus, to avoid averaging out potential eye movements (negative correlations) with shared EOG artifacts (positive correlations) we set all positive values to 0 before calculating the average. This index also yielded a flat average (**Figure 5.5E**), confirming that eye movements did not co-occur with replay events.

Across cells, this time-locking of an LFP delta wave was evident on an event-by-event basis (**Figure 5.6A**). The sign of the time-locked event varied across individuals. Interestingly, in two different cells recorded from the same bird (Bird 6), the pattern was similar: a negative wave beginning just after the start of the replay event, followed by a positive wave. In Bird 3, the oscillation appeared primarily as a positive wave, while in Bird 2 it appeared as a negative wave slightly preceding the replay event, followed by a positive wave coinciding with the replay event.

In contrast to the LFPs, while the EEGs contained numerous and often large deflections, a time-locked pattern did not emerge (**Figure 5.6B**). The possible exception is Bird 2, for which the unreferenced array LFP was used in lieu of the EEG (see Methods); this signal contains a mixture of local and global signals. Time-locking of the LFPs occurred only very faintly for compressed events (**Figure 5.6C**; compare to the same cell in **Figure 5.6A**) and not at all for reverse events (**Figure 5.6D**). This rules out the possibility that this LFP signal can be ascribed solely to sleep bursting in general.

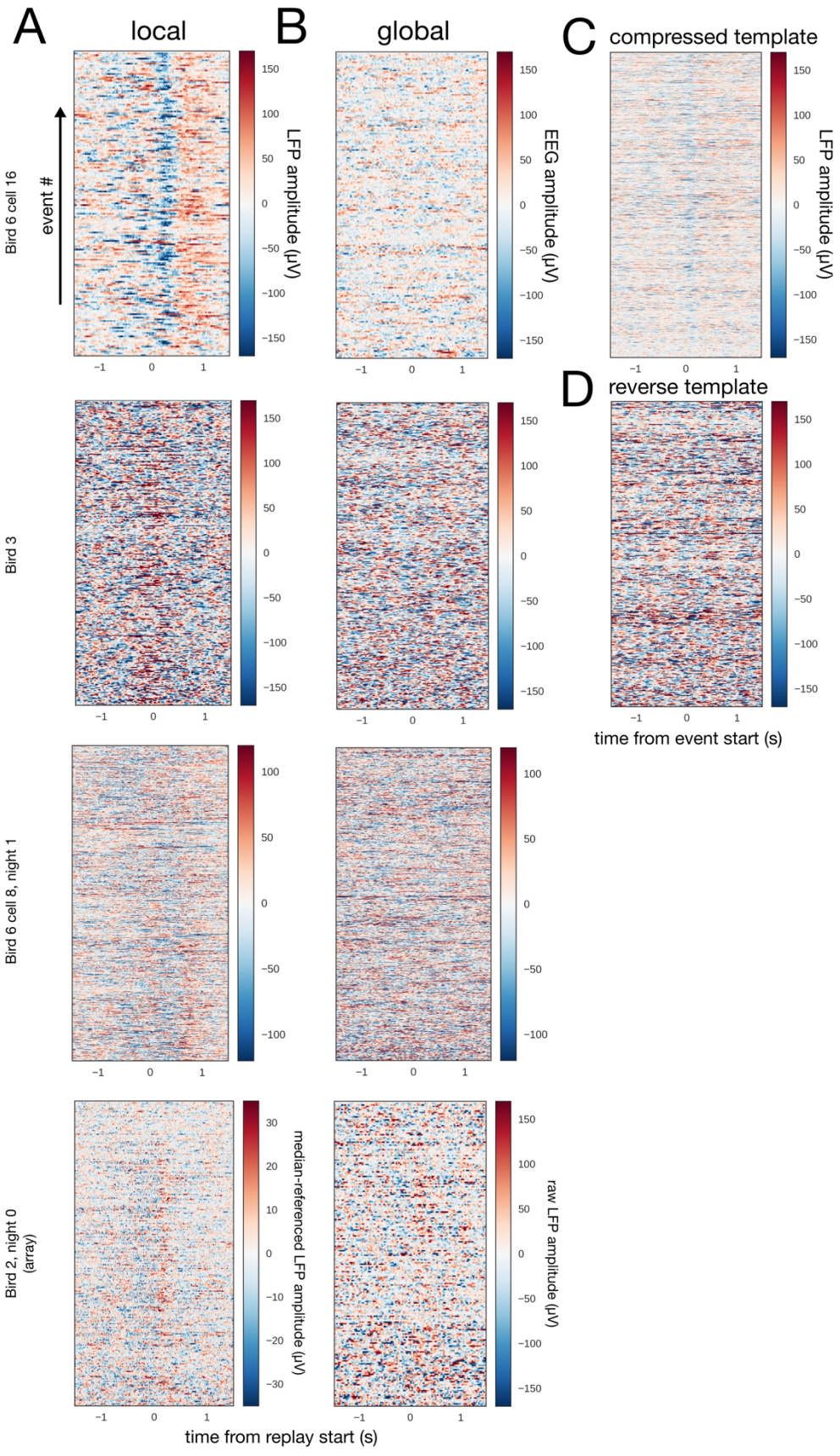

Figure 5.6. Replay-triggered EEG and LFP. For each subplot, rows correspond to individual replay events across one night, with the start of each event centered at 0 s. Events are ordered by start time, with events from earlier in the night at the bottom. Color indicates signal amplitude. A) EEG (Birds 3 and 6) or the unreferenced array LFP (Bird 2), centered on near-real-time replay events. B) LFP traces, centered on near-real-time replay events. C) LFP traces centered on compressed (< 0.4x) events. D) LFP traces centered on near-real-time events identified with the reversed template.

Global sleep structure and replay frequency

Is replay associated with overall sleep architecture? We examined the EEG and LFP of 3-s epochs of nighttime sleep, comparing epochs with no replay to epochs containing at least one instance of replay. Given the results of Chapters 2-3, we chose to focus on mean log-transformed delta power as a measure of slow wave activity, and the number of peaks per second (nPeaks) as a relatively independent measure of high-frequency activity.

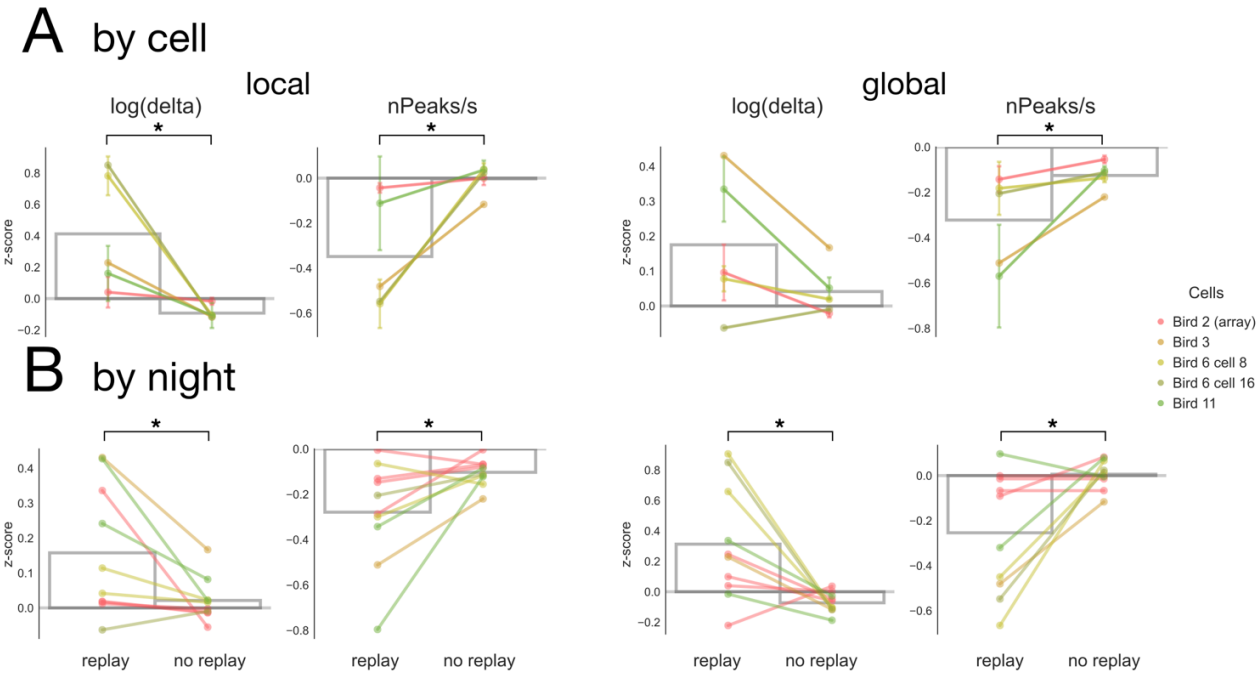

Figure 5.7. Spectral characteristics of epochs containing replay. Nighttime sleep epochs (3 s) with and without replay were compared. "Local" spectral measures were calculated from the LFP. "Global" measures were calculated from either the EEG or the unreferenced LFP (i.e., referenced only to the EEG ground; see Methods). A) For each cell, the mean across all nights is shown. Error bars show the SEM. Gray bars indicate the grand mean across all cells. B) Data from all nights. Gray bars indicate the grand mean across all nights. *, $p < 0.05$ (Wilcoxon signed-rank test).

During epochs containing replay, log(delta) was significantly higher in the LFP (Wilcoxon signed-rank test, $p = 0.04$); this was a trend but not significant in the EEG ($p = 0.08$) (**Figure 5.7A**). Conversely, replay-containing epochs had significantly lower nPeaks, in both the LFP ($p = 0.04$) and the EEG ($p = 0.04$) (**Figure 5.7A**). These patterns were also found when each night

was considered independently (**Figure 5.7B**; local log(delta) p = 0.02; local nPeaks p = 0.03; global log(delta) p = 0.02; global nPeaks p = 0.03). This suggests that replay tends to occur during NREM rather than REM. The sets of results were also highly consistent, in that almost all individual comparisons were in the significant direction.

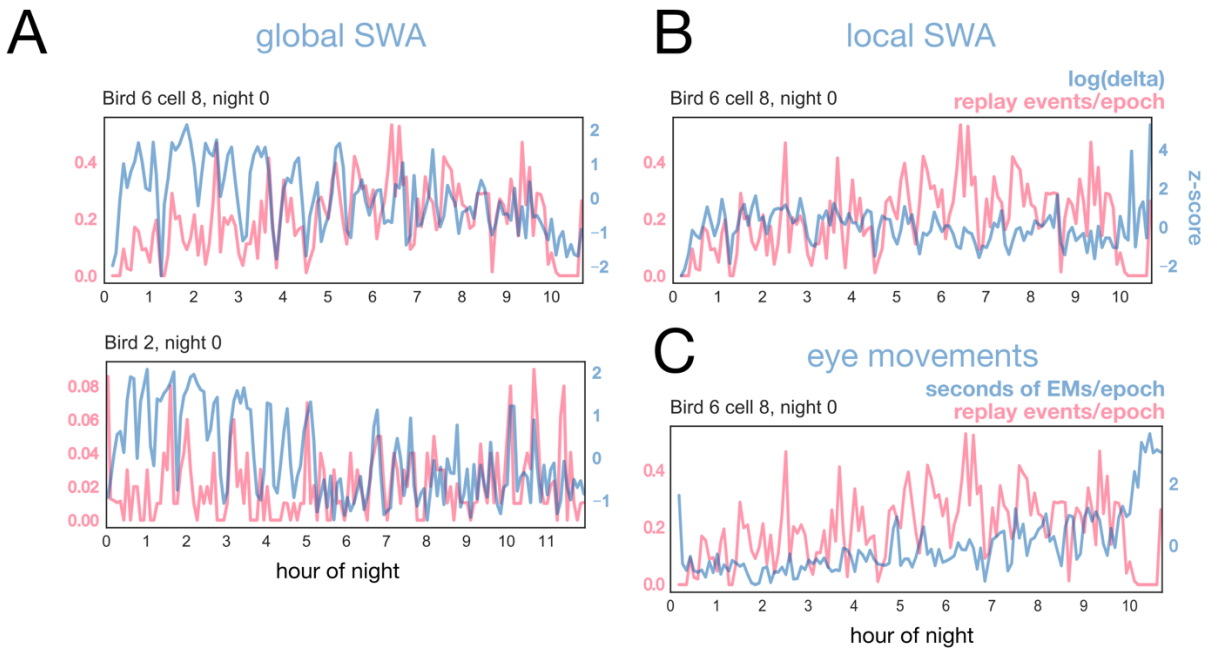

Figure 5.8. Sleep structure vs replay frequency across the night. Red, number of replay events per 3-s epoch. Blue, measure of sleep structure. Data are binned in 5-minute bins. A) Delta power in the EEG (Bird 6) or the unreferenced array LFP (Bird 2). B) Delta power in the LFP. C) Eye movements, measured in s/epoch (z-scored). SWA, slow wave activity.

Over the course of the night, the amount of replay per epoch often seemed to oscillate, usually with a period between 30 and 60 minutes (**Figure 5.8**, red traces). We asked whether this rhythm was related to the ultradian rhythms present in sleep structure. Indeed, global slow wave activity **(Figure 5.8A**, blue traces) appeared to oscillate in tandem with replay during many nights. The co-oscillation of replay activity with delta also appeared locally, albeit to a lesser degree (**Figure 5.8B**); the LFP is likely less reflective of global sleep structure than the EEG (compare blue traces in **Figure 5.8A**, top, and **Figure 5.8B**). Conversely, replay occurred out of

phase with nPeaks (not shown) and eye movements (**Figure 5.8C**). Interestingly, while delta decreased across the night, replay did not necessarily follow this pattern and in some cases appeared to increase over the night. This could indicate that replay is associated with NREM, but not SWS specifically.

Replay content

What parts of the song are replayed? To measure replay content, we used the spike synchronization profile, a modified variant of event synchronization which tracks the synchrony of two or more spiketrains over time (Kreuz et al., 2015; Mulansky and Kreuz, 2016). This measure was calculated between each replay event and its template (**Figure 5.9**, black traces), and across all templates to evaluate consistency across singing activity (**Figure 5.9**, red traces).

In the case of RA neurons, peaks in the spike synchronization profile correspond to bursts, as many cells are firing simultaneously. The height of a given peak reflects how many events contained spikes at that timepoint.

The frequency with which any given burst appeared in replay varied widely across the song, and did not appear to be closely linked to how consistent the burst was across templates (**Figure 5.9**). This suggests that different parts of the song may be replayed in disproportionate amounts. Most cells had one or two especially prominent peaks, indicating segments of the motif that appeared in replay events most reliably. For instance, in Bird 2 the most prominent peaks are clustered near syllable B and the following gap; in Bird 3 the two largest peaks bracket the first half of syllable B; and in Bird 11 the largest peak occurs at the onset of syllable A. Interestingly, the two cells that came from the same bird (Bird 6) both had a major peak near the same point, near the transition from syllable A to B.

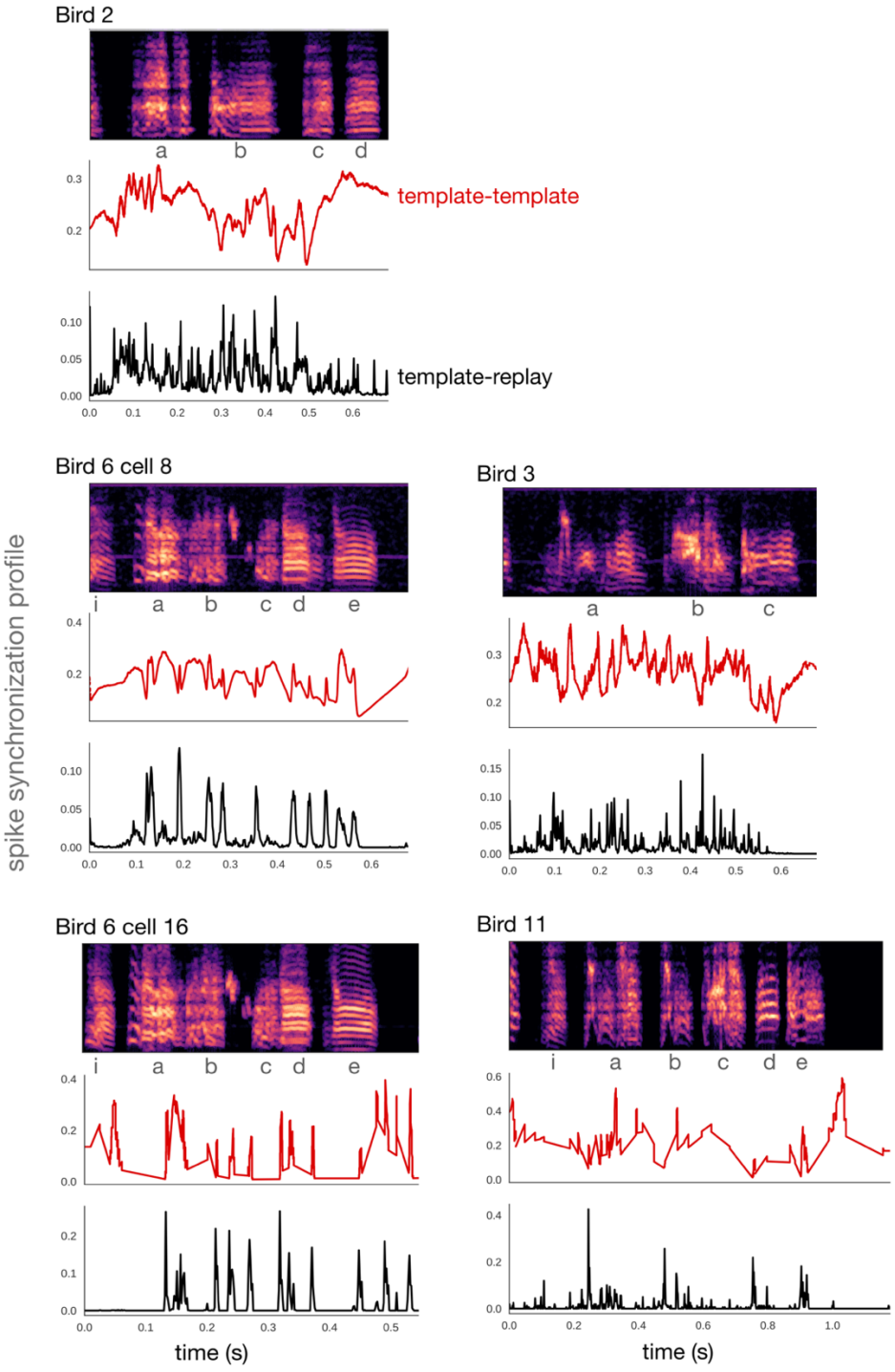

Figure 5.9. Replay content. For each cell, the song spectrogram is shown with syllables labeled in grey. Below the spectrogram, the aligned spike synchronization profile is shown for both singing activity and sleep replay. Red, shared content across motif spiketrains used as templates. Black, mean content across all replay events, calculated by averaging the spike synchronization profile of each replay event with its template.

Compressed events

Additional examination of the events found with compressed templates (0.1x – 0.3x) showed a surprisingly close correspondence to the template (**Figure 5.10A**). The compressed events co-occurred with a very slightly deflection in the LFP (**Figure 5.10B-C**), and they did not appear to be associated with EEG events (**Figure 5.10D**) or eye movements (**Figure 5.10E**). The difference in the magnitude of the LFP effect (compare to **Figure 5.5**) suggests these events are fundamentally different from real-time replay.

We confirmed this by examining the LFP effect over multiple scales and birds (**Figure 5.11**). In both examples, the amplitude of the replay-triggered LFP is higher over a broad range of timescales centered around real time, and drops off for both highly compressed and highly expanded timescales.

While the majority of compressed events are likely artifacts, this does not rule out the possibility that some of these events may be actual instances of compressed replay. During sleep, RA neurons were often seen firing "slow" bursts – short trains of spikes faster than the surrounding tonic firing of ~20 Hz, but slower than is typical for RA bursts during singing activity. It could be that some of these singular "slow" bursts are recapitulating a compressed version of song interburst intervals, with each burst replaced by a single spike as can occur even during real time replay. Given our knowledge of the system, however, it is unclear what the purpose of such events might be, or how they would be generated.

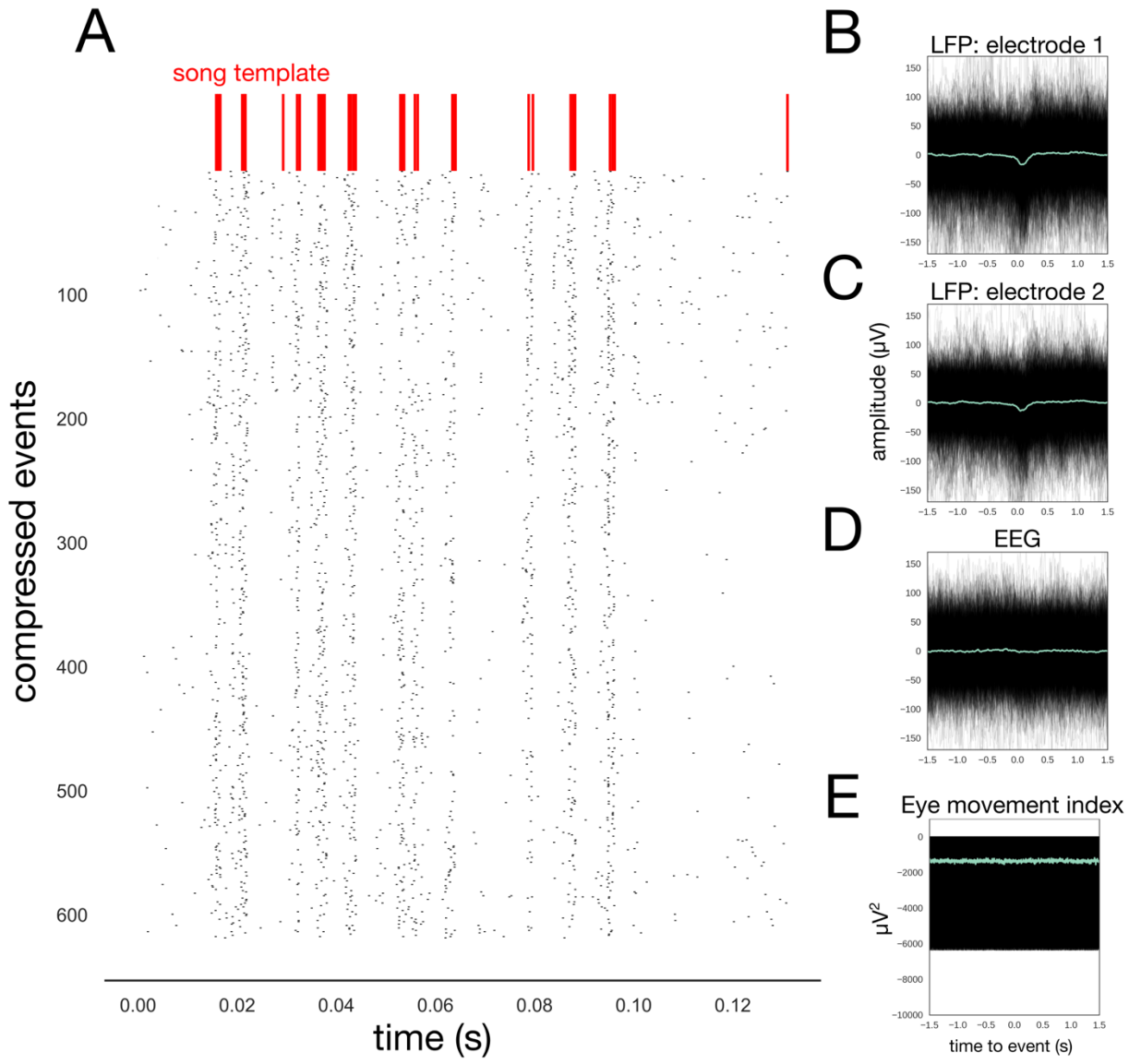

Figure 5.10. Compressed events and event-triggered averages of LFP, EEG, and EOG. Data are from the same cell shown in Figure 5.2. A) Raster of all events identified at timescale 0.2x with $p < 0.02$. The compressed version of a representative template is shown in red. B-E) Replay-triggered traces from the PSG, with 0 seconds corresponding to the start of each replay event. Thin black lines, individual traces. Thick green line, mean of all traces. In B-D, traces with artifacts > 500 μV were excluded. B) LFP from electrode 1, the same electrode on which the RA neuron was recorded. C) LFP from electrode 2, a nearby quiet electrode. D) Surface EEG. E) Replay-triggered eye movement index, calculated from the anticorrelation of the LEOG and REOG. Eye movements would appear on this index as negative deflections.

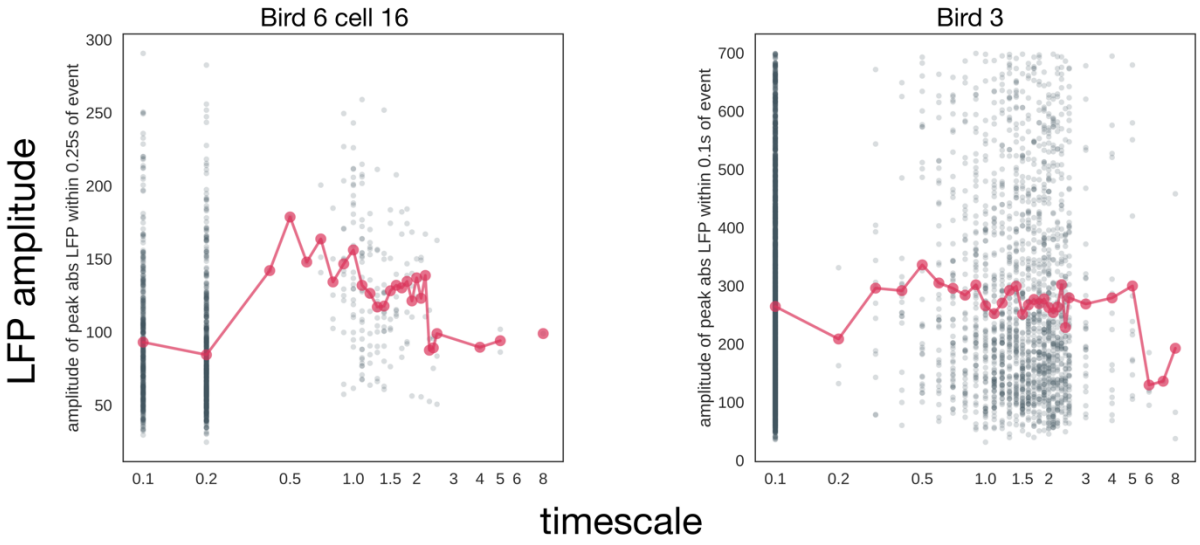

Figure 5.11. Timescale of replay events vs amplitude of LFP. For each replay event, the peak amplitude of the LFP within 0.25s (Bird 6) or 0.1s (Bird 3) is plotted. The value of this time window was chosen based on the timing of the average LFP slow wave that co-occurred with real-time replay. Each grey dot corresponds to a single replay events, and means at each timescale are plotted in red. Timescale is defined such that 1 indicates real time, timescales between 0 and 1 indicate time compression, and >1 indicates time expansion.

Non-canonical replay

The results so far have been based on templates derived from the full motif that a bird commonly produced during singing, and even ignoring observed cases when birds would occasionally drop a syllable. We plan to analyze the data sets collected during sleep for uncommon singing events (such as dropping individual syllables) and unobserved singing events. We will modify the existing templates by eliminating the spikes representing a given syllable (thereby shortening the templates) and re-running the analyses, then eliminating any overlap with previously identified replay events. It remains to be seen if this will identify additional replay events, ones that are not directly related to typically singing. A particularly interesting analysis will be to prepare templates where the sequence of individual syllables is reversed but the temporal structure within each syllable is preserved. This is more analogous to reverse replay in the hippocampus, and also is worth pursuing.

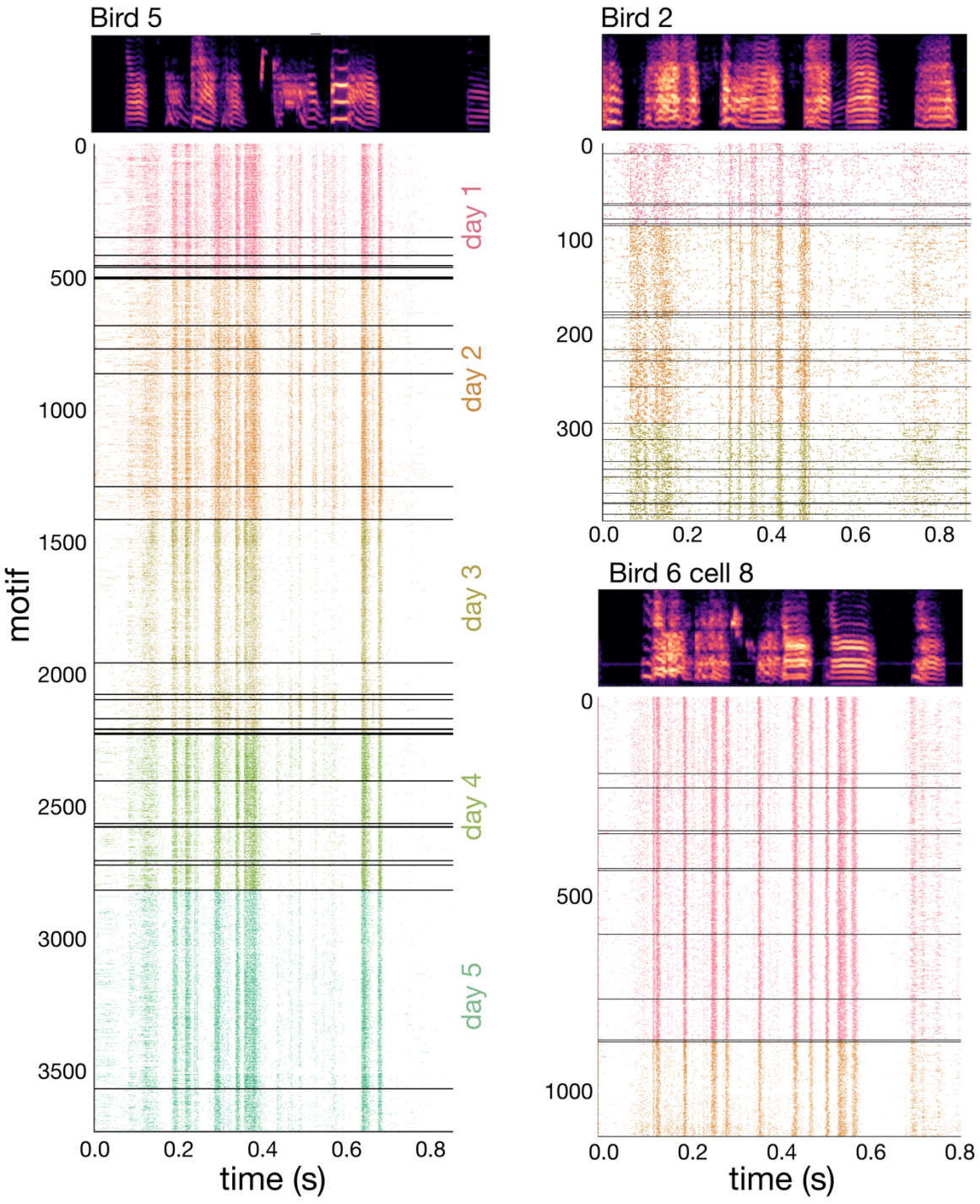

Figure 5.12. Motor coding across multiple sleep-wake cycles: whole-motif activity. Each raster shows activity of the RA cell during all canonical motifs, aligned to the song spectrogram used for dynamic time warping. Different colors indicate different days. Horizontal black lines indicate periods of sleep > 1 minute.

Changes in burst structure during sleep

Previously it has been reported that a subset of RA replay bursts subtly change structure (typically dropping spikes) comparing singing activity before and after sleep (Rauske et al., 2010). We examined three datasets in which a single cell was tracked over 2 – 5 days of singing (**Figure 5.12**).

We saw evidence of this phenomenon in our data but at a much lower frequency than the roughly 20% of bursts that changed nightly in the prior study (**Figure 5.13**). There may be two explanations for this difference. Firstly, our recordings had generally lower SNR than did those reported in Rauske et al. This will adversely affect the ability to see changes in individual spikes within bursts. Second, our birds were quite old (258 – 389 days post hatch), whereas the birds in Rauske et al. were "> 120 days posthatch" (Rauske, 2005). [We do not yet know if we can more accurately ascertain the age of the Rauske et al. 2005 birds.] Since age is a factor affecting adult song variation (Lombardino and Nottebohm, 2000) an age effect cannot be ruled out comparing the two studies. We did not pursue this further.

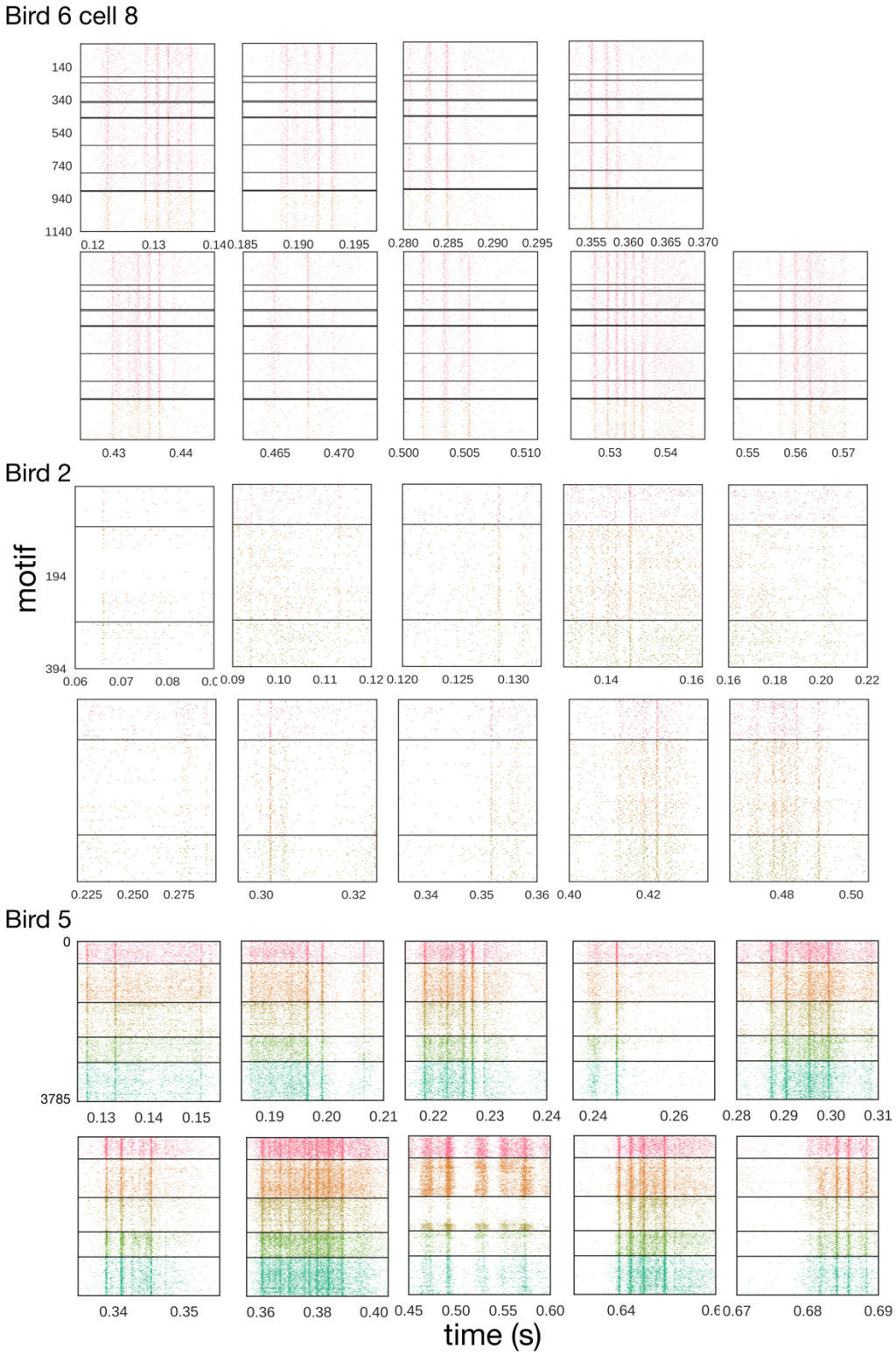

Figure 5.13. Motor coding across multiple sleep-wake cycles: individual bursts. Each raster shows a single burst from the activity of the RA cell during canonical motifs. Different colors indicate different days. Horizontal black lines indicate periods of sleep > 1 minute.

Discussion

Here we show the first evidence linking procedural replay to sleep structure and local oscillatory activity. Song replay occurred close to real time, consistent with previous observations (Dave and Margoliash, 2000; Chi et al., 2003b). Replay tended to occur during periods of probable NREM – sleep rich in slow waves with little high-frequency activity. Slow waves in the LFP, but not the EEG, were time-locked to replay events. The amount of replay oscillated in phase with slow wave content in the ~40-minute ultradian rhythm. The motif was not represented evenly across all replay events, with specific points being replayed more than others.

The time-locking to slow waves bears remarkable similarity to hippocampal replay, which is triply phase-locked to slow waves, spindles, and sharp-wave ripples. This phase-locking is not invariable; in one study it was estimated that about 30% of replay events occurred during sharp wave ripples (O'Neill et al., 2017). However, it is thought to be critical for sleep effects on learning. Memory consolidation improved if spindles were triggered in phase with slow waves (Latchoumane et al., 2017) or if slow waves were triggered in phase with sharp wave ripples (Maingret et al., 2016), but not if the same oscillations were triggered even slightly out of phase. These findings lead to the hypotheses that these oscillations help to coordinate replay events across disparate areas. Slow waves, which travel across broad regions of cortex (Massimini et al., 2004) are particularly poised to carry out this function, and indeed the enhancement of slow waves that auditory stimulation has been shown to benefit memory consolidation (Ngo et al., 2013; Ong et al., 2016; Papalambros et al., 2017; Ong et al., 2018). The results shown here suggest that slow waves may serve an analogous function in the song system of zebra finches.

The sign of the local slow waves we observed is somewhat difficult to interpret: in mammals, negative slow waves recorded extracellularly typically correspond to the UP state and positive waves to the DOWN state (Steriade et al., 1993d). However, very little is known about slow waves in birds; although there is evidence they are generated and function similarly to slow waves in mammals (Reiner et al., 2001; Lesku et al., 2011b; van der Meij et al., 2019), they can travel in multiple directions (Beckers et al., 2014; van der Meij et al., 2018). Moreover the nuclear organization of the avian brain makes it difficult to predict how UP and DOWN states, if they indeed underlie slow waves, might correspond to the LFP.

In a previous report on replay measured in the syrinx, the amount of replay appeared to oscillate over the night with a period of approximately 30 minutes (Young et al., 2017). However, this was not remarked on, and consequently it was not clear if this rhythm appeared across all of the datasets. Nevertheless we speculated this was due to a link between replay and sleep structure, as this approximately matches the sleep cycle duration we had previously found in budgerigars (Chapter 2); subsequently, we observed a sleep cycle of similar duration in zebra finches (Chapter 3). The present findings confirm this speculation, showing that replay activity fluctuates in tandem with large-scale slow wave activity.

The time course of replay, however, was not fully predicted by either NREM or REM. On the scale of the 30-40-minute ultradian rhythm, it increased during periods of heightened slow wave activity. But on the scale of the whole night, it did not follow the SWS trend of decreasing over the course of the night. This could suggest a link to intermediate sleep (IS). The total amount of IS remain consistent over the night in zebra finches and budgerigars, but its delta content should decrease, matching the decline in SWS. In humans, stage 2 remains similarly consistent, but over the night it exhibit changes in delta content, high-frequency activity, spindle

frequency (Himanen et al., 2002), and associated dream mentation (McNamara et al., 2010). Thus, the pattern of replay could reflect a tendency to occur during periods of NREM, correlated with some property of IS that remains consistent or increases over the night.

An alternative possibility is that the intervening REM episodes could affect the amount of replay during surrounding NREM periods. The interleaving of REM and NREM has been hypothesized as a crucial mechanism for sleep processing of memory. This has been supported by behavioral studies of both procedural (Kirov et al., 2015; Buchegger and Meier-Koll, 2016) and declarative memory (Ficca et al., 2000; Batterink et al., 2017) and by studies of structural dendritic changes associated with motor task learning, in which NREM and REM had opposing but complimentary effects (Yang et al., 2014; Li et al., 2017).

We observed uneven representation of the motif across replay. However, with this small sample size it is difficult to draw conclusions about what characterizes these segments of the song. One speculation, consistent with the results shown here is that especially complex syllables are replayed more than others; large peaks did not occur during simple syllables such as harmonic stacks. Additional recordings across multiple birds would help to clarify this. Other approaches to measuring replay content could provide further insights: for example, running shorter segments of the template, or versions of the template with individual syllables removed. The whole-motif approach used here is unlikely to detect replay in which the syllables are out of order, as has been reported (albeit rarely) in syringeal replay (Young et al., 2017).

The replay identification algorithm used here was developed to detect HVC replay occurring close to real-time (Chi et al., 2003a; 2003b). It uses Poisson-based spiketrains to generate its nulls, both when simulating background spiketrains to determine the threshold and when calculating p-values. However, Poisson statistics may not adequately capture the background

spiking of RA, with its highly regular rate, or RA's bursting activity, with long intervals of silence punctuated by superfast bursts. Further optimization of this algorithm for RA would include developing more representative null conditions, especially to test for the presence of highly compressed or expanded replay.

Following the initial discovery of song replay, much evidence has accumulated supporting a link between sleep and learning in songbirds. Behaviorally, sleep appears to benefit sensorimotor song learning (Derégnaucourt et al., 2005) and perceptual learning of auditory memories (Brawn et al., 2013; 2018). Juveniles develop RA sleep bursting, a possible form of proto-replay, after first hearing the tutor song; the structure of this bursting is shaped by which tutor song is heard, and the bursting emerges prior to changes in the bird's own vocalizations (Shank and Margoliash, 2009).

CHAPTER 6. GENERAL DISCUSSION

"There is a time for many words, and there is also a time for sleep."

– Homer, ~850 B.C. (Homer, 1909)

Overview of findings

Specialized forms of sleep may be more widespread in all animals than previously thought. Some mammalian species once thought to lack REM may express it after all (Siegel et al., 1996; Lyamin et al., 2002; Miller et al., 2008). Birds are still able to sleep in extreme situations once assumed incompatible with sleep, underscoring the necessity of the sleep stages (Stahel et al., 1984; Buchet et al., 1986; Rattenborg et al., 1999; 2016). Moreover, recent evidence has challenged the commonly held idea that specialized sleep is unique to birds and mammals. Reptiles may exhibit multiple sleep stages that could be the precursors to SWS and REM (Shein-Idelson et al., 2016; Libourel et al., 2018; Tisdale et al., 2018). Finally, very basic traits of complex sleep such as muscle twitches or EEG slowing may appear in amphibians (Libourel and Herrel, 2016), fish (Leung et al., 2019), insects (Klein et al., 2008; Cassill et al., 2009), cephalopods (Frank et al., 2012), and even jellyfish (Nath et al., 2017). The present results build on these accumulated findings by demonstrating complex sleep architecture in two species of birds and linking this sleep structure to circuit-level mechanisms of sleep function.

In Chapter 2 I examined the sleep architecture of budgerigars. I found highly complex sleep structure with many similarities to mammalian sleep, contradicting previous knowledge of sleep in parrots. For many decades, avian sleep has been characterized as more rudimentary than that of mammals, with low levels of REM and less-developed SWS. Despite recent advances, many sleep researchers working in mammals continue to characterize avian sleep as more primitive

and more fragmented with lower SWA amplitudes (Vorster and Born, 2015) and smaller amounts of REM (Siegel, 2009). However, I demonstrated that experimental conditions used in older studies caused large disruptions in sleep/wake behavior and likely led to incorrect conclusions. In contrast, I showed that budgerigars had very high levels of REM, possibly exceeding that of humans. Furthermore, their sleep was organized into clear patterns resembling those found in many mammals: SWS decrease, REM increase, and ultradian sleep cycles of about 35 minutes. I also confirmed the single previous report of intermediate sleep in birds.

In Chapter 3 I extended these observations to zebra finch sleep, confirming a key set of results that originally challenged the prevailing view of sleep in songbirds. In the course of this work I developed a method for automating the scoring of sleep/wake behavior, one of the major rate limiting steps of sleep studies in birds. Confirming many previous studies, I found no evidence of sleep spindles in surface EEG of budgerigars and zebra finches, nor were they evident in arcopallial LFP. Finally, I showed that zebra finches exhibit an ultradian sleep cycle on the order of 35-40 minutes.

The changing views of avian sleep took place in the broader context of a paradigmatic shift in our understanding of avian brains (Reiner et al., 2001; 2005; Pfenning et al., 2014; Olkowicz et al., 2016) and cognitive abilities (Gentner et al., 2006; Ditz and Nieder, 2015; Kabadayi and Osvath, 2017; Elie and Theunissen, 2018). In subsequent chapters I transitioned to studying song replay, a possible circuit-level mechanism for sleep effects on memory, and one of only two clearly established forms of sleep replay. In Chapter 4 I detailed a method for chronic array recordings that provides an avenue for future studies of replay across neuronal populations and long time periods. In Chapter 5, I examined the features of song replay and its relationship to sleep structure. Song replay occurred at or near real time, confirming earlier reports. Replay was

most prevalent during NREM-like sleep, and fluctuated throughout the night in tandem with the 35-minute ultradian rhythm seen earlier. However, the total amount did not follow the SWS trend of decreasing over the night. Finally, individual replay events were time-locked to local slow waves in RA.

The association of replay with NREM and the coupling of replay to slow waves are both strikingly similar to hippocampal replay in rodents. These similarities between mechanisms in different memory systems, in two distantly related species, suggest that sleep replay and its links to broader sleep structure are very old. The findings here are also consistent with previous reports of reactivation in M1, which occurred during NREM and were time-locked to slow waves (Gulati et al., 2014; Ramanathan et al., 2015). An ancient origin of sleep replay is further supported by recent evidence for sleep reactivation in Drosophila (Dag et al., 2019).

In the context of hippocampal replay, slow waves and other oscillations are thought to co-occur with replay in order to promote the simultaneous participation of many cells, especially across disparate brain areas (Siapas and Wilson, 1998; Maingret et al., 2016; Wang and Ikemoto, 2016; Khodagholy et al., 2017; Latchoumane et al., 2017). Therefore, the present results also support a broadly expressed role of slow waves in coordinating replay events.

Future directions

Function of REM

The enormous amount of REM in budgerigars suggests an important functional contribution of this stage. The present study did not attempt to draw any link with daytime behavior, but this could be a fruitful avenue of future study. Multiple behavioral tests of learning have been developed in budgerigars (Eda-Fujiwara et al., 2012; Tu and Dooling, 2012; Seki and Dooling,

2016; Spierings and Cate, 2016); some are highly ethologically relevant, such as birds learning to imitate the calls of new conspecifics in order to become socially integrated and to impress potential mates (Hile et al., 2005; Dahlin et al., 2014).

Laboratory rodents have relatively little REM; for example, in the "reverberation" study, which tracked replay for 24 - 48 consecutive hours, REM took up only 8% of recording time (Ribeiro et al., 2004). This is almost certainly why hippocampal REM replay has only ever been described in a single study (Louie and Wilson, 2001), despite the prolific nature of the hippocampal replay field. Budgerigars and zebra finches therefore provide an important opportunity to study REM function in species which have evolved high amounts of REM.

Tonic and phasic REM in birds

In Chapter 2, I presented preliminary evidence of both tonic REM (without eye movements) and phasic REM (with eye movements). In mammals these subtypes of REM, although not very thoroughly studied, occur rhythmically (Ktonas et al., 2003), may serve different functions (Molinari and Foulkes, 1969; De Carli et al., 2016)and have subtly different electrophysiological properties (Brankačk et al., 2012; Usami et al., 2017; Simor et al., 2018). If REM subtypes in birds exhibit similar patterns, this would strengthen the case for a common precursor of REM in mammals and birds. One of the simplest ways to test for this could be to measure the arousal threshold, which should be higher during phasic (Sallinen et al., 1996; Wehrle et al., 2007).

In mammals, the eye movements of phasic REM are accompanied by pontine-geniculo-occipital (PGO) waves sweeping through the visual system (Callaway et al., 1987), PGO waves appear to have important functional properties in their own right (Datta, 2000; Datta et al., 2004), although they are not as well studied as slow waves. Birds have never been shown to have PGO waves, but one study that recorded from optic tectum did observe EEG spikes that were

associated with eye movements (Sugihara and Gotoh, 1973); the optic tectum is analogous to the superior colliculus, which may also receive PGO waves in mammals (Syka et al., 1973). Finding avian PGO-like waves (or their absence) would be a major mechanistic clue as to the evolutionary origins of rapid eye movements during REM.

Slow waves and evoked BOS responses

If BOS-evoked responses in sleeping birds are indeed analogous to evoked replay, as we predict, then these responses should be similarly linked to NREM and local slow waves. There is evidence for the association with NREM already. BOS responses appear very quickly after the bird falls asleep (Dave et al., 1998); REM is unlikely to occur with such a short latency. Additionally, injections of acetylcholine into HVC suppressed BOS responses (Shea and Margoliash, 2003), and acetylcholine innervation to Uva has been hypothesized to drive Uva_{HVC} neurons, which suppress sleep bursting (Hahnloser et al., 2008). In mammals acetylcholine levels are very high during REM and low during NREM (Vazquez and Baghdoyan, 2001; Lee and Dan, 2012), although it is unknown if this is true in birds as well.

Such experiments would require PSG and video to fully distinguish between wake and REM. Recordings would be needed over many more trials and a longer period of time than is typical of an acute recording of a single site. A more challenging variant of this experiment would be to specifically target auditory stimuli to different phases of the slow wave, as has been done in human sleep cueing experiments (Batterink et al., 2016).

Properties of slow waves in birds

Despite the known similarities between avian and mammalian slow waves there is much that still remains unknown. For example, the sole evidence for the intracellular generation of avian

slow waves comes from a single figure in a single paper (Reiner et al., 2001). Much confusion remains over how delta waves can appear in the EEG of birds at all, given that neurons in the avian brain are not organized into columnar sheets as is mammalian cortex (Wester and Contreras, 2012). Avian slow waves travel across the forebrain, but do so in three-dimensional "plumes" and do not travel in a consistent direction (Beckers et al., 2014; van der Meij et al., 2018; 2019). Future experiments, including slice experiments, are needed to further investigate the possibility of UP and DOWN states (Steriade et al., 1993c) in avian neurons, how these rhythms might be synchronized across cells (Steriade et al., 1993b) and modulated by neurotransimitters (Steriade et al., 1993a), and how they are expressed in the EEG (Steriade et al., 1993d).

Adult neurogenesis

New neurons are added to the song system throughout the bird's adult life; in zebra finches they almost double in number from the beginning of adulthood (Walton et al., 2012). These adult-born neurons migrate to HVC (Goldman and Nottebohm, 1983; Alvarez-Buylla and Nottebohm, 1988; Scott et al., 2012), project to RA (Kirn et al., 1991), and eventually become fully integrated HVC_{RA} neurons that are active during song (Tokarev et al., 2015).

While HVC neurogenesis has never been examined in the context of sleep, a study that imaged adult-born neurons migrating to HVC observed migration happening at night (Scott et al., 2012). The authors hypothesized that the relatively crowded extracellular space in the mature brain was a key barrier to migration, resulted in the unusual "wandering" form of migration they saw the new neurons using. Sleep is known to expand the extracellular space in mammals, increasing the flow of cerebrospinal fluid and hastening the removal of metabolic byproducts and waste (Xie et al., 2013). Perhaps another function of expanded extracellular space could be to

facilitate the migration of adult-born neurons as the bird sleeps. The observation of post-sleep changes in RA spike burst structure (Rauske et al., 2010) may indicate the nighttime establishment of new synapses from HVC_{RA} neurons that are newly engaging RA circuitry.

Functional effects of sleep and sleep replay

Auditory feedback manipulation

In pitch shifting experiments, birds are induced to alter the pitch of a single syllable (Tumer and Brainard, 2007). The syllable's normal distribution of pitch is determined, and then one half of the distribution (either higher or lower) is targeted by an aversive auditory stimulus (typically a loud noise burst (Tumer and Brainard, 2007; Hoffmann et al., 2016; Roberts et al., 2017) or more recently, pharmacogenetic (Heston et al., 2018) or optogenetic stimulation (Hisey et al., 2018) of the ventral tegmental area). This process unfolds over several days, and is reversible but not immediately so: if the training is stopped, birds usually slowly return the syllable to its original baseline pitch (Ali et al., 2013). In most cases such experiments have focused on harmonic stacks for technical reasons.

A sleep effect was observed in one pitch shifting study that used juvenile and young adult birds (Andalman and Fee, 2009). During training, the pitch tended to shift in the direction of learning overnight. If LMAN was inactivated during the day, the pitch returned to what it had been that morning. This led the researchers to hypothesize that learning was taking place in two steps: during the day, the AFP drove changes in pitch, while during the night, the HVC-RA circuit 'updated' or consolidated the day's learning (Andalman and Fee, 2009).

However, a sleep-dependent change in the direction of learning ("enhancement") contrasts with effects of sleep during normal juvenile learning, in which sleep causes song to become less

structured, lower in entropy variance, and less like the tutor song ("deterioration") (Derégnaucourt et al., 2005). It could be that during pitch shifting, sleep is actually functioning to revert the bird's song to normal, with the result that the song "deteriorates" from normal post sleep and thus moves in the direction of pitch shifting. While speculative, this possibility could be studied by examining the course of recovery from pitch shifting, and whether adding or removing the aversive stimulus change the type of sleep effects seen.

An advantage of this paradigm is that it targets an individual element of song while leaving the rest intact. This raises the possibility that such training could be reflected in replay content.

Other approaches, such as delayed auditory feedback (Leonardo and Konishi, 1999; Fukushima and Margoliash, 2015) or temporary deafening (Zevin et al., 2004; Shank and Margoliash, 2009), could also be employed to examine sleep-dependent changes in behavior and/or replay, especially during the recovery process. These methods are capable of inducing large-scale changes in song relatively quickly, and would have the advantage of amplifying the magnitude of any potential sleep effects. For example, such a disruption of the song might be expected to alter overall sleep architecture.

Replay in juvenile birds

Replay has never been formally demonstrated in juvenile birds, partially because of the computational challenge it poses. Juvenile plastic song is not stereotyped and can shift rapidly (Tchernichovski, 2001), which means that a precise song structure and multiple related spike templates is not available. However, the approach used to identify replay here was designed for use with multiple templates, and could make such an experiment more plausible. With a range of templates that are more variable than in adult birds, this opens up the possibility of identifying phenomena such as preplay. (There is also preliminary evidence for preplay in RA in adult birds

(Rauske, 2005), comparing templates of spike bursts before and after they changed structure as reported in Rauske et al. 2010).This could be combined with paradigms such as the ABAB method, in which birds are taught one song until it becomes relative stable, and then presented with a new song in which only one syllable is different from the original (Ravbar et al., 2012). This induces local variability around the new syllable while leaving the rest stereotyped, which could facilitate the reliable identification of replay in juveniles.

Manipulating sleep in birds

How can one test for a causal link between learning and specific sleep stages in birds? The traditional approach used in mammals, specific sleep deprivation, is unlikely to work in birds, even putting aside the confounds of stress and the disruption of non-targeted sleep stages. Birds fluctuate so rapidly between sleep stages that it is implausible to simply awaken them each time they enter the sleep stage in question, as is done in humans (Karni et al., 1994) and some rodent studies (Datta et al., 2004). In rodents, a common REM deprivation method relies on loss of muscle tone (i.e. the "flowerpot method," in which muscle atonia causes the animal to fall off a small platform into shallow water whenever a REM episode begins) (Smith and Rose, 1996). As confirmed in chapters 2-3, birds do not exhibit this total loss of muscle tone during REM.

One method for testing such a causal link arises from the human literature: auditory manipulation of slow waves. This technique uses acoustic stimuli, delivered at specific phases of the slow wave, to either suppress or enhance slow wave activity (Ngo et al., 2013). It does not appear to alter other aspects of sleep architecture, and can induce both physiological effects (Tasali et al., 2008; Grimaldi et al., 2019) and effects on learning (Ngo et al., 2013; Papalambros et al., 2017). Such a technique, if developed in birds, would provide a powerful way to test for an association of slow waves with behavior and with replay.

Interestingly, some species of birds gain the ability to resist the deleterious effects of sleep deprivation in specific contexts. For example, during the migratory season, white-crowned sparrows sleep far less than normal, but nevertheless retain high levels of performance on a learned cognitive task (Rattenborg et al., 2004). But outside of the migratory season equivalent amounts of sleep deprivation caused decrements in performance on the same task (Rattenborg et al., 2004). It is not known if this is true of all memory tasks, or is limited to only some categories as is true of certain patient populations with sleep disruptions (Dresler et al., 2011a). Further study of this phenomenon could lead to remarkable insights into resilience to sleep deprivation and compensatory mechanisms.

REFERENCES

Abt K (1987) Descriptive data analysis: a concept between confirmatory and exploratory data analysis. Methods Inf Med 26:77–88.

Agnew HW, Webb WB (1973) The influence of time course variables on REM sleep. Bull Psychon Soc 2:131–133.

Albouy G, Sterpenich V, Balteau E, Vandewalle G, Desseilles M, Dang-Vu T, Darsaud A, Ruby P, Luppi P-H, Degueldre C, Peigneux P, Luxen A, Maquet P (2008) Both the hippocampus and striatum are involved in consolidation of motor sequence memory. Neuron 58:261–272.

Aldredge JL, Welch AJ (1973) Variations of heart rate during sleep as a function of the sleep cycle. Electroencephalography and Clinical Neurophysiology 35:193–198.

Ali F, Otchy TM, Pehlevan C, Fantana AL, Burak Y (2013) The basal ganglia is necessary for learning spectral, but not temporal, features of birdsong. Neuron 80:494–506.

Alonso RG, Trevisan MA, Amador A, Goller F, Mindlin GB (2015) A circular model for song motor control in Serinus canaria. Front Comput Neurosci 9:943–949.

Alvarez-Buylla A, Nottebohm F (1988) Migration of young neurons in adult avian brain. Nature 335: 353-354.

Amlaner CJ Jr., McFarland DJ (1981) Sleep in the herring gull (Larus argentatus). Animal Behaviour 29:551–556.

Amzica F, Steriade M (1998) Cellular substrates and laminar profile of sleep K-complex. Neuroscience 82:671–686.

Ancoli-Israel S, Chesson A, Quan SF (2007) The AASM manual for the scoring of sleep and associated events: rules, terminology and technical specifications. American Academy of Sleep Medicine.

Andalman AS, Fee MS (2009) A basal ganglia-forebrain circuit in the songbird biases motor output to avoid vocal errors. Proc Natl Acad Sci USA 106:12518–12523.

Antrobus J, Kondo T, Reinsel R, Fein G (1995) Dreaming in the late morning: summation of REM and diurnal cortical activation. Conscious Cogn 4:275–299.

Aristotle (350BCa) On Sleep and Sleeplessness. Available at: http://classics.mit.edu/Aristotle/sleep.html.

Aristotle (350BCb) The History of Animals. Available at: http://classics.mit.edu//Aristotle/history_anim.html.

Armitage R, Trivedi M, Hoffmann R, Rush AJ (1997) Relationship between objective and subjective sleep measures in depressed patients and healthy controls. Depress Anxiety 5:97–102.

Aschoff J (1965) Circadian Rhythms in Man. Science 148:1427–1432.

Aserinsky E, Kleitman N (1953) Regularly occurring periods of eye motility, and concomitant phenomena, during sleep. Science 118:273–274.

Aton SJ, Seibt J, Dumoulin M, Jha SK, Steinmetz N, Coleman T, Naidoo N, Frank MG (2009) Mechanisms of sleep-dependent consolidation of cortical plasticity. Neuron 61:454–466.

Axmacher N, Elger CE, Fell J (2008) Ripples in the medial temporal lobe are relevant for human memory consolidation. Brain 131:1806–1817.

Ayala-Guerrero F (1989) Sleep patterns in the parakeet Melopsittacus undulatus. Physiol Behav 46:787–791.

Ayala-Guerrero F, Mexicano G, Ramos JI (2003) Sleep characteristics in the turkey Meleagris gallopavo. Physiol Behav 78:435–440.

Ayala-Guerrero F, Pérez MC, Calderón A (1988) Sleep patterns in the bird Aratinga canicularis. Physiol Behav 43:585–589.

Ayala-Guerrero F, Vasconcelos-Dueñas I (1988) Sleep in the dove Zenaida asiatica. Behavioral and Neural Biology 49:133–138 Available at: http://linkinghub.elsevier.com/retrieve/pii/S0163104788904517.

Ball NJ, Amlaner CJ (1983) A Synthesis of Sleep in Wild Birds. Behaviour 87:85–119.

Batterink LJ, Creery JD, Paller KA (2016) Phase of Spontaneous Slow Oscillations during Sleep Influences Memory-Related Processing of Auditory Cues. J Neurosci 36:1401–1409.

Batterink LJ, Westerberg CE, Paller KA (2017) Vocabulary learning benefits from REM after slow-wave sleep. Neurobiology of Learning and Memory 144:102–113.

Beckers GJL, van der Meij J, Lesku JA, Rattenborg NC (2014) Plumes of neuronal activity propagate in three dimensions through the nuclear avian brain. BMC Biol 12:16.

Begin M (1979) White Nights. New York: Harper & Row.

Bendor D, Wilson MA (2012) Biasing the content of hippocampal replay during sleep. Nat Neurosci 15:1439–1444.

Berger RJ, Phillips NH (1994) Constant light suppresses sleep and circadian rhythms in pigeons without consequent sleep rebound in darkness. Am J Physiol 267:R945–R952.

Berger RJ, Walker JM (1972) Sleep in the burrowing owl (Speotyto cunicularia hypugaea). Behav Biol 7:183–194.

Bergmann BM, Everson CA, Kushida CA, Fang VS, Leitch CA, Schoeller DA, Refetoff S, Rechtschaffen A (1989) Sleep deprivation in the rat: V. Energy use and mediation. Sleep 12:31–41.

Bergmann BM, Gilliland MA, Feng PF, Russell DR, Shaw P, Wright M, Rechtschaffen A, Alverdy JC (1996) Are physiological effects of sleep deprivation in the rat mediated by bacterial invasion? Sleep 19:554–562.

Beyaert L, Greggers U, Menzel R (2012) Honeybees consolidate navigation memory during sleep. J Exp Biol 215:3981–3988.

Bédard C, Kröger H, Destexhe A (2006) Does the 1/f frequency scaling of brain signals reflect self-organized critical states? Phys Rev Lett 97:118102.

Blake H, Gerard RW (1937) Brain potentials during sleep. American Journal of Physiology - Legacy Content 119:692–703.

Blumberg MS, Coleman CM, Gerth AI, McMurray B (2013) Spatiotemporal structure of REM sleep twitching reveals developmental origins of motor synergies. Curr Biol 23:2100–2109.

Bonnet MH (1983) Memory for events occurring during arousal from sleep. Psychophysiology 20:81–87.

Borbély AA, Achermann P (2005) Sleep Homeostasis and Models of Sleep Regulation. In: Principles and Practice of Sleep Medicine (Kryger MH, Roth T, Dement WC, eds), pp 405–417. Philadelphia, PA: Elsevier Saunders.

Borquez M, Born J, Navarro V, Betancourt R, Inostroza M (2013) Sleep enhances inhibitory behavioral control in discrimination learning in rats. Experimental Brain Research 232:1469–1477.

Boyce R, Glasgow SD, Williams S, Adamantidis A (2016) Causal evidence for the role of REM sleep theta rhythm in contextual memory consolidation. Science 352:812–816.

Böhner J (1990) Early acquisition of song in the zebra finch, Taeniopygia guttata. Animal Behaviour 39:369–374.

Brankačk J, Scheffzük C, Kukushka VI, Vyssotski AL, Tort ABL, Draguhn A (2012) Distinct features of fast oscillations in phasic and tonic rapid eye movement sleep. Journal of Sleep Research 21:630–633.

Brawn TP, Fenn KM, Nusbaum HC, Margoliash D (2010) Consolidating the effects of waking and sleep on motor-sequence learning. J Neurosci 30:13977–13982.

Brawn TP, Nusbaum HC, Margoliash D (2013) Sleep consolidation of interfering auditory memories in starlings. Psychol Sci 24:439–447.

Brawn TP, Nusbaum HC, Margoliash D (2018) Sleep-dependent reconsolidation after memory destabilization in starlings. Nat Comms 9:3093.

Buchegger J, Meier-Koll A (2016) Motor Learning and Ultradian Sleep Cycle: An Electroencephalographic Study of Trampoliners:. Perceptual and Motor Skills 67:635–645.

Buchet C, Dewasmes G, Le Maho Y (1986) An electrophysiological and behavioral study of sleep in emperor penguins under natural ambient conditions. Physiol Behav 38:331–335.

Buckley DP, Duggan MR, Anderson MJ (2017) Budgie in the mirror: An exploratory analysis of social behaviors and mirror use in the Budgerigar (Melopsittacus undulatus). Behav Processes 135:66–70.

Callaway CW, Lydic R, Baghdoyan HA, Hobson JA (1987) Pontogeniculooccipital waves: spontaneous visual system activity during rapid eye movement sleep. Cell Mol Neurobiol 7:105–149.

Campbell SS, Tobler I (1984) Animal sleep: a review of sleep duration across phylogeny. Neurosci Biobehav Rev 8:269–300.

Cantero JL, Atienza M, Stickgold R, Kahana MJ, Madsen JR, Kocsis B (2003) Sleep-dependent theta oscillations in the human hippocampus and neocortex. J Neurosci 23:10897–10903.

Capellini I, Barton RA, McNamara P, Preston BT, Nunn CL (2008) Phylogenetic analysis of the ecology and evolution of mammalian sleep. Evolution 62:1764–1776.

Carskadon MA, Dement WC (2011) Normal human sleep: an overview. In: Principles and practice of sleep medicine, 5 ed. (Kryger MH, Roth T, Dement WC, eds), pp 16–26. St Louis.

Cassill DL, Brown S, Swick D, Yanev G (2009) Polyphasic Wake/Sleep Episodes in the Fire Ant, Solenopsis Invicta. J Insect Behav 22:313–323.

Cassone VM (2014) Avian circadian organization: a chorus of clocks. Front Neuroendocrinol 35:76–88.

Celis-Murillo A, Stodola KW, Pappadopoli B, Burton JM, Ward MP (2016) Seasonal and daily patterns of nocturnal singing in the Field Sparrow (Spizella pusilla). J Ornithol 157:853–860.

Chellappa SL, Frey S, Knoblauch V, Cajochen C (2011) Cortical activation patterns herald successful dream recall after NREM and REM sleep. Biol Psychol 87:251–256.

Chi Z, L Rauske P, Margoliash D (2003a) Detection of spike patterns using pattern filtering, with applications to sleep replay in birdsong. Neurocomputing 52-54:19–24.

Chi Z, Margoliash D (2001) Temporal Precision and Temporal Drift in Brain and Behavior of Zebra Finch Song. Neuron 32:899–910.

Chi Z, Rauske PL, Margoliash D (2003b) Pattern Filtering for Detection of Neural Activity, with Examples from HVc Activity During Sleep in Zebra Finches. Neural Computation 15:2307–2337.

Chung JE, Magland JF, Barnett AH, Tolosa VM, Tooker AC, Lee KY, Shah KG, Felix SH, Frank LM, Greengard LF (2017) A Fully Automated Approach to Spike Sorting. Neuron 95:1381–1394.e1386.

Cicogna P, Natale V, Occhionero M, Bosinelli M (2000) Slow wave and REM sleep mentation. Sleep Res Online 3:67–72.

Cirelli C, Tononi G (2015) Sleep and synaptic homeostasis. Sleep 38:161–162.

Clemens Z, Fabó D, Halász P (2006) Twenty-four hours retention of visuospatial memory correlates with the number of parietal sleep spindles. Neurosci Lett 403:52–56.

Clemens Z, Mölle M, Eross L, Barsi P, Halász P, Born J (2007) Temporal coupling of parahippocampal ripples, sleep spindles and slow oscillations in humans. Brain 130:2868–2878.

Corkin S (1968) Acquisition of motor skill after bilateral medial temporal-lobe excision. Neuropsychologia 6:255–265.

Cousins JN, El-Deredy W, Parkes LM, Hennies N, Lewis PA (2016) Cued Reactivation of Motor Learning during Sleep Leads to Overnight Changes in Functional Brain Activity and Connectivity. Battaglia FP, ed. PLoS Biol 14:e1002451.

Crandall SR, Adam M, Kinnischtzke AK, Nick TA (2007) HVC neural sleep activity increases with development and parallels nightly changes in song behavior. J Neurophysiol 98:232–240.

Csicsvari J, O'Neill J, Allen K, Senior T (2007) Place-selective firing contributes to the reverse-order reactivation of CA1 pyramidal cells during sharp waves in open-field exploration. Eur J Neurosci 26:704–716.

d'Antonio-Bertagnolli AJ, Anderson MJ (2017) Lateral asymmetry in the freely occurring behaviour of budgerigars (Melopsittacus undulatus) and its relation to cognitive performance. Laterality 42:1–20.

Dag U, Lei Z, Le JQ, Wong A, Bushey D, Keleman K (2019) Neuronal reactivation during post-learning sleep consolidates long-term memory in Drosophila. Elife 8:229.

Dahlin CR, Young AM, Cordier B, Mundry R, Wright TF (2014) A test of multiple hypotheses for the function of call sharing in female budgerigars, Melopsittacus undulatus. Behav Ecol Sociobiol (Print) 68:145–161.

Daliparthi VK, Tachibana RO, Cooper BG, Hahnloser RH, Kojima S, Sober SJ, Roberts TF (2019) Transitioning between preparatory and precisely sequenced neuronal activity in production of a skilled behavior. Elife 8:3086.

Darwin C (1882) Comparison of the Mental Powers of Man and the Lower Animals. In: The Descent of Man and Selection in Relation to Sex. London: John Murray.

Datta S (2000) Avoidance task training potentiates phasic pontine-wave density in the rat: A mechanism for sleep-dependent plasticity. J Neurosci 20:8607–8613.

Datta S, Mavanji V, Ulloor J, Patterson EH (2004) Activation of phasic pontine-wave generator prevents rapid eye movement sleep deprivation-induced learning impairment in the rat: a mechanism for sleep-dependent plasticity. J Neurosci 24:1416–1427.

Dave AS, Margoliash D (2000) Song replay during sleep and computational rules for sensorimotor vocal learning. Science 290:812–816.

Dave AS, Yu AC, Margoliash D (1998) Behavioral State Modulation of Auditory Activity in a Vocal Motor System. Science 282:2250–2254.

Davidson TJ, Kloosterman F, Wilson MA (2009) Hippocampal replay of extended experience. Neuron 63:497–507.

Day NF, Kinnischtzke AK, Adam M, Nick TA (2009) Daily and developmental modulation of "premotor" activity in the birdsong system. Dev Neurobiol 69:796–810.

Day NF, Nick TA (2013) Rhythmic cortical neurons increase their oscillations and sculpt basal ganglia signaling during motor learning. Dev Neurobiol 73:754–768.

De Carli F, Proserpio P, Morrone E, Sartori I, Ferrara M, Gibbs SA, De Gennaro L, Russo Lo G, Nobili L (2016) Activation of the motor cortex during phasic rapid eye movement sleep. Ann Neurol 79:326–330.

de Cervantes Saavedra M (1949) Don Quixote. New York: The Viking Press. Available at: https://archive.org/stream/in.ernet.dli.2015.45341/2015.45341.Don-Quixote_djvu.txt.

de Vivo L, Bellesi M, Marshall W, Bushong EA, Ellisman MH, Tononi G, Cirelli C (2017) Ultrastructural evidence for synaptic scaling across the wake/sleep cycle. Science 355:507–510.

Dement W (1958) The occurrence of low voltage, fast, electroencephalogram patterns during behavioral sleep in the cat. Electroencephalography and Clinical Neurophysiology 10:291–296.

Derbyshire AJ, Rempel B, Forbes A, Lambert EF (1936) The effects of anesthetics on action potentials in the cerebral cortex of the cat. American Journal of Physiology - Legacy Content.

Derégnaucourt S, Mitra PP, Feher O, Pytte C, Tchernichovski O (2005) How sleep affects the developmental learning of bird song. Nature 433:710–716.

Derégnaucourt S, Saar S, Gahr M (2012) Melatonin affects the temporal pattern of vocal signatures in birds. J Pineal Res 53:245–258.

Dewasmes G, Cohen-Adad F, Koubi H, Le Maho Y (1985) Polygraphic and behavioral study of sleep in geese: existence of nuchal atonia during paradoxical sleep. Physiol Behav 35:67–73.

Diba K, Buzsáki G (2007) Forward and reverse hippocampal place-cell sequences during ripples. Nat Neurosci 10:1241–1242.

Diekelmann S, Born J (2010) The memory function of sleep. Nat Rev Neurosci 11:114–126.

Diering GH, Nirujogi RS, Roth RH, Worley PF, Pandey A, Huganir RL (2017) Homer1a drives homeostatic scaling-down of excitatory synapses during sleep. Science 355:511–515.

Dijk DJ, Brunner DP, Borbély AA (1990) Time course of EEG power density during long sleep in humans. Am J Physiol 258:R650–R661.

Dijk DJ, Franken P (2005) Interaction of Sleep Homeostasis and Circadian Rhythmicity: Dependent or Independent Systems? In: Principles and Practice of Sleep Medicine, 4 ed. (Kryger MH, Roth T, Dement WC, eds), pp 418–434. Philadelphia, PA: Elsevier Saunders.

Ditz HM, Nieder A (2015) Neurons selective to the number of visual items in the corvid songbird endbrain. Proc Natl Acad Sci USA 112:7827–7832.

Donlea JM, Thimgan MS, Suzuki Y, Gottschalk L, Shaw PJ (2011) Inducing sleep by remote control facilitates memory consolidation in Drosophila. Science 332:1571–1576.

Doupe AJ, Kuhl PK (1999) BIRDSONG AND HUMAN SPEECH: Common Themes and Mechanisms. Annu Rev Neurosci 22:567–631.

Dragoi G, Tonegawa S (2013) Distinct preplay of multiple novel spatial experiences in the rat. Proc Natl Acad Sci USA 110:9100–9105.

Dresler M, Eibl L, Fischer CFJ, Wehrle R, Spoormaker VI, Steiger A, Czisch M, Pawlowski M (2014) Volitional components of consciousness vary across wakefulness, dreaming and lucid dreaming. Front Psychol 4:987.

Dresler M, Kluge M, Pawlowski M, Schüssler P, Steiger A, Genzel L (2011a) A double dissociation of memory impairments in major depression. J Psychiatr Res 45:1593–1599.

Dresler M, Koch SP, Wehrle R, Spoormaker VI, Holsboer F, Steiger A, Sämann PG, Obrig H, Czisch M (2011b) Dreamed movement elicits activation in the sensorimotor cortex. Curr Biol 21:1833–1837.

Duffy FH, Jones K, Bartels P, Albert M, McAnulty GB, Als H (1990) Quantified Neurophysiology with mapping: Statistical inference, Exploratory and Confirmatory data analysis. Brain Topogr 3:3–12.

Dugas-Ford J, Ragsdale CW (2015) Levels of homology and the problem of neocortex. Annu Rev Neurosci 38:351–368.

Dugas-Ford J, Rowell JJ, Ragsdale CW (2012) Cell-type homologies and the origins of the neocortex. Proc Natl Acad Sci USA 109:16974–16979.

Ebbinghaus H (1912) Über das Gedächtnis.

Eda-Fujiwara H, Imagawa T, Matsushita M, Matsuda Y, Takeuchi H-A, Satoh R, Watanabe A, Zandbergen MA, Manabe K, Kawashima T, Bolhuis JJ (2012) Localized brain activation related to the strength of auditory learning in a parrot. Hausberger M, ed. PLoS ONE 7:e38803.

Edgin JO, Tooley U, Demara B, Nyhuis C, Anand P, Spanò G (2015) Sleep Disturbance and Expressive Language Development in Preschool-Age Children With Down Syndrome. Child Dev 86:1984–1998 Available at: http://doi.wiley.com/10.1111/cdev.12443.

Ego-Stengel V, Wilson MA (2010) Disruption of ripple-associated hippocampal activity during rest impairs spatial learning in the rat. Hippocampus 20:1–10.

Ekambaram V, Maski K (2017) Non-Rapid Eye Movement Arousal Parasomnias in Children. Pediatr Ann 46:e327–e331.

Elie JE, Theunissen FE (2018) Zebra finches identify individuals using vocal signatures unique to each call type. Nat Comms 9:4026.

Emery NJ, Clayton NS (2004) The mentality of crows: convergent evolution of intelligence in corvids and apes. Science 306:1903–1907.

Empson JA, Clarke PR (1970) Rapid eye movements and remembering. Nature 227:287–288.

Euston DR, Tatsuno M, McNaughton BL (2007) Fast-forward playback of recent memory sequences in prefrontal cortex during sleep. Science 318:1147–1150.

Everson CA, Bergmann BM, Rechtschaffen A (1989) Sleep deprivation in the rat: III. Total sleep deprivation. Sleep 12:13–21.

Fenn KM, Margoliash D, Nusbaum HC (2013) Sleep restores loss of generalized but not rote learning of synthetic speech. Cognition 128:280–286.

Fenn KM, Nusbaum HC, Margoliash D (2003) Consolidation during sleep of perceptual learning of spoken language. Nature 425:614–616.

Ferrara M, Fablo M, De Gennaro L, Nobili L (2012) Hippocampal sleep features: relations to human memory function. Front Neurol 3:1–9.

Ferrarelli F, Huber R, Peterson MJ, Massimini M, Murphy M, Riedner BA, Watson A, Bria P, Tononi G (2007) Reduced sleep spindle activity in schizophrenia patients. Am J Psychiatry 164:483–492.

Ficca G, Lombardo P, Rossi L, Salzarulo P (2000) Morning recall of verbal material depends on prior sleep organization. Behavioural Brain Research 112:159–163.

Findley LJ, Wilhoit SC, Suratt PM (1985) Apnea Duration and Hypoxemia During REM Sleep in Patients with Obstructive Sleep Apnea. Chest 87:432–436.

Foster DJ, Wilson MA (2006) Reverse replay of behavioural sequences in hippocampal place cells during the awake state. Nature 440:680–683.

Fox SE, Wolfson S, Ranck JB (1986) Hippocampal theta rhythm and the firing of neurons in walking and urethane anesthetized rats. Exp Brain Res 62:495–508.

Frank MG (2012) Erasing Synapses in Sleep: Is It Time to Be SHY? Neural Plast 2012:1–15.

Frank MG, Waldrop RH, Dumoulin M, Aton S, Boal JG (2012) A preliminary analysis of sleep-like states in the cuttlefish Sepia officinalis. Balaban E, ed. PLoS ONE 7:e38125.

Fukushima M, Margoliash D (2015) The effects of delayed auditory feedback revealed by bone conduction microphone in adult zebra finches. Sci Rep 5:8800.

Gabrieli JDE, Corkin S, Mickel SF, Growdon JH (1993) Intact acquisition and long-term retention of mirror-tracing skill in Alzheimer's disease and in global amnesia. Behavioral Neuroscience 107:899–910.

Gais S, Born J (2004) Declarative memory consolidation: mechanisms acting during human sleep. Learn Mem 11:679–685.

Galea JM, Albert NB, Ditye T, Miall RC (2010) Disruption of the dorsolateral prefrontal cortex facilitates the consolidation of procedural skills. J Cogn Neurosci 22:1158–1164.

Gallup AC, Swartwood L, Militello J, Sackett S (2015) Experimental evidence of contagious yawning in budgerigars (Melopsittacus undulatus). Anim Cogn 18:1051–1058.

Garst-Orozco J, Babadi B, Olveczky BP (2015) A neural circuit mechanism for regulating vocal variability during song learning in zebra finches. Elife 3: e03697.

Gentner TQ, Fenn KM, Margoliash D, Nusbaum HC (2006) Recursive syntactic pattern learning by songbirds. Nature 440:1204–1207.

Girardeau G, Benchenane K, Wiener SI, Buzsáki G, Zugaro MB (2009) Selective suppression of hippocampal ripples impairs spatial memory. Nat Neurosci 12:1222–1223.

Girardeau G, Zugaro M (2011) Hippocampal ripples and memory consolidation. Curr Opin Neurobiol 21:452–459.

Glaze CM, Troyer TW (2006) Temporal structure in zebra finch song: implications for motor coding. J Neurosci 26:991–1005.

Goldman SA, Nottebohm F (1983) Neuronal production, migration, and differentiation in a vocal control nucleus of the adult female canary brain. Proc Natl Acad Sci USA 80:2390–2394.

Gomez RL, Bootzin RR, Nadel L (2006) Naps promote abstraction in language-learning infants. Psychol Sci 17:670–674.

Gottesmann C (1996) The transition from slow-wave sleep to paradoxical sleep: evolving facts and concepts of the neurophysiological processes underlying the intermediate stage of sleep. Neurosci Biobehav Rev 20:367–387.

Grewe BF, Langer D, Kasper H, Kampa BM, Helmchen F (2010) High-speed in vivo calcium imaging reveals neuronal network activity with near-millisecond precision. Nat Methods 7:399–405.

Grimaldi D, Papalambros NA, Reid KJ, Abbott SM, Malkani RG, Gendy M, Iwanaszko M, Braun RI, Sanchez DJ, Paller KA, Zee PC (2019) Strengthening sleep-autonomic interaction via acoustic enhancement of slow oscillations. Sleep 328:343.

Guitchounts G, Markowitz JE, Liberti WA, Gardner TJ (2013) A carbon-fiber electrode array for long-term neural recording. J Neural Eng 10:046016.

Gujar N, McDonald SA, Nishida M, Walker MP (2011) A Role for REM Sleep in Recalibrating the Sensitivity of the Human Brain to Specific Emotions. Cereb Cortex 21:115–123.

Gulati T, Ramanathan DS, Wong CC, Ganguly K (2014) Reactivation of emergent task-related ensembles during slow-wave sleep after neuroprosthetic learning. Nat Neurosci 17:1107–1113.

Gulevich G, Dement W, Johnson L (1966) Psychiatric and EEG observations on a case of prolonged (264 hours) wakefulness. Arch Gen Psychiatry 15:29–35.

Guzmán DA, Flesia AG, Aon MA, Pellegrini S, Marin RH, Kembro JM (2017) The fractal organization of ultradian rhythms in avian behavior. Sci Rep 7:684.

Hackett SJ, Kimball RT, Reddy S, Bowie RCK, Braun EL, Braun MJ, Chojnowski JL, Cox WA, Han K-L, Harshman J, Huddleston CJ, Marks BD, Miglia KJ, Moore WS, Sheldon FH, Steadman DW, Witt CC, Yuri T (2008) A phylogenomic study of birds reveals their evolutionary history. Science 320:1763–1768.

Hahnloser RHR, Fee MS (2007) Sleep-related spike bursts in HVC are driven by the nucleus interface of the nidopallium. J Neurophysiol 97:423–435.

Hahnloser RHR, Kozhevnikov AA, Fee MS (2002) An ultra-sparse code underlies the generation of neural sequences in a songbird. Nature 419:65–70.

Hahnloser RHR, Kozhevnikov AA, Fee MS (2006) Sleep-related neural activity in a premotor and a basal-ganglia pathway of the songbird. J Neurophysiol 96:794–812.

Hahnloser RHR, Wang CZ-H, Nager A, Naie K (2008) Spikes and bursts in two types of thalamic projection neurons differentially shape sleep patterns and auditory responses in a songbird. J Neurosci 28:5040–5052.

Halász P (2016) The K-complex as a special reactive sleep slow wave - A theoretical update. Sleep Med Rev 29:34–40.

Harrison Y, Horne JA (2000) Sleep loss and temporal memory. Q J Exp Psychol A 53:271–279.

Hartse KM (1994) Sleep in insects and nonmammalian vertebrates. In: Principles and Practice of Sleep Medicine, 2nd ed. (Kryger MH, Roth T, Dement WC, eds), pp 95–104. Philadelphia: Elsevier.

Heston JB, Simon J, Day NF, Coleman MJ, White SA (2018) Bidirectional scaling of vocal variability by an avian cortico-basal ganglia circuit. Physiol Rep 6:e13638.

Hile AG, Burley NT, Coopersmith CB, Foster VS, Striedter GF (2005) Effects of Male Vocal Learning on Female Behavior in the Budgerigar, Melopsittacus undulatus. Ethology 111:901–923.

Himanen S-L, Virkkala J, Huhtala H, Hasan J (2002) Spindle frequencies in sleep EEG show U-shape within first four NREM sleep episodes. Journal of Sleep Research 11:35–42.

Hindmarsh AH (1984) Vocal mimicry in starlings. Behaviour 90:302–324.

Hisey E, Kearney MG, Mooney R (2018) A common neural circuit mechanism for internally guided and externally reinforced forms of motor learning. Nat Neurosci 21:589–597.

Hobson JA (1965) The effects of chronic brain-stem lesions on cortical and muscular activity during sleep and waking in the cat. Electroencephalography and Clinical Neurophysiology 19:41–62.

Hobson JA, McCarley RW, Wyzinski PW (1975) Sleep cycle oscillation: reciprocal discharge by two brainstem neuronal groups. Science 189:55–58.

Hoffman KL, McNaughton BL (2002) Coordinated Reactivation of Distributed Memory Traces in Primate Neocortex. Science 297:2070–2073.

Hoffmann LA, Saravanan V, Wood AN, He L, Sober SJ (2016) Dopaminergic Contributions to Vocal Learning. J Neurosci 36:2176–2189.

Homer (1909) The Odyssey (Eliot CW, ed). New York: P.F Collier & Son. Available at: https://www.bartleby.com/br/02201.html.

Honaker SM, Gozal D, Bennett J, Capdevila OS, Spruyt K (2009) Sleep-disordered breathing and verbal skills in school-aged community children. Dev Neuropsychol 34:588–600.

Horne JA, McGrath MJ (1984) The consolidation hypothesis for REM sleep function: stress and other confounding factors--a review. Biol Psychol 18:165–184.

Huber R, Ghilardi MF, Massimini M, Tononi G (2004) Local sleep and learning. Nature 430:78–81.

Hume KI, Van F, Watson A (1998) A field study of age and gender differences in habitual adult sleep. Journal of Sleep Research 7:85–94.

Hupbach A, Gomez RL, Bootzin RR, Nadel L (2009) Nap-dependent learning in infants. Dev Sci 12:1007–1012.

Immelmann K (1969) Song development in the zebra finch and other estrildid finches. In: Bird Vocalizations (Hinde RA, ed), pp 61–77. London: Cambridge University Press.

Jackson C, McCabe BJ, Nicol AU, Grout AS, Brown MW, Horn G (2008) Dynamics of a memory trace: effects of sleep on consolidation. Curr Biol 18:393–400 Available at: http://linkinghub.elsevier.com/retrieve/pii/S0960982208001693.

Janik VM (2014) Cetacean vocal learning and communication. Curr Opin Neurobiol 28:60–65.

Jarvis ED et al. (2005) Avian brains and a new understanding of vertebrate brain evolution. Nat Rev Neurosci 6:151–159.

Jenkins JG, Dallenbach KM (1924) Obliviscence during Sleep and Waking. The American Journal of Psychology 35:605.

Ji D, Wilson MA (2007) Coordinated memory replay in the visual cortex and hippocampus during sleep. Nat Neurosci 10:100–107.

Johnson BP, Scharf SM, Verceles AC, Westlake KP (2019) Use of targeted memory reactivation enhances skill performance during a nap and enhances declarative memory during wake in healthy young adults. Journal of Sleep Research 2:263.

Johnson LA, Blakely T, Hermes D, Hakimian S, Ramsey NF, Ojemann JG (2012) Sleep spindles are locally modulated by training on a brain-computer interface. Proc Natl Acad Sci USA 109:18583–18588.

Jones SG, Vyazovskiy VV, Cirelli C, Tononi G, Benca RM (2008) Homeostatic regulation of sleep in the white-crowned sparrow (Zonotrichia leucophrys gambelii). BMC Neurosci 9:47–14.

Jouvet M (1965) Paradoxical Sleep--A Study of its Nature and Mechanisms. Prog Brain Res 18:20–62 Available at: https://sommeil.univ-lyon1.fr/articles/jouvet/pbr_65/print.php.

Jouvet M, Michel F, Courjon J (1959) Sur un stade d'activité électrique cérébrale rapide au cours du sommeil physiologique. Comptes rendus des séances de l'Académie des Sciences 153:1024.

Jouvet Mounier D, Astic L, Lacote D (1969) Ontogenesis of the states of sleep in rat, cat, and guinea pig during the first postnatal month. Developmental Psychobiology 2:216–239.

Kabadayi C, Osvath M (2017) Ravens parallel great apes in flexible planning for tool-use and bartering. Science 357:202–204.

Kao MH, Doupe AJ, Brainard MS (2005) Contributions of an avian basal ganglia-forebrain circuit to real-time modulation of song. Nature 433:638–643.

Karni A, Tanne D, Rubenstein BS, Askenasy JJ, Sagi D (1994) Dependence on REM sleep of overnight improvement of a perceptual skill. Science 265:679–682.

Kavanau JL (1998) Vertebrates that never sleep: implications for sleep's basic function. Brain Research Bulletin 46:269–279.

Keijzer F, Van Duijn M, Lyon P (2013) What nervous systems do: early evolution, input–output, and the skin brain thesis. Adaptive Behavior 21:67–85.

Keklund G, Akerstedt T (1997) Objective components of individual differences in subjective sleep quality. Journal of Sleep Research 6:217–220.

Khodagholy D, Gelinas JN, Buzsáki G (2017) Learning-enhanced coupling between ripple oscillations in association cortices and hippocampus. Science 358:369–372.

Kirn JR, Alvarez-Buylla A, Nottebohm F (1991) Production and survival of projection neurons in a forebrain vocal center of adult male canaries. J Neurosci 11:1756–1762.

Kirov R, Kolev V, Verleger R, Yordanova J (2015) Labile sleep promotes awareness of abstract knowledge in a serial reaction time task. Front Psychol 6:1354.

Kis A, Szakadát S, Kovács E, Gácsi M, Simor P, Gombos F, Topál J, Miklósi Á, Bódizs R (2014) Development of a non-invasive polysomnography technique for dogs (Canis familiaris). Physiol Behav 130:149–156.

Klein BA, Olzsowy KM, Klein A, Saunders KM, Seeley TD (2008) Caste-dependent sleep of worker honey bees. Journal of Experimental Biology 211:3028–3040.

Klein M, Jouvet M, Michel F (1964) Etude polygraphique du sommeil chez les oiseaux. In, pp 99–103. Paris. Available at: https://sommeil.univ-lyon1.fr/articles/jouvet/crssb_63/print.php.

Klinzing JG, Mölle M, Weber F, Supp G, Hipp JF, Engel AK, Born J (2016) Spindle activity phase-locked to sleep slow oscillations. Neuroimage 134:607–616.

Knörnschild M (2014) Vocal production learning in bats. Curr Opin Neurobiol 28:80–85.

Kobayashi R, Kohsaka M, Fukuda N, Honma H, Sakakibara S, Koyama T (1998) Gender differences in the sleep of middle-aged individuals. Psychiatry Clin Neurosci 52:186–187.

Konishi M (1963) The Role of Auditory Feedback in the Vocal Behavior of the Domestic Fowl1. Z Tierpsychol 20:349–367.

Konishi M (1965) The role of auditory feedback in the control of vocalization in the white-crowned sparrow. Z Tierpsychol 22:770–783.

Koumura T, Okanoya K (2016) Automatic Recognition of Element Classes and Boundaries in the Birdsong with Variable Sequences. Vicario DS, ed. PLoS ONE 11:e0159188.

Kreuz T, Mulansky M, Bozanic N (2015) SPIKY: a graphical user interface for monitoring spike train synchrony. J Neurophysiol 113:3432–3445.

Krieger J (2005) Respiratory Physiology: Breathing in Normal Subjects. In: Principles and Practice of Sleep Medicine, 4 ed. (Kryger MH, Roth T, Dement WC, eds), pp 232–244. Philadelphia, PA: Elsevier Saunders.

Ktonas P, Nygren A, Frost J (2003) Two-minute rapid eye movement (REM) density fluctuations in human REM sleep. Neurosci Lett 353:161–164.

Kudrimoti HS, Barnes CA, McNaughton BL (1999) Reactivation of hippocampal cell assemblies: effects of behavioral state, experience, and EEG dynamics. J Neurosci 19:4090–4101.

Kuriyama K, Stickgold R, Walker MP (2004) Sleep-dependent learning and motor-skill complexity. Learn Mem 11:705–713 Available at: http://walkerlab.berkeley.edu/reprints/Kuriyama,Stickgold,Walker_L%26M_2004.pdf.

Lansink CS, Goltstein PM, Lankelma JV, McNaughton BL, Pennartz CMA (2009) Hippocampus Leads Ventral Striatum in Replay of Place-Reward Information Stevens CF, ed. PLoS Biol 7:e1000173.

Latchoumane C-FV, Ngo H-VV, Born J, Shin H-S (2017) Thalamic Spindles Promote Memory Formation during Sleep through Triple Phase-Locking of Cortical, Thalamic, and Hippocampal Rhythms. Neuron 95:424–435.e426.

Lee AK, Wilson MA (2002) Memory of Sequential Experience in the Hippocampus during Slow Wave Sleep. Neuron 36:1183–1194.

Lee BS (1950) Effects of Delayed Speech Feedback. The Journal of the Acoustical Society of America 22:824–826.

Lee S-H, Dan Y (2012) Neuromodulation of brain states. Neuron 76:209–222.

Leonardo A, Fee MS (2005) Ensemble coding of vocal control in birdsong. J Neurosci 25:652–661.

Leonardo A, Konishi M (1999) Decrystallization of adult birdsong by perturbation of auditory feedback. Nature 399:466–470.

Leschziner G (2014) Narcolepsy: a clinical review. Pract Neurol 14:323–331.

Lesku JA, Meyer LCR, Fuller A, Maloney SK, Dell'Omo G, Vyssotski AL, Rattenborg NC (2011a) Ostriches sleep like platypuses. PLoS ONE 6:e23203.

Lesku JA, Rattenborg NC, Valcu M, Vyssotski AL, Kuhn S, Kuemmeth F, Heidrich W, Kempenaers B (2012) Adaptive sleep loss in polygynous pectoral sandpipers. Science 337:1654–1658.

Lesku JA, Roth TC II, Amlaner CJ, Lima SL (2006) A Phylogenetic Analysis of Sleep Architecture in Mammals: The Integration of Anatomy, Physiology, and Ecology. The American Naturalist 168:441–453.

Lesku JA, Roth TC, Rattenborg NC, Amlaner CJ, Lima SL (2008) Phylogenetics and the correlates of mammalian sleep: a reappraisal. Sleep Med Rev 12:229–244.

Lesku JA, Vyssotski AL, Martinez-Gonzalez D, Wilzeck C, Rattenborg NC (2011b) Local sleep homeostasis in the avian brain: convergence of sleep function in mammals and birds? Proceedings of the Royal Society B: Biological Sciences 278:2419–2428.

Leung LC, Wang GX, Madelaine R, Skariah G, Kawakami K, Deisseroth K, Urban AE, Mourrain P (2019) Neural signatures of sleep in zebrafish. Nature 571:198–204.

Li W, Ma L, Yang G, Gan W-B (2017) REM sleep selectively prunes and maintains new synapses in development and learning. Nat Neurosci 20:427–437.

Liao S-Q, Hou G-Q, Liu X-L, Long C, Li D-F (2011) Electrophysiological properties of neurons in the robust nucleus of the arcopallium of adult male zebra finches. Neurosci Lett 487:234–239.

Libourel PA, Barrillot B, Arthaud S, Massot B, Morel A-L, Beuf O, Herrel A, Luppi P-H (2018) Partial homologies between sleep states in lizards, mammals, and birds suggest a complex evolution of sleep states in amniotes. PLoS Biol 16:e2005982.

Libourel PA, Herrel A (2016) Sleep in amphibians and reptiles: a review and a preliminary analysis of evolutionary patterns. Biological Reviews 91:833–866.

Linden DJ (2012) Sleeping and Dreaming. In: The Accidental Mind. Harvard University Press.

Lomb NR (1976) Least-Squares Frequency-Analysis of Unequally Spaced Data. Astrophysics and Space Science 39:447–462.

Lombardino AJ, Nottebohm F (2000) Age at deafening affects the stability of learned song in adult male zebra finches. J Neurosci 20:5054–5064.

Louie K, Wilson MA (2001) Temporally Structured Replay of Awake Hippocampal Ensemble Activity during Rapid Eye Movement Sleep. Neuron 29:145–156.

Low PS, Shank SS, Sejnowski TJ, Margoliash D (2008) Mammalian-like features of sleep structure in zebra finches. Proc Natl Acad Sci USA 105:9081–9086.

Lustenberger C, Boyle MR, Alagapan S, Mellin JM, Vaughn BV, Fröhlich F (2016) Feedback-Controlled Transcranial Alternating Current Stimulation Reveals a Functional Role of Sleep Spindles in Motor Memory Consolidation. Curr Biol 26:2127–2136.

Lyamin OI, Shpak OV, Nazarenko EA, Mukhametov LM (2002) Muscle jerks during behavioral sleep in a beluga whale (Delphinapterus leucas L.). 76:265–270.

Lynch GF, Okubo TS, Hanuschkin A, Hahnloser RHR, Fee MS (2016) Rhythmic Continuous-Time Coding in the Songbird Analog of Vocal Motor Cortex. Neuron 90:877–892.

Mahowald MW, Bornemann MAC (2005) NREM sleep-arousal parasomnias. In: Principles and Practice of Sleep Medicine, 4 ed. (Kryger MH, Roth T, Dement WC, eds), pp 889–896. Philadelphia, PA: Elsevier Saunders.

Maingret N, Girardeau G, Todorova R, Goutierre M, Zugaro M (2016) Hippocampo-cortical coupling mediates memory consolidation during sleep. Nat Neurosci 19:959–964.

Manoach DS, Cain MS, Vangel MG, Khurana A, Goff DC, Stickgold R (2004) A failure of sleep-dependent procedural learning in chronic, medicated schizophrenia. Biol Psychiatry 56:951–956.

Manoach DS, Thakkar KN, Stroynowski E, Ely A, McKinley SK, Wamsley E, Djonlagic I, Vangel MG, Goff DC, Stickgold R (2010) Reduced overnight consolidation of procedural learning in chronic medicated schizophrenia is related to specific sleep stages. J Psychiatr Res 44:112–120.

Maquet P (2001) The role of sleep in learning and memory. Science 294:1048–1052.

Maquet P, Laureys S, Peigneux P, Fuchs S, Petiau C, Phillips C, Aerts J, Del Fiore G, Degueldre C, Meulemans T, Luxen A, Franck G, Van Der Linden M, Smith C, Cleeremans A (2000) Experience-dependent changes in cerebral activation during human REM sleep. Nat Neurosci 3:831–836.

Maquet P, Péters J, Aerts J, Delfiore G, Degueldre C, Luxen A, Franck G (1996) Functional neuroanatomy of human rapid-eye-movement sleep and dreaming. Nature 383:163–166.

Margoliash D (1983) Acoustic parameters underlying the responses of song-specific neurons in the white-crowned sparrow. J Neurosci 3:1039–1057.

Margoliash D (1986) Preference for autogenous song by auditory neurons in a song system nucleus of the white-crowned sparrow. J Neurosci 6:1643–1661.

Margoliash D, Brawn TP (2012) Sleep and Learning in Birds: Rats! There's More to Sleep. In: Sleep and Brain Activity (Frank MG, ed). Sleep and Brain Activity.

Margoliash D, Fortune ES (1992) Temporal and harmonic combination-sensitive neurons in the zebra finch's HVc. J Neurosci 12:4309–4326.

Margoliash D, Fortune ES, Sutter ML, Yu AC, Wren-Hardin BD, Dave A (1994) Distributed representation in the song system of oscines: evolutionary implications and functional consequences. Brain Behav Evol 44:247–264.

Margoliash D, Konishi M (1985) Auditory representation of autogenous song in the song system of white-crowned sparrows. PNAS 82:5997–6000.

Markowitz JE, Liberti WA, Guitchounts G, Velho T, Lois C, Gardner TJ (2015) Mesoscopic patterns of neural activity support songbird cortical sequences. Ashe J, ed. PLoS Biol 13:e1002158.

Marks GA, Shaffery JP, Oksenberg A, Speciale SG, Roffwarg HP (1995) A functional role for REM sleep in brain maturation. Behavioural Brain Research 69:1–11.

Marler P, Tamura M (1964) Culturally Transmitted Patterns of Vocal Behavior in Sparrows. Science 146:1483–1486.

Marshall L, Born J (2007) The contribution of sleep to hippocampus-dependent memory consolidation. Trends in Cognitive Sciences 11:442–450.

Marshall L, Helgadóttir H, Mölle M, Born J (2006) Boosting slow oscillations during sleep potentiates memory. Nature 444:610–613.

Martin P (2004) Counting sheep : the science and pleasures of sleep and dreams. New York: Thomas Dunne Books/St. Martin's Press.

Martinez-Gonzalez D, Lesku JA, Rattenborg NC (2008) Increased EEG spectral power density during sleep following short-term sleep deprivation in pigeons (Columba livia): evidence for avian sleep homeostasis. Journal of Sleep Research 17:140–153.

Massimini M, Huber R, Ferrarelli F, Hill S, Tononi G (2004) The sleep slow oscillation as a traveling wave. J Neurosci 24:6862–6870.

McKellar P, Simpson L (1954) Between wakefulness and sleep: hypnagogic imagery. Br J Psychol 45:266–276.

McNamara P, Johnson P, McLaren D, Harris E, Beauharnais C, Auerbach S (2010) REM and NREM sleep mentation. Int Rev Neurobiol 92:69–86.

Mensen A, Riedner B, Tononi G (2016) Optimizing detection and analysis of slow waves in sleep EEG. J Neurosci Methods 274:1–12.

Mexicano G, Montoya-Loaiza B, Ayala-Guerrero F (2014) Sleep characteristics in the quail Coturnix coturnix. Physiol Behav 129:167–172.

Miller ML, Gallup AC, Vogel AR, Vicario SM, Clark AB (2012) Evidence for contagious behaviors in budgerigars (Melopsittacus undulatus): an observational study of yawning and stretching. Behav Processes 89:264–270.

Miller PJO, Aoki K, Rendell LE, Amano M (2008) Stereotypical resting behavior of the sperm whale. Curr Biol 18:R21–R23.

Milner B, Corkin S, Teuber HL (1968) Further analysis of the hippocampal amnesic syndrome: 14-year follow-up study of H.M. Neuropsychologia 6:215–234.

Molinari S, Foulkes D (1969) Tonic and phasic events during sleep: psychological correlates and implications. Perceptual and Motor Skills 29:343–368.

Montaigne M de (1877) Essays of Michel de Montaigne — Complete (Hazlit WC, ed). Available at: http://www.gutenberg.org/files/3600/3600-h/3600-h.htm.

Mooney R (1992) Synaptic basis for developmental plasticity in a birdsong nucleus. J Neurosci 12:2464–2477.

Morden B, Mitchell G, Dement W (1967) Selective REM sleep deprivation and compensation phenomena in the rat. Brain Res 5:339–349.

Morin A, Doyon J, Dostie V, Barakat M, Tahar AH, Korman M, Benali H, Karni A, Ungerleider LG, Carrier J (2008) Motor Sequence Learning Increases Sleep Spindles and Fast Frequencies in Post-Training Sleep. Sleep 31:1149–1156.

Morris D (1954) The Reproductive Behaviour of the Zebra Finch (Poephila Guttata), With Special Reference To Pseudofemale Behaviour and Displacement Activities. Behaviour 6:271–322.

Morris GO, Williams HL, Lubin A (1960) Misperception and Disorientation During Sleep Deprivation. Arch Gen Psychiatry 2:247.

Moser M-B, Rowland DC, Moser EI (2015) Place cells, grid cells, and memory. Cold Spring Harb Perspect Biol 7:a021808.

Mölle M, Marshall L, Gais S, Born J (2002) Grouping of spindle activity during slow oscillations in human non-rapid eye movement sleep. J Neurosci 22:10941–10947.

Mölle M, Yeshenko O, Marshall L, Sara SJ, Born J (2006) Hippocampal sharp wave-ripples linked to slow oscillations in rat slow-wave sleep. J Neurophysiol 96:62–70.

Mulansky M, Kreuz T (2016) PySpike—A Python library for analyzing spike train synchrony. SoftwareX 5:183–189.

Nath RD, Bedbrook CN, Abrams MJ, Basinger T, Bois JS, Prober DA, Sternberg PW, Gradinaru V, Goentoro L (2017) The Jellyfish Cassiopea Exhibits a Sleep-like State. Curr Biol 27:2984–2990.e3.

Nádasdy Z, Hirase H, Czurkó A, Csicsvari J, Buzsáki G (1999) Replay and time compression of recurring spike sequences in the hippocampus. J Neurosci 19:9497–9507.

Nemeth D, Janacsek K, Londe Z, Ullman MT, Howard DV, Howard JH Jr (2010) Sleep has no critical role in implicit motor sequence learning in young and old adults. Experimental Brain Research 201:351–358.

Ngo H-VV, Martinetz T, Born J, Mölle M (2013) Auditory closed-loop stimulation of the sleep slow oscillation enhances memory. Neuron 78:545–553.

Nick TA, Konishi M (2001) Dynamic control of auditory activity during sleep: Correlation between song response and EEG. Proc Natl Acad Sci USA 98:14012–14016.

Nick TA, Konishi M (2005a) Neural auditory selectivity develops in parallel with song. J Neurobiol 62:469–481.

Nick TA, Konishi M (2005b) Neural song preference during vocal learning in the zebra finch depends on age and state. J Neurobiol 62:231–242.

Nicolelis MAL, Ribeiro S (2002) Multielectrode recordings: the next steps. Curr Opin Neurobiol 12:602–606.

Nieder A (2018) Evolution of cognitive and neural solutions enabling numerosity judgements: lessons from primates and corvids. Philosophical Transactions of the Royal Society B: Biological Sciences 373:20160514.

Nietzsche F (1909) Thus Spake Zarathustra. Edinburgh and London: T.N. Foulis.

Nishida M, Pearsall J, Buckner RL, Walker MP (2009) REM Sleep, Prefrontal Theta, and the Consolidation of Human Emotional Memory. Cereb Cortex 19:1158–1166.

Nishida M, Walker MP (2007) Daytime naps, motor memory consolidation and regionally specific sleep spindles. Miall C, ed. PLoS ONE 2:e341.

Niven JE, Laughlin SB (2008) Energy limitation as a selective pressure on the evolution of sensory systems. Journal of Experimental Biology 211:1792–1804.

Nordeen KW, Nordeen EJ (1992) Auditory feedback is necessary for the maintenance of stereotyped song in adult zebra finches. Behavioral and Neural Biology 57:58–66.

Nottebohm F (1970) Ontogeny of bird song. Science 167:950–956.

Nottebohm F (1972) The Origins of Vocal Learning. The American Naturalist 106:116–140.

Nottebohm F, Nottebohm ME, Crane L (1986) Developmental and seasonal changes in canary song and their relation to changes in the anatomy of song-control nuclei. Behavioral and Neural Biology 46:445–471.

Nottebohm F, Stokes TM, Leonard CM (1976) Central control of song in the canary, Serinus canarius. Journal of Comparative Neurology 165:457–486.

O T, P M (2002) Towards quantification of vocal imitation in the zebra finch. J Comp Physiol 188:867–878.

O'Neill J, Boccara CN, Stella F, Schoenenberger P, Csicsvari J (2017) Superficial layers of the medial entorhinal cortex replay independently of the hippocampus. Science 355:184–188.

Ohayon MM, Carskadon MA, Guilleminault C, Vitiello MV (2004) Meta-analysis of quantitative sleep parameters from childhood to old age in healthy individuals: developing normative sleep values across the human lifespan. Sleep 27:1255–1273.

Olkowicz S, Kocourek M, Lučan RK, Porteš M, Fitch WT, Herculano-Houzel S, Němec P (2016) Birds have primate-like numbers of neurons in the forebrain. Proc Natl Acad Sci USA 113:7255-7260.

Ong JL, Lo JC, Chee NIYN, Santostasi G, Paller KA, Zee PC, Chee MWL (2016) Effects of phase-locked acoustic stimulation during a nap on EEG spectra and declarative memory consolidation. Sleep Med 20:88–97.

Ong JL, Patanaik A, Chee NIYN, Lee XK, Poh J-H, Chee MWL (2018) Auditory stimulation of sleep slow oscillations modulates subsequent memory encoding through altered hippocampal function. Sleep 41:114.

Ookawa T, Gotoh J (1964) Electroencephalographs Study of Chickens: Periodic Recurrence of Low Voltage and Fast Waves during Behavioral Sleep. Poultry Science 43:1603–1604.

Ookawa T, Gotoh J (1965) Electroencephalogram of the chicken recorded from the skull under various conditions. Journal of Comparative Neurology 124:1–14.

Oudiette D, Constantinescu I, Leclair-Visonneau L, Vidailhet M, Schwartz S, Arnulf I (2011) Evidence for the re-enactment of a recently learned behavior during sleepwalking. Thomas A, ed. PLoS ONE 6:e18056.

O'Neill J, Pleydell-Bouverie B, Dupret D, Csicsvari J (2010) Play it again: reactivation of waking experience and memory. Trends in Neurosciences 33:220–229.

Pachitariu M, Steinmetz NA, Kadir SN, Carandini M, Harris KD (2016) Fast and accurate spike sorting of high-channel count probes with KiloSort. In 30th Conference on Neural Information Processing Systems, pp 4448–4456. Barcelona, Spain.

Papalambros NA, Santostasi G, Malkani RG, Braun R, Weintraub S, Paller KA, Zee PC (2017) Acoustic Enhancement of Sleep Slow Oscillations and Concomitant Memory Improvement in Older Adults. Front Hum Neurosci 11:109.

Patel PR, Zhang H, Robbins MT, Nofar JB, Marshall SP, Kobylarek MJ, Kozai TDY, Kotov NA, Chestek CA (2016) Chronic in vivo stability assessment of carbon fiber microelectrode arrays. J Neural Eng 13:066002.

Pavlides C, Winson J (1989) Influences of hippocampal place cell firing in the awake state on the activity of these cells during subsequent sleep episodes. J Neurosci 9:2907–2918.

Peever J, Fuller PM (2017) The Biology of REM Sleep. Curr Biol 27:R1237–R1248.

Peh WYX, Roberts TF, Mooney R (2015) Imaging auditory representations of song and syllables in populations of sensorimotor neurons essential to vocal communication. J Neurosci 35:5589–5605.

Peigneux P, Laureys S, Fuchs S, Collette F, Perrin F, Reggers J, Phillips C, Degueldre C, Del Fiore G, Aerts J, Luxen A, Maquet P (2004) Are Spatial Memories Strengthened in the Human Hippocampus during Slow Wave Sleep? Neuron 44:535–545.

Petkov CI, Jarvis ED (2012) Birds, primates, and spoken language origins: behavioral phenotypes and neurobiological substrates. Front Evol Neurosci 4:12.

Peyrache A, Khamassi M, Benchenane K, Wiener SI, Battaglia FP (2009) Replay of rule-learning related neural patterns in the prefrontal cortex during sleep. Nat Neurosci 12:919–926.

Pfenning AR et al. (2014) Convergent transcriptional specializations in the brains of humans and song-learning birds. Science 346:1256846.

Phillips NH, Berger RJ (1992) Melatonin infusions restore sleep suppressed by continuous bright light in pigeons. Neurosci Lett 145:217–220.

Picardo MA, Merel J, Katlowitz KA, Vallentin D, Okobi DE, Benezra SE, Clary RC, Pnevmatikakis EA, Paninski L, Long MA (2016) Population-Level Representation of a Temporal Sequence Underlying Song Production in the Zebra Finch. Neuron 90:866–876.

Plihal W, Born J (1997) Effects of early and late nocturnal sleep on declarative and procedural memory. J Cogn Neurosci 9:534–547.

Poe GR, Nitz DA, McNaughton BL, Barnes CA (2000) Experience-dependent phase-reversal of hippocampal neuron firing during REM sleep. Brain Res 855:176–180.

Portfors CV, Perkel DJ (2014) The role of ultrasonic vocalizations in mouse communication. Curr Opin Neurobiol 28:115–120.

Prather JF (2013) Auditory signal processing in communication: perception and performance of vocal sounds. Hear Res 305:144–155.

Prather JF, Peters S, Nowicki S, Mooney R (2008) Precise auditory-vocal mirroring in neurons for learned vocal communication. Nature 451:305–310.

Qin YL, McNaughton BL, Skaggs WE, Barnes CA (1997) Memory reprocessing in corticocortical and hippocampocortical neuronal ensembles. Burgess N, Oapos Keefe J, eds. Philos Trans R Soc Lond, B, Biol Sci 352:1525–1533.

Ramanathan DS, Gulati T, Ganguly K (2015) Sleep-Dependent Reactivation of Ensembles in Motor Cortex Promotes Skill Consolidation. Ashe J, ed. PLoS Biol 13:e1002263.

Ramm P, Smith CT (1990) Rates of cerebral protein synthesis are linked to slow wave sleep in the rat. Physiol Behav 48:749–753.

Rasch B, Büchel C, Gais S, Born J (2007) Odor cues during slow-wave sleep prompt declarative memory consolidation. Science 315:1426–1429.

Rasch B, Pommer J, Diekelmann S, Born J (2009) Pharmacological REM sleep suppression paradoxically improves rather than impairs skill memory. Nat Neurosci 12:396–397.

Rattenborg NC (2006) Evolution of slow-wave sleep and palliopallial connectivity in mammals and birds: a hypothesis. Brain Research Bulletin 69:20–29.

Rattenborg NC, Lima SL, Amlaner CJ (1999) Facultative control of avian unihemispheric sleep under the risk of predation. Behavioural Brain Research 105:163–172.

Rattenborg NC, Mandt BH, Obermeyer WH, Winsauer PJ, Huber R, Wikelski M, Benca RM (2004) Migratory sleeplessness in the white-crowned sparrow (Zonotrichia leucophrys gambelii). PLoS Biol 2:0924–0936.

Rattenborg NC, Martinez-Gonzalez D (2015) Avian versus mammalian sleep: the fruits of comparing apples and oranges. Neuroscience Translations 1:55–63.

Rattenborg NC, Martinez-Gonzalez D, Lesku JA (2009) Avian sleep homeostasis: convergent evolution of complex brains, cognition and sleep functions in mammals and birds. Neurosci Biobehav Rev 33:253–270.

Rattenborg NC, Martinez-Gonzalez D, Roth TC, Pravosudov VV (2011) Hippocampal memory consolidation during sleep: a comparison of mammals and birds. Biological Reviews 86:658–691.

Rattenborg NC, Martinez-Gonzalez D, van der Meij J, Beckers GJL, Vyssotski AL, Pompeiano M, Balaban E (2015) Can sleeping birds preen? Dissociation between sleep-related EEG activity and behavior in pigeons. Society for Neuroscience, Chicago, IL.

Rattenborg NC, Voirin B, Cruz SM, Tisdale R, Dell'Omo G, Lipp H-P, Wikelski M, Vyssotski AL (2016) Evidence that birds sleep in mid-flight. Nat Comms 7:12468.

Rauske PL (2005) The modulation of sensorimotor activity by sleep. Doctoral dissertation, University of Chicago. Margoliash D, ed.

Rauske PL, Chi Z, Dave AS, Margoliash D (2010) Neuronal stability and drift across periods of sleep: premotor activity patterns in a vocal control nucleus of adult zebra finches. J Neurosci 30:2783–2794.

Rauske PL, Shea SD, Margoliash D (2003) State and neuronal class-dependent reconfiguration in the avian song system. J Neurophysiol 89:1688–1701.

Ravbar P, Lipkind D, Parra LC, Tchernichovski O (2012) Vocal Exploration Is Locally Regulated during Song Learning. 32:3422–3432.

Rechtschaffen A, Gilliland M, Bergmann B, Winter J (1983) Physiological correlates of prolonged sleep deprivation in rats. Science 221:182–184.

Rechtschaffen A, Kales A (1968) A manual of standardized, techniques and scoring system for sleep stages of human sleep. Los Angeles: Brain Information Service. Brain Research Institute.

Reichmuth C, Casey C (2014) Vocal learning in seals, sea lions, and walruses. Curr Opin Neurobiol 28:66–71.

Reiner A et al. (2004) Revised nomenclature for avian telencephalon and some related brainstem nuclei. Journal of Comparative Neurology 473:377–414.

Reiner A, Stern EA, Wilson CJ (2001) Physiology and morphology of intratelencephalically projecting corticostriatal-type neurons in pigeons as revealed by intracellular recording and cell filling. Brain Behav Evol 58:101–114.

Reiner A, Yamamoto K, Karten HJ (2005) Organization and evolution of the avian forebrain. The Anatomical Record 287A:1080–1102.

Rial RV, Nicolau MC, Gamundi A, Akaârir M, Garau C, Aparicio S, Tejada S, Moranta D, Gené L, Esteban S (2007a) Comments on evolution of sleep and the palliopallial connectivity in mammals and birds. Brain Research Bulletin 72:183–186.

Rial RV, Nicolau MC, Gamundí A, Akaârir M, Aparicio S, Garau C, Tejada S, Roca C, Gené L, Moranta D, Esteban S (2007b) The trivial function of sleep. Sleep Med Rev 11:311–325.

Ribeiro S, Gervasoni D, Soares ES, Zhou Y, Lin S-C, Pantoja J, Lavine M, Nicolelis MAL (2004) Long-lasting novelty-induced neuronal reverberation during slow-wave sleep in multiple forebrain areas. Wolfram Schultz, ed. PLoS Biol 2:E24.

Rickard TC, Cai DJ, Rieth CA, Jones J, Ard MC (2008) Sleep does not enhance motor sequence learning. J Exp Psychol Learn Mem Cogn 34:834–842.

Riedner BA, Hulse BK, Murphy MJ, Ferrarelli F, Tononi G (2011) Temporal dynamics of cortical sources underlying spontaneous and peripherally evoked slow waves. Prog Brain Res 193:201–218.

Roberts TF, Hisey E, Tanaka M, Kearney MG, Chattree G, Yang CF, Shah NM, Mooney R (2017) Identification of a motor-to-auditory pathway important for vocal learning. Nat Neurosci 20:978–986.

Robertson EM, Pascual-Leone A, Press DZ (2004) Awareness Modifies the Skill-Learning Benefits of Sleep. Curr Biol 14:208–212.

Robinson KS (2014) Icehenge. New York: Orb Books.

Rojas-Ramírez JA, Tauber ES (1970) Paradoxical Sleep in Two Species of Avian Predator (Falconiformes). Science 168:956–956.

Roth TC, Lesku JA, Amlaner CJ, Lima SL (2006) A phylogenetic analysis of the correlates of sleep in birds. Journal of Sleep Research 15:395–402.

Roxin A, Brunel N, Hansel D, Mongillo G, van Vreeswijk C (2011) On the Distribution of Firing Rates in Networks of Cortical Neurons. J Neurosci 31:16217–16226.

Roxin A, Hakim V, Brunel N (2008) The statistics of repeating patterns of cortical activity can be reproduced by a model network of stochastic binary neurons. J Neurosci 28:10734–10745.

Rudoy JD, Voss JL, Westerberg CE, Paller KA (2009) Strengthening individual memories by reactivating them during sleep. Science 326:1079.

Sagan C (1977) Dragons of Eden. New York: Random House.

Sagan C (1996) The Demon-Haunted World. New York: Ballantine Books.

Sallinen M, Kaartinen J, Lyytinen H (1996) Processing of auditory stimuli during tonic and phasic periods of REM sleep as revealed by event-related brain potentials. Journal of Sleep Research 5:220–228.

Sanchez-Vives MV, McCormick DA (2000) Cellular and network mechanisms of rhythmic recurrent activity in neocortex. Nat Neurosci 3:1027–1034.

Saucier D, Astic L (1975) Etude polygraphique du sommeil chez le poussin a l'eclosion. Evolution aux 3ème ET 4ème jours. Electroencephalography and Clinical Neurophysiology 38:303–306.

Scargle JD (1982) Studies in Astronomical Time-Series Analysis .2. Statistical Aspects of Spectral-Analysis of Unevenly Spaced Data. Astrophysical Journal 263:835–853.

Schabus M, Dang-Vu TT, Albouy G, Balteau E, Boly M, Carrier J, Darsaud A, Degueldre C, Desseilles M, Gais S, Phillips C, Rauchs G, Schnakers C, Sterpenich V, Vandewalle G, Luxen A, Maquet P (2007) Hemodynamic cerebral correlates of sleep spindles during human non-rapid eye movement sleep. PNAS 104:13164–13169.

Scharff C, Nottebohm F (1991) A comparative study of the behavioral deficits following lesions of various parts of the zebra finch song system: implications for vocal learning. J Neurosci 11:2896–2913.

Schiappa C, Scarpelli S, D'Atri A, Gorgoni M, De Gennaro L (2018) Narcolepsy and emotional experience: a review of the literature. Behav Brain Funct 14:19.

Schmidt DF (1994) A Comparative Analysis of Avian Sleep. Doctoral dissertation, University of Arkansas. Amlaner CJ Jr., ed.

Schmidt MH (2014) The energy allocation function of sleep: a unifying theory of sleep, torpor, and continuous wakefulness. Neurosci Biobehav Rev 47:122–153.

Schönauer M, Geisler T, Gais S (2013) Strengthening procedural memories by reactivation in sleep. J Cogn Neurosci 26:143–153.

Schulz H (2008) Rethinking sleep analysis. JCSM 4:99–103.

Schulz H, Salzarulo P (2012) Forerunners of REM sleep. Sleep Med Rev 16:95–108.

Schwartz JRL, Roth T (2008) Neurophysiology of Sleep and Wakefulness: Basic Science and Clinical Implications. Curr Neuropharmacol 6:367–378.

Scott BB, Gardner T, Ji N, Fee MS, Lois C (2012) Wandering neuronal migration in the postnatal vertebrate forebrain. J Neurosci 32:1436–1446 Available at: http://people.bu.edu/timothyg/resources/lab-publications/Scott_Gardner_Lois.pdf.

Scriba MF, Ducrest A-L, Henry I, Vyssotski AL, Rattenborg NC, Roulin A (2013) Linking melanism to brain development: expression of a melanism-related gene in barn owl feather follicles covaries with sleep ontogeny. Front Zool 10:42.

Seki Y, Dooling RJ (2016) Effect of auditory stimuli on conditioned vocal behavior of budgerigars. Behav Processes 122:87–89.

Shanahan LK, Gjorgieva E, Paller KA, Kahnt T, Gottfried JA (2018) Odor-evoked category reactivation in human ventromedial prefrontal cortex during sleep promotes memory consolidation. Elife 7:203.

Shank SS (2008) Sleep and sensorimotor learning in an oscine. Doctoral dissertation, University of Chicago. Margoliash D, ed.

Shank SS, Margoliash D (2009) Sleep and sensorimotor integration during early vocal learning in a songbird. Nature 458:73–77.

Shapovalov ASN (1970) Monosynaptic control over spinal motoneurons at different levels. Neuroscience Translations 4:123–134.

Shaw PJ, Tononi G, Greenspan RJ, Robinson DF (2002) Stress response genes protect against lethal effects of sleep deprivation in Drosophila. 417:287–291.

Shea SD, Margoliash D (2003) Basal Forebrain Cholinergic Modulation of Auditory Activity in the Zebra Finch Song System. Neuron 40:1213–1226.

Shein-Idelson M, Ondracek JM, Liaw H-P, Reiter S, Laurent G (2016) Slow waves, sharp waves, ripples, and REM in sleeping dragons. Science 352:590–595.

Shimizu A, Himwich HE (1968) The ontogeny of sleep in kittens and young rabbits. Electroencephalography and Clinical Neurophysiology 24:307–318.

Siapas AG, Wilson MA (1998) Coordinated interactions between hippocampal ripples and cortical spindles during slow-wave sleep. Neuron 21:1123–1128.

Siegel JM (1995) Phylogeny and the function of REM sleep. Behavioural Brain Research 69:29–34.

Siegel JM (2009) Sleep viewed as a state of adaptive inactivity. Nat Rev Neurosci 10:747–753.

Siegel JM, Manger PR, Nienhuis R, Fahringer HM, Pettigrew JD (1996) The Echidna Tachyglossus aculeatus Combines REM and Non-REM Aspects in a Single Sleep State: Implications for the Evolution of Sleep. J Neurosci 16:3500–3506.

Siegel JM, Manger PR, Nienhuis R, Fahringer HM, Pettigrew JD (1998) Monotremes and the evolution of rapid eye movement sleep. Philos Trans R Soc Lond, B, Biol Sci 353:1147–1157.

Siegel JM, Manger PR, Nienhuis R, Fahringer HM, Shalita T, Pettigrew JD (1999) Sleep in the platypus. Neuroscience 91:391–400.

Siegle JH, López AC, Patel YA, Abramov K, Ohayon S, Voigts J (2017) Open Ephys: an open-source, plugin-based platform for multichannel electrophysiology. J Neural Eng 14:045003.

Simonyan K (2014) The laryngeal motor cortex: its organization and connectivity. Curr Opin Neurobiol 28:15–21 Available at: http://linkinghub.elsevier.com/retrieve/pii/S095943881400107X.

Simor P, Gombos F, Blaskovich B, Bódizs R (2018) Long-range alpha and beta and short-range gamma EEG synchronization distinguishes phasic and tonic REM periods. Sleep 41:16.

Simor P, Horváth K, Ujma PP, Gombos F, Bódizs R (2013) Fluctuations between sleep and wakefulness: wake-like features indicated by increased EEG alpha power during different sleep stages in nightmare disorder. Biol Psychol 94:592–600.

Sinha AK, Smythe H, Zarcone VP, Barchas JD, Dement WC (1972) Human sleep-electroencephalogram: A damped oscillatory phenomenon. Journal of Theoretical Biology 35:387–393.

Skaggs WE, McNaughton BL (1996) Replay of neuronal firing sequences in rat hippocampus during sleep following spatial experience. Science 271:1870–1873.

Smith C (1985) Sleep states and learning: a review of the animal literature. Neurosci Biobehav Rev 9:157–168.

Smith C (1995) Sleep states and memory processes. Behavioural Brain Research 69:137–145.

Smith C (2011) Sleep States and Memory Processing in Rodents: A Review. 6:59–70.

Smith C, Macneill C (1994) Impaired motor memory for a pursuit rotor task following Stage 2 sleep loss in college students. Journal of Sleep Research 3:206–213.

Smith C, Rose GM (1996) Evidence for a paradoxical sleep window for place learning in the Morris water maze. Physiol Behav 59:93–97.

Snyder JM, Molk DM, Treuting PM (2013) Increased mortality in a colony of zebra finches exposed to continuous light. J Am Assoc Lab Anim Sci 52:301–307.

Solodkin M, Cardona A, Corsi-Cabrera M (1985) Paradoxical sleep augmentation after imprinting in the domestic chick. Physiol Behav 35:343–348.

Song S, Howard JH, Howard DV (2007) Sleep Does Not Benefit Probabilistic Motor Sequence Learning. J Neurosci 27:12475–12483.

Sossinka R, Böhner J (1980) Song Types in the Zebra Finch Poephila guttata castanotis. Z Tierpsychol 53:123–132.

Spencer RMC, Sunm M, Ivry RB (2006) Sleep-dependent consolidation of contextual learning. Curr Biol 16:1001–1005.

Spierings MJ, Cate Ten C (2016) Budgerigars and zebra finches differ in how they generalize in an artificial grammar learning experiment. Proc Natl Acad Sci USA 113:E3977–E3984.

Spiro JE, Dalva MB, Mooney R (1999) Long-range inhibition within the zebra finch song nucleus RA can coordinate the firing of multiple projection neurons. J Neurophysiol 81:3007–3020.

Stafstrom CE, Schwindt PC, Crill WE (1984) Repetitive firing in layer V neurons from cat neocortex in vitro. J Neurophysiol 52:264–277.

Stahel CD, Megirian D, Nicol SC (1984) Sleep and metabolic rate in the little penguin, Eudyptula minor. J Comp Physiol B 154:487–494.

Steriade M (1997) Synchronized activities of coupled oscillators in the cerebral cortex and thalamus at different levels of vigilance. Cereb Cortex 7:583–604.

Steriade M (2003) The corticothalamic system in sleep. Front Biosci 8:d878–d899.

Steriade M, Amzica F, Nunez A (1993a) Cholinergic and noradrenergic modulation of the slow (approximately 0.3 Hz) oscillation in neocortical cells. J Neurophysiol 70:1385–1400.

Steriade M, Contreras D, Curró Dossi R, Nunez A (1993b) The slow (< 1 Hz) oscillation in reticular thalamic and thalamocortical neurons: scenario of sleep rhythm generation in interacting thalamic and neocortical networks. J Neurosci 13:3284–3299.

Steriade M, Domich L, Oakson G, Deschênes M (1987) The deafferented reticular thalamic nucleus generates spindle rhythmicity. J Neurophysiol 57:260–273.

Steriade M, Nunez A, Amzica F (1993c) A novel slow (< 1 Hz) oscillation of neocortical neurons in vivo: depolarizing and hyperpolarizing components. J Neurosci 13:3252–3265.

Steriade M, Nunez A, Amzica F (1993d) Intracellular analysis of relations between the slow (< 1 Hz) neocortical oscillation and other sleep rhythms of the electroencephalogram. J Neurosci 13:3266–3283.

Sterman MB, Knauss T, Lehmann D, Clemente CD (1965) Circadian sleep and waking patterns in the laboratory cat. Electroencephalography and Clinical Neurophysiology 19:509–517.

Stickgold R (1998) Sleep: off-line memory reprocessing. Trends in Cognitive Sciences 2:484–492.

Stickgold R, James L, Hobson JA (2000a) Visual discrimination learning requires sleep after training. Nat Neurosci 3:1237–1238 Available at: http://www.nature.com/doifinder/10.1038/81756.

Stickgold R, Malia A, Maguire D, Roddenberry D, O'Connor M (2000b) Replaying the Game: Hypnagogic Images in Normals and Amnesics. Science 290:350–353.

Stoeger AS, Manger P (2014) Vocal learning in elephants: neural bases and adaptive context. Curr Opin Neurobiol 28:101–107.

Stosiek C, Garaschuk O, Holthoff K, Konnerth A (2003) In vivo two-photon calcium imaging of neuronal networks. PNAS 100:7319–7324.

Sugihara K, Gotoh J (1973) Depth-electroencephalograms of chickens in wakefulness and sleep. Jpn J Physiol 23:371–379 Available at: http://eutils.ncbi.nlm.nih.gov/entrez/eutils/elink.fcgi?dbfrom=pubmed&id=4357906&retmode=ref&cmd=prlinks.

Swift KM, Gross BA, Frazer MA, Bauer DS, Clark KJD, Vazey EM, Aston-Jones G, Li Y, Pickering AE, Sara SJ, Poe GR (2018) Abnormal Locus Coeruleus Sleep Activity Alters Sleep Signatures of Memory Consolidation and Impairs Place Cell Stability and Spatial Memory. Curr Biol 28:3599–3609.e4.

Swisher JE (1962) Manifestaions of "Activated" Sleep in the Rat. Science 138:1110–1110.

Syka J, Kovacevic N, Radil-Weiss T (1973) Tectal activity and eye movements during paradoxical sleep in cats. Physiol Behav 10:203–207.

Szymczak JT (1985) Sleep pattern in the starling (Sturnus vulgaris). Acta Physiol Pol 36:323–331.

Szymczak JT (1986a) Daily distribution of sleep states in the jackdaw, Corvus monedula. Chronobiologia 13:227–235.

Szymczak JT (1986b) Daily rhythm of sleep-wakefulness in the starling, Sturnus vulgaris. Acta Physiol Pol 37:199–206.

Szymczak JT (1987) Daily distribution of sleep states in the rook Corvus frugilegus. J Comp Physiol A 161:321–327.

Szymczak JT (1989) Influence of environmental temperature and photoperiod on temporal structure of sleep in corvids. Acta Neurobiol Exp (Wars) 49:359–366.

Szymczak JT, Helb HW, Kaiser W (1993) Electrophysiological and behavioral correlates of sleep in the blackbird (Turdus merula). Physiol Behav 53:1201–1210.

Szymczak JT, Kaiser W, Helb HW, Beszczyńska B (1996) A study of sleep in the European blackbird. Physiol Behav 60:1115–1120.

Šušić VT, Kovačević RM (1973) Sleep patterns in the owl Strix aluco. Physiol Behav 11:313–317.

Tamaki M, Matsuoka T, Nittono H, Hori T (2008) Fast sleep spindle (13-15 hz) activity correlates with sleep-dependent improvement in visuomotor performance. Sleep 31:204–211.

Tasali E, Leproult R, Ehrmann DA, Van Cauter E (2008) Slow-wave sleep and the risk of type 2 diabetes in humans. Proc Natl Acad Sci USA 105:1044–1049.

Tassi P, Muzet A (2000) Sleep inertia. Sleep Med Rev 4:341–353.

Tchernichovski O (2001) Dynamics of the Vocal Imitation Process: How a Zebra Finch Learns Its Song. Science 291:2564–2569.

Thorpe WH (1958) The learning of song patterns by birds, with especial reference to the song of the chaffinch Fringilla coelebs. Ibis 100:535–570.

Tilley AJ, Empson JA (1978) REM sleep and memory consolidation. Biol Psychol 6:293–300.

Tisdale RK, Lesku JA, Beckers GJL, Rattenborg NC (2018) Bird-like propagating brain activity in anesthetized Nile crocodiles. Sleep 41:1–11.

Tisdale RK, Vyssotski AL, Lesku JA, Rattenborg NC (2017) Sleep-Related Electrophysiology and Behavior of Tinamous (Eudromia elegans): Tinamous Do Not Sleep Like Ostriches. Brain Behav Evol 89:249–261.

Tobler I (2005) Phylogeny of Sleep Regulation. In: Principles and Practice of Sleep Medicine, 4 ed. (Kryger MH, Roth T, Dement WC, eds), pp 77–90. Philadelphia: Elsevier.

Tobler I, Borbély AA (1988) Sleep and EEG spectra in the pigeon (Columba livia) under baseline conditions and after sleep deprivation. J Comp Physiol 163:729–738.

Tokarev K, Boender AJ, Claßen GAE, Scharff C (2015) Young, active and well-connected: adult-born neurons in the zebra finch are activated during singing. Brain Struct Funct 221:1833–1843.

Tononi G, Cirelli C (2003) Sleep and synaptic homeostasis: a hypothesis. Brain Research Bulletin 62:143–150.

Tu H-W, Dooling RJ (2012) Perception of warble song in budgerigars (Melopsittacus undulatus): evidence for special processing. Anim Cogn 15:1151–1159.

Tumer EC, Brainard MS (2007) Performance variability enables adaptive plasticity of "crystallized" adult birdsong. Nature 450:1240–1244.

Uchida S, Maloney T, March JD, Azari R, Feinberg I (1991) Sigma (12–15 Hz) and Delta (0.3–3 Hz) EEG oscillate reciprocally within NREM sleep. Brain Research Bulletin 27:93–96.

Uguccioni G, Pallanca O, Golmard J-L, Dodet P, Herlin B, Leu-Semenescu S, Arnulf I (2013) Sleep-Related Declarative Memory Consolidation and Verbal Replay during Sleep Talking in Patients with REM Sleep Behavior Disorder Paul F, ed. PLoS ONE 8:e83352.

Ulinski PS, Margoliash D (1990) Neurobiology of the Reptile—Bird Transition. In: Comparative Structure and Evolution of Cerebral Cortex, Part I, pp 217–265. Springer, Boston, MA.

Usami K, Matsumoto R, Kobayashi K, Hitomi T, Matsuhashi M, Shimotake A, Kikuchi T, Yoshida K, Kunieda T, Mikuni N, Miyamoto S, Takahashi R, Ikeda A (2017) Phasic REM

Transiently Approaches Wakefulness in the Human Cortex-A Single-Pulse Electrical Stimulation Study. Sleep 40:1–7.

Van Cauter E, Spiegel K, Tasali E, Leproult R (2008) Metabolic consequences of sleep and sleep loss. Sleep Med 9 Suppl 1:S23–S28.

van der Helm E, Yao J, Dutt S, Rao V, Saletin JM, Walker MP (2011) REM Sleep Depotentiates Amygdala Activity to Previous Emotional Experiences. Current Biology 21:2029–2032.

van der Meij J, Martinez-Gonzalez D, Beckers GJL, Rattenborg NC (2018) Intra-"cortical" activity during avian non-REM and REM sleep: variant and invariant traits between birds and mammals. Sleep 13:3252.

van der Meij J, Martinez-Gonzalez D, Beckers GJL, Rattenborg NC (2019) Neurophysiology of Avian Sleep: Comparing Natural Sleep and Isoflurane Anesthesia. Front Neurosci 13:262.

Van Der Werf YD, Altena E, Schoonheim MM, Sanz-Arigita EJ, Vis JC, De Rijke W, Van Someren EJW (2009) Sleep benefits subsequent hippocampal functioning. Nat Neurosci 12:122–123.

Van Dongen H, Maislin G, Mullington JM, Dinges DF (2003) The cumulative cost of additional wakefulness: dose-response effects on neurobehavioral functions and sleep physiology from chronic sleep restriction and total sleep deprivation. Sleep 26:117-126.

van Luijtelaar EL, van der Grinten CP, Blokhuis HJ, Coenen AM (1987) Sleep in the domestic hen (Gallus domesticus). Physiol Behav 41:409–414.

Van T La (2012) Diurnal and Nocturnal Birds Vocalize at Night: A Review. The Condor 114:245–257.

Van Twyver H, Allison T (1972) A polygraphic and behavioral study of sleep in the pigeon (Columba livia). Experimental Neurology 35:138–153.

Vandecasteele M, M S, Royer S, Belluscio M, Berényi A, Diba K, Fujisawa S, Grosmark A, Mao D, Mizuseki K, Patel J, Stark E, Sullivan D, Watson B, Buzsáki G (2012) Large-scale recording of neurons by movable silicon probes in behaving rodents. J Vis Exp:e3568–e3568.

VanderPlas J, Connolly AJ, Ivezic Z, Gray A (2012) Introduction to astroML: Machine learning for astrophysics. Proceedings of Conference on Intelligent Data Understanding (CIDU), pp 47-54, 2012:47–54.

VanderPlas JT, Ivezic Ž (2015) *Periodograms for Multiband Astronomical Time Series*. ApJ 812:18.

Vanderwolf CH (1969) Hippocampal electrical activity and voluntary movement in the rat. Electroencephalography and Clinical Neurophysiology 26:407–418.

Varga AW et al. (2016) Reduced Slow-Wave Sleep Is Associated with High Cerebrospinal Fluid Aβ42 Levels in Cognitively Normal Elderly. Sleep 39:2041–2048.

Vazquez J, Baghdoyan HA (2001) Basal forebrain acetylcholine release during REM sleep is significantly greater than during waking. Am J Physiol Regul Integr Comp Physiol 280:R598–R601.

Vertes RP (2004) Memory consolidation in sleep; dream or reality. Neuron 44:135–148.

Vicario DS (1991) Organization of the zebra finch song control system: Functional organization of outputs from nucleus robustus archistriatalis. Journal of Comparative Neurology 309:486–494.

Vorster AP, Born J (2015) Sleep and memory in mammals, birds and invertebrates. Neurosci Biobehav Rev 50:103–119.

Voss U, Schermelleh-Engel K, Windt J, Frenzel C, Hobson A (2013) Measuring consciousness in dreams: the lucidity and consciousness in dreams scale. Conscious Cogn 22:8–21.

Waldstein RS (1990) Effects of postlingual deafness on speech production: Implications for the role of auditory feedback. The Journal of the Acoustical Society of America 88:2099–2114.

Walk JW, Kershner EL, Warner RE (2000) Nocturnal Singing in Grassland Birds. Wilson Bull 112:289–292.

Walker JM, Berger RJ (1972) Sleep in the domestic pigeon (Columba livia). Behav Biol 7:195–203.

Walker MP, Brakefield T, Morgan A, Hobson JA, Stickgold R (2002) Practice with sleep makes perfect: sleep-dependent motor skill learning. Neuron 35:205–211.

Walker MP, Brakefield T, Seidman J, Morgan A, Hobson JA, Stickgold R (2003) Sleep and the time course of motor skill learning. Learn Mem 10:275–284.

Walker MP, Stickgold R (2004) Sleep-Dependent Learning and Memory Consolidation. Neuron 44:121–133.

Walker MP, Stickgold R (2006) Sleep, memory, and plasticity. Annu Rev Psychol 57:139–166.

Walker MP, van Der Helm E (2009) Overnight therapy? The role of sleep in emotional brain processing. Psychological Bulletin 135: 731-748.

Walton C, Pariser E, Nottebohm F (2012) The zebra finch paradox: song is little changed, but number of neurons doubles. J Neurosci 32:761–774.

Wamsley EJ, Tucker MA, Shinn AK, Ono KE, McKinley SK, Ely AV, Goff DC, Stickgold R, Manoach DS (2012) Reduced sleep spindles and spindle coherence in schizophrenia: mechanisms of impaired memory consolidation? Biol Psychiatry 71:154–161.

Wang DV, Ikemoto S (2016) Coordinated Interaction between Hippocampal Sharp-Wave Ripples and Anterior Cingulate Unit Activity. J Neurosci 36:10663–10672.

Wang G, Harpole CE, Trivedi AK, Cassone VM (2012) Circadian regulation of bird song, call, and locomotor behavior by pineal melatonin in the zebra finch. J Biol Rhythms 27:145–155.

Watts A, Gritton HJ, Sweigart J, Poe GR (2012) Antidepressant suppression of non-REM sleep spindles and REM sleep impairs hippocampus-dependent learning while augmenting striatum-dependent learning. J Neurosci 32:13411–13420.

Webb WB, Agnew HW (1971) Stage 4 sleep: influence of time course variables. Science 174:1354–1356.

Wehrle R, Kaufmann C, Wetter TC, Holsboer F, Auer DP, Pollmächer T, Czisch M (2007) Functional microstates within human REM sleep: first evidence from fMRI of a thalamocortical network specific for phasic REM periods. Eur J Neurosci 25:863–871.

Weiss SK (2013) Sleep Starts and Sleep Talking. In: Parasomnias, pp 139–154. New York, NY: Springer, New York, NY.

Weitzmann ED (1961) A note on the EEG and eye movements during behavioral sleep in monkeys. Electroencephalography and Clinical Neurophysiology 13:790–794.

Wester JC, Contreras D (2012) Columnar interactions determine horizontal propagation of recurrent network activity in neocortex. J Neurosci 32:5454–5471.

Wierzynski CM, Lubenov EV, Gu M, Siapas AG (2009) State-dependent spike-timing relationships between hippocampal and prefrontal circuits during sleep. Neuron 61:587–596.

Wild JM (1993) Descending projections of the songbird nucleus robustus archistriatalis. J Comp Neurol 338:225–241 Available at: http://doi.wiley.com/10.1002/cne.903380207.

Wild JM, Goller F, Suthers RA (1998) Inspiratory muscle activity during bird song. J Neurobiol. 36:441-453.

Wilhelm I, Metzkow Mészàros M, Knapp S, Born J (2012) Sleep-dependent consolidation of procedural motor memories in children and adults: the pre-sleep level of performance matters. Dev Sci 15:506–515.

Wilson M, McNaughton B (1994) Reactivation of hippocampal ensemble memories during sleep. Science 265:676–679.

Wood WE, Osseward PJ, Roseberry TK, Perkel DJ (2013) A daily oscillation in the fundamental frequency and amplitude of harmonic syllables of zebra finch song. PLoS ONE 8:e82327–14.

Xie L, Kang H, Xu Q, Chen MJ, Liao Y, Thiyagarajan M, O'Donnell J, Christensen DJ, Nicholson C, Iliff JJ, Takano T, Deane R, Nedergaard M (2013) Sleep drives metabolite clearance from the adult brain. Science 342:373–377.

Yanagihara S, Hessler NA (2011a) Common features of neural activity during singing and sleep periods in a basal ganglia nucleus critical for vocal learning in a juvenile songbird. PLoS ONE 6:e25879–e25879.

Yanagihara S, Hessler NA (2011b) Phasic basal ganglia activity associated with high-gamma oscillation during sleep in a songbird. J Neurophysiol 107:424–432.

Yanagihara S, Yazaki-Sugiyama Y (2016) Auditory experience-dependent cortical circuit shaping for memory formation in bird song learning. Nat Comms 7:11946.

Yang G, Lai CSW, Cichon J, Ma L, Li W, Gan W-B (2014) Sleep promotes branch-specific formation of dendritic spines after learning. Science 344:1173–1178.

Yger P, Spampinato GL, Esposito E, Lefebvre B, Deny S, Gardella C, Stimberg M, Jetter F, Zeck G, Picaud S, Duebel J, Marre O (2018) A spike sorting toolbox for up to thousands of electrodes validated with ground truth recordings in vitro and in vivo. Elife 7:608.

Young BK, Goller F (2012) Playback-induced syringeal motor rehearsal of song without concurrent respiratory movements. In Society for Neuroscience, New Orleans, LA. Available at: http://www.abstractsonline.com/Plan/ViewAbstract.aspx?sKey=aa9e58eb-d394-4797-a602-979f35831500&cKey=db6c0d9e-4db7-4c27-b412-0ed7cde26024.

Young BK, Mindlin GB, Arneodo E, Goller F (2017) Adult zebra finches rehearse highly variable song patterns during sleep. PeerJ 5:e4052.

Yu AC, Margoliash D (1996) Temporal Hierarchical Control of Singing in Birds. Science 273:1871–1875.

Zepelin H, Siegel JM, Tobler I (2005) Mammalian Sleep. In: Principles and Practice of Sleep Medicine, 4 ed., pp 91–100. Philadelphia, PA: Elsevier Saunders.

Zevin JD, Seidenberg MS, Bottjer SW (2004) Limits on reacquisition of song in adult zebra finches exposed to white noise. J Neurosci 24:5849–5862.

Zhang G et al. (2014) Comparative genomics reveals insights into avian genome evolution and adaptation. Science 346:1311–1320.